THE MICRORNA DEREGULATION IN COLORECTAL CANCER

YONG FUNG LIN

THESIS SUBMITTED IN FULFILMENT OF THE REQUIREMENT FOR THE DEGREE OF DOCTOR OF PHILOSOPHY

FACULTY OF MEDICINE
UNIVERSITY OF MALAYA
KUALA LUMPUR

2014

ORIGINAL LITERARY WORK DECLARATION FORM

Name of candidate: **Yong Fung Lin** (IC: **881115-56-5590**)

Registration/Matric No: **MHA100040**

Name of Degree: **Doctor of Philosophy**

Title of Thesis ("this Work"): **The microRNA Deregulation in Colorectal Cancer**

Field of Study: **Molecular Biology of Colorectal Cancer**

I do solemnly and sincerely declare that:

(1) I am the sole author/writer of this Work;

(2) This Work is original;

(3) Any use of my work in which copyright exists was done by way of fair dealing and for permitted purposes and any excerpt or extract from, or reference to or reproduction of any copyright work has been disclosed expressly and sufficiently and the title of the Work and its authorship have been acknowledged in this Work;

(4) I do not have any actual knowledge nor do I ought reasonably to know that the making of this work constitutes an infringement of any copyright work;

(5) I hereby assign all and every rights in the copyright to this work to the University of Malaya ("UM"), who henceforth shall be owner of the copyright in this Work and that any reproduction or use in any form or by any means whatsoever is prohibited without the written consent of UM having been first had and obtained;

(6) I am fully aware that if in the course of making this Work I have infringed any copyright whether intentionally or otherwise, I may be subject to legal action or any other action as may be determined by UM.

Candidate's Signature Date

Subscribed and solemnly declared before,

Witness's Signature Date

Name :

Designation :

ABSTRACT

Colorectal cancer (CRC) is the carcinoma of the colon and rectum in the gastrointestinal system. CRC is the third most common cancer in men and the second in women worldwide. The limitations of the currently available biomarkers and technologies for CRC screening and surveillance have highlighted the necessity of finding novel biomarkers. Recently, microRNA (miRNA)-based studies have rendered remarkable contribution in the elucidation of mechanisms of carcinogenesis. miRNAs are short, non-coding RNA molecules that act as regulators of gene expression through messenger RNA (mRNA) degradation or translational inhibition. Blood miRNA expression profiles offer great potential as non-invasive biomarkers. In the present study, the aims were to characterise and correlate the tissue and blood miRNA expression patterns of primary CRC patients, and establish the functional roles of the identified miRNAs in the carcinogenesis of CRC. Firstly, the miRNA profiling study was divided into two phases: (I) marker discovery by miRNA microarray using paired cancer tissues (n = 30) and blood samples (CRC, n = 42; control, n = 18); (II) marker validation by reverse transcription-quantitative real-time polymerase chain reaction (RT-qPCR) using an independent set of paired cancer tissues (n = 30) and blood samples (CRC, n = 70; control, n = 32). Logistic regression and receiver operating characteristic curve analyses were applied to obtain diagnostic utility of the miRNAs. Seven miRNAs (miR-150, miR-193a-3p, miR-23a, miR-23b, miR-338-5p, miR-342-3p and miR-483-3p) were found to be differentially expressed in both tissue and blood samples. Significant positive correlations were observed in the tissue and blood levels of miR-193a-3p, miR-23a and miR-338-5p. These miRNAs were demonstrated as a classifier for CRC detection, with a receiver operating characteristic curve area of 0.887 (80.0% sensitivity, 84.4% specificity and 83.3% accuracy). Next, these miRNAs were subjected to functional and miRNA:mRNA target validation studies via miRNA mimics and

inhibitors transfections. SW480 and SW620 CRC cell lines were utilised. Cell viability, apoptosis, migration and invasion assays were conducted. Luciferase assays were performed for the validation of target mRNAs. The expression levels of target mRNAs and proteins in clinical CRC samples and cell lines were assessed using RT-qPCR and Western blot. miR-193a-3p was identified to be involved in CRC cell migration and invasion by targeting *FOXO4*. miR-23a was determined to possess apoptosis resistance function by targeting *APAF1*. However, the transfection of miR-338-5p did not reveal significant findings in the cell viability, apoptosis, migration and invasion analyses. In conclusion, miRNA deregulation in the blood is reflective of that in the CRC tissue. The triple miRNA classifier of miR-193a-3p, miR-23a and miR-338-5p may serve as potential blood biomarkers for CRC detection. The miRNA:mRNA target validation studies have highlighted the potential application of miR-193a-3p:*FOXO4* and miR-23a:*APAF1* regulation axes in miRNA-based therapy and prognostication.

ABSTRAK

Kanser kolorektal adalah karsinoma kolon dan rektum dalam sistem gastrointestinal. Kanser kolorektal adalah kanser ketiga paling lazim di kalangan lelaki dan yang kedua di kalangan wanita di seluruh dunia. Batasan dalam biomarker dan teknologi sedia ada bagi pemeriksaan dan pemantauan kanser kolorektal telah mengetengahkan keperluan untuk mencari biomarker yang novel. Kebelakangan ini, kajian berasaskan microRNA (miRNA) amat menyerlah dalam penerangan mengenai mekanisme karsinogenesis. miRNA adalah molekul RNA pendek, bukan pengekodan yang terlibat dalam penyeliaan gen melalui degradasi 'messenger RNA (mRNA)' atau perencatan translasional protein. Profil ekspresi miRNA darah menawarkan potensi besar sebagai biomarker tidak invasif. Objektif-objektif penyelidikan ini adalah demi mencirikan dan mengaitkan pola ekspresi miRNA tisu dan darah pesakit kanser kolorektal, dan menentukan peranan miRNA yang terpilih dalam karsinogenesis kanser kolorektal. Pertama sekali, kajian profil miRNA telah dibahagikan kepada dua fasa: (I) penemuan marker melalui miRNA microarray dengan menggunakan sampel tisu (n = 30) dan darah (kanser, n = 42; kawalan, n = 18); (II) pengesahan marker melalui 'reverse transcription-quantitative real-time polymerase chain reaction (RT-qPCR)' dengan menggunakan set sampel tisu (n = 30) dan darah (kanser, n = 70; kawalan, n = 32) yang baru. Analisis-analisis seperti 'logistic regression' dan 'receiver operating characteristic curve' telah dilaksanakan untuk memperoleh utiliti diagnostik daripada miRNA-miRNA yang terlibat. Berdasarkan sampel-sampel tisu dan darah yang telah diuji, tujuh miRNAs (miR-150, miR-193a-3p, miR-23a, miR-23b, miR-338-5p, miR-342-3p dan miR-483-3p) telah memaparkan tahap ekspresi yang unik. Tahap miR-193a-3p, miR-23a dan miR-338-5p telah menunjukkan korelasi positif yang ketara di antara sampel tisu dan darah. miRNA-miRNA tersebut telah didemonstrasikan sebagai sekumpulan miRNA yang boleh digunakan dalam pengesanan kanser kolorektal, dengan keluasan

‘receiver operating characteristic curve’ sebanyak 0.887 (sensitiviti 80.0%, kekhususan 84.4% dan ketepatan 83.3%). Seterusnya, kajian fungsional dan pengesahan target miRNA:mRNA melalui transfeksi mimik dan perencatan telah dijalankan. Sel kanser kolorektal SW480 dan SW620 telah digunakan. Eksperimen-eksperimen seperti tahap kegiatan sel, apoptosis, migrasi dan invasi telah dijalankan. Uji kaji ‘luciferase’ telah dilaksanakan bagi pengesahan target mRNA. Tahap ekspresi target mRNA dan protein dalam sampel klinikal dan sel kanser kolorektal telah dinilai melalui ‘RT-qPCR’ dan ‘Western blot’. Penglibatan miR-193a-3p dalam sel migrasi dan invasi melalui target *FOXO4* telah dikenal pasti manakala miR-23a telah didapati mempunyai fungsi rintangan apoptosis melalui target *APAF1*. Walau bagaimanapun, transfeksi miR-338-5p tidak memaparkan penemuan penting dalam analisis-analisis tahap kegiatan sel, apoptosis, migrasi dan invasi. Kesimpulannya, ketidakseimbangan tahap miRNA dalam darah telah mencerminkan tahap miRNA dalam tisu kanser kolorektal. Sekumpulan tiga miRNA, miR-193a-3p, miR-23a dan miR-338-5p dicadangkan sebagai biomarker-biomarker yang berpotensi dalam pengesanan kanser kolorektal. Kajian pengesahan target miRNA:mRNA juga menekankan bahawa paksi pengawalseliaan tahap miR-193a-3p:*FOXO4* dan miR-23a:*APAF1* berkemungkinan boleh diterapkan dalam terapi berasaskan miRNA dan pemantauan kanser.

ACKNOWLEDGEMENTS

First and foremost, I would like to express my deepest gratitude to my supervisors, Professor Dr. Wang Chee Woon and Associate Professor Dr. Law Chee Wei, for giving me an opportunity to work in this challenging research and for their continuous support and invaluable guidance.

I would like to convey my sincere regards to Professor Dr. April Camilla Roslani and clinical doctors from the UMMC Colorectal Surgery Unit for their help in clinical sample collection. I would like to thank Professor Dr. Kandiah Jeyaseelan and his co-workers from the National University of Singapore for the introductory training on microRNA research. I am also grateful to Professor Dr. Tan Kay Sin from the Department of Medicine for allowing me to widen my knowledge through several mini projects.

Special thanks to all lecturers, administrative staffs and graduate students from the Departments of Surgery and Molecular Medicine for their help in all means towards the completion of my research.

Most importantly, I would like to express my heartfelt thanks to my family for their unconditional love, motivation, support and encouragement. I love you all and thank you very much!

Lastly, I would like to acknowledge the financial sponsorship received from the Ministry of Higher Education Malaysia (MyBrain15-MyPhD) and research funding from the University of Malaya Research Grants (RG313-11HTM and PV020-2011A).

TABLE OF CONTENTS

PAGE

LIST OF FIGURES

PAGE

LIST OF TABLES

PAGE

LIST OF ABBREVIATIONS AND SYMBOLS

3D	three dimensional
3’-UTR	3’-untranslated region
5-FU	5-fluorouracil
AATK	apoptosis-associated tyrosine kinase
ABCC	ATP-binding cassette, sub-family C
ACVR1C	activin A receptor, type 1C
ADAM17	ADAM metallopeptidase domain 17
Ago	Argonaute
AJCC	American Joint Committee on Cancer
AKT	protein kinase B
ANOVA	analysis of variance
ANXA8	annexin A8
APAF1	apoptotic peptidase activating factor 1
APC	adenomatous polyposis coli
APS	ammonium persulphate
ASO(s)	antisense oligonucleotide(s)
ATP	adenosine triphosphate
AUC	area under the ROC curve
BAK	BCL2-antagonist/killer
BAX	BCL2-associated X protein
BBC3	BCL2-binding component 3
BCL2	B-cell lymphoma 2
BCL2L2	BCL2-like 2
BID	BH3-interacting domain death antagonist

BIM	BCL2-interacting mediator of cell death
BLAST	Basic Local Alignment Search Tool
bp	base pair
BRAF	B-Raf proto-oncogene
BSA	bovine serum albumin
CA19-9	carbohydrate antigen 19-9
CARD	N-terminal caspase recruitment domain
CCND1	cyclin D1
CCNG1	cyclin G1
CDC42	cell division control protein 42 homologue
CDK6	cyclin-dependent kinase 6
CEA	carcinoembryonic antigen
CED-4	cell death 4
cel	*Caenorhabditis elegans*
CI	confidence interval
CIMP	CpG island methylator phenotype
CIN	chromosomal instability
CK1	casein kinase 1
cm	centimetre
COX2	cyclooxygenase 2
CpG	cytosine-phosphate-guanine
CRC	colorectal cancer
CREB	cAMP response element-binding protein
CREBBP	CREB-binding protein
CREF	carcinoma-related EF-hand
C_T	cycle threshold

CTC	computed tomographic colonography
CTGF	connective tissue growth factor
dATP	deoxyadenosine triphosphate
DCBE	double contrast barium enema
DGCR8	DiGeorge syndrome critical region gene 8
DLL1	delta-like 1
DMEM	Dulbecco's modified Eagle's medium
DMSO	dimethyl sulphoxide
DNA	deoxyribonucleic acid
DVL	dishevelled
DYRK1A	dual-specificity tyrosine-phosphorylated and regulated kinase 1A
e.g.	exemplī grātiā (for example)
ECM	extracellular matrix
EDTA	ethylenediaminetetraacetic acid
EGFR	epidermal growth factor receptor
EGR2	early growth response 2
ELOSA	enzyme-linked oligosorbent assay
EMT	epithelial-to-mesenchymal transition
ERBB	v-erb-b2 erythroblastic leukaemia viral oncogene homologue
EtBr	ethidium bromide
EVL	Enah/Vasp-like
EZH2	enhancer of zeste homologue 2
FADD	Fas-associated death domain
FAP	familial adenomatous polyposis
FBS	foetal bovine serum
FIT	faecal immunochemical test

FITC	fluorescein isothiocyanate
FOBT	faecal occult blood test
FOX	forkhead box
FOXO4	forkhead box O4
FZD	frizzled
g	gram
G1	grade 1
G2	grade 2
G3	grade 3
G4	grade 4
GADD45	growth arrest and DNA damage-inducible protein 45
GAPDH	glyceraldehyde-3-phosphate dehydrogenase
GDP	guanosine diphosphate
GEO	Gene Expression Omnibus
gFOBT	guaiac-based FOBT
GRB2	growth factor receptor-bound protein 2
GSK3β	glycogen synthase kinase 3β
GTP	guanosine triphosphate
h	hour
hsa	*Homo sapiens*
HBV	hepatitis B virus
HCl	hydrochloric acid
HCV	hepatitis C virus
HIF1	hypoxia-inducible factor 1
HNPCC	hereditary non-polyposis colorectal cancer
HRP	horseradish peroxidase

i.e.	id est (that is)
IARC	International Agency for Research on Cancer
iASPP	inhibitor of apoptosis-stimulating protein of p53
IGF2	insulin-like growth factor 2
IKKB	inhibitor kappa-B kinase β
IL6R	interleukin 6 receptor
IRF1	interferon regulatory factor 1
JNK	c-Jun N-terminal kinase
kDa	kilodalton
KRAS	Kirsten rat sarcoma viral oncogene homologue
L	litre
LB	Luria-Bertani
LC3	microtubule-associated protein 1A/1B-light chain 3
LEF	lymphocyte enhancer factor
LNA	locked nucleic acid
LRP	low density lipoprotein receptor-related protein
M	molar
MAC	modified Astler-Coller
MAP3K1	mitogen-activated protein kinase kinase kinase 1
MAPK	mitogen-activated protein kinase
MDM2	mouse double minute 2 homologue
mg	milligram
MIAME	Minimum Information About a Microarray Experiment
MIQE	Minimum Information for Publication of Quantitative Real-time PCR Experiments
miRISC	miRNA-RISC

miRNA(s)	microRNA(s)
ml	millilitre
mm	millimetre
mM	millimolar
MMP(s)	matrix metalloproteinase(s)
MMR	mismatch repair
MOPS	3-(N-Morpholino)propanesulphonic acid
mRNA(s)	messenger RNA(s)
MSI	microsatellite instability
MTSS1	metastasis suppressor 1
MTT	3-(4,5-dimethylthiazol-2-yl)-2,5,-diphenyltetrazolium bromide
MUC4	mucin 4
NaCl	sodium chloride
NC	negative control
NCBI	National Centre for Biotechnology Information
NEDD1	neural precursor cell expressed, developmentally down-regulated 1
NES	nuclear export sequence
NLS	nuclear localisation sequence
nm	nanometre
nmol	nanomole
NTC	non-transfected control
PACT	protein kinase RNA activator
PAGE	polyacrylamide gel electrophoresis
PAK2	p21 protein (Cdc42/Rac)-activated kinase 2
P-body	processing body
PBS	phosphate-buffered saline

PCA	principal component analysis
PCAF	p300/CBP-associated factor
PDCD4	programmed cell death 4
PI	propidium iodide
PI3K	phosphatidylinositol 3-kinase
PIK3CA	phosphatidylinositol-4,5-bisphosphate 3-kinase, catalytic sub-unit alpha
PIK3C3	phosphatidylinositol 3-kinase, catalytic sub-unit type 3
PIP2	phosphatidylinositol-4,5-biphosphate
PIP3	phosphatidylinositol-3,4,5-triphosphate
pmol	picomole
POX	proline oxidase
PTEN	phosphatase and tensin homologue
QC	quality control
qPCR	quantitative real-time PCR
RIN	RNA integrity number
RIPA	radio-immunoprecipitation assay
RISC	RNA-induced silencing complex
RMA	robust multichip averaging
RNA	ribonucleic acid
RNA pol II	RNA polymerase II
RNAi	RNA interference
RNase(s)	ribonuclease(s)
ROC	receiver operating characteristic
rpm	revolutions per minute
RRAS2	related RAS viral oncogene homologue 2

rRNA	ribosomal RNA
RT	reverse transcription
RT-qPCR	reverse transcription-quantitative real-time polymerase chain reaction
S6K2	S6 kinase 2
SD	standard deviation
sdH_2O	sterile deionised water
SDS	sodium dodecyl sulphate
SEM	standard error of mean
SEPT9	septin 9
SGK	serum and glucocorticoid-inducible kinase
SHC	SH2-containing
shRNA(s)	short hairpin RNA(s)
siRNA(s)	small interfering RNA(s)
SIRT1	silent information regulator 1
SKP2	S-phase kinase-associated protein 2
SMAD	mothers against decapentaplegic homologue
SOCS3	suppressor of cytokine signalling 3
SRSF2	serine/arginine-rich splicing factor 2
SSC	saline-sodium citrate
STAT	signal transducer and activator of transcription
STK4	serine/threonine kinase 4
TBE	tris-borate-ethylenediaminetetraacetic acid
TCF	T-cell factor
TEMED	tetramethylethylenediamine
TGFBR	TGF-β receptor

TGF-β	transforming growth factor beta
TNM	tumour-node-metastasis
TRBP	transactivation response RNA-binding protein
tRNA	transfer RNA
TSP1	thrombospondin 1
U	unit (enzyme)
UICC	International Union for Cancer Control
UMMC	University of Malaya Medical Centre
uPA	urokinase-type plasminogen activator
USF1	upstream stimulating factor 1
UV	ultraviolet
V	volt
VEGF	vascular endothelial growth factor
WIP1	wild-type p53-induced phosphatase 1
ZEB	zinc finger E-box binding homeobox
α	alpha
β	beta
µg	microgram
µl	microlitre
µm	micrometre
µM	micromolar
°C	degree Celsius
%	percent
†	symbol for mutation
=	equal to
~	approximately

$<$	less than
$>$	greater than
$\leq$	less than or equal to
$\geq$	greater than or equal to

LIST OF APPENDICES

PAGE

CHAPTER 1

INTRODUCTION

Colorectal cancer (CRC) is the carcinoma of the colon and rectum in the gastrointestinal system. CRC is the third most common cancer in men and the second in women worldwide, with an estimation of 1.36 million new cases, 0.69 million deaths and 3.54 million people living with CRC (Ferlay et al., 2013). The carcinogenesis of CRC is heterogeneous, multi-factorial and may take several decades. CRC is a curable disease if the growth is detected at an early, localised stage. However, most cases are diagnosed at late stages due to low population compliance to CRC screening. The concerns of invasive nature, radiation exposure and false-positivity of currently available screening tests have highlighted the necessity of exploring other non-invasive biomarkers to complement and improve CRC screening in the average-risk population. Blood-based tests are easy to perform as only standard blood collection procedure is required. The deregulation of various messenger RNAs (mRNAs), tumour associated antigens, cytokines, anti-apoptotic proteins and cell proliferation proteins has been detected in the blood circulation of CRC patients (Creeden, Junker, Vogel-Ziebolz, & Rex, 2011). In recent years, the emergence of microRNAs (miRNAs) as endogenous regulators of gene expression has rendered remarkable contribution in the elucidation of cancer initiation, promotion and progression. miRNAs are short, non-coding RNA molecules of approximately 22 nucleotides that bind to the 3'-untranslated region (3'-UTR) of target mRNAs (Bartel, 2004). In the event of full complementarity, the target mRNA will be subjected to mRNA cleavage. In contrast, partial complementarity will lead to translational repression and/or deadenylation whereby the mRNA will be localised to processing body (P-body) for storage or degradation (Bartel, 2009; Chan & Slack, 2006;

L. Wu, Fan, & Belasco, 2006). miRNAs appear to be cell type- and disease-specific, enabling them to serve as more superior biomarkers than mRNAs or proteins (Esquela-Kerscher & Slack, 2006). miRNA expression patterns are being extensively studied in order to aid in the diagnosis and treatment of cancer. Nevertheless, most publications on miRNA deregulation in CRC are focused either on the tissue or blood component. The absolute hypothesis of whether the circulating blood miRNAs are reflective of those in the CRC tissues is yet to be answered. The ideal blood biomarker should be able to detect the early presence of a tumour before the growth could otherwise be easily detected.

Hence, the main objective of the present study was to characterise and correlate the tissue and blood miRNA expression patterns of primary CRC patients. The specific objectives are as follows:

(a) To assess the diagnostic utility of the significantly correlated miRNAs in the tissue and blood samples.
(b) To establish the functional roles of the identified miRNAs in the carcinogenesis of CRC.
(c) To identify the potential genes and pathways targeted by the identified miRNAs.
(d) To determine the feasibility of the identified miRNA:mRNA markers for discriminating early and advanced CRC.

On the whole, the present study revolved around a marker discovery phase via miRNA microarray and a marker validation phase via reverse transcription-quantitative real-time polymerase chain reaction (RT-qPCR). Since a single miRNA is capable of regulating multiple targets and regulatory pathways in a particular disease, the identification of concurrently expressed miRNAs was of utmost importance in this research. The potential exploitation of miRNAs in therapeutic intervention has driven

the investigation of their biological functions in the carcinogenesis of CRC via *in vitro* miRNA mimics and inhibitors studies. SW480 and SW620 cell lines derived from the spontaneous progression of a human CRC in a single patient were used for the analysis of gene expression changes during the transition from early to advanced carcinoma. A focused approach on the effects of the deregulated miRNAs in cell viability, apoptosis, migration and invasion were examined. Eventually, the causal associations between the differentially expressed miRNAs and the predicted target genes were established. The findings from this study would contribute to the scientific knowledge pertaining to the feasibility of the identified miRNAs as diagnostic, prognostic and therapeutic biomarkers in CRC.

CHAPTER 2

LITERATURE REVIEW

2.1 Colorectal cancer (CRC)

2.1.1 Overview of large intestine

Large intestine is part of the gastrointestinal system. The length of the large intestine is about five feet long (American Cancer Society, 2011). It functions to absorb water and minerals from food and excrete the indigestible waste from the body as faeces. The large intestine is made up of several sections: caecum, ascending colon, transverse colon, descending colon, sigmoid colon and rectum (Tortora & Derrickson, 2007).

2.1.2 Prevalence of CRC

CRC is the carcinoma of the colon and rectum in the gastrointestinal system. CRC is the third most common cancer in men and the second in women worldwide (Bray, Jemal, Grey, Ferlay, & Forman, 2012; Ferlay et al., 2013). Data from the latest GLOBOCAN 2012 project conducted by the International Agency for Research on Cancer (IARC) have revealed an estimation of 1.36 million new CRC cases, 0.69 million deaths and 3.54 million people living with CRC in 2012 worldwide (Ferlay et al., 2013). Almost 55% of the cases occur in the developed regions. The CRC burden is predicted to rise at 1% per year by 2030, assuming the population growth and ageing occur based on the United Nations's world population prospects (Bray et al., 2012; United Nations Population Division, 2013). The incidence rate of CRC has been increasing in Asian countries as well (Wan Puteh et al., 2013). In Malaysia, it ranks the second after lung

cancer and breast cancer in men and women, respectively (Zainal Ariffin & Nor Saleha, 2011). Among Malaysians, the highest incidence of CRC has been observed in the Chinese population, followed by the Malay and Indian populations (Sung, Lau, Goh, & Leung, 2005; Zainal Ariffin & Nor Saleha, 2011). Moreover, the incidence is disproportionately higher in males as compared to females. The five-year survival rate exceeds 90% when CRC is detected at an early, localised stage (McFarland et al., 2008). However, most cases are diagnosed at late stages due to insufficient public awareness and inconvenient nature of certain screening tests.

2.1.3 Aetiology of CRC

The pathogenesis of CRC is heterogeneous, multi-factorial and may take several decades. CRC may develop sporadically (85%) with no well-defined aetiology, as part of hereditary cancer syndrome (10%) such as familial adenomatous polyposis (FAP) and hereditary non-polyposis colorectal cancer (HNPCC), or on a background of inflammatory bowel disease (5%) (Half, Bercovich, & Rozen, 2009; Lynch & Lynch, 2005; Robinson et al., 2007; Søreide et al., 2009). Nevertheless, the development of sporadic CRC has been suggested to arise from randomly acquired somatic mutations in several of the common genes found in hereditary CRC (Choong & Tsafnat, 2012).

The hallmarks of CRC include autonomous growth signals, insensitivity to anti-growth signals, evasion of apoptosis, unlimited replicative potential, sustained angiogenesis and the ability for tumour invasion and metastasis (Hanahan & Weinberg, 2011). Genetic and epigenetic alterations that cause the disruption of homeostatic regulation between cell proliferation and cell death transform the normal colonic epithelium to an adenomatous intermediate and eventually into invasive adenocarcinoma.

2.1.4 Genomic instability pathways in CRC

The loss of genomic stability greatly influences the development of CRC by facilitating the acquisition of various tumour-associated mutations (Markowitz & Bertagnolli, 2009). The three major genomic instabilities in CRC are chromosomal instability (CIN), microsatellite instability (MSI) and epigenetic silencing through cytosine-phosphate-guanine (CpG) island methylator phenotype (CIMP) (Søreide et al., 2009).

The CIN pathway is recognised by cytogenetic abnormalities, aneuploidy and allelic losses at chromosomal arms (Harrison & Benziger, 2011; Lanza et al., 2007). FAP is an autosomal dominant disorder associated with CIN and caused by germline mutations of the adenomatous polyposis coli (*APC*) gene (Konishi et al., 1996). FAP is defined by the presence of numerous polyps in the colon (Harrison & Benziger, 2011).

The MSI pathway is characterised by mutations in nucleotide repetitive sequences, especially due to defects in the DNA mismatch repair system (Harrison & Benziger, 2011; Lanza et al., 2007). HNPCC is an autosomal dominant condition associated with MSI and caused by germline mutations of the DNA mismatch repair (*MMR*) genes (*MLH1*, *MSH2*, *MSH6* and *PMS2*) (Earle et al., 2010; Konishi et al., 1996).

CIMP is a phenomenon of epigenetic silencing of genes through aberrant DNA methylation at certain cytosine residues of the cytosine- and guanine-rich regions known as the CpG islands (Markowitz & Bertagnolli, 2009). Although the molecular mechanism of the CIMP pathway has not been fully elucidated, several studies on DNA methylation have revealed that sporadic CRC exhibits concurrent methylation of at least three loci from a selected panel of CpG island-associated genes (S. Lee, Cho, Yoo, Kim, & Kang, 2008; McKenna & Roberts, 2009; Toyota et al., 1999). CIMP-positive tumours can be sub-divided into CIMP-high and CIMP-low, characterised by the quantitative differences in CpG island methylation (Teodoridis, Hardie, & Brown, 2008). These

tumours are associated with poorer prognosis in CRC (S. Lee et al., 2008; Toyota et al., 1999; Weisenberger et al., 2006). Based on a study by Shen et al. (2007), the CIMP-high tumours are usually presented with MSI status and B-Raf proto-oncogene (*BRAF*) mutations while the CIMP-low tumours are less microsatellite unstable but possess higher percentages of Kirsten rat sarcoma viral oncogene homologue (*KRAS*) mutations. In contrast, CIMP-negative tumours have a high rate of *TP53* mutations and low rates of *BRAF* and *KRAS* mutations (Shen et al., 2007).

2.1.5 Risk factors of CRC

There are many risk factors underlying the pathogenesis of CRC. The presence of colorectal polyps, which may be hyperplastic or adenomatous in nature, places one at increased risk of acquiring CRC (Morimoto et al., 2002). Colorectal polyps are benign growths protruding from the colon and rectal mucosa. The polyps may undergo genetic changes to become malignant. An individual with a family history of CRC or colorectal adenoma may have an increased risk of developing CRC (Levin et al., 2008). In addition, a background of an inflammatory bowel disease such as Crohn's disease or ulcerative colitis, may also lead to CRC (Monteleone, Pallone, & Stolfi, 2012). Other risk factors of CRC are environmental exposure to carcinogens and unhealthy lifestyle such as high intakes of red meats and animal fats, low intakes of vegetables, fruits and fibres, smoking, alcohol consumption, obesity and physical inactivity (American Cancer Society, 2011; Bruce, Wolever, & Giacca, 2000). Moreover, the risk of CRC increases with age, whereby most cases are diagnosed in the older generation above 50 years old (Levin et al., 2008).

2.1.6 Symptoms of CRC

Patients with pre-cancerous polyps or early-stage CRC seldom reveal any symptom until the growth obstructs the large intestine (Sung et al., 2005). In addition, several gastrointestinal tract diseases such as irritable bowel syndrome, inflammatory bowel disease, diverticulosis, haemorrhoid and peptic ulcer disease may mimic the symptoms of CRC. The main symptoms of CRC are rectal bleeding and blood in the stool (Levin et al., 2008). Other symptoms may include a change in the shape of the stool, prolonged constipation or diarrhoea, weight loss, abdominal cramp and frequent urge for bowel movements (American Cancer Society, 2011). Since the growth can be present for a long duration before any symptom develops, CRC screening is vital for early detection of CRC.

2.1.7 Screening, diagnostic and prognostic tests for CRC

CRC is a curable disease if the growth is detected at an early, localised stage. Screening can reduce CRC morbidity and mortality by prevention through polypectomy or early diagnosis for immediate surgical resection. Nonetheless, the awareness of CRC screening in Malaysia is low and community-based screening programmes are limited (Wan Puteh et al., 2013). CRC screening is strongly recommended for high-risk population at young ages and average-risk population aged 50 years old and above (Levin et al., 2008). The advantages and disadvantages of the common screening, diagnostic and prognostic tests for CRC are discussed in the following sub-sections.

2.1.7.1 Colonoscopy

Colonoscopy is an invasive endoscopic procedure that allows the visualisation of the entire colon and rectum. Bowel preparation with laxative agents is necessary. Sedation is often administered to reduce abdominal discomfort. Colonoscopy is the most sensitive and ultimate tool in the screening, diagnosis and post-operative surveillance of CRC (Young & Womeldorph, 2013). Patients with positive findings from other screening tests are commonly referred for a colonoscopy. Polypectomy and biopsy can be performed during the procedure. Colonoscopy is greatly recommended for high-risk individuals and those aged 50 and above with the screening interval of five and ten years, respectively (Levin et al., 2008). Numerous studies have shown that colonoscopy screening has significant contribution in the detection of neoplastic lesions and reduction of CRC incidence and mortality (Brenner et al., 2013; Kahi, Imperiale, Juliar, & Rex, 2009; Young & Womeldorph, 2013). However, the requirement of bowel preparation and sedation, and possible bowel complications such as perforation and bleeding, have hindered its widespread application as a screening tool (Castro, Azrak, Seeff, & Royalty, 2013).

2.1.7.2 Flexible sigmoidoscopy

Flexible sigmoidoscopy is similar to colonoscopy, but the examination is limited to the inner lining of the rectum and sigmoid colon up to 60 cm (Austin et al., 2009). Bowel preparation is needed prior to the procedure. No sedation is required and the procedure typically lasts about few minutes with minimal discomfort. Bowel perforation and infection following flexible sigmoidoscopy are rare (Schoen et al., 2012). However, colonoscopy is necessary if large polyps or growths are discovered. Flexible sigmoidoscopy is recommended to be done every five years (Levin et al., 2008).

2.1.7.3 Computed tomographic colonography (CTC)

CTC is an imaging technique characterised by the generation of cross-sectional two- or three-dimensional x-ray images of the colon and rectum (Fenlon et al., 1999). It is also known as virtual colonoscopy (Cotton et al., 2004). A flexible tube is inserted into the rectum; air is blown to insufflate the colon and the patient is positioned through a helical computed tomography scanner (Fenlon et al., 1999). Bowel preparation is needed but does not require sedation. CTC can be performed fairly quickly with minimal discomfort or risk. This procedure is less invasive as it involves low-dose radiation (Halligan et al., 2013). The feasibility of the CTC test in average-risk symptomatic patients has been investigated (Simons, Van Steenbergen, De Witte, & Janssen-Heijnen, 2013). The results revealed a detection sensitivity of 94.3% with a miss rate of only 3.8%. Colonoscopy is then conducted if abnormality is discovered. Moreover, two independent population studies by Gluecker et al. (2003) and Moawad (2010) have revealed higher preferences of CTC to colonoscopy in CRC screening. The suggested test time interval for CTC is every five years (Levin et al., 2008).

2.1.7.4 Double contrast barium enema (DCBE)

DCBE is a radiological examination of the colon (Halligan et al., 2013). Bowel preparation is needed prior to the procedure. Barium sulphate enema is injected into the colon via a rectal tube followed by insufflation with air (Gluecker et al., 2003). X-ray images of the colon are captured and analysed. However, small polyps may be missed and referral for a colonoscopy is needed if there is any positive finding. The screening interval for DCBE is every five years (Levin et al., 2008). This radiological imaging technique is less preferable today as CTC has been shown to possess higher precision

and lower radiation effects as compared to DCBE (Halligan et al., 2013; Neri et al., 2010)

2.1.7.5 Faecal-based tests

Faecal-based tests are non-invasive screening tests. The two common faecal-based tests are faecal occult blood test (FOBT) and stool DNA test.

Large polyps or growths may cause intermittent bleeding into the large intestine. Dark- or black-coloured stool is one of the symptoms of CRC. FOBT detects blood in the stool and is available as a test kit. The procedure involves placing a tiny stool sample on a special card and adding the provided chemicals to detect the presence of blood (Allison, Tekawa, Ransom, & Adrain, 1996). FOBT can be divided into guaiac-based FOBT (gFOBT) and immunochemical-based FOBT, known as faecal immunochemical test (FIT) (Levin et al., 2008). gFOBT is a low-cost test that involves several samplings of bowel movements. Although gFOBT does not require a bowel preparation, there is a pre-test dietary restriction on certain types of food and drugs such as red meats, citrus juices, vitamin C and non-steroidal anti-inflammatory drugs (American Cancer Society, 2011). Since gFOBT detects blood from any source, there is a higher rate of false-positivity (Bandi, Cokkinides, Smith, & Jemal, 2012). In contrast, FIT detects only human blood and thus, gives a better accuracy as compared to gFOBT (Flitcroft, Irwig, Carter, Salkeld, & Gillespie, 2012). The cost for FIT is slightly higher but it does not involve a pre-test dietary restriction. Moreover, FIT is more convenient as it requires fewer samplings of stool samples. gFOBT or FIT is recommended to be performed annually in conjunction with flexible sigmoidoscopy (Levin et al., 2008). Patients with positive FOBT results will then be referred for further examination via colonoscopy. Although FOBT is confined by low sensitivity and specificity against the detection of

small polyps and pre-malignant lesions, FOBT is considered a useful screening method due to its non-invasive property (Bandi et al., 2012; Quintero et al., 2012).

Stool DNA test is an emerging technology in CRC screening. It detects abnormal DNA shed from polyp or tumour cells in the stool using a panel of molecular markers (McFarland et al., 2008). *KRAS*, *BRAF*, *APC* and *TP53* are the common targets incorporated in the stool DNA test (Imperiale, Ransohoff, Itzkowitz, Turnbull, & Ross, 2004; Zou et al., 2009). The test enables the discovery of somatic mutations (U.S. Preventive Services Task Force, 2008). Several limitations of the stool DNA test are uncertainty of screening interval, high cost and inadequacy in the number of markers tested (McFarland et al., 2008). Numerous studies are being carried out to improve the panel of molecular markers. A recent investigation by Ahlquist et al. (2012) on next-generation stool DNA test has revealed promising preliminary results that warrant further optimisation and validation in a larger population. The method integrates the use of a preservative buffer during stool collection, direct measurement of target genes from the stool supernatant, a panel of molecular markers that are more specific in the detection of CRC and a highly sensitive assay known as quantitative allele-specific real-time target and signal amplification. Patients with positive findings will then be referred for further examination via colonoscopy.

2.1.7.6 Blood-based tests

Blood-based tests for CRC screening and surveillance provide substantial clinical benefits. Blood-based tests are easy to perform and non-invasive as only standard blood collection procedure is required. Moreover, the tests can be repeated regularly with minimal risk to the patients. The potential classes of blood biomarkers are tumour associated antigens, cytokines, anti-apoptotic proteins, cell proliferation proteins, cell

free DNAs, hypermethylated genes, mRNAs and miRNAs (Creeden et al., 2011). Among these, the two clinically available blood-based screening tests are ColonSentry mRNA expression panel test and septin 9 (*SEPT9*) methylated DNA test (Heichman, 2014).

ColonSentry test was developed by GeneNews Limited in 2008 and it is the world's first blood-based molecular test that can be used to evaluate an individual's risk of developing CRC (Novak, Liew, & Liew, 2012). mRNA from whole blood is subjected to RT-qPCR for the measurement of a seven-gene biomarker panel (*ANXA3*, *CLEC4D*, *IL2RB*, *LMNB1*, *PRRG4*, *TNFAIP6* and *VNN1*) (Marshall et al., 2010). Based on the gene profiles, a current relative risk score that compares the probability of developing CRC over the prevalence of the disease is calculated (Novak et al., 2012). A validation study in the Malaysian population has revealed a test sensitivity of 61%, specificity of 77% and accuracy of 70% (Yip et al., 2010). The ColonSentry test is currently available in Canada, China, Malaysia and the USA.

SEPT9 methylated DNA test was developed by Epigenomics AG in 2008 and subsequently licensed to several companies such as Quest Diagnostics, ARUP Laboratories, Warnex Medical Laboratories and QIAGEN (deVos et al., 2009; Heichman, 2014). The sample needed is blood plasma (Lofton-Day et al., 2008). Methylation-based real-time PCR principle is used in the measurement of the *SEPT9* methylated DNA expression (deVos et al., 2009). The test has been shown to exhibit a sensitivity of 90% and specificity of 88% in defining CRC (Warren et al., 2011).

On the other hand, carcinoembryonic antigen (CEA) test is a common blood-based test used in post-operative surveillance and monitoring therapy in patients with advanced CRC (H. Kobayashi et al., 2007; Tan et al., 2009). CEA is an oncofoetal antigen discovered in 1965 (Gold & Freedman, 1965). It is produced mainly by normal foetal

gut, liver and pancreas tissues, and by epithelial tumours of the gastrointestinal system (Gold & Freedman, 1965). CEA is not a highly sensitive and specific marker as the level can rise in smokers and patients with inflammatory bowel disease, liver disease, pancreatitis or epithelial tumours at other areas (Tan et al., 2009). The test is often dependent on the cut-off value for a positive result and some CRC patients do not show elevated serum CEA levels during recurrence (C. Liu et al., 2010; Su, Shi, & Wan, 2012). Carbohydrate antigen 19-9 (CA19-9) test works the same way as CEA test (Sisik, Kaya, Bas, Basak, & Alimoglu, 2013). It may serve as an additional marker for CRC patients with normal CEA levels (P. C. Lin et al., 2012).

2.1.8 Staging of CRC

The most commonly used staging system in cancer is tumour-node-metastasis (TNM) system (Edge & Compton, 2010). The system is based on the size and degree of primary tumour invasion (T), regional lymph node involvement (N) and distant metastasis (M). It is maintained collaboratively by the International Union for Cancer Control (UICC) and the American Joint Committee on Cancer (AJCC) (Edge & Compton, 2010). The TNM system is revised periodically in every six to eight years. The latest revision was released on January 1, 2010 and is known as the 7th edition of the AJCC Cancer Staging Manual (Obrocea, Sajin, Marinescu, & Stoica, 2011). Nevertheless, the older versions such as the 5th and 6th editions of the AJCC Cancer Staging Manual are still being used among clinicians (Hari et al., 2013). The TNM system encompasses both clinical (pre-operative) and pathological (post-operative) classifications (Compton et al., 2012; Labianca, Nordlinger, Beretta, Brouquet, & Cervantes, 2010). The clinical classification is designated as cTNM and it forms the basis of treatment regimen selection. The pathological classification is designated as pTNM and it is crucial for prognostic

evaluation. Other less commonly used staging systems are Dukes' classification and modified Astler-Coller (MAC) classification (Dukes & Bussey, 1958). The Dukes' classification is a pathological staging that relies only on the degree of primary tumour invasion while the MAC classification is a modification of the Dukes' classification. The definitions of the terms used in the latest TNM system are listed in Table 2.1. The TNM system, together with the equivalent Dukes' and MAC classifications are summarised in Table 2.2.

Table 2.1: Definitions of TNM system.

TNM system	Description
Primary tumour (T)	
TX	Assessment of primary tumour cannot be performed
T0	No evidence of primary tumour
Tis	Carcinoma *in situ*: tumour confinement within the glandular basement membrane or mucosal lamina propria
T1	Tumour invasion into sub-mucosa
T2	Tumour invasion into muscularis propria
T3	Tumour invasion through the muscularis propria into pericolorectal tissues
T4a	Tumour penetration to the surface of the visceral peritoneum
T4b	Tumour invasion and adherence to other organs or structures
Regional lymph nodes (N)	
NX	Assessment of regional nodes cannot be performed
N0	No regional lymph node metastasis
N1	Metastasis in one to three regional lymph nodes
N1a	Metastasis in one regional lymph node
N1b	Metastasis in two to three regional lymph nodes
N1c	Tumour deposit(s) in the sub-serosa, mesentery, or non-peritonealised pericolic or perirectal tissues without regional nodal metastasis
N2	Metastasis in four or more regional lymph nodes
N2a	Metastasis in four to six regional lymph nodes
N2b	Metastasis in seven or more regional lymph nodes
Distant metastasis (M)	
M0	No distant metastasis
M1	Distant metastasis
M1a	Metastasis confined to one organ or site
M1b	Metastases in more than one organ or site or the peritoneum

(Source: Compton et al., 2012)

Table 2.2: TNM system with equivalent Dukes' and MAC classifications for CRC.

Stage	**TNM**	**Dukes**	**MAC**
0	Tis, N0, M0	-	-
I	T1, N0, M0	A	A
	T2, N0, M0	A	B1
IIA	T3, N0, M0	B	B2
IIB	T4a, N0, M0	B	B2
IIC	T4b, N0, M0	B	B3
IIIA	T1-T2, N1/N1c, M0	C	C1
	T1, N2a, M0	C	C1
IIIB	T3-T4a, N1/N1c, M0	C	C2
	T2-T3, N2a, M0	C	C1/C2
	T1-T2, N2b, M0	C	C1
IIIC	T4a, N2a, M0	C	C2
	T3-T4a, N2b, M0	C	C2
	T4b, N1-N2, M0	C	C3
IVA	Any T, Any N, M1a	-	-
IVB	Any T, Any N, M1b	-	-

(Source: Compton et al., 2012)

2.1.9 Treatment of CRC

Surgical resection is the ultimate treatment for CRC. Based on the data published by Labianca et al. (2010), the five-year survival rate after surgical resection alone was 85-95% for stage I cancer, 60-80% for stage II cancer and 30-60% for stage III cancer. Adjuvant therapies, which include chemotherapy (anti-cancer drug), radiotherapy (radiation) and chemoradiotherapy (anti-cancer drug and radiation), are standard treatments for patients with advanced CRC (Carrato, 2008). Fluoropyrimidine drugs are common chemotherapeutic agents used in the treatment of CRC (Wolpin, Meyerhardt, Mamon, & Mayer, 2007). A widely used example is 5-fluorouracil (5-FU). It is often administered in combination with other cytotoxic drugs like oxaliplatin, irinotecan or leucovorin (André et al., 2009; Thorn et al., 2011).

Post-surgical adjuvant therapies are normally administered to stage IIB, IIC and III colon cancer patients to improve their survival rates (Labianca et al., 2010). Besides adjuvant therapies, neoadjuvant chemoradiotherapy is highly recommended for stage IIB, IIC and III rectal cancer patients to increase the chances of curative resection (Carrato, 2008). Although stage I and IIA cancers carry a better prognosis, some of the patients still develop recurrence. The routine use of adjuvant therapies in early-stage patients is controversial, as not all of them are likely to benefit, which may lead to the adverse effects of under-treatments or over-treatments (Schepeler et al., 2008; Wolpin et al., 2007).

2.1.10 Prognosis of CRC

Prognosis of CRC plays an important role in the prediction of distant metastasis and recurrence, thus allowing adjuvant therapy or surgery where appropriate. Prevention of recurrence is crucial as CRC relapse is often life-threatening. Based on the TNM system, the extent of tumour penetration, the involvement of regional lymph nodes and the presence of metastasis are crucial prognostic parameters (Compton et al., 2012). Adenocarcinomas can be graded based on the percentages of gland formation, grade 1 (G1): well differentiated (> 95%), grade 2 (G2): moderately differentiated (50-95%), grade 3 (G3): poorly differentiated (5-50%) and grade 4 (G4): undifferentiated (< 5%) (Hamilton & Aaltonen, 2000). The tumour grading system is considered as a stage-independent prognostic factor in CRC, in which G1 and G2 tumours give better prognosis than G3 and G4 tumours. Other prognostic factors that are independent of the TNM system include pre-operative CEA level, tumour deposits, circumferential resection margin, perineural invasion, MSI status, tumour regression grade following neoadjuvant therapy, *KRAS* mutation analysis and 18q loss of heterozygosity status (Compton et al., 2012). All in all, compliance to surgical follow-up is the utmost goal in CRC surveillance.

2.2 microRNA (miRNA)

2.2.1 miRNA discovery

miRNAs are short (~22 nucleotides), endogenous, non-coding RNA molecules that act as regulators of gene expression (Bartel, 2004; He & Hannon, 2004). The pioneer discovery of miRNAs was initiated by Lee and his colleagues in 1993 when they found lin-4, a small RNA molecule that is capable of controlling the larval development of

Caenorhabditis elegans via post-transcriptional regulation of *lin-14* gene at the 3'-UTR (R. C. Lee, Feinbaum, & Ambros, 1993). Seven years later, the discovery of the second miRNA, let-7, that shares a similar role as a regulator of developmental transition, has incurred more curiosity in miRNA research (Reinhart et al., 2000). The let-7 has been determined to bind to the 3'-UTR of *lin-41* and *hbl-1* mRNAs (He & Hannon, 2004). To date, there are more than 2000 entries of human miRNAs in the latest miRBase release (version 21; June 2014) (http://www.mirbase.org/), constituting around 1% of total genes that can regulate up to one third of the human genome (Babashah & Soleimani, 2011; Koturbash, Zemp, Pogribny, & Kovalchuk, 2011; Kozomara & Griffiths-Jones, 2014).

miRBase is the primary online repository for all miRNA sequences and annotation. The numbering of miRNA genes is based on chronological discovery (Kozomara & Griffiths-Jones, 2014). The miRBase registry for mature miRNA sequences begins with the accession MIMAT. The naming convention for mature miRNA is "miR" while the precursor stem-loop or miRNA gene is designated as "*mir*" (Ambros et al., 2003). For instance, miR-338 represents the mature miRNA sequence while *mir-338* represents the precursor stem-loop sequence. Distinct precursor sequences that produce identical mature sequences are named as *mir-338-1* and *mir-338-2* (Lagos-Quintana, Rauhut, Lendeckel, & Tuschl, 2001). On the other hand, lettered suffixes are used to differentiate closely related mature sequences, like miR-23a, miR-23b and miR-23c (Ambros et al., 2003). miR/miR* nomenclature has been widely used to determine the predominantly expressed mature miRNA arm from a stem-loop precursor (Griffiths-Jones, Grocock, van Dongen, Bateman, & Enright, 2006). For example, miR-150 is the predominant sequence while miR-150* is from the opposite arm of the precursor. However, the use of the miR/miR* nomenclature has been ceased in the latest release of miRBase version 21 (Kozomara & Griffiths-Jones, 2014). It is replaced by the inclusion

of a -5p or -3p suffix to specify the arm origin of the mature miRNA sequence. For instance, miR-150-5p is derived from the 5' end of the stem-loop precursor while miR-150-3p is derived from the 3' end. Nonetheless, the names for miRNAs (e.g. lin-4 and let-7) that are discovered prior to the invention of the miRBase naming convention are being retained for historical reasons (Griffiths-Jones et al., 2006).

2.2.2 miRNA biogenesis

miRNA genes are located either within the intragenic (protein-coding) or intergenic (non-protein-coding) regions of the genome (V. N. Kim, Han, & Siomi, 2009). In human, most of the miRNA genes are localised within the intragenic regions (70%) (Garzon, Calin, & Croce, 2009). There are two types of processing pathways in miRNA biogenesis, namely, canonical and mirtron pathways (Sotillo & Thomas-Tikhonenko, 2011) (Figure 2.1).

Canonical maturation involves miRNA genes that are found in either the intronic or exonic regions of the protein-coding genes (V. N. Kim et al., 2009). The miRNA gene is transcribed by RNA polymerase II (RNA pol II) into a long primary transcript (pri-miRNA) that contains a 7-methylguanosine cap and a poly-adenosine tail (Weimer, 2007). The pri-miRNA is cleaved by ribonuclease (RNase) III Drosha-DiGeorge syndrome critical region gene 8 (DGCR8) microprocessor complex to generate a ~70-nucleotide-long precursor stem-loop structure (pre-miRNA) (Garzon et al., 2009). The pre-miRNA is then exported from the nucleus to the cytoplasm by Exportin 5-Ran-GTP complex for a second cleavage by the cytoplasmic RNA-induced silencing complex (RISC) to yield a double-stranded miRNA:miRNA* duplex (Winter, Jung, Keller, Gregory, & Diederichs, 2009). The RISC is made up of RNase III Dicer, transactivation response RNA-binding protein (TRBP) and protein kinase RNA activator (PACT)

(Redfern et al., 2013). The miRNA strand with weaker thermodynamic stability at the 5' end will complex with Argonaute (Ago) proteins in the RISC to form a miRNA-RISC (miRISC) complex that guides the interaction with the target mRNA (Weimer, 2007). On the contrary, the non-functional miRNA* passenger strand will be degraded (Khvorova, Reynolds, & Jayasena, 2003; X. Liu, Fortin, & Mourelatos, 2008). In mirtron pathway, miRNA genes are transcribed from small intronic regions of the non-protein-coding genes (Garzon et al., 2009). They share similar processing steps with the canonical pathway except that the Drosha-mediated cleavage is replaced by splicing in the generation of pre-miRNA (Sotillo & Thomas-Tikhonenko, 2011).

2.2.3 miRNA mechanism of action

Once the mature miRNA is incorporated into the RISC complex, the miRISC complex guides the interaction with the target mRNA based on their sequence complementarity (Figure 2.1). The common pairing region is between the miRNA seed sequence (nucleotides 2-8 from the 5' end of miRNA) and the 3'-UTR of mRNA (Filipowicz, 2005). In the event of full complementarity, the miRISC complex is directed to cleave and degrade the target mRNA (Bartel, 2004). This mechanism is also known as post-transcriptional silencing or RNA interference (RNAi). In the event of partial complementarity, the mechanism of action is achieved through translational repression at the pre-initiation and/or post-initiation stages of protein synthesis (Garzon et al., 2009). Translational repression is only reflected at the protein level as the mRNA level is unaffected. Perfect complementarity is commonly observed in plants while partial complementarity is usually detected in animals (Bartel, 2004). Nevertheless, partial complementarity has also resulted in both mRNA degradation and translational inhibition, as in the case of lin-4 and let-7 in *C. elegans* (Bagga et al., 2005). This

mechanism is accomplished through mRNA destabilisation or deadenylation in which deadenylases and decapping enzymes are recruited to the target region (Bagga et al., 2005; Bartel, 2009;). The target mRNA is then localised to P-body for degradation or storage (Chan & Slack, 2006; L. Wu et al., 2006). Nonetheless, in response to certain stress stimuli, the translationally repressed mRNA in the P-body can re-enter the translational machinery (Bhattacharyya, Habermacher, Martine, Closs, & Filipowicz, 2006). On the other hand, several reports have indicated that miRNAs may positively induce gene transcription (L. C. Li et al., 2006; Place, Li, Pookot, Noonan, & Dahiya, 2008). Although the exact mechanism of RNA activation is yet to be determined, the binding of a miRNA to the 5' non-coding regulatory region in the gene promoter has been suggested to result in a sequence-specific induction process that redirects the sequence into the nucleus for gene activation (L. C. Li et al., 2006).

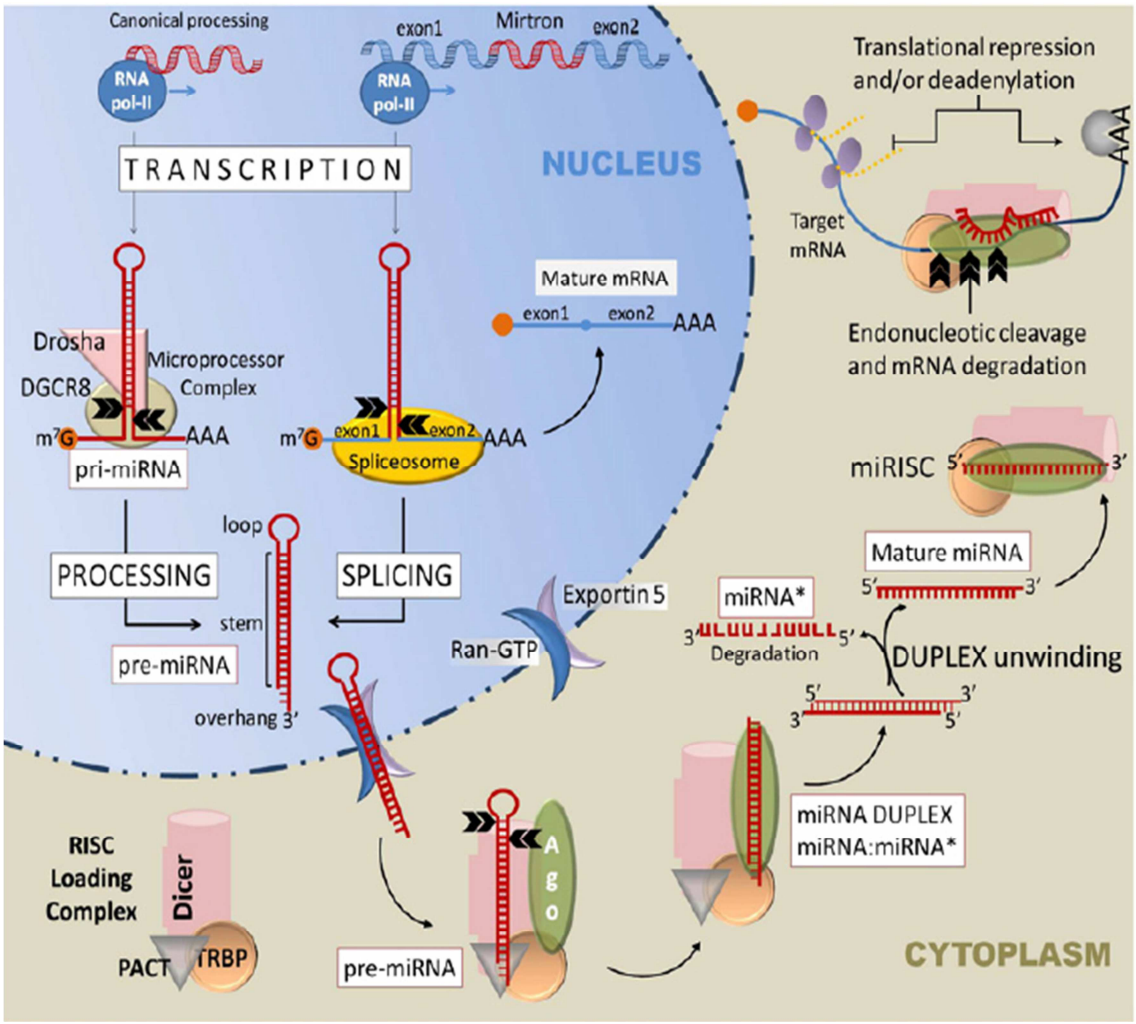

Figure 2.1: miRNA biogenesis and mechanism of action. The two processing pathways in miRNA biogenesis are canonical and mirtron pathways. Once the mature miRNA is loaded onto the RISC complex and bound to the 3'-UTR of the target mRNA, the mechanism of action involved is either mRNA degradation or translational repression. (Source: Sotillo & Thomas-Tikhonenko, 2011)

2.2.4 miRNA target prediction and validation

2.2.4.1 Computational prediction

Computational prediction of miRNA targets in plants is straightforward as most plant miRNAs show perfect complementarity with their target genes (Sun et al., 2013). Simple pattern matching or National Centre for Biotechnology Information-Basic Local Alignment Search Tool (NCBI-BLAST) search is usually sufficient (Rehmsmeier, Steffen, Hochsmann, & Giegerich, 2004). In contrast, prediction of miRNA targets in animals is more complicated as partial complementarity produces many secondary structures of miRNA:mRNA duplexes (Rehmsmeier et al., 2004). The binding of a mature miRNA to its target is largely dependent on the free energy of binding between the miRNA seed region and the 3'-UTR of mRNA (Doench & Sharp, 2004). Some common miRNA target prediction programmes are DIANA-microT, miRanda, MirTarget2/miRDB, PicTar, RNA22, RNAhybrid and TargetScan/TargetScanS (Table 2.3). The common principles governing these target prediction programmes are base pairing pattern, thermodynamic stability of miRNA:mRNA hybrid, comparative sequence analysis, determination of multiple targets sites per target transcript and statistical evaluation (Min & Yoon, 2010; Sotillo & Thomas-Tikhonenko, 2011).

Table 2.3: Computational tools for miRNA target prediction.

Programme	**Recommended target species**	**Algorithm**	**Web address**	**Reference**
DIANA-microT	Any species	Thermodynamics	http://diana.cslab.ece.ntua.gr/microT/	Maragkakis et al. (2009)
miRanda	Flies, vertebrates	Seed complementarity	http://www.microrna.org/microrna/home.do	Enright et al. (2003)
MirTarget2/miRDB	Humans, mice, rats, dogs, chickens	Support vector machine classifier	http://mirdb.org/miRDB/	X. Wang (2008)
PicTar	Vertebrates, flies, worms	Thermodynamics	http://www.pictar.org/	Krek et al. (2005)
RNA22	Any species	Pattern recognition	http://cbcsrv.watson.ibm.com/rna22.html	Miranda et al. (2006)
RNAhybrid	Any species	Thermodynamics, statistical model	http://bibiserv.techfak.uni-bielefeld.de/rnahybrid/	Rehmsmeier, Steffen, Hochsmann, and Giegerich (2004)
TargetScan/TargetScanS	Vertebrates	Seed complementarity	http://www.targetscan.org/	Lewis, Burge, and Bartel (2005); Lewis, Shih, Jones-Rhoades, Bartel, and Burge (2003)

2.2.4.2 Experimental validation

Computationally predicted miRNA targets require experimental validation. It is necessary to determine whether a target is directly regulated by a particular miRNA in order to provide substantial evidence of their interaction in the biological context. Each technology has its own advantages and disadvantages. It is important to identify the appropriate experimental design that fits the objective of the study.

The determination of miRNA and target mRNA expression levels in a particular disease is a prerequisite step in miRNA studies. miRNA/mRNA microarray and next-generation sequencing are recent technological advancements in miRNA profiling. Microarray technology is based on nucleic acid hybridisation between the target miRNAs/mRNAs and their corresponding complementary probes (Callari et al., 2012). Next-generation sequencing is a high-throughput technology that allows parallel sequencing of millions of DNA and/or RNA fragments from the genome, transcriptome and epigenome of any species within a short duration (Burgos et al., 2013; Grada & Weinbrecht, 2013). On the other hand, quantitative real-time polymerase chain reaction (qPCR) is the preferred method in the validation and quantification of miRNA and mRNA expression levels (Min & Yoon, 2010). Besides qPCR, *in situ* hybridisation is applicable in determining the relative abundance and localisation of a particular miRNA/mRNA at the cellular level (Nielsen, 2012). Northern blot analysis is another experimental technique that provides information on the size and expression of the predicted mRNA targets (Berezikov, Cuppen, & Plasterk, 2006). However, northern blot assay has limited sensitivity and is rarely used today. For the determination of target protein expression levels, the common approaches include Western blot, enzyme-linked immunosorbent assay and immunocytochemistry (Min & Yoon, 2010).

In terms of miRNA:mRNA target validation, luciferase reporter assay is the preferred technique (Nicolas, 2011). The 3'-UTR of mRNA containing the miRNA seed pairing site is cloned into a luciferase reporter. miRNA mimic or inhibitor is co-transfected with the luciferase reporter into a cell line and the binding of the miRNA will either suppress or enhance the luciferase protein production (Takane et al., 2010). A luciferase assay is then used to measure the luminescence generated by the luciferase reporter. Simultaneously, the 3'-UTR of the mRNA with mutated miRNA seed pairing region is included as the experimental control. This is to confirm that the mediation of luciferase activity is based on the base pairing between the miRNA seed sequence and the predicted 3'-UTR pairing region, and is not due to secondary indirect effects (Sotillo & Thomas-Tikhonenko, 2011). Once the regulation of a particular miRNA:mRNA has been confirmed, it is possible to demonstrate this interaction in the biological context via various *in vitro* cell-based assays (e.g. cell proliferation, cell differentiation and cell death assays). In addition, *in vivo* effects of a specific miRNA can be investigated via the use of animal models. For instance, S. L. Lin, Chang, and Ying (2006) have shown that transgene-like animal models that are generated using intronic miRNAs are useful in the study of miRNA-associated target genes.

2.2.5 miRNAs as novel molecular biomarkers

Recent advances in microRNAome have made miRNAs a compelling novel class of molecular biomarker to complement and improve current screening, diagnostic, prognostic and therapeutic tools in various diseases. miRNAs are detectable in tissue, blood, faeces and other body fluids such as saliva, tears and urine (Link et al., 2010; Volinia et al., 2006; Weber et al., 2010; D. C. Yu, Li, Ding, & Ding, 2011). miRNAs are evolutionary conserved across species and expressed in a tissue-specific manner

(Esquela-Kerscher & Slack, 2006). They have been shown to participate in many biological processes such as cell proliferation, differentiation, apoptosis and metastasis (Koturbash et al., 2011). A single miRNA is predicted to have multiple mRNA targets (~200 transcripts) that work in concert in controlling a common pathway (Krek et al., 2005).

In cancer, miRNA genes are frequently located at fragile sites and genomic regions of deletion and amplification (Calin et al., 2004). The first report on miRNA down-regulation in cancer was published in 2002 when Calin and his colleagues discovered that the down-regulation of miR-15a and miR-16-1 in chronic lymphocytic leukaemia has contributed to the enhanced expression of oncogene B-cell lymphoma 2 *(BCL2)* (Calin et al., 2002). On the other hand, miR-155 was the first miRNA that was demonstrated to have an increased expression in cancer, with 10- to 30-fold higher copy number in the diffuse large B-cell lymphoma than the normal circulating B cells (Eis et al., 2005).

2.2.6 Therapeutic modulation of miRNAs in cancer pathophysiology

miRNA deregulation has been characterised in many human cancers. Thus, normalising the miRNA expression may pose a new dimension for therapeutic approach. The therapeutic modulation of miRNAs involves the inhibition and restoration of miRNA activity. The delivery of exogenous miRNA inhibition and restoration strategies can be achieved through transient or stable transfection, liposomal nanoparticles and viral transduction (Sotillo & Thomas-Tikhonenko, 2011). Efficiency in the delivery, dosage, sustainability in the *in vivo* condition and off-target effects are the main concerns of miRNA-based therapeutic intervention.

2.2.6.1 Inhibition of miRNA activity

A common modulator in miRNA inhibition is antisense oligonucleotides (ASOs). ASOs, also known as antagomirs, are short, single-stranded RNA or DNA molecules that can trigger the degradation of miRNAs or mRNAs by Watson-Crick base pairing mechanism and tailling at the adenosines or uridines bases (Broderick & Zamore, 2011). The common backbone modifications in ASOs are phosphorothioate, 2'-*O*-methyl, 2'-*O*-methoxyethyl, 2'-fluoro and locked nucleic acid (LNA) modifications (Broderick & Zamore, 2011; Seto, 2010) (Figure 2.2). The incorporation of several backbone modifications within a single construct such as 2'-*O*-methyl/LNA/phosphorothioate ASO has been shown to greatly increase the efficiency of miRNA inhibition in HeLa cervical cancer cells (Lennox & Behlke, 2010). A cholesterol-conjugated 2'-*O*-methyl ASO with phosphorothioate modification has been administered successfully to inhibit the liver-specific miR-122 in mice (Krützfeldt et al., 2005). Its use has also been shown to inhibit the autonomous cell proliferation caused by the over-expression of miR-221 and miR-222 in MDA-MB-231 breast and U87 glioblastoma cell lines (le Sage et al., 2007). Although an unconjugated 2'-*O*-methoxyethyl ASO with phosphorothioate backbone has also been tested, the use of an ASO with cholesterol conjugation has been determined to improve cell penetration and association with the transmembrane lipoproteins (C. Esau et al., 2006; Krützfeldt et al., 2005). In other instance, the administration of a miR-21-2'-*O*-methyl-modified ASO has been shown to inhibit tumour growth and angiogenesis in HCT116 CRC cells (Castanotto et al., 2007; Song & Rossi, 2014).

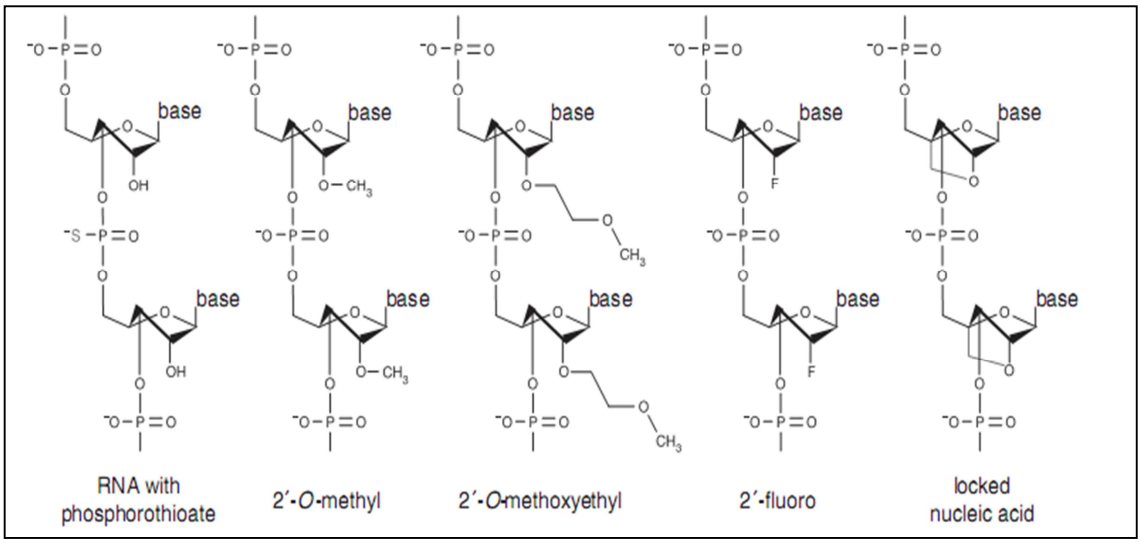

Figure 2.2: ASOs of different backbone modifications for miRNA inhibition. RNA with phosphorothioate contains a sulphur substitution of a non-bridging oxygen; 2'-*O*-methyl RNA contains a methyl group bound to the 2' oxygen of the ribose; 2'-*O*-methoxyethyl RNA contains a methoxy group bound to the 2' oxygen of the ribose; 2'-fluoro RNA contains a fluorine molecule bound to the 2' oxygen of the ribose; locked nucleic acid contains a 2',4' methylene bridge in the ribose that formed a bicyclic nucleotide. (Source: Broderick & Zamore, 2011)

An alternative method to the use of ASOs is miRNA 'sponges'. miRNA 'sponges' are miRNA inhibitory transgenes that possess multiple tandem binding sites to miRNAs of interest (Ebert & Sharp, 2010). The advantages of using miRNA 'sponges' are extensive binding affinity and sequence complementarity to a specific miRNA seed region and possibility of delivery via viral vectors (Ebert & Sharp, 2010). Open reading frames for reporter genes and selectable markers such as fluorescent tags and antibiotic resistant genes can be included to monitor the characteristics of 'sponge'-expressing cells (Sotillo & Thomas-Tikhonenko, 2011). Recently, Kluiver et al. (2012) have demonstrated the usage of a single miRNA 'sponge' that inhibits a whole seed family of

miRNAs from miR-17-92 cluster in murine WEHI231 B-cell lymphoma cell line. Even though the use of miRNA 'sponges' in CRC is still in the infancy stage, this approach has been applied by Valastyan et al. (2009) to confirm the tumour suppressor role of miR-31 in breast cancer. The miR-31 'sponge'-expressing breast cancer cells (MCF7-Ras-sp31) have been identified to be more invasive and metastatic when compared to the control MCF7-Ras cells.

2.2.6.2 Restoration of miRNA activity

The restoration of miRNA activity caused by the absence or reduced expression of miRNAs can be achieved through the introduction of miRNA mimics. miRNA mimics are chemically modified double-stranded RNAs with similarity to the endogenous Dicer products (Z. Liu, Sall, & Yang, 2008). They can be loaded directly onto RISC to restore the levels of altered miRNAs. For instance, the restoration of miR-195 expression in CRC via miR-195 mimic has been shown to promote apoptosis and suppress tumourigenicity by down-regulating the level of the anti-apoptotic *BCL2* gene (L. Liu, Chen, Xu, Li, & Du, 2010). Furthermore, the use of miR-101 mimic in CRC has been demonstrated to suppress the expression of the oncogenic cyclooxygenase 2 (*COX2*) mRNA (Strillacci et al., 2009). In prostate cancer, systemic delivery of miR-34a mimic has been shown to inhibit clonogenic expansion, tumour regeneration and metastasis by down-regulating the CD44 expression (C. Liu et al., 2011). Based on a recent report by S. Li et al. (2014), the re-introduction of miR-206 into CAOV3 and BG1 estrogen receptor alpha(α)-positive ovarian cancer cell lines has successfully inhibited cell proliferation and invasion.

Besides the use of miRNA mimics, small interfering RNA (siRNA) approach has also been utilised for gene knockdown in RNAi-based silencing. The characteristic of a siRNA duplex that binds to the target mRNA can attenuate the oncogenic expression of the gene. siRNAs have been used to inhibit the over-expression of c-*MYC* proto-oncogene and vascular endothelial growth factor (*VEGF*) gene that control cell proliferation, apoptosis and invasion in Volo CRC cells (Tai et al., 2012). Intraperitoneal delivery of a siRNA targeting the neural precursor cell expressed, developmentally down-regulated 1 (*NEDD1*) gene has been shown to improve the survival of a mouse scirrhous gastric cancer model (Fujita et al., 2013). However, miRNA mimics and siRNAs have short term duration of effects. Multiple doses may be necessary to achieve a desired regulation (John et al., 2007).

Another method to restore reduced miRNAs involves the use of short hairpin RNAs (shRNAs), delivered through DNA or viral vectors. shRNAs are tight hairpin RNAs generated from polymerase II or III promoters and processed by Dicer into mature miRNAs prior loading onto the RISC complex (C. C. Esau & Monia, 2007). Lentiviruses have been widely used as vectors for shRNA expression in cancer (Blosser et al., 2014; Wei, Lv, Chen, & Guan, 2014). This technique provides a more stable and persistent silencing as compared to the use of miRNA mimics and siRNAs. However, the possibility of insertional mutagenesis in the expression vectors and the potentiality of Exportin 5 pathway saturation may impede the therapeutic usage of shRNAs (Grimm et al., 2006).

Recently, the development of artificial miRNAs that combines the existing miRNA and siRNA technologies has emerged as a major breakthrough in RNAi-based therapeutics. An artificial miRNA is constructed using a pre-miRNA transcript as the scaffold or backbone, with the central stem sequence being substituted with a synthetic siRNA (Boudreau, Martins, & Davidson, 2009). The artificial miRNA is then processed like the

pre-miRNA transcript used for the scaffold. It is noteworthy that the administration of artificial miRNAs does not disrupt miRNA biogenesis and is well tolerated by endogenous miRNAs (McManus, Petersen, Haines, Chen, & Sharp, 2002). The use of artificial miRNAs for gene silencing has resolved the cytotoxicity issue caused by the saturation of shRNAs (Maczuga et al., 2012). A recombinant adenoviral construct that expresses p53 protein and harbours an artificial miRNA targeting the 3'-UTR of *p21* mRNA has been experimented in the p53-mutated DLD1 CRC cell line to induce p53-mediated apoptosis and enhance the chemosensitivity of the cancer cells to doxorubicin (Idogawa et al., 2009). Moreover, the use of a lentiviral-mediated artificial miRNA that targets the signal transducer and activator of transcription 5 (*STAT5*) gene has been shown to increase the chemosensitivity of SW1116 CRC cells to cisplastin and 5-FU (Hong et al., 2012). This technique has also been applied to target the up-regulated multidrug resistance ATP-binding cassette, sub-family C 1 and 2 (*ABCC1* and *ABCC2*) genes in a mouse hepatocellular carcinoma model (Borel et al., 2011).

2.2.6.3 miRNA therapeutics in clinical trial

The first miRNA-based therapeutic that enters into human clinical trial is an inhibitor of miR-122 (Miravirsen, a β-D-oxy-LNA-modified phosphorothioate ASO developed by Santaris Pharma A/S), and it is currently in phase 2a for the treatment of chronic Hepatitis C virus (HCV) infection (Gupta, Swaminathan, Martin-Garcia, & Navas-Martin, 2012; Janssen et al., 2013). Miravirsen can be administered via sub-cutaneous injection and its use has demonstrated dose-dependent reductions in HCV RNA levels with absence of viral resistance. Following that, the second miRNA-based therapeutic, mimic of miR-34a (MRX34, a double-stranded RNA oligonucleotide developed by Mirna Therapeutics), has reached phase 1 trial as a replacement therapy for primary

liver cancer and metastatic cancers with liver involvement (Bouchie, 2013). MRX34 can be administered systemically to liver via NOV340 liposome technology (SMARTICLES) developed by Marina Biotech (Bader, 2012). Data generated in animal studies have confirmed that the use of MRX34 is well-tolerated by normal tissues and effectively inhibits tumour growth (Bouchie, 2013).

2.2.7 miRNA involvement in the carcinogenesis of CRC

miRNAs can confer both oncogenic and tumour suppressive roles, depending upon their downstream targets (Esquela-Kerscher & Slack, 2006; Garzon et al., 2009). Based on the Fearon and Vogelstein model of colorectal carcinogenesis, the adenoma-carcinoma sequence begins with Wnt/beta(β)-catenin pathway activation, epidermal growth factor receptor (EGFR) signalling activation, transforming growth factor beta (TGF-β) response inactivation, loss of p53 function and finally extracellular matrix (ECM) breakdown and epithelial-to-mesenchymal transition (EMT) (Fearon & Vogelstein, 1990) (Figure 2.3). Up-regulation and down-regulation of various miRNAs have been reported in CRC. The up-regulation of mature miRNAs is possible during transcriptional activation or amplification of the miRNA genes while the down-regulation is due to deletions from chromosomal regions, epigenetic silencing and defects in the biogenesis (Rossi, Kopetz, Davuluri, Hamilton, & Calin, 2010). The involvement of miRNAs in the molecular events that drive the initiation, promotion and progression of CRC is being extensively investigated.

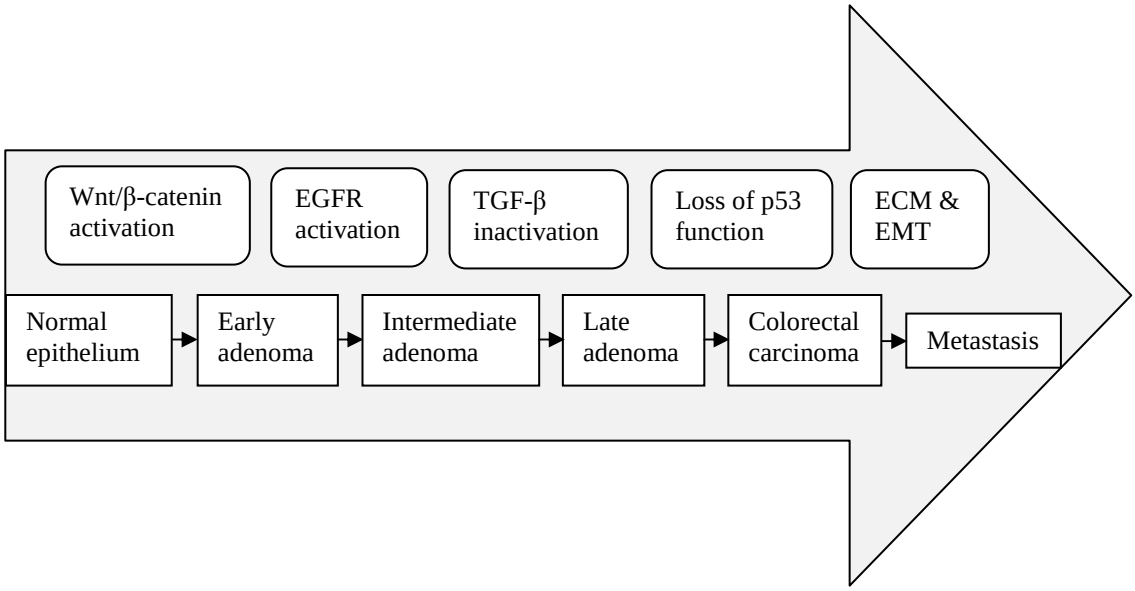

Figure 2.3: Molecular events in the carcinogenesis of CRC.

(Source: Fearon & Vogelstein, 1990; Slaby, Svoboda, Michalek, & Vyzula, 2009)

2.2.7.1 Wnt/beta(β)-catenin pathway

The Wnt/β-catenin pathway is essential for cell proliferation and tissue development via the regulation of β-catenin level (Willert & Jones, 2006). In the absence of Wnt ligand, cytoplasmic β-catenin is dissociated from the E-cadherin/β-catenin/α-catenin complex, phosphorylated by the activated glycogen synthase kinase 3β (GSK3β) and directed for ubiquitination and degradation (Giles, van Es, & Clevers, 2003). On the contrary, the binding of Wnt to the transmembrane receptor frizzled (FZD) and low density lipoprotein receptor-related protein 5 and 6 (LRP5 and LRP6) will result in the activation of phosphoprotein dishevelled (DVL) that inhibits the GSK3β and prevents β-catenin degradation (C. Liu et al., 2002). The free β-catenin in the nucleus will then bind to the T-cell factor/lymphocyte enhancer factor (TCF/LEF) to form a β-catenin/TCF/LEF complex, leading to the transcriptional activation of genes involved in cell proliferation and differentiation (e.g. c-*MYC*, cyclin D1 [*CCND1*] and matrix metalloproteinase 7 [*MMP7*]) (Tejpar & Van Cutsem, 2002; Willert & Jones, 2006). In

colorectal neoplasia, mutations in the genes encoding Wnt, β-catenin, GSK3β, Axin and APC proteins are associated with the advancement of dysplasia in aberrant crypt foci during the initiation of adenoma-carcinoma sequence (Suehiro et al., 2008).

Various miRNAs have been determined to regulate the Wnt/β-catenin pathway during early transformation of colonic epithelial cells. Nagel et al. (2008) have demonstrated the ability of miR-135a and miR-135b to down-regulate the translation of *APC* transcript in CRC cells and to activate the Wnt/β-catenin signalling in the absence of Wnt ligand. miR-122a, which was initially recognised as a liver-specific miRNA, has been found to function as a novel tumour suppressor in colorectal and other gastrointestinal cancers (X. Wang, Lam, Zhang, Jin, & Sung, 2009). The inhibition of miR-122a has been shown to reverse the wild-type APC-induced cell growth inhibition while the restoration of miR-122a has been demonstrated to inhibit cell growth. Several validated targets of miR-122a include ADAM metallopeptidase domain 17 (*ADAM17*), BCL2-like 2 (*BCL2L2*) and cyclin G1 (*CCNG1*) genes (Gramantieri et al., 2007; Tsai et al., 2009; H. Xu et al., 2010). Moreover, the activated c-*MYC* gene in the Wnt/β-catenin pathway has been identified as a direct target of miR-145 (Slaby, Svoboda, Michalek, & Vyzula, 2009). Elevation of c-*MYC* expression as a result of miR-145 down-regulation is associated with aggressive and poorly differentiated tumours (J. Zhang et al., 2010). Besides that, the down-regulation of several downstream c-*MYC* targets such as anti-angiogenic thrombospondin 1 (*TSP1*) and connective tissue growth factor (*CTGF*) genes has been shown to be under the influence of miR-18 and miR-19 from the miR-17-92 cluster (Dews et al., 2006; Sachdeva & Mo, 2010). The down-regulation of *TSP1* and *CTGF* has been linked to increased proliferation, angiogenesis and metastasis.

2.2.7.2 Epidermal growth factor receptor (EGFR) pathway

EGFR is a member of the v-erb-b2 erythroblastic leukaemia viral oncogene homologue (ERBB) family of transmembrane tyrosine kinase receptors (Krasinskas, 2011). EGFR signalling cascade begins with extracellular ligand binding, receptor dimerisation and phosphorylation of cytoplasmic tyrosine kinase residues, leading to the activation of intracellular signal transduction pathways (Fang & Richardson, 2005). EGFR signalling is made up of two interlinked pathways, namely, mitogen-activated protein kinase (MAPK) pathway and phosphatidylinositol 3-kinase (PI3K)-protein kinase B (AKT) pathway. Deregulation in the EGFR signalling has been linked to tumour promotion and progression of numerous malignancies, including CRC.

Growth factor stimulation in the EGFR-MAPK pathway will initiate the intrinsic activation of two adaptor proteins, namely, SH2-containing (SHC) protein and growth factor receptor-bound protein 2 (GRB2) (Fang & Richardson, 2005). These proteins will trigger the activation of RAS, in particularly KRAS in CRC, and the signalling cascade involving RAF-MEK-MAPK. The KRAS oncoprotein is a GTPase that is involved in the regulation of cell proliferation, differentiation and apoptosis. In the normal state, KRAS activity is switched off when it cleaves the terminal phosphate of guanosine triphosphate (GTP) and converts it to guanosine diphosphate (GDP) (Krasinskas, 2011). miR-143, miR-18a* and let-7 have been reported to regulate KRAS expression (Slaby et al., 2009). These miRNAs have been validated to possess inverse relationship with KRAS protein levels in clinical CRC samples and cell culture studies (Akao, Nakagawa, & Naoe, 2006; X. Chen et al., 2009; Tsang & Kwok, 2009).

In the EGFR-PI3K pathway, growth factor stimulation will lead to the generation of a second messenger phosphatidylinositol-3,4,5-triphosphate (PIP3) that promotes AKT activation (Vara et al., 2004). PI3K is a lipid kinase that is made up of a p110 catalytic

sub-unit and a p85β regulatory sub-unit (Vara et al., 2004). The PI3K is a mediator that controls downstream processes affecting cell growth, proliferation and survival (Krasinskas, 2011). The down-regulation of miR-126 in CRC has been found to promote cell proliferation via an increase in the level of p85β regulatory protein (C. Guo et al., 2008). Recently, miR-375 involvement has been demonstrated to inhibit CRC cell proliferation and cell cycle arrest by targeting the phosphatidylinositol-4,5-bisphosphate 3-kinase, catalytic sub-unit alpha (*PIK3CA*) gene (Y. Wang, Tang, Li, Jiang, & Wang, 2014). In addition, the up-regulation of miR-223 and the down-regulation of miR-133a, miR-143 and miR-145 have been reported to be associated with both PI3K-AKT and insulin growth factor pathways in inflammation-induced CRC (Josse et al., 2014). On the other hand, the tumour suppressor phosphatase and tensin homologue (*PTEN*) gene, a negative regulator in the PI3K-AKT signalling with a function to dephosphorylate PIP3 to the initial substrate phosphatidylinositol-4,5-biphosphate (PIP2), has been determined to be repressed by miR-21, miR-92a and miR-103 in CRC (Geng et al., 2014; Krasinskas, 2011; Krichevsky & Gabriely, 2009; G. Zhang et al., 2014).

2.2.7.3 Transforming growth factor-beta (TGF-β) pathway

TGF-β pathway is involved in the regulation of cell proliferation, differentiation and apoptosis (Massagué, Blain, & Lo, 2000). TGF-β signalling is initiated via the binding of TGF-β ligand to TGF-β receptor type II (TGFBR2), followed by the phosphorylation of TGF-β receptor type I (TGFBR1) (Y. Xu & Pasche, 2007). Several downstream mediators of TGF-β signalling are mothers against decapentaplegic homologue (SMAD) proteins and components of the MAPK, c-Jun N-terminal kinase (JNK) and PI3K-AKT pathways (ten Dijke & Hill, 2004). TGF-β signalling may exert opposite effects of tumour-suppressive functions in normal intestinal epithelium and tumour-promoting

functions in late stages of colorectal carcinogenesis (Y. Xu & Pasche, 2007). Mutated *TGFBR1* and *TGFBR2* genes are commonly associated with malignant transformation of CRC (Biswas et al., 2004; Grady et al., 1999). Moreover, the diminishing expression of SMAD proteins, typically SMAD2, SMAD3 and SMAD4, greatly contributes to the loss of growth inhibitory effect in TGF-β signalling (ten Dijke & Hill, 2004; Y. Xu & Pasche, 2007). miR-106a, a highly up-regulated miRNA in metastatic CRC, has been found to exert its function by targeting the *TGFBR2* gene (Feng et al., 2012). In addition, L. Liu et al. (2013) have revealed an association between the up-regulation of miR-130a/301a/454 family and the down-regulation of SMAD4 protein in CRC. The miR-130a/301a/454 family has been suggested to possess oncogenic functions by enhancing cell proliferation and migration. Recently, Reid et al. (2012) have unveiled several novel miRNAs that are involved in the TGF-β signalling pathway, namely, miR-130b, miR-21 and miR-301b that target the activin A receptor, type 1C (*ACVR1C*); miR-424 that targets the *SMAD3*; miR-130, miR-135b, miR-183, miR-19a, miR-19b, miR-449a and miR-449b that target the *SMAD4*.

2.2.7.4 p53 pathway

TP53 gene mutation is considered a mandatory event during the transition of a large adenoma into an invasive carcinoma in CRC. Generally, in response to DNA damage, cellular stress and hypoxia, the p53 transcription factor functions to regulate a variety of genes involved in cell cycle arrest and apoptosis (Levine, 1997). The p53 expression is tightly regulated by E3 ubiquitin ligase mouse double minute 2 homologue (MDM2) and p19ARF (Juven-Gershon & Oren, 1999). The MDM2 binds and exports the nuclear p53 to cytoplasm for ubiquitination and degradation. In contrast, the p19ARF, a tumour suppressor protein transcribed from the INK4a-ARF locus, acts to attenuate the MDM2-

mediated degradation of p53 by forming a complex with the MDM2 in the nucleus (Tao & Levine, 1999). miRNA involvement in the p53 pathway has been greatly reported. Members of the miR-34a-c family have been validated as transcriptional regulators of p53 pathway (Corney, Flesken-Nikitin, Godwin, Wang, & Nikitin, 2007; Yamakuchi, Ferlito, & Lowenstein, 2008). The miR-34a, miR-34b and miR-34c are considered as tumour suppressors in CRC (Slaby et al., 2009). These miRNAs have been found to regulate several downstream genes of the p53 pathway (e.g. delta-like 1 [*DLL1*], enhancer of zeste homologue 2 [*EZH2*], *MET*, *NOTCH1* and silent information regulator 1 [*SIRT1*]) (Corney et al., 2007; Yamakuchi et al., 2008). miR-16 is a miRNA that shares similar roles with the miR-34a-c family. The target genes of miR-16 include *survivin*, *CCND1* and cyclin-dependent kinase 6 (*CDK6*) (Q. Ma et al., 2013). The miR-16 acts as a tumour suppressor in CRC and its expression is often found to be down-regulated (Yan et al., 2013). On the other hand, miR-107 functions as a mediator of p53 regulation in hypoxic signalling and tumour angiogenesis in CRC (Yamakuchi et al., 2010). The miR-107 decreases hypoxic signalling by down-regulating the hypoxia inducible factor 1 (*HIF1*) expression. Another miRNA with validated involvement in the p53 signalling is miR-124 (K. Liu et al., 2013). The expression of miR-124 has been identified to be down-regulated in CRC (J. Zhang et al., 2013). It is capable of regulating the proliferation of CRC cells by targeting the inhibitor of apoptosis-stimulating protein of p53 (*iASPP*) and *STAT3* genes (K. Liu et al., 2013; J. Zhang et al., 2013).

2.2.7.5 Extracellular matrix (ECM) breakdown and epithelial-to-mesenchymal transition (EMT)

Metastasis is a complex process involving tumour cells detachment from the primary tumour, local invasion into the stroma, intravasation into blood or lymphatic vessels, extravasation at a distant organ and proliferation into clinically detectable metastases (Liotta, Steeg, & Stetler-Stevenson, 1991; Wan, Pantel, & Kang, 2013). The tumour stroma mainly consists of basement membrane, ECM, fibroblasts, immune cells and vasculature (Bremnes et al., 2011). Among these, ECM breakdown is the definite step in tumour invasion. The key enzymes involved are urokinase-type plasminogen activator (uPA) and matrix metalloproteinases (MMPs) (Takayama, Miyanishi, Hayashi, Sato, & Niitsu, 2006). The involvement of miR-21 in ECM remodelling and cell motility has been described (Asangani et al., 2008). mir-21, a miRNA that targets the programmed cell death 4 (*PDCD4*) gene, has been found to be up-regulated in CRC (K. H. Chang et al., 2011). Generally, *PDCD4* is a tumour suppressor gene that inhibits the tissue plasminogen activator-induced neoplastic transformation (Jansen, Camalier, & Colburn, 2005). Loss of *PDCD4* often leads to tumour invasion and metastasis. In other instance, Ke et al. (2014) have revealed that the restoration of miR-224 in CRC can inhibit the expression of cell division control protein 42 homologue (*CDC42*) gene that is involved in filamentous actin-mediated cell migration.

Following ECM remodelling, the tumour cells are able to detach from the primary epithelial cluster by undergoing EMT. EMT is characterised by the reduction of epithelial markers (e.g. E-cadherin and claudin) and the up-regulation of mesenchymal markers (e.g. N-cadherin, vimentin and fibronectin), leading to the loss of cell adhesion and increase in cell motility (Natalwala, Spychal, & Tselepis, 2008). The mesenchymal-like cells are able to move freely into the vasculature (van Zijl, Krupitza, & Mikulits, 2011). The transcriptional repressor zinc finger E-box binding homeobox 1 and 2

(ZEB1 and ZEB2) are crucial inducers of EMT (Paterson et al., 2013). During EMT, members of the miR-200 family (miR-200a, miR-200b, miR-200c, miR-141 and miR-429) are commonly suppressed by the ZEB factors (Lamouille, Subramanyam, Blelloch, & Derynck, 2013). However, the miR-200 family may initiate a miRNA-mediated feedforward loop that inhibits the expression of TGF-β2 and ZEB factors, thereby stabilising the EMT process (Burk et al., 2008; Slaby et al., 2009). Besides ZEB factors, other downstream EMT factors that have been shown to be targeted by miRNAs include Snail (miR-34 and miR-203), Slug (miR-1 and miR-200b) and vimentin (miR-138) (Lamouille et al., 2013; J. Zhang & Ma, 2012).

CHAPTER 3

MATERIALS AND METHODS

3.1 Materials

3.1.1 Sterile deionised water (sdH_2O)

The sdH_2O was prepared by autoclaving ultrapure water obtained from PURELAB Option S-R 7-15 water purification system (ELGA LabWater, High Wycombe, UK). The water was used in the preparation of buffers and solutions.

3.1.2 Cell lines and culture reagents

3.1.2.1 Cell lines

SW480 (CCL-228) and SW620 (CCL-227) CRC cell lines were obtained from American Type Culture Collection (ATCC, Manassas, VA, USA).

3.1.2.2 Commercially available cell culture reagents

Dulbecco's modified Eagle's medium (DMEM), 1X trypsin-ethylenediaminetetraacetic acid (EDTA) solution and dimethyl sulphoxide (DMSO) were purchased from Sigma-Aldrich (St. Louis, MO, USA). Foetal bovine serum (FBS) and 100X penicillin-streptomycin were obtained from Gibco (Carlsbad, CA, USA).

3.1.2.3 Complete medium

Basal DMEM	445 ml
FBS	50 ml
100X Penicillin-streptomycin	5 ml

3.1.2.4 Freezing medium

Basal DMEM	3 ml
FBS	7 ml
DMSO	100 µl

Freshly prepared freezing medium was used for cryopreservation.

3.1.2.5 1X Phosphate-buffered saline (PBS)

The 1X PBS was prepared by mixing one part of 10X PBS (Vivantis, Oceanside, CA, USA) with nine parts of sdH_2O.

3.1.3 1X siRNA resuspension buffer

5X siRNA buffer	50 µl
Nuclease-free water	200 µl

The 5X siRNA buffer was purchased from Dharmacon (Lafayette, CO, USA). Nuclease-free water was purchased from Ambion (Carlsbad, CA, USA). The 1X siRNA resuspension buffer was used to resuspend lyophilised miRIDIAN miRNA mimics and inhibitors (Dharmacon, Lafayette, CO, USA) of 5 nmol into 20 μM stocks. miRIDIAN miRNA mimics are double-stranded RNA oligonucleotides designed to mimic the function of endogenous mature miRNAs. miRIDIAN miRNA inhibitors are single-stranded, chemically enhanced RNA oligonucleotides designed to inhibit the function of endogenous mature miRNAs.

3.1.4 Reagents for total RNA extraction

3.1.4.1 5 M Sodium chloride (NaCl)

NaCl	29.22 g
sdH_2O	100 ml

NaCl (Sigma-Aldrich, St. Louis, MO, USA) was dissolved in sdH_2O. The solution was autoclaved and kept at room temperature.

3.1.4.2 Wash solution 1 (70% Ethanol:30% Denaturation solution)

Absolute ethanol	70 ml
Denaturation solution	30 ml

Absolute ethanol was obtained from Sigma-Aldrich (St. Louis, MO, USA). Denaturation solution was purchased from Ambion (Carlsbad, CA, USA).

3.1.4.3 Wash solution 2 (80% Ethanol:50 mM NaCl)

Absolute ethanol	80 ml
5 M NaCl (section 3.1.4.1)	1 ml
Nuclease-free water	19 ml

3.1.5 Reagents for RNA agarose gel electrophoresis

3.1.5.1 1X 3-(N-Morpholino)propanesulphonic acid (MOPS) buffer

The 1X MOPS running buffer was prepared by diluting one part of 10X MOPS buffer (Nacalai Tesque, Nakagyo-ku, Kyoto, Japan) with nine parts of sdH_2O.

3.1.5.2 RNA loading buffer

Glycerol, 50% (*v*/*v*)	5 ml
Bromophenol blue, 0.25% (*w*/*v*)	25 mg
EDTA, 1 mM	3.72 mg
sdH_2O	Top up to 10 ml

Glycerol was purchased from VWR (Lutterworth, Leicestershire, UK). Bromophenol blue and EDTA were purchased from Sigma-Aldrich (St. Louis, MO, USA).

3.1.5.3 RNA sample buffer (per sample)

10X MOPS buffer	2 µl
37% Formaldehyde	3.5 µl
Deionised formamide	10 µl
RNA loading buffer (section 3.1.5.2)	2 µl

The 37% formaldehyde and deionised formamide were purchased from Sigma-Aldrich (St. Louis, MO, USA).

3.1.5.4 1% RNA agarose gel

Agarose	0.5 g
sdH_2O	43.5 ml
37% Formaldehyde	1.5 ml
10X MOPS buffer	5 ml
Ethidium bromide (EtBr) (10 mg/ml)	1 µl

Agarose powder and EtBr reagent were purchased from Sigma-Aldrich (St. Louis, MO, USA). Agarose was first dissolved in sdH_2O and heated to 100°C in a microwave oven. The solution was then cooled to approximately 60°C before the addition of 37% formaldehyde, 10X MOPS buffer and EtBr.

3.1.6 Reagents for RNA polyacrylamide gel electrophoresis (PAGE)

3.1.6.1 1X Tris-borate-ethylenediaminetetraacetic acid (TBE) buffer

The 1X TBE running buffer was prepared by diluting one part of 10X TBE buffer (Vivantis, Oceanside, CA, USA) with nine parts of sdH_2O.

3.1.6.2 10% Ammonium persulphate (APS)

APS	0.1 g
sdH_2O	1 ml

APS was obtained from Bio-Rad (Hercules, CA, USA). The solution was prepared fresh for each use.

3.1.6.3 15% RNA polyacrylamide gel

Urea	3.6 g
40% Acrylamide/bis-acrylamide (29:1)	2.82 ml
10X TBE buffer	0.75 ml
sdH_2O	0.95 ml
10% APS (section 3.1.6.2)	37.5 µl
Tetramethylethylenediamine (TEMED)	7.5 µl

Urea, 40% acrylamide/bis-acrylamide (29:1) and TEMED were obtained from Bio-Rad (Hercules, CA, USA). The mixture of urea, 40% acrylamide/bis-acrylamide (29:1) and 10X TBE buffer was initially heated to 60°C. Once urea has dissolved, sdH_2O, 10% APS and TEMED were added to the gel mixture.

3.1.6.4 RNA sample buffer (per sample)

10X TBE buffer	2 µl
Deionised formamide	10 µl
RNA loading buffer (section 3.1.5.2)	3 µl
EtBr (10 mg/ml)	1 µl

3.1.7 Reagents for miRNA microarray

3.1.7.1 1 M Tris-HCl, pH 8

Tris base	6 g
sdH_2O	Top up to 50 ml

Tris base (Sigma-Aldrich, St. Louis, MO, USA) was dissolved in 30 ml of sdH_2O. The pH was adjusted to 8 using concentrated hydrochloric acid (HCl). The stock solution was then adjusted to 50 ml and autoclaved. The working concentration, 1 mM Tris-HCl was prepared by mixing 5 µl of the stock solution with 4.995 ml of nuclease-free water.

3.1.7.2 ATP mix dilution (1:500)

ATP mix stock	1 µl
1 mM Tris-HCl, pH 8	499 µl

The ATP mix stock was obtained from the FlashTag Biotin HSR RNA Labelling kit (Affymetrix, Santa Clara, CA, USA).

3.1.7.3 Poly(A) tailling master mix (per sample)

10X Reaction buffer	1.5 µl
25 mM $MnCl_2$	1.5 µl
ATP mix dilution (section 3.1.7.2)	1 µl
PAP enzyme	1 µl

The individual components were obtained from the FlashTag Biotin HSR RNA Labelling kit (Affymetrix, Santa Clara, CA, USA).

3.1.7.4 Array hybridisation cocktail (per sample)

2X Hybridisation mix	50 µl
27.5% Formamide	15 µl
DMSO	10 µl
20X Eukaryotic hybridisation controls	5 µl

3 nM Control oligo B2	1.7 µl

The 2X hybridisation mix and DMSO were obtained from the GeneChip Hybridisation, Wash and Stain kit (Affymetrix, Santa Clara, CA, USA). The 20X eukaryotic hybridisation controls and 3 nM control oligo B2 were obtained from the GeneChip Eukaryotic Hybridisation Control kit (Affymetrix, Santa Clara, CA, USA). The 27.5% formamide was obtained from the FlashTag Biotin HSR RNA Labelling kit (Affymetrix, Santa Clara, CA, USA).

3.1.8 Reagents for enzyme-linked oligosorbent assay (ELOSA)

3.1.8.1 1X PBS, 0.02% Tween-20

10X PBS	10 ml
Tween-20	20 µl
sdH_2O	90 ml

Tween-20 was obtained from Sigma-Aldrich (St. Louis, MO, USA).

3.1.8.2 5% Bovine serum albumin (BSA) in 1X PBS

BSA	0.5 g
1X PBS (section 3.1.2.5)	10 ml

BSA powder (Sigma-Aldrich, St. Louis, MO, USA) was dissolved in 1X PBS. The resulting solution was aliquoted and kept at -20°C.

3.1.8.3 10% Sodium dodecyl sulphate (SDS)

SDS	10 g
sdH_2O	100 ml

SDS powder (Bio-Rad, Hercules, CA, USA) was dissolved in sdH_2O. The resulting solution was filtered using a 0.2 μm syringe filter (Sartorius, Goettingen, Germany).

3.1.8.4 5X Saline-sodium citrate (SSC), 0.05% SDS, 0.005% BSA

20X SSC buffer	1.25 ml
10% SDS (section 3.1.8.3)	25 μl
5% BSA in 1X PBS (section 3.1.8.2)	5 μl
sdH_2O	3.72 ml

The 20X SSC buffer was purchased from Sigma-Aldrich (St. Louis, MO, USA). The resulting solution was aliquoted and kept at -20°C.

3.1.8.5 ELOSA hybridisation cocktail (per sample)

5X SSC, 0.05% SDS, 0.005% BSA (section 3.1.8.4)	48 μl
25% Dextran sulphate	2.5 μl

The 25% dextran sulphate was obtained from Genisphere (Hatfield, PA, USA).

3.1.8.6 Streptavidin-horseradish peroxidase (HRP) dilution (1:6000)

Streptavidin-HRP	1 µl
5% BSA in 1X PBS (section 3.1.8.2)	5.999 ml

Streptavidin-HRP was purchased from Pierce (Rockford, IL, USA).

3.1.9 Reagents for reverse transcription (RT)

3.1.9.1 RT master mix for miRNA (per sample)

10X TaqMan RT buffer	1.5 µl
100 mM dNTPs	0.15 µl
20 U/µl RNase inhibitor	0.19 µl
50 U/µl MultiScribe reverse transcriptase	1 µl
Nuclease-free water	4.16 µl

The individual components were obtained from the TaqMan miRNA RT kit (Applied Biosystems, Carlsbad, CA, USA).

3.1.9.2 RT master mix for mRNA (per sample)

10X TaqMan RT buffer	1 µl
25 mM $MgCl_2$	2.2 µl
2.5 mM dNTPs	2 µl

50 μM Random hexamers	0.5 μl
20 U/μl RNase inhibitor	0.2 μl
50 U/μl MultiScribe reverse transcriptase	0.25 μl

The individual components were obtained from the TaqMan RT kit (Applied Biosystems, Carlsbad, CA, USA).

3.1.10 Reagents for quantitative real-time polymerase chain reaction (qPCR)

3.1.10.1 qPCR for miRNA (96-well)

2X TaqMan Fast Advanced master mix	10 μl
20X TaqMan miRNA assay	1 μl
Nuclease-free water	7.67 μl

The 2X TaqMan Fast Advanced master mix and 20X TaqMan miRNA assay were purchased from Applied Biosystems (Carlsbad, CA, USA). The assays obtained were hsa-miR-150 (Assay ID: 000473; MIMAT0000451), hsa-miR-16 (Assay ID: 000391; MIMAT0000069), hsa-miR-193a-3p (Assay ID: 002250; MIMAT0000459), hsa-miR-23a (Assay ID: 000399; MIMAT0000078), hsa-miR-23b (Assay ID: 000400; MIMAT0000418), hsa-miR-338-5p (Assay ID: 002658; MIMAT0004701), hsa-miR-342-3p (Assay ID: 002260; MIMAT0000753), hsa-miR-483-3p (Assay ID: 002339; MIMAT0002173) and RNU48 (Assay ID: 001006; NR_002745).

3.1.10.2 qPCR for mRNA (96-well)

2X TaqMan Fast Advanced master mix	10 µl
20X TaqMan gene expression assay	1 µl
Nuclease-free water	8 µl

The 20X TaqMan gene expression assay was purchased from Applied Biosystems (Carlsbad, CA, USA). The assays obtained were *β-actin* (Assay ID: Hs99999903_m1; NM_001101.3), *APAF1* (Assay ID: Hs00559441_m1; NM_013229.2), *FOXO4* (Assay ID: Hs00936217_g1; NM_005938.3) and *GAPDH* (Assay ID: Hs99999905_m1; NM_002046.5).

3.1.11 Reagent for total protein quantification

Triton X-100	5 ml
sdH_2O	45 ml

A 10% Triton X-100 working solution was prepared by diluting one part of Triton X-100 (Sigma-Aldrich, St. Louis, MO, USA) with nine parts of sdH_2O.

3.1.12 Reagents for sodium dodecyl sulphate-polyacrylamide gel electrophoresis (SDS-PAGE)

3.1.12.1 0.5% Bromophenol blue

Bromophenol blue	0.5 g
sdH_2O	100 ml

3.1.12.2 1.5 M Tris-HCl, pH 8.8

Tris base	27.23 g
sdH_2O	Top up to 150 ml

Tris base was dissolved in 100 ml of sdH_2O. The pH of the solution was adjusted to 8.8 using concentrated HCl. The solution was then adjusted to 150 ml and stored at 4°C.

3.1.12.3 0.5 M Tris-HCl, pH 6.8

Tris base	6 g
sdH_2O	Top up to 100 ml

Tris base was dissolved in 70 ml of sdH_2O. The pH of the solution was adjusted to 6.8 using concentrated HCl. The solution was then adjusted to 100 ml and stored at 4°C.

3.1.12.4 SDS reducing sample buffer

sdH_2O	3.55 ml
0.5 M Tris-HCl, pH 6.8 (section 3.1.12.3)	1.25 ml
Glycerol	2.5 ml
10% SDS (section 3.1.8.3)	2 ml
0.5% Bromophenol blue (section 3.1.12.1)	0.2 ml

The above stock solution was prepared. Fifty µl of β-mercaptoethanol (Bio-Rad, Hercules, CA, USA) was added to an aliquot of 950 µl of SDS reducing sample buffer prior to use.

3.1.12.5 10X Electrode stock buffer, pH 8.3

Tris base	30.3 g
Glycine	144 g
SDS	10 g
sdH_2O	Top up to 1 L

Tris base, glycine (Bio-Rad, Hercules, CA, USA) and SDS were dissolved in sdH_2O to produce a 10X electrode stock buffer. The stock buffer was further diluted to 1X strength for each electrophoresis run.

3.1.12.6 Tris-glycine SDS-PAGE gel

	10%	4%
	Resolving gel (10 ml)	Stacking gel (5 ml)
sdH_2O	4.1 ml	3 ml
30% acrylamide/bis (37.5:1)	3.3 ml	650 µl
Gel buffer	2.5 ml	1.25 ml
	(section 3.1.12.2)	(section 3.1.12.3)
10% SDS (section 3.1.8.3)	100 µl	50 µl
10% APS (section 3.1.6.2)	50 µl	25 µl
TEMED	5 µl	5 µl

The 30% acrylamide/bis (37.5:1) was purchased from Bio-Rad (Hercules, CA, USA). The 10% APS and TEMED were added to the gel mixture just prior to gel-casting.

3.1.13 Reagent for membrane transfer

Tris base	3.03 g
Glycine	14.4 g
Methanol	200 ml
sdH_2O	Top up to 1 L

Methanol was purchased from Sigma-Aldrich (St. Louis, MO, USA). The transfer buffer was kept cold at 4°C.

3.1.14 Reagents for Western blot

Western blot was performed using the Fast Western Blot kit, ECL substrate (Pierce, Rockford, IL, USA). Preparations of the working solutions were based on an 8 x 10 cm blot probed with either a mouse or rabbit primary antibody. All working solutions were prepared just prior to use.

3.1.14.1 Fast Western 1X wash buffer

Fast Western 10X wash buffer	10 ml
sdH_2O	90 ml

Fast Western 1X wash buffer was prepared by mixing one part of the Fast Western 10X wash buffer with nine parts of sdH_2O.

3.1.14.2 Primary antibody working solution

Primary antibody	10 µl
Fast Western antibody diluent	10 ml

Primary antibody was diluted at a ratio of 1:1000 with Fast Western antibody diluent.

3.1.14.3 Fast Western optimised HRP reagent working solution

Fast Western optimised HRP reagent	1 ml
Fast Western antibody diluent	10 ml

3.1.14.4 Detection reagent working solution

Detection reagent 1	2 ml
Detection reagent 2	2 ml

3.1.15 Reagents for sub-cloning

3.1.15.1 1% DNA agarose gel

Agarose	0.25 g
1X TBE (section 3.1.6.1)	25 ml
EtBr (10 mg/ml)	0.5 µl

Agarose powder was dissolved in 1X TBE and heated to 100°C in a microwave oven. The mixture was cooled to about 60°C before the addition of EtBr.

3.1.15.2 Restriction enzyme digestion

10X FastDigest green buffer	2 µl
FastDigest enzyme (HindIII and/or SpeI)	1 µl

Nuclease-free water	Top up to 20 µl

The 10X FastDigest green buffer and enzymes were purchased from Fermentas (Waltham, MA, USA).

3.1.15.3 Luciferase reporter and plasmid DNA vectors

The luciferase reporter vectors used in this study were pMIR-REPORT firefly luciferase miRNA expression reporter vector (Ambion, Carlsbad, CA, USA) and pRL-SV40 *Renilla* luciferase control reporter vector (Promega, Madison, WI, USA).

Plasmid DNA vectors containing the putative 3'-UTR fragments or the site-directed mutants were assembled from synthetic oligonucleotides and/or PCR products and cloned into pMA-T vectors using GeneArt gene synthesis service (Invitrogen, Carlsbad, CA, USA). The gene fragment sequences were derived from the NCBI database. Each customised fragment was inclusive of HindIII and SpeI restriction sites.

3.1.15.4 Ligation

10X T4 DNA ligase buffer	2 µl
T4 DNA ligase (5 U/µl)	0.5 µl
Vector DNA:insert DNA	1:5
Nuclease-free water	Top up to 10 µl

The T4 DNA ligase buffer and enzyme were purchased from Fermentas (Waltham, MA, USA).

3.1.15.5 Ampicillin (10 mg/ml)

A stock solution at 10 mg/ml was made by dissolving 200 mg of ampicillin, sodium salt (Gibco, Carlsbad, CA, USA) in 20 ml of nuclease-free water. The stock solution was aliquoted into smaller volumes and stored at -80°C.

3.1.15.6 Luria-Bertani (LB)-ampicillin broth

LB broth	12.5 g
sdH_2O	500 ml
Ampicillin (10 mg/ml) (section 3.1.15.5)	5 ml

LB broth, Miller powder (BD Biosciences, Franklin Lakes, NJ, USA) was dissolved in 500 ml of sdH_2O with frequent agitation. The medium was autoclaved and cooled to 50-55°C before the addition of ampicillin. The working concentration for ampicillin was 100 μg/ml. The medium was stored at 4°C and warmed to room temperature before use.

3.1.15.7 LB-ampicillin agar plates

LB agar	20 g
sdH_2O	500 ml
Ampicillin (10 mg/ml) (section 3.1.15.5)	5 ml

LB agar, Miller powder (BD Biosciences, Franklin Lakes, NJ, USA) was dissolved in 500 ml of sdH_2O with frequent agitation. The medium was autoclaved and cooled to 50-55°C before the addition of ampicillin. The working concentration for ampicillin was

100 µg/ml. The molten agar was poured into 10 cm sterile petri dishes until 1/3 full and allowed to be hardened at room temperature. The LB-ampicillin agar plates were sealed with parafilm and stored at 4°C in an inverted position. The plates were pre-warmed at 37°C for 30 minutes before use.

3.1.15.8 80% Glycerol

Glycerol	80 ml
sdH_2O	20 ml

The 80% glycerol solution was autoclaved and kept at room temperature.

3.1.16 1X 3-(4,5-Dimethylthiazol-2-yl)-2,5,-diphenyltetrazolium bromide (MTT)

The MTT Cell Proliferation kit from OZ Biosciences (Marseille, France) was utilised. The 10X MTT stock solution in the kit was diluted to 1X working solution using sterile 1X PBS. The 1X MTT was stored at -20°C for three months.

3.1.17 Reagents for migration and invasion assays

3.1.17.1 0.01 M Tris (pH 8), 0.7% NaCl

NaCl	0.7 g
1 M Tris-HCl (pH 8) (section 3.1.7.1)	1 ml
sdH_2O	99 ml

NaCl was dissolved in the mixture of 1 M Tris-HCl and sdH_2O. The solution was filtered using a 0.2 μm syringe filter (Sartorius, Goettingen, Germany) and kept at 4°C.

3.1.17.2 Matrigel coating solution (250 μg/ml)

Matrigel basement membrane matrix (8.5 mg/ml)	29.4 μl
0.01 M Tris (pH 8), 0.7% NaCl (section 3.1.17.1)	70.6 μl

The Matrigel basement membrane matrix was purchased from BD Biosciences (Franklin Lakes, NJ, USA). The concentration of the Matrigel matrix is lot-specific. Aliquots of the Matrigel matrix were stored at -80°C and thawed overnight on ice at 4°C prior to use. A 100 μl of Matrigel coating solution with the working concentration of 250 μg/ml was sufficient to coat one 24-well cell culture insert. The coating solution was prepared fresh for each use.

3.1.17.3 3.7% Formaldehyde in 1X PBS

37% Formaldehyde	1 ml
1X PBS	9 ml

The solution was prepared fresh for each use.

3.1.18 Essential research services

RNA integrity analysis via Agilent 2100 Bioanalyzer (Agilent, Santa Clara, CA, USA) was outsourced to Malaysia Genome Institute, Selangor, Malaysia. RNA integrity number (RIN) was obtained using Eukaryote Total RNA Nano Chip (Agilent, Santa Clara, CA, USA).

Oligonucleotide synthesis and DNA sequencing services were obtained from First BASE Laboratories Sdn. Bhd., Selangor, Malaysia. The company is using the Applied Biosystems BigDye® Terminator v3.1 Cycle Sequencing kit chemistry on 3730XL Genetic Analyzer platform (Carlsbad, CA, USA) for all *de novo* sequencing and re-sequencing purposes.

3.2 Methods

3.2.1 Clinical study design and sample collection

A case-control study was designed to identify blood miRNAs that are reflective of those in CRC tissues. The study was performed according to the principles of the Declaration of Helsinki and has gained an approval from the Medical Ethics Committee of the University of Malaya Medical Centre (UMMC), Malaysia (reference number: 805.9) (Appendix 1). A total of 112 whole blood samples and a sub-set of 60 paired cancer tissue with normal colonic mucosa samples were collected from primary CRC patients. The tissue samples were obtained from the same group of patients who have donated their blood samples. All patients were diagnosed and treated at the UMMC, Malaysia, from January 2011 to January 2013. The recruited patients did not receive any pre-operative chemotherapy and/or radiotherapy prior to sample collection. Tumour histology was confirmed by pathological analysis and staged according to the TNM

staging system (Edge & Compton, 2010). For the control group, 50 whole blood samples that were age-, gender- and race-matched were collected from colonoscopy-confirmed colonic disease-free individuals. All clinical samples were obtained with written informed consent. Demographic data and medical record were retrieved from the Department of Medical Records, UMMC, Malaysia.

Whole blood samples were collected in EDTA blood collection tubes (BD Vacutainer, BD Diagnostics, Franklin Lakes, NJ, USA). An aliquot of 400 µl of whole blood was mixed with 1.3 ml of RNA*later* solution (Ambion, Carlsbad, CA, USA) to stabilise and protect the cellular RNA. Tissue samples, cut into small pieces, were collected directly in 5 ml of RNA*later* solution immediately after resection. The blood and tissue samples were stored at -80°C.

3.2.2 Cell culture

SW480 and SW620 CRC cells were cultured in complete medium (section 3.1.2.3). The cells were maintained in a 5% CO_2-humidified incubator (MCO-17A1, Sanyo, Osaka, Japan) at 37°C. The SW480 and SW620 cell lines were adherent cell lines. Cell culture experiments were performed in the laminar flow cabinet and culture media were warmed to 37°C in a water bath before use.

3.2.2.1 Thawing of frozen culture

A cryovial containing cryopreserved cells was obtained from liquid nitrogen tank or -80°C freezer and thawed immediately in a water bath at 37°C with gentle swirling. The content was transferred to a 15 ml centrifuge tube and 3 ml of complete medium was

added. The cell suspension was centrifuged at 2,000 rpm for 5 minutes and the supernatant was discarded. The cell pellet was resuspended with 5 ml of complete medium and transferred to a T-25 culture flask. The culture flask was maintained in the 5% CO_2-humidified incubator. Complete medium was changed every 2-3 days.

3.2.2.2 Sub-culturing of adherent cells

Cells were sub-cultured when the confluency reached 80-90%. T-75 culture flask was used for subsequent sub-culturing of the cells. The medium in the culture flask was discarded and the cells were rinsed twice with 10 ml of 1X PBS. The cells were trypsinised with 1 ml of trypsin-EDTA at 37°C for 10-15 minutes. The cells were viewed under a phase contrast microscope for detachment. Two ml of complete medium was then added into the flask to stop the trypsinisation procedure. The cell suspension was transferred to a 15 ml centrifuge tube and centrifuged at 2,000 rpm for 5 minutes. The supernatant was discarded and the cell pellet was resuspended with 3 ml of complete medium. Meanwhile, the required number of T-75 culture flask was prepared and 9 ml of complete medium was added into each flask. The cell suspension was then dispensed in equal volume into each flask.

3.2.2.3 Cryopreservation

Freezing medium (section 3.1.2.4) was freshly prepared for cryopreservation. After the cells were trypsinised and centrifuged, the supernatant was discarded and the cell pellet was resuspended with the freezing medium. Cells from one T-75 culture flask could be stocked up into five cryovials, with 1 ml each. The cryovials were then labelled and stored in -80°C freezer for short term storage or liquid nitrogen for long term storage.

3.2.2.4 Cell counting by haemocytometer

Following trypsinisation and resuspension with complete medium, a small aliquot of the cells was obtained for cell counting. Ten µl of the cell suspension was diluted with 10 µl of trypan blue solution (Bio-Rad, Hercules, CA, USA) for cell viability screening. Ten µl of the mixture was pipetted onto a haemocytometer and viewed under a phase contrast microscope at 100X magnification. The mean number of cells from the four edges was counted using a tally counter.

The total cell count was calculated as follows:

Total cell count = mean number of cells x dilution factor x volume of cell suspension x 10^4

3.2.3 miRNA transfection

miRNA transfections for mRNA and protein analyses were performed on 48-well and 6-well plates, respectively. Cells were seeded in antibiotic-free complete medium at 1 x 10^5 cells per well (48-well) or 1 x 10^6 cells per well (6-well) one day before transfection. These cell densities were chosen after seeding optimisation. Lipofectamine 2000 transfection reagent (Invitrogen, Carlsbad, CA, USA) and Opti-MEM I reduced serum medium (Gibco, Carlsbad, CA, USA) were complexed at a ratio of 0.5:25 µl (48-well) or 5:250 µl (6-well) and incubated at room temperature for 5 minutes. miRIDIAN miRNA mimic or inhibitor (Dharmacon, Lafayette, CO, USA) was diluted to a concentration of 10 pmol in 25 µl (48-well) or 100 pmol in 250 µl (6-well) of Opti-MEM I reduced serum medium. Both mixtures were then combined and incubated at room temperature for another 20 minutes. After the incubation, the plated medium was removed and the miRNA-transfection mixture was added dropwise to each well. The medium was changed to antibiotic-free complete medium after 6 hours of transfection.

The cells were incubated in the 5% CO_2-humidified incubator at 37°C for 48 hours for mRNA analysis or 72 hours for protein analysis.

The miRNA mimics and inhibitors tested were for hsa-miR-193a-3p, hsa-miR-23a and hsa-miR-338-5p. miRNA mimic negative control (mimic NC) and miRNA inhibitor negative control (inhibitor NC) were included in each transfection experiment. The negative control molecules were based on the mature sequence of *C. elegans* cel-miR-67-3p (MIMAT0000039). The molecules have been confirmed to have minimal sequence identity with human miRNAs and no identifiable effect on tested miRNAs. Moreover, miRNA mimic positive control that targets the 3'-UTR of glyceraldehyde-3-phosphate dehydrogenase (*GAPDH*) gene and miRNA inhibitor positive control that targets the endogenous miR-16 were also included. Other experimental controls include non-transfected control (NTC) cells and mock-transfected control cells with only the transfection reagent. Each transfection experiment was performed in triplicates in three independent experiments.

3.2.4 Total RNA extraction

3.2.4.1 Total RNA extraction from whole blood

The procedure was adapted from RiboPure-Blood RNA Purification kit (Ambion, Carlsbad, CA, USA) with slight modification to enable the isolation of miRNA and other small RNAs. RNA*later*-stabilised blood sample that was kept at -80°C was thawed on ice and centrifuged at maximum speed for 5 minutes. The supernatant was discarded and 1 ml of lysis solution was added. The mixture was vigorously vortexed to resuspend the pellet. Next, 10 µl of acetic acid was added and the cell lysate was vortexed and kept on ice for 5 minutes. Following that, 400 µl of acid-

phenol:chloroform from beneath the overlying layer of the aqueous buffer was added. The cell lysate was vortexed and centrifuged at maximum speed for 5 minutes to separate the aqueous and organic phases. The aqueous phase containing the RNA was then transferred to a 15 ml centrifuge tube while the organic phase was discarded. One ml of Denaturation solution (Ambion, Carlsbad, CA, USA) was added and vortexed. The solution was then mixed with 2.7 ml of absolute ethanol. A clear suspension should be observed. Otherwise, 300 µl increments of nuclease-free water were added until the suspension turned clear. The clear solution was filtered through the provided spin column by successively centrifuging 700 µl of sample for 10 seconds. The column flow-through was discarded. The spin column was washed with 700 µl of wash solution 1 (section 3.1.4.2) once and 700 µl of wash solution 2 (section 3.1.4.3) twice via brief centrifugation. After the washing steps, the spin column was spun at maximum speed for 1 minute to remove any residual fluid before being transferred to a new collection tube. A volume of 150 µl of elution solution (pre-heated to 78°C) was applied to the centre of the column. The column was left at room temperature for 1 minute before the final centrifugation for 2 minutes to elute the RNA into the collection tube. The sample was aliquoted in equal volume into two tubes and stored at -80°C.

3.2.4.2 Total RNA extraction from CRC tissue and cultured cells

Total RNA extraction from CRC tissue and cultured cells was performed based on the protocol in miRNeasy Mini kit (Qiagen, Venlo, Limburg, Netherlands). For CRC tissue, 30 mg of RNA*later*-stabilised tissue was weighed and placed in 700 µl of QIAzol reagent. The sample was homogenised until no visible piece of tissue was observed. For cultured cells, the cells were washed with 1X cold PBS and 200 µl of QIAzol reagent was added into three wells of a 48-well plate. The reagent was pipetted up and down to

lyse the cells. The lysed cells from the three wells were pooled into a 1.5 ml microcentrifuge tube. The tissue/cell lysate was either subjected to immediate extraction or stored at -80°C.

The sample extraction began with a vigorous mixing of the tissue/cell lysate with 140 µl chloroform for 15 seconds. The mixture was incubated at room temperature for 3 minutes and centrifuged at maximum speed for 15 minutes at 4°C. The aqueous phase was transferred to a new collection tube and 525 µl of absolute ethanol was added. The solution was mixed and 700 µl of the solution was successively centrifuged through the provided spin column at 10,000 rpm for 15 seconds at room temperature. The column flow-through was discarded. Next, 350 µl of buffer RWT was added and centrifuged at 10,000 rpm for 15 seconds. DNase I solution (80 µl) was added and the spin column was incubated at room temperature for 15 minutes before the addition of another 350 µl of buffer RWT. The spin column was again centrifuged at 10,000 rpm for 15 seconds. Following that, 500 µl of buffer RPE was added and briefly centrifuged. The step was repeated with another 500 µl of buffer RPE and centrifuged at 10,000 rpm for 2 minutes. After the washing steps, the spin column was spun at maximum speed for 1 minute to remove any residual fluid before being transferred to a new collection tube. A volume of 50 µl of nuclease-free water was applied to the centre of the column and incubated at room temperature for 1 minute. Finally, the column was centrifuged at maximum speed for 2 minutes to elute the RNA. The sample was aliquoted in equal volume into two tubes and stored at -80°C.

3.2.5 Quantification of total RNA

The concentration and purity of the extracted total RNA was determined by NanoDrop 2000 spectrophotometer (Thermo Scientific, Waltham, MA, USA). Nuclease-free water

was used as the blank. The A_{260}/A_{280} and A_{260}/A_{230} ratios indicate the purity of the RNA. Values ranging from 1.8-2.2 are acceptable for downstream experiments.

3.2.6 Assessment of RNA quality

3.2.6.1 Denaturing RNA agarose gel electrophoresis

Molten RNA gel (section 3.1.5.4) was allowed to set in the gel-casting tray with a comb inserted to create wells for sample loading. After the gel has solidified, it was placed in the electrophoresis tank filled with 1X MOPS buffer (section 3.1.5.1). RNA sample of 200-300 ng was mixed with 17.5 µl of sample buffer (section 3.1.5.3) and placed in a water bath at 65°C for 10 minutes to denature the RNA. The sample was placed on ice until loading. Electrophoresis was conducted at 90V for approximately 40 minutes. RNA marker (18S + 28S ribosomal RNA [rRNA] from calf liver) (Sigma-Aldrich, St.Louis, MO, USA) was loaded as the positive control. The gel image was captured using a gel documentation system (UVP, Upland, CA, USA). RNA of good quality should reveal two distinct bands at the intensity ratio of 2:1 for 28S:18S rRNA.

3.2.6.2 Denaturing RNA PAGE

Denaturing RNA PAGE was used to assess the integrity of small RNAs (5.8S rRNA, 5S rRNA and transfer RNA [tRNA]). Molten RNA gel (section 3.1.6.3) was poured into the gel-casting tray with a comb inserted to create wells for sample loading. After the gel has solidified, it was placed in the electrophoresis tank filled with 1X TBE buffer (section 3.1.6.1) and pre-run at 100V for 30 minutes. RNA sample of 200-300 ng was mixed with 16 µl of sample buffer (section 3.1.6.4). The mixture was placed in a water

bath at 95°C for 2 minutes to denature the RNA. The sample was placed on ice until loading. Electrophoresis was conducted at 100V for approximately 1.5 hours. The gel image was captured using a gel documentation system (UVP, Upland, CA, USA). RNA of good quality should reveal three distinct bands, indicating the presence of 5.8S rRNA, 5S rRNA and tRNA.

3.2.7 miRNA microarray

Two independent miRNA microarray profiling studies of tissue and blood were conducted. In tissue miRNA array, 30 paired cancer tissue and the normal colonic mucosa samples were pooled according to stages II (n = 10), III (n = 10) and IV (n = 10). In blood miRNA array, blood samples from 42 CRC cases were grouped by tumour location (colon; rectum) and pooled into stages I (n = 3; n = 3), II (n = 9; n = 3), III (n = 9; n = 3) and IV (n = 9; n = 3). Blood samples from 18 healthy controls were used for the profiling study. Due to limited availability of stage I CRC cases, only one replicate was performed for both colon and rectal samples. Similarly, the profiling analyses of rectal samples for stages II, III and IV were also performed in one replicate. On the other hand, the profiling analyses of colon samples for stages II, III and IV were performed in triplicates and control samples in six replicates, with n = 3 each.

3.2.7.1 Sample labelling

The FlashTag Biotin HSR RNA Labelling kit (Affymetrix, Santa Clara, CA, USA) was used to label total RNA samples for the analysis by GeneChip miRNA 2.0 array (Affymetrix, Santa Clara, CA, USA). The array contains 15,644 probe sets, covering

131 organisms and detecting 1,105 human mature miRNAs. The content was derived from miRBase database version 15.0.

Total RNA was adjusted to a concentration of 1 μg in 8 μl of nuclease-free water. Two μl of RNA spike control oligos and 5 μl of poly(A) tailling master mix (section 3.1.7.3) were added. The sample was mixed and briefly centrifuged. The tube was incubated at 37°C in a thermal cycler for 15 minutes. After the incubation, 4 μl of 5X FlashTag biotin HSR ligation mix and 2 μl of T4 DNA ligase were added. The sample was mixed and briefly centrifuged. The tube was incubated at room temperature for 30 minutes. The enzyme reaction was inactivated by adding 2.5 μl of HSR stop solution. The 23.5 μl of biotin-labelled sample was mixed and briefly centrifuged. Two μl of the sample was transferred to a new PCR tube for ELOSA quality control (QC) assay (section 3.2.7.2). The remaining 21.5 μl of the sample was kept on ice until the sample hybridisation procedure (section 3.2.7.3).

3.2.7.2 ELOSA QC assay

ELOSA is a colorimetric assay that serves as a quality assurance test that the sample labelling has taken place. The assay is designed to detect successful hybridisation of RNA spike control oligos to ELOSA spotting oligos immobilised onto the ELOSA plate (Genisphere, Hatfield, PA, USA). Appropriate negative and positive controls were included. The negative control was the biotin-labelled sample without RNA spike control oligos and total RNA. The positive control was the biotinylated ELOSA positive control provided in the FlashTag Biotin HSR Labelling kit (Affymetrix, Santa Clara, CA, USA).

The number of wells needed was calculated accordingly. Each well was coated with 1.5 µl of ELOSA spotting oligos in 73.5 µl of 1X PBS. The ELOSA plate was sealed and incubated overnight at 4°C. After the overnight incubation, the coated plate was equilibrated to room temperature for 5 minutes. The plate was rinsed twice with 1X PBS, 0.02% Tween-20 (section 3.1.8.1) and blotted to dry. A volume of 150 µl of 5% BSA in 1X PBS (blocking solution) (section 3.1.8.2) was added into each well and the plate was incubated at room temperature for 1 hour. Meanwhile, the 2 µl of biotin-labelled sample (section 3.2.7.1) and the negative and positive controls for ELOSA assay were mixed with 50.5 µl of ELOSA hybridisation cocktail (section 3.1.8.5) and briefly centrifuged. After the 1 hour incubation, the blocking solution was discarded and the plate was blotted to dry. The 52.5 µl of hybridisation solution was loaded into each well and the plate was incubated at room temperature for another 1 hour. Following that, the hybridisation solution was discarded and the plate was rinsed thrice with 1X PBS, 0.02% Tween-20 and blotted to dry. An aliquot of 75 µl of the streptavidin-HRP dilution (section 3.1.8.6) was loaded into each well and left at room temperature for 30 minutes. The solution was then discarded and the wells were rinsed thrice with 1X PBS, 0.02% Tween-20. Subsequently, 100 µl of TMB substrate (Pierce, Rockford, IL, USA) was added into each well and the plate was incubated at room temperature for 30 minutes in the dark. The substrate would turn to blue colour for a successful sample labelling reaction or remain colourless for an unsuccessful reaction. After a successful ELOSA QC assay, the remaining 21.5 µl of biotin-labelled sample from section 3.2.7.1 was used for sample hybridisation.

3.2.7.3 Sample hybridisation

The Hybridisation Oven 640 (Affymetrix, Santa Clara, CA, USA) was switched on and the temperature and rotation speed were set at 48°C and 60 rpm, respectively. The

GeneChip miRNA 2.0 array (Affymetrix, Santa Clara, CA, USA) was warmed to room temperature for 15 minutes. The GeneChip Hybridisation, Wash and Stain kit (Affymetrix, Santa Clara, CA, USA) and the GeneChip Eukaryotic Hybridisation Control kit (Affymetrix, Santa Clara, CA, USA) were used in the sample preparation for hybridisation. The GeneChip Hybridisation, Wash and Stain kit consists of a hybridisation module (2X hybridisation mix and DMSO), a stain module (stain cocktail 1, stain cocktail 2 and array holding buffer), wash buffer A and wash buffer B. The GeneChip Eukaryotic Hybridisation Control kit consists of a vial of 20X eukaryotic hybridisation controls and a vial of 3 nM control oligo B2. The 20X eukaryotic hybridisation controls vial was thawed and heated at 65°C for 5 minutes. The 21.5 µl of biotin-labelled sample (section 3.2.7.1) was mixed with 81.7 µl of array hybridisation cocktail (section 3.1.7.4). The mixture was initially incubated at 99°C for 5 minutes and then at 45°C for 5 minutes. A 200 µl yellow tip was inserted into the upper right septum of the array to enable proper venting during sample injection. At the end of the incubation, 100 µl of the sample was injected into the array via the lower left septum. Precaution was taken to avoid any air bubble. The yellow tip was then removed from the upper right septum and both septa were sealed to minimise evaporation and prevent leaks. The array was placed into the hybridisation tray and loaded into the hybridisation oven. The array was incubated at 48°C; 60 rpm for 16 hours.

3.2.7.4 Washing, staining and scanning

After 16 hours of hybridisation, the array was recovered from the hybridisation oven. The sample was extracted from the array and discarded. The array was filled with 100 µl of array holding buffer and equilibrated to room temperature for 15 minutes. The Fluidics Station 450 with fluidics script FS450_0003 (Affymetrix, Santa Clara, CA,

USA) was employed in the automation of the washing and staining steps. Three 1.5 ml microcentrifuge tubes were each filled with 600 µl of stain cocktail 1, 600 µl of stain cocktail 2 and 800 µl of array holding buffer. These tubes were placed into the tube holders on the fluidics station. The washing and staining steps lasted about 1.5 hours. The GeneChip Command Console software (Affymetrix, Santa Clara, CA, USA) was used to operate the washing, staining and scanning interfaces.

At the end of the washing and staining steps, the array was filled with array holding buffer. If there were air bubbles, the array holding buffer would be extracted and re-filled manually. Once the array was confirmed to be free from air bubbles, both septa were re-sealed and sent for scanning. Scanning of the miRNA array was performed using the GeneChip Scanner 3000 7G (Affymetrix, Santa Clara, CA, USA). Data summarisation, normalisation and quality control of the raw signal intensity data in relation to the RNA spike control oligos (spike in-control-2, -23, -29, -31 and -36) were performed using miRNA QC Tool software (Affymetrix, Santa Clara, CA, USA). Each probe set of the RNA spike control oligos should reveal a signal background higher than 1,000 units. The data were then saved as CEL file format and exported into third party software for further analysis.

3.2.7.5 Microarray data analysis

The miRNA microarray data analysis was conducted using GeneSpring GX 12.0 software (Agilent, Santa Clara, CA, USA). Robust multichip averaging (RMA) algorithm was applied for background correction and probe summarisation of perfect match values in each array. Median intensity values for each miRNA from the same replicates were calculated and subjected to quantile normalisation to normalise the data across different arrays (Irizarry et al., 2003). The normalised data were analysed using *t*-

test/analysis of variance (ANOVA) with *p*-value computation done asymptotically at $p < 0.05$. Subsequently, the gene list was filtered at a fold change cut-off of 1.5. Hierarchical clustering was computed using similarity measure of Euclidean distance and average-linkage rule, and expressed in the form of heat map and three dimensional (3D) principal component analysis (PCA) plot (Gibbons & Roth, 2002).

3.2.8 RT

3.2.8.1 RT for miRNA

RT procedure is needed to synthesise complementary DNA strands. For a 15 µl of miRNA RT reaction, 7 µl of RT master mix (section 3.1.9.1) was mixed with 3 µl of miRNA RT primer and 5 µl of total RNA (10 ng) in a 0.2 ml PCR tube. The mixture was mixed gently and centrifuged. RT was carried out in a thermal cycler (PerkinElmer, Waltham, MA, USA) at 16°C for 30 minutes; 42°C for 30 minutes; 85°C for 5 minutes and hold at 4°C. miRNA RT primer was supplied as a separate tube in the TaqMan miRNA assay (Applied Biosystems, Carlsbad, CA, USA).

3.2.8.2 RT for mRNA

For a 10 µl of mRNA RT reaction, 6.15 µl of RT master mix (section 3.1.9.2) was mixed with 3.85 µl of total RNA (200 ng) in a 0.2 ml PCR tube. The mixture was mixed gently and centrifuged. RT was performed using a thermal cycler (PerkinElmer, Waltham, MA, USA) at 25°C for 10 minutes; 48°C for 30 minutes; 95°C for 5 minutes and hold at 4°C.

3.2.9 qPCR for miRNA and mRNA

For miRNA, qPCR mastermix of 18.67 µl (section 3.1.10.1) was prepared and mixed with 1.33 µl of miRNA RT product (section 3.2.8.1). For mRNA, qPCR mastermix of 19 µl (section 3.1.10.2) was prepared and mixed with 1 µl of mRNA RT product (section 3.2.8.2). qPCR reaction was performed in triplicates using MicroAmp Fast Optical 96-well reaction plate (Applied Biosystems, Carlsbad, CA, USA). The plate was sealed with MicroAmp Optical adhesive film (Applied Biosystems, Carlsbad, CA, USA). qPCR reaction was conducted using StepOnePlus Real-Time PCR machine (Applied Biosystems, Carlsbad, CA, USA) based on the fast mode parameters: uracil N-glycosylase incubation (50°C for 2 minutes); AmpliTaq Fast DNA polymerase activation (95°C for 20 seconds); 40 cycles of denaturing (95°C for 1 second) and annealling/extending (60°C for 20 seconds).

Relative expression was determined using comparative cycle threshold (C_T) method, via $2^{-\Delta\Delta CT}$ formula (Schmittgen & Livak, 2008). A C_T value above 36 was set as the cut-off for defining as non-detected (Caraguel, Stryhn, Gagné, Dohoo, & Hammell, 2011; Jordan & Durso, 2005). The expression of each miRNA or mRNA relative to the respective endogenous control, RNU48 or *β-actin*, was presented as ΔC_T (C_T gene of interest – C_T endogenous control). The ΔC_T values of the cancer and control groups were subjected to paired/unpaired *t*-test (Yuan, Reed, Chen, & Stewart Jr, 2006). The fold change ($2^{-\Delta\Delta CT}$) value was calculated using the equation: $2^{-\ (\Delta CT\ cancer\ sample\ -\ \Delta CT\ control\ sample)}$.

3.2.10 Total protein extraction from CRC tissue and cultured cells

Total protein from CRC tissue and cultured cells was extracted using T-PER tissue protein extraction reagent (Pierce, Rockford, IL, USA) and radio-immunoprecipitation assay (RIPA) buffer (Pierce, Rockford, IL, USA), respectively. Halt protease and phosphatase inhibitor cocktail (Pierce, Rockford, IL, USA) was added at the concentration of 10 µl/ml prior to use. For CRC tissue, 30 mg of tissue was weighed and immersed in 600 µl of T-PER reagent. The sample was homogenised until no visible piece of tissue was observed. For cultured cells, the cells were washed twice with 1X cold PBS before the addition of 250 µl of RIPA buffer into three wells of a 6-well plate. The plate was placed on a shaker for 5 minutes and the cells were scraped using a cell scraper. The lysed cells from the three wells were pooled into a 1.5 ml microcentrifuge tube. The tissue/cell lysate was centrifuged at maximum speed for 10 minutes. The supernatant containing the total protein was collected and aliquoted in equal volume into two tubes. The extracted total protein was stored at -80°C.

3.2.11 Quantification of total protein

The concentration of the extracted total protein was determined by Pierce 660 nm assay (Pierce, Rockford, IL, USA). Pre-diluted BSA protein assay standards (125 µg/ml; 250 µg/ml; 500 µg/ml; 750 µg/ml; 1000 µg/ml; 1500 µg/ml; 2000 µg/ml) (Pierce, Rockford, IL, USA) were utilised to generate a standard curve for the determination of protein concentration from unknown samples. Nuclease-free water was used as the blank. Protein quantification was carried out with a sample:protein assay reagent ratio of 1:15. One µl of each assay standard/unknown sample/blank was added to 15 µl of protein assay reagent. The mixture was vortexed and incubated at room temperature for 5 minutes in the dark. The absorbance was measured at a wavelength of 660 nm by

NanoDrop 2000 spectrophotometer (Thermo Scientific, Waltham, MA, USA). For cell lysates prepared in RIPA buffer, 0.4 µl of 10% Triton X-100 (section 3.1.11) was added to 4.6 µl of each sample prior to the addition of protein assay reagent. The exact protein concentration was calculated by multiplying the concentration obtained with a dilution factor of 1.087.

3.2.12 SDS-PAGE and Western blot

3.2.12.1 Preparation of SDS-PAGE

The apparatus for SDS-PAGE, Mini-PROTEAN Tetra Cell (Bio-Rad, Hercules, CA, USA) was set up. Briefly, the spacer and short plates were sandwiched together. The comb was inserted and a line around 1 cm from the bottom of the comb was marked. The line served as the maximum level for resolving gel loading. The glass cassette sandwich was then placed in the casting frame and casting stand. The recipe for the preparation of resolving (10%) and stacking (4%) gels is provided in section 3.1.12.6. Resolving gel was prepared first and loaded until the marked line. Distilled water was added immediately to the top of the gel to level the surface and remove any air bubble. The resolving gel was allowed to set for 45 minutes. After the resolving gel has polymerised, the distilled water was decanted and excess water was blotted by using an absorbent tissue. Stacking gel was then loaded to fill the glass cassette sandwich. A 1 mm comb was inserted to create wells for sample loading. The stacking gel was left to polymerise for 30 minutes. The glass cassette sandwich was then assembled in the electrophoresis tank and filled with 1X electrode running buffer (section 3.1.12.5). Forty µg of protein sample (10 µl) was mixed with 10 µl of SDS reducing sample buffer (section 3.1.12.4) and heated at 95°C for 10 minutes. The sample was loaded into the well and SDS-PAGE was run at 100V for about 1.5 hours. Five µl of SuperSignal

molecular weight protein ladder (Pierce, Rockford, IL, USA) was also loaded and used to monitor the electrophoresis run and membrane transfer.

3.2.12.2 Membrane transfer

After the completion of SDS-PAGE, the stacking gel was discarded while the resolving gel was equilibrated in cold transfer buffer (section 3.1.13) for 15 minutes with agitation. Wet transfer system using Mini Trans-Blot Cell (Bio-Rad, Hercules, CA, USA) was applied. Nitrocellulose transfer membrane of 0.45 μm (Pierce, Rockford, IL, USA) was utilised. The 8 x 10 cm nitrocellulose membrane, sponges and thick blot papers needed for the membrane transfer were also soaked in cold transfer buffer for 15 minutes. The transfer cassette sandwich was assembled from anode to cathode in the following order: sponge, thick blot paper, nitrocellulose membrane, resolving gel, thick blot paper and sponge. A 15 ml centrifuge tube was used to roll over the thick blot paper to remove any air bubble. The assembly was then placed in the transfer tank and filled with cold transfer buffer. Membrane transfer was performed at 100V for 1 hour.

After the 1 hour of membrane transfer, the transfer cassette sandwich was disassembled and the membrane was stained using the MemCode Reversible Protein Stain kit (Pierce, Rockford, IL, USA) to evaluate the transfer efficiency. The blot was initially rinsed with distilled water prior to incubation with 25 ml of MemCode reversible protein stain for 1 minute with agitation. Protein bands would appear turquoise-blue. Once the presence of protein bands was confirmed, the blot was rinsed thrice with 25 ml of MemCode destain reagent. The procedure was followed by rinsing the blot with distilled water for four times. Thirty ml of MemCode stain eraser was then added and incubated for 5 minutes with agitation. The blot was eventually rinsed with distilled water for four times and followed by a final wash for 5 minutes with agitation.

3.2.12.3 Western blot

After confirming the efficiency of protein transfer, the blot was processed using the Fast Western Blot kit (Pierce, Rockford, IL, USA). The blot was briefly rinsed with 15 ml of Fast Western 1X wash buffer (section 3.1.14.1). Primary antibody working solution (section 3.1.14.2) of mouse monoclonal anti-β-actin, rabbit polyclonal anti-APAF1 or rabbit polyclonal anti-FOXO4 (Pierce, Rockford, IL, USA) was added to the blot and incubated at 4°C for 1 hour. After the primary antibody incubation, the blot was placed in a clean tray and rinsed with 15 ml of Fast Western 1X wash buffer. Fast Western optimised HRP reagent working solution (section 3.1.14.3) was added and incubated at room temperature for 15 minutes. The blot was then placed in a clean tray and washed with 20 ml of Fast Western 1X wash buffer for 5 minutes with agitation. The washing step was repeated twice. Subsequently, the blot was removed and placed in a plastic wrap. Four ml of detection reagent working solution (section 3.1.14.4) was applied onto the blot and incubated at room temperature for 1 minute. Precaution was taken to avoid any air bubble. The blot was visualised via a chemiluminescence imager (UVP, Upland, CA, USA) with 3-5 minutes exposure. The intensities of the bands were quantitated using the imager's VisionWorksLS software.

3.2.12.4 Resolving polyacrylamide gel staining

After the membrane transfer procedure in section 3.2.12.2, the resolving gel was retrieved from the transfer cassette sandwich and rinsed twice with distilled water for 5 minutes on a shaking platform. The resolving gel was submerged in 50 ml of Bio-Safe Coomassie stain (Bio-Rad, Hercules, CA, USA) for 30 minutes. Following that, the stain solution was decanted and the gel was destained with distilled water for 15 minutes. Protein bands would be visible on the gel if the membrane transfer was

unsuccessful. This method serves as an additional assay to access the efficiency of protein transfer.

3.2.13 Bacterial culture and sub-cloning

3.2.13.1 Bacterial culture

The pMIR-REPORT firefly luciferase miRNA expression reporter vector (Ambion, Carlsbad, CA, USA) was supplied as *Escherichia coli* glycerol stock and stored at -80°C. GeneArt pMA-T vectors containing the putative 3'-UTR fragments or the site-directed mutants (Invitrogen, Carlsbad, CA, USA) were supplied as stab cultures of *E. coli* and stored at -20°C. All stock cultures were slightly thawed on ice and two loopfuls (around 20 µl) of each culture were transferred aseptically into round bottom tubes containing 2 ml of LB-ampicillin broth (section 3.1.15.6). The bacterial cultures were grown overnight at 37°C; 180 rpm to propagate the plasmids.

3.2.13.2 Plasmid DNA extraction

Plasmid DNA extraction was carried out using the PureLink Quick Plasmid Miniprep kit (Invitrogen, Carlsbad, CA, USA). Two ml of an overnight culture was transferred to a microcentrifuge tube and spun at maximum speed for 5 minutes. The supernatant was discarded by pouring. The steps were repeated twice for a total of 6 ml of bacterial culture. The pellet was then resuspended with 250 µl of L7 lysis buffer and incubated at room temperature for 5 minutes. Next, 350 µl of N4 precipitation buffer was added. The tube was mixed by inversion and centrifuged at 12,000 rpm for 10 minutes at room temperature. The supernatant was loaded onto the provided spin column and centrifuged

at 12,000 rpm for 1 minute. The flow-through was discarded and 500 µl of W10 wash buffer was added. The spin column was left at room temperature for 1 minute and centrifuged at 12,000 rpm for 1 minute. The flow-through was again discarded and 700 µl of W9 wash buffer was added and centrifuged at 12,000 rpm for 1 minute. A final centrifugation at maximum speed for 1 minute was performed to remove any residual wash buffer from the spin column. Subsequently, the spin column was transferred to a new microcentrifuge tube and 75 µl of TE buffer (pre-heated to 67°C) was added to the centre of the column. The spin column was incubated at room temperature for 3 minutes and centrifuged at maximum speed for 2 minutes to elute the plasmid DNA. The purified plasmid DNA was stored at -20°C. The concentration of the plasmid DNA was determined by NanoDrop 2000 spectrophotometer, similar to the method in section 3.2.5. The quality of the plasmid DNA was assessed using DNA gel electrophoresis (section 3.2.13.4).

3.2.13.3 Restriction enzyme digestion

Restriction enzyme digestion was carried out to linearise and create sticky ends at the pMIR-REPORT firefly luciferase vector and the 3'-UTR fragment of the pMA-T vector prior to sub-cloning. This procedure was also performed to determine the presence of the cloned fragment after transformation. One µg of plasmid DNA was added to the restriction enzyme mixture (section 3.1.15.2). The mixture was incubated at 37°C in a thermal cycler for 20 minutes. The enzymes were then inactivated via incubation at 80°C for 10 minutes. The restriction enzyme digestion was analysed using DNA gel electrophoresis (section 3.2.13.4).

3.2.13.4 DNA gel electrophoresis

Molten DNA gel (section 3.1.15.1) was allowed to set in the gel-casting tray with a comb inserted to create wells for sample loading. Once the gel has solidified, it was placed in the electrophoresis tank filled with 1X TBE buffer (section 3.1.6.1). An aliquot of 2.5 µl of plasmid DNA sample (section 3.2.13.2) was mixed with 0.5 µl of 6X DNA loading dye (Fermentas, Waltham, MA, USA) prior to sample loading. For restriction enzyme digestion (section 3.2.13.3), the usage of FastDigest green buffer enabled a direct loading of the reaction mixture. Two µl of GeneRuler 1 kb DNA ladder (Fermentas, Waltham, MA, USA) was used as the molecular weight marker. Electrophoresis was conducted at 100V for approximately 40 minutes. The gel image was captured using a gel documentation system (UVP, Upland, CA, USA). For sub-cloning purposes, the digested fragments were excised using a clean scalpel and used in DNA gel extraction (section 3.2.13.5).

3.2.13.5 DNA gel extraction

DNA gel extraction was carried out using the GeneJET Gel Extraction and DNA Cleanup Micro kit (Thermo Scientific, Waltham, MA, USA). A total of 200-250 mg of gel slice containing the DNA fragment was excised using a clean scalpel and transferred to a microcentrifuge tube. The gel slice was loaded with 200 µl of extraction buffer and incubated at 58°C for 10-20 minutes until the gel slice has completely dissolved. The tube was mixed by inversion every 3 minutes to facilitate the melting process. A volume of 200 µl of absolute ethanol was added and mixed by pipetting. The sample was loaded onto the provided purification column and centrifuged at 14,000 rpm for 1 minute. The flow-through was discarded and the column was washed once with 200 µl of prewash buffer and twice with 700 µl of wash buffer via centrifugation at 14,000 rpm for 1

minute. Subsequently, the column was spun at maximum speed for 1 minute to remove any residual wash buffer. The column was then transferred to a new microcentrifuge tube and 10 µl of elution buffer was loaded. The column was incubated at room temperature for 2 minutes. The DNA was eluted by centrifuging the column at maximum speed for 2 minutes. The extracted DNA was stored at -20°C. The concentration of the extracted DNA was determined by NanoDrop 2000 spectrophotometer, similar to method in section 3.2.5.

3.2.13.6 Ligation and transformation

Ligation reaction between vector DNA and insert DNA was performed using a vector DNA:insert DNA molar ratio of 1:5, which indicated a reaction involving 50 ng of vector DNA (pMIR-REPORT firefly luciferase vector) and 250 ng of excised insert DNA. The ligation mixture (section 3.1.15.4) was incubated at 22°C in a thermal cycler for 1 hour. The ligation mixture was then used for transformation.

One vial (50 µl) of One Shot Top10 Chemically Competent *E. coli* cells (Invitrogen, Carlsbad, CA, USA) was thawed on ice. Five µl of the ligation mixture was added into the vial. The vial was mixed by flicking and left standing on ice for 30 minutes. Next, heat shock method was conducted, whereby the vial was immediately returned to ice after a short incubation at 42°C for 1 minute. Two hundred and fifty µl of the provided SOC medium was then added and the vial was incubated at 37°C; 180 rpm in a shaking incubator for 1 hour. Finally, the transformation mix was spreaded onto two LB-ampicillin agar plates (section 3.1.15.7), each with 150 µl of transformation mix. The agar plates were incubated overnight at 37°C. Single colonies were then picked using sterile loops and allowed to grow overnight in tubes containing 2 ml of LB-ampicillin broth (section 3.1.15.6) at 37°C; 180 rpm. Two loopfuls (around 20 µl) of each

overnight culture were then transferred to new tubes containing LB-ampicillin broth to propagate more clones necessary for plasmid DNA extraction (section 3.2.13.2). An aliquot of 0.5 ml of the bacterial culture was stocked in 0.5 ml of 80% glycerol (section 3.1.15.8).

3.2.13.7 Plasmid DNA sequencing

Ten µl of the purified plasmid DNA (50 ng/µl) was sent for sequencing service. According to the sequencing primers listed in the pMIR-REPORT firefly luciferase miRNA expression reporter vector system (Ambion, Carlsbad, CA, USA), three sequencing primers were chosen: forward 5'–AGGCGATTAAGTTGGGTA–3', forward 5'–GAGGTAGATGAGATGTGA–3' and reverse 5'–ATTGCAACGATTTAGGTG–3'. Sequence alignment was then conducted via BLASTN software offered by the NCBI database. This step was performed to confirm a successful ligation reaction between the vector backbone and insert DNA after transformation.

3.2.14 miRNA and luciferase reporter co-transfection

SW480 cell line was used as the host in the co-transfection study. Cells were seeded in antibiotic-free complete medium at 2 x 10^4 cells per well on a 96-well white plate one day before transfection. In the first phase of transfection involving miRNA, 0.25 µl of Lipofectamine 2000 transfection reagent (Invitrogen, Carlsbad, CA, USA) was diluted in 25 µl of Opti-MEM I reduced serum medium (Gibco, Carlsbad, CA, USA) and incubated at room temperature for 5 minutes. miRIDIAN miRNA mimic or inhibitor (Dharmacon, Lafayette, CO, USA) was diluted to a concentration of 5 pmol in 25 µl of Opti-MEM I reduced serum medium. Both mixtures were combined and incubated at

room temperature for 20 minutes. After the incubation, the plated medium was removed and the miRNA-transfection mixture was added into each well. The plate was incubated in the 5% CO_2-humidified incubator at 37°C for 3 hours.

In the second phase of transfection involving plasmid DNA, 0.25 µl of Lipofectamine 2000 transfection reagent was complexed with 25 µl of Opti-MEM I reduced serum medium and incubated at room temperature for 5 minutes. pMIR-REPORT firefly luciferase reporter vector containing either the target recognition or mutated site (100 ng) and pRL-SV40 *Renilla* luciferase control reporter vector (10 ng) were diluted in 25 µl of Opti-MEM I reduced serum medium. Both mixtures were combined and incubated at room temperature for 20 minutes.

At the end of the 3 hours of miRNA transfection, the medium was removed and the cells were washed with 50 µl of Opti-MEM I reduced serum medium. The plasmid-transfection mixture was then added into each well and incubated in the 5% CO_2-humidified incubator for another 3 hours. After that, the medium was changed to antibiotic-free complete medium and the cells were left to grow for 48 hours, following which luciferase assay (section 3.2.15) was conducted. The transfection controls included were NTC cells and cells co-transfected with miRNA and pMIR-REPORT firefly luciferase reporter vector without target recognition or mutated site. Each transfection experiment was performed in triplicates in three independent experiments.

3.2.15 Luciferase assay

The Dual-Glo Luciferase assay (Promega, Madison, WI, USA) was used to study the interaction between miRNA and its predicted target gene. The assay allows the measurement of two independent reporter enzymes within a single system. Firefly

luciferase vector was the main reporter used in the evaluation of miRNA interaction while *Renilla* luciferase vector was used to determine the transfection efficiency. After 48 hours of co-transfection (section 3.2.14), the plate was equilibrated to room temperature for 5 minutes and 75 µl of Dual-Glo Luciferase reagent was added into each well. The plate was incubated for 10 minutes in the dark before the measurement of firefly luminescence. Once the measurement has completed, 75 µl of Dual-Glo Stop and Glo reagent was added to quench the luminescence signal from the firefly reaction. The plate was incubated for 10 minutes in the dark and the *Renilla* luminescence was measured. Infinite M200-Pro plate reader (Tecan, Männedorf, Zurich, Switzerland) was used for the luminescence measurements. Transfection efficiency was normalised by dividing the firefly luciferase signal with the *Renilla* luciferase signal.

3.2.16 MTT assay

MTT assay was performed according to the guidelines in MTT Cell Proliferation kit (OZ Biosciences, Marseille, France). It is a colorimetric assay that measures the activity of mitochondrial reductase enzyme in reducing MTT to formazan dye in viable cells. Cell viability following miRNA mimics and inhibitors transfections was determined. Cells (2×10^4) were seeded in 96-well plate and miRNA transfections were carried out accordingly in triplicates for 24, 48 and 72 hours. At the end of each transfection period, cultured cells were washed with pre-warmed 1X PBS. One hundred µl of 1X MTT (section 3.1.16) was added into each well and the plate was incubated in the 5% CO_2-humidified incubator at 37°C for 4 hours. At the end of the incubation, 100 µl of solubilisation solution was added. The plate was placed on a shaker for 15 minutes to ensure that the converted dye has completed dissolved. The absorbance was measured at a wavelength of 570 nm and a reference wavelength at 650 nm using Infinite M200-Pro

plate reader (Tecan, Männedorf, Zurich, Switzerland). Wells with complete medium were used as the blank. The viability of the transfected sample was expressed as a percentage of the NTC sample.

3.2.17 Apoptosis assay and image-based cytometry

Apoptosis assay was performed using the Annexin V-Fluorescein Isothiocyanate (FITC) Apoptosis Detection kit (BioVision, Milpitas, CA, USA). During apoptosis, membrane phosphatidylserine is translocated from the inner surface to the outer surface of the plasma membrane. Annexin V is a calcium-dependent phospholipid-binding protein that has a high affinity for phosphatidylserine. Annexin V-FITC fluorescent dye is used to stain cells that are undergoing apoptosis while propidium iodide (PI) stain is used to identify necrotic cells that have lost their membrane integrity. Cells that are stained positive for Annexin V-FITC but negative for PI are apoptotic cells. Cells with positive results for both Annexin V-FITC and PI are either late apoptotic or dead cells while cells with negative results for both Annexin V-FITC and PI are live cells.

miRNA transfection procedure was conducted according to section 3.2.3 using 6-well plate. After 48 hours of transfection, the cells were harvested and a cell pellet containing 5 x 10^5 cells was collected in a microcentrifuge tube. The cell pellet was resuspended with 500 µl of 1X binding buffer. Five µl of both Annexin V-FITC and PI reagents were added. The cell suspension was gently vortexed and left in the dark at room temperature. Measurement was performed within one hour of staining. The sample (25 µl) was loaded onto a Tali cellular analysis slide (Invitrogen, Carlsbad, CA, USA). Quantitative analysis of live (Annexin V-negative/PI-negative), dead (Annexin V-positive/PI-positive) and apoptotic (Annexin V-positive/PI-negative) cell populations was evaluated using Tali image-based cytometer (Invitrogen, Carlsbad, CA, USA). An unstained

sample was initially analysed and set as the background in order to determine the fluorescent thresholds. Each sample was then gated according to the initial thresholds. An anti-cancer drug doxorubicin (50 μM) was used as the positive control. All assays were performed in triplicates in three separate experiments.

3.2.18 Caspase 3/7 assay

The Caspase-Glo 3/7 assay (Promega, Madison, WI, USA) was used to measure the activation of caspase-3 and -7 activities. Cells (2×10^4 cells/well) were seeded in 96-well white plate and miRNA transfections were carried out accordingly in triplicates. After 48 hours of transfection, the plate was removed from the incubator and equilibrated to room temperature for 5 minutes. One hundred μl of Caspase-Glo 3/7 reagent was added into each well and the plate was incubated at room temperature for 3 hours prior to luminescence detection using Infinite M200-Pro plate reader (Tecan, Männedorf, Zurich, Switzerland). Wells with complete medium were used as the blank. The caspase 3/7 activity of the transfected sample was expressed as a percentage of the NTC sample.

3.2.19 Migration and invasion assays

Migration and invasion assays were performed on 24-well transwell plates containing inserts of 8 μm pore size (BD Biosciences, Franklin Lakes, NJ, USA). Uncoated chambers were used for migration assay while Matrigel-coated chambers were used for invasion assay. Matrigel matrix aliquot was thawed overnight on ice in a cold room at 4°C. Since Matrigel matrix would gel at a temperature above 10°C, pre-cooled pipettes, tips and tubes have to be used during the handling of the Matrigel matrix. Matrigel

coating solution with a working concentration of 250 μg/ml (section 3.1.17.2) was prepared and the solution was kept on ice until use. A volume of 100 μl of Matrigel coating solution was sufficient to coat one 24-well cell culture insert. The transwell plate was allowed to coat in the 5% CO_2-humidified incubator at 37°C for 2 hours. An equal number of uncoated inserts was prepared. Following incubation, the inserts were rinsed with 200 μl of serum-free basal medium.

miRNA transfection procedure was carried out according to section 3.2.3 using 6-well plate. After 48 hours of transfection, the cells were harvested and a 500 μl of cell suspension containing 2.5 x 10^5 cells in basal medium was prepared. The cell suspension was loaded onto the 24-well cell culture insert. Complete medium containing 10% serum (750 μl) was used as the chemoattractant in the lower chamber. The plate was incubated in the 5% CO_2-humidified incubator at 37°C for 24 hours. Following that, the medium was removed and the inner side of the 24-well insert was swabbed to remove the non-migrating or non-invading cells. Cells on the lower surface of the insert were rinsed with 1X PBS, fixed with 3.7% formaldehyde in 1X PBS (section 3.1.17.3) for 5 minutes and permeabilised with 100% methanol for 15 minutes. The cells were then stained with Wright-Giemsa stain (Sigma-Aldrich, St.Louis, MO, USA) for 15 minutes, rinsed twice with 1X PBS and air-dried for 15 minutes. Finally, the cells were counted using an inverted microscope (ECLIPSE Ti-S, Nikon, Tokyo, Japan) at 100X magnification. Five random fields from each insert were captured and analysed using Image-J software (National Institute of Health; http://imagej.nih.gov/ij/). The migration and invasion assays were repeated in three independent experiments.

3.2.20 miRNA target prediction analysis

miRNA target prediction was computed using miRWalk (http://www.umm.uni-heidelberg.de/apps/zmf/mirwalk), a database that integrates several miRNA target prediction programmes (Dweep, Sticht, Pandey, & Gretz, 2011). An informative prediction was assumed when a putative target was concordantly identified by five of the most common algorithms (DIANA-MicroT, miRanda, miRWalk, MirTarget2/miRDB, PicTar, RNA22, RNAhybrid and TargetScan Human). TargetScan Human (version 6.2) was chosen as the main algorithm in determining the predicted miRNA:mRNA pairing region. The algorithm produces a list of hundreds of target genes based on the presence of conserved sites (8mer, 7mer-m8 or 7mer-1A) at the 3'-UTR of mRNAs that match the seed region of the selected miRNA. Human miRNA is typically represented with the prefix "hsa", which stands for *Homo sapiens*. For simplicity, all miRNAs stated in the present study are human miRNAs, unless stated otherwise.

3.2.21 Statistical analysis

The patients' demographics were reported as mean ± standard deviation (SD) or frequencies and percentages for continuous and categorical variables, respectively. Chi-square test was used in the analysis of age distribution while Fisher's exact test was used in the analysis of gender and race distributions. Microarray data analysis was carried out as outlined in section 3.2.7.5. Data from RT-qPCR and cell culture experiments were expressed as mean ± standard error of mean (SEM). Statistical significance was determined by paired/unpaired *t*-test and a two-tailed *p*-value of < 0.05 was considered to be statistically significant. Correlation analysis was determined by Pearson's test. Logistic regression and receiver operating characteristic (ROC) curve

analyses were applied to obtain diagnostic utility of the selected miRNAs. Statistical analysis was performed using SPSS version 16.0 software (IBM, Armonk, NY, USA).

CHAPTER 4

RESULTS

4.1 Demographics

A total of 112 CRC patients and 50 healthy controls were recruited in this study. Tables 4.1 and 4.2 summarise the distribution of the whole blood and paired cancer tissue cohorts. No significant differences were observed between the CRC patients and controls in the distribution of age (p = 0.171) and gender (p = 0.174). Malaysia is made up of a multi-ethnic population. The National Cancer Registry of Malaysia has reported a higher proportion of CRC cases in the Malaysian Chinese population (Zainal Ariffin & Nor Saleha, 2011). Thus, approximately 52.47% of the samples obtained were from the Malaysian Chinese and the remainders were from the Malays (25.31%) and Malaysian Indians (22.22%) (p = 0.202). All CRC cases in this study were adenocarcinomas. The detailed demographic data of the participants are given in Appendix 2.

Table 4.1: Distribution of the CRC patient and healthy control blood cohorts.

Characteristics		**CRC patient blood cohort (*n* = 112), *n* (%)**	**Control blood cohort (*n* = 50), *n* (%)**	***p*-value[a]**
Age (mean year ± SD)		64.43 ± 9.05	61.54 ± 10.31	0.171
Gender	Male	67 (59.82%)	24 (48.00%)	0.174
	Female	45 (40.18%)	26 (52.00%)	
Race	Malay	26 (23.12%)	15 (30.00%)	0.202
	Chinese	64 (57.14%)	21 (42.00%)	
	Indian	22 (19.64%)	14 (28.00%)	
TNM stage	I	25 (22.32%)		
	II	32 (28.57%)		
	III	31 (27.68%)		
	IV	24 (21.43%)		
Tumour location	Colon	72 (64.29%)		
	Rectum	40 (35.71%)		
Tumour grading	G1	25 (22.32%)		
(adenocarcinoma)	G2	76 (67.86%)		
	G3	11 (9.82%)		

[a]*p*-value for age was calculated by chi-square test; *p*-values for gender and race were calculated by Fisher's exact test.

Table 4.2: Distribution of the sub-set of paired cancer tissue.

Characteristics		**Sub-set of paired cancer tissue (*n* = 60), *n* (%)**
Age (mean year ± SD)		63.78 ± 8.55
Gender	Male	33 (55.00%)
	Female	27 (45.00%)
Race	Malay	10 (16.67%)
	Chinese	38 (63.33%)
	Indian	12 (20.00%)
TNM stage	I	0
	II	20 (33.33%)
	III	20 (33.33%)
	IV	20 (33.33%)
Tumour location	Colon	60 (100.00%)
	Rectum	0
Tumour grading	G1	13 (21.67%)
(adenocarcinoma)	G2	43 (71.67%)
	G3	4 (6.67%)

4.2 Assessment of RNA quality and integrity

High quality total RNA is crucial for obtaining reliable microarray and RT-qPCR results. The concentration and purity of the extracted total RNA from blood and tissue samples were determined spectrophotometrically. The A_{260}/A_{280} and A_{260}/A_{230} ratios for all the extracted total RNA samples were in the range of 1.8-2.2. The 1.8-2.2 range indicates the absence of protein, phenol and other contaminants in a sample. The RNA band integrity was assessed using denaturing RNA agarose and polyacrylamide gels. High quality RNA would reveal two sharp bands at the intensity ratio of 2:1 for 28S:18S rRNA on the agarose gel (Figure 4.1) and three distinct bands for 5.8S rRNA, 5S rRNA

and tRNA on the polyacrylamide gel (Figure 4.2) (Skrypina, Timofeeva, Khaspekov, Savochkina, & Beabealashvilli, 2003; Yeh & Lee, 1988). All the agarose and polyacrylamide gel electrophoresis images are shown in Appendices 3 and 4, respectively. Moreover, samples that were used in miRNA microarray assays were evaluated using Agilent 2100 Bioanalyzer (Figure 4.3). A RIN of 1.0 represents almost fragmented and degraded RNA while a RIN of 10.0 represents intact and non-fragmented RNA (Schroeder et al., 2006). RNA samples with RIN ≥ 7.0 and absence of DNA contamination were used (Appendix 5).

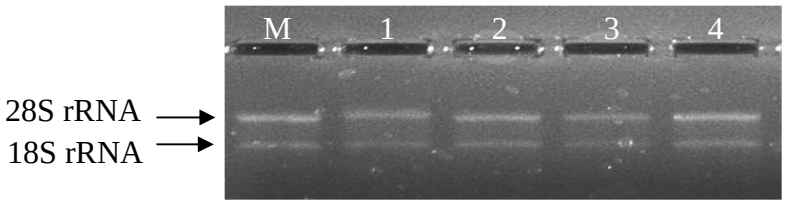

Figure 4.1: Denaturing agarose gel electrophoresis. High quality total RNA preparation was demonstrated by the sharp bands for 28S rRNA and 18S rRNA.

Lane M: 18S + 28S rRNA marker

Lane 1: CRC blood RNA

Lane 2: Control blood RNA

Lane 3: CRC tissue RNA

Lane 4: Normal colonic tissue RNA

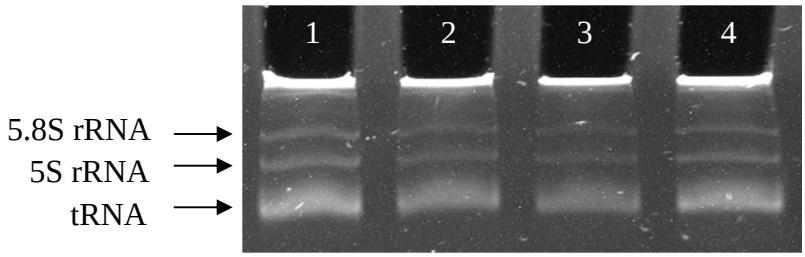

Figure 4.2: Denaturing polyacrylamide gel electrophoresis. High quality total RNA preparation was demonstrated by the distinct bands for 5.8S rRNA, 5S rRNA and tRNA.

Lane 1: CRC blood RNA

Lane 2: Control blood RNA

Lane 3: CRC tissue RNA

Lane 4: Normal colonic tissue RNA

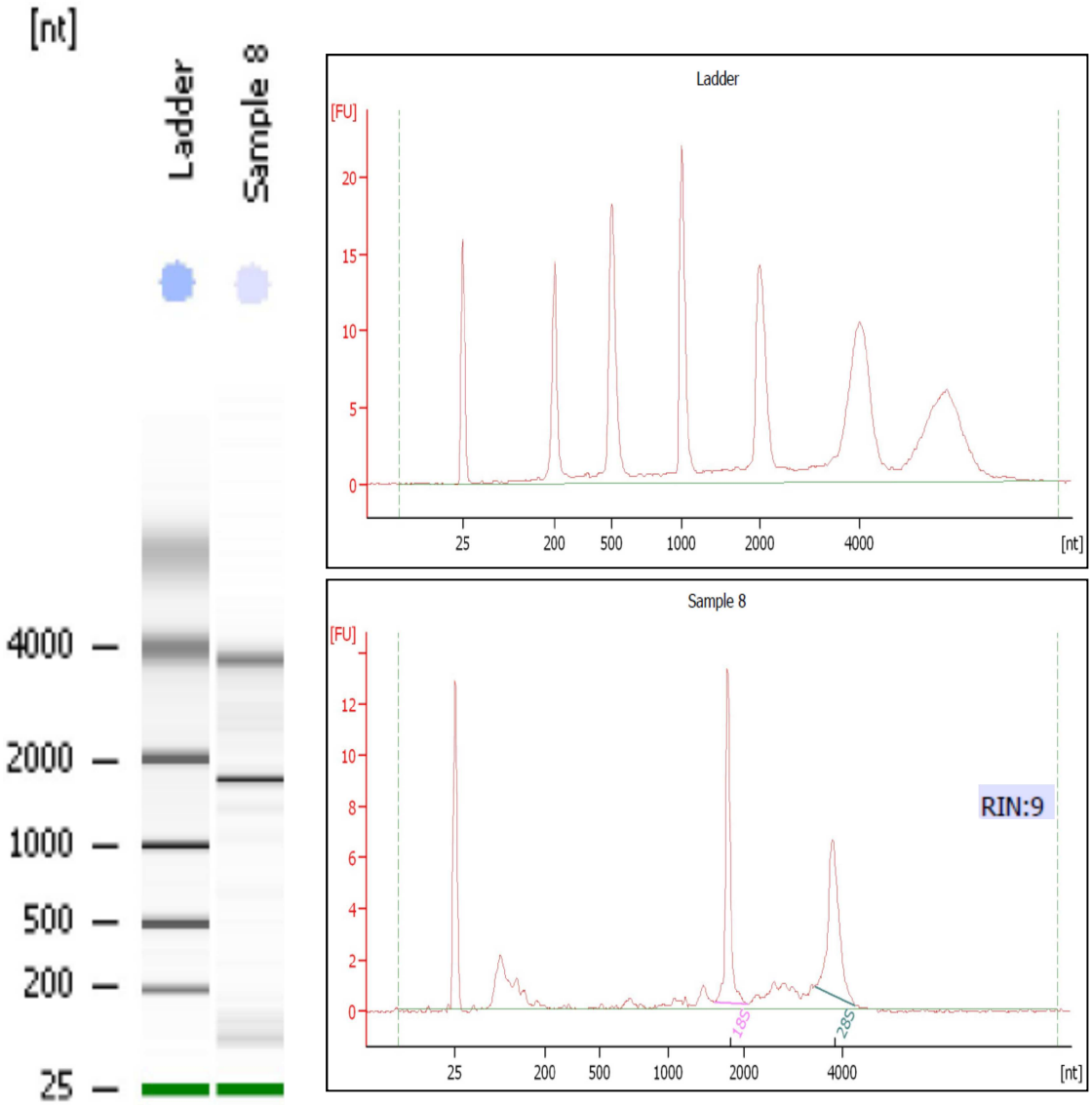

Figure 4.3: RNA integrity analysis. The figure shows the gel (left) and electropherogram (right) of the RNA ladder and sample obtained from Agilent 2100 Expert software. The RNA integrity analysis for Sample 8 (CRC blood RNA) revealed a RIN of 9. The two distinct 18S and 28S peaks observed in the sample electropherogram indicated high integrity total RNA.

4.3 Tissue and blood miRNA microarray profiling studies

In the discovery of global miRNA expression in cancer tissue and whole blood, two independent miRNA microarray profiling studies were conducted. Prior to pursuing with the microarray data analysis, data summarisation, normalisation and quality control of the raw signal intensity data for all arrays (n = 26) were performed (Figure 4.4).

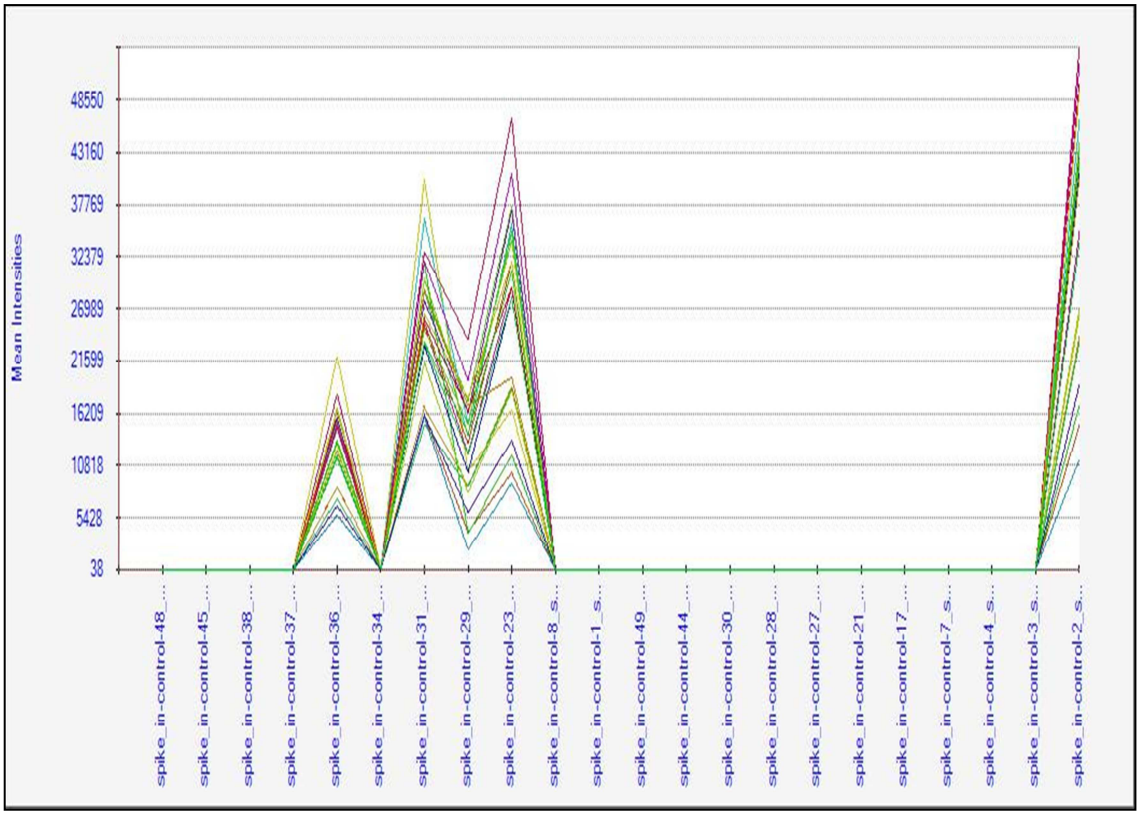

Figure 4.4: miRNA QC Tool analysis. Data summarisation, normalisation and quality control of the raw signal intensity data in relation to the RNA spike control oligos (spike in-control-2, -23, -29, -31 and -36) were conducted. Each probe set of the RNA spike control oligos revealed a signal background higher than 1,000 units. Thus, all arrays have passed the quality control analysis.

The miRNA microarray data reported in this study are in accordance with the Minimum Information About a Microarray Experiment (MIAME) guidelines (Brazma et al., 2001). The data have been submitted to the NCBI Gene Expression Omnibus (GEO) database (Accession: GSE39845). Hierarchical clustering analysis was performed based on the similarity measure of Euclidean distance and average-linkage rule, and expressed in the form of heat map and 3D PCA plot (Gibbons & Roth, 2002). The heat map indicated the number of miRNAs that were differentially regulated between the cancer and the normal/control group. Many miRNAs that were poorly expressed in the normal/control samples have been determined to be highly expressed in the CRC samples. The 3D PCA plot was computed to provide a visual representation of the samples. The samples were distributed into a three dimensional space based on the variances in miRNA gene expression. Samples from the same group or stage were found to be clustered together in distinctive patterns.

4.3.1 Tissue miRNA array

In tissue miRNA array, 30 paired cancer tissue with normal colonic mucosa samples were included (Appendix 6). At the fold change cut-off of 1.5, the tissue miRNA array revealed 40 significantly up-regulated and 32 significantly down-regulated miRNAs (Table 4.3). Since the profiling experiment for each cancer stage was performed in only one replicate, the miRNA expression was calculated as a general fold change of cancer tissue versus normal colonic mucosa. The heat map and 3D PCA plot for the tissue miRNA array are depicted in Figures 4.5 and 4.6, respectively.

Table 4.3: List of 72 significantly deregulated miRNAs in tissue miRNA array. The miRNA expression was calculated as a general fold change of cancer tissue versus normal colonic mucosa ($p < 0.05$). Positive values denote up-regulation and negative values denote down-regulation.

miRNA	**Fold change**	**miRNA**	**Fold change**	**miRNA**	**Fold change**
hsa-let-7i-star	1.76	hsa-miR-193a-3p	8.72	hsa-miR-378-star	-2.75
hsa-miR-10b	-1.79	hsa-miR-195	-2.03	hsa-miR-383	-3.45
hsa-miR-10b-star	-1.86	hsa-miR-198	1.54	hsa-miR-422a	-2.72
hsa-miR-105	2.13	hsa-miR-20a	1.94	hsa-miR-424-star	2.20
hsa-miR-1224-5p	1.63	hsa-miR-203	3.54	hsa-miR-429	2.03
hsa-miR-124	-6.64	hsa-miR-21-star	2.33	hsa-miR-431	1.75
hsa-miR-1244	1.77	hsa-miR-215	-3.21	hsa-miR-483-3p	1.63
hsa-miR-1246	4.74	hsa-miR-224	8.44	hsa-miR-493-star	2.25
hsa-miR-1247	8.74	hsa-miR-23a	2.79	hsa-miR-497	-2.90
hsa-miR-1292	1.62	hsa-miR-23b	3.56	hsa-miR-501-5p	1.71
hsa-miR-1296	-1.63	hsa-miR-23b-star	-2.20	hsa-miR-503	2.42
hsa-miR-1308	3.43	hsa-miR-27b	-1.72	hsa-miR-509-3p	3.65
hsa-miR-138	-3.56	hsa-miR-27b-star	-1.80	hsa-miR-548x	-1.76
hsa-miR-139-3p	-5.91	hsa-miR-28-3p	-2.29	hsa-miR-550-star	2.57
hsa-miR-139-5p	-5.61	hsa-miR-29b-2-star	-2.10	hsa-miR-552	8.89
hsa-miR-140-3p	-1.79	hsa-miR-30a	-2.76	hsa-miR-622	8.66
hsa-miR-146b-3p	2.34	hsa-miR-30a-star	-4.25	hsa-miR-663b	5.40
hsa-miR-148a	1.82	hsa-miR-30c-1	-2.48	hsa-miR-767-5p	2.62
hsa-miR-149	-2.41	hsa-miR-30c-2	-4.12	hsa-miR-887	-2.02
hsa-miR-150	-1.61	hsa-miR-3162	1.90	hsa-miR-940	1.58
hsa-miR-18a-star	3.47	hsa-miR-338-5p	8.20	hsa-miR-941	2.65
hsa-miR-181d	1.63	hsa-miR-342-3p	-1.59	hsa-miR-96	1.86
hsa-miR-182	3.64	hsa-miR-378	-2.81	hsa-miR-99a	-1.57
hsa-miR-183-star	5.01	hsa-miR-378c	-3.15	hsa-miR-99b	-1.85

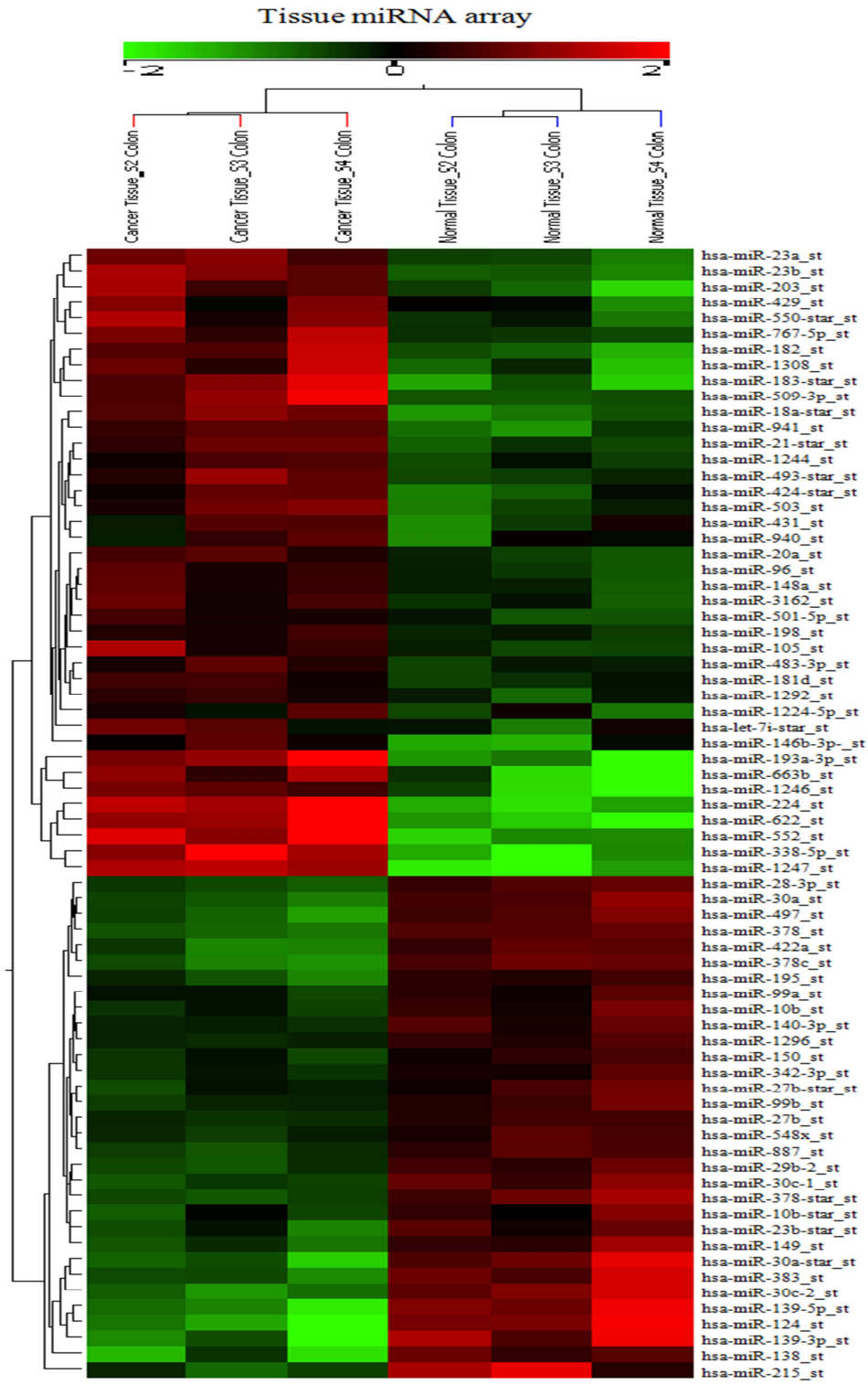

Figure 4.5: Heat map of tissue miRNA array. The heat map shows the hierarchical clustering analysis of 72 miRNAs that were found to be differentially regulated between the cancer tissue and the normal colonic mucosa.

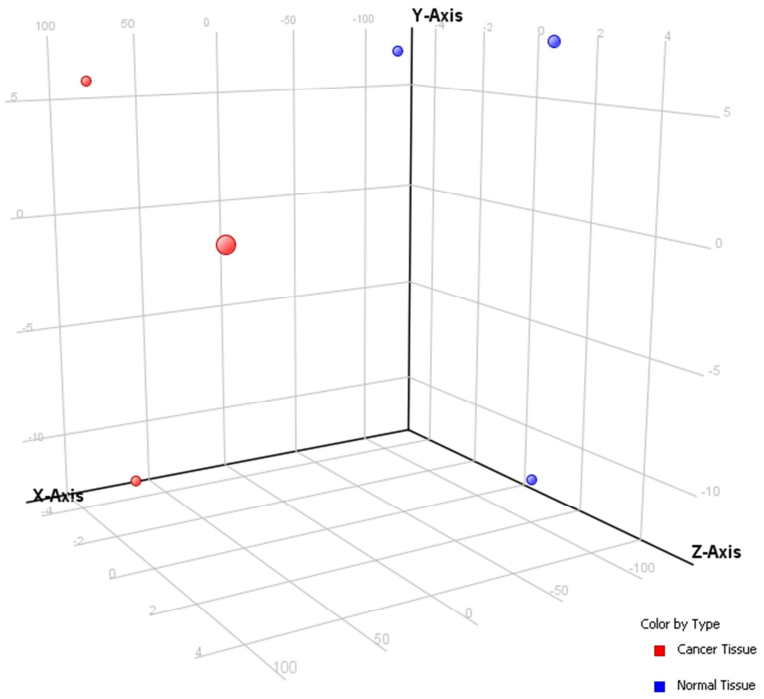

Figure 4.6: 3D PCA plot of tissue miRNA array. The 3D PCA plot shows a distinguished distribution of the paired cancer tissue and normal colonic mucosa. Colour by type, red: cancer tissue; blue: normal colonic mucosa.

4.3.2 Blood miRNA array

In blood miRNA array, 42 CRC and 18 healthy control samples were included (Appendix 6). Blood miRNAs with fold change values of ≥ 1.5 or ≤ -1.5 in any TNM stage were included. A total of 15 significantly up-regulated and 9 significantly down-regulated miRNAs were discovered (Table 4.4). The heat map and 3D PCA plot for the blood miRNA array are depicted in Figures 4.7 and 4.8, respectively.

Table 4.4: List of 24 significantly deregulated miRNAs in blood miRNA array. The miRNA expression was calculated as a fold change of TNM stage (I, II, III or IV) versus control group ($p < 0.05$). Values of ≥ 1.5 or ≤ -1.5 are highlighted in bold. Positive values denote up-regulation and negative values denote down-regulation.

miRNA	**Fold change**			
	Stage I	**Stage II**	**Stage III**	**Stage IV**
hsa-miR-122	**-1.90**	**1.89**	-1.18	**7.34**
hsa-miR-122-star	1.10	-1.08	**1.52**	-1.02
hsa-miR-1245	**1.55**	-1.01	1.12	1.08
hsa-miR-1274b	**1.79**	-1.03	-1.14	1.00
hsa-miR-130a-star	**1.64**	-1.04	-1.15	-1.02
hsa-miR-150	**-2.56**	**-1.52**	**-3.91**	-1.47
hsa-miR-18b-star	**1.54**	-1.03	1.41	1.09
hsa-miR-193a-3p	1.01	1.21	-1.00	**1.85**
hsa-miR-2116-star	**2.21**	1.13	1.17	-1.05
hsa-miR-23a	-1.05	**1.55**	-1.07	1.45
hsa-miR-23b	**1.58**	**1.51**	1.41	**1.74**
hsa-miR-296-5p	**1.88**	-1.05	1.31	-1.07
hsa-miR-3122	**-1.58**	1.07	-1.04	-1.20
hsa-miR-3183	**2.22**	1.00	-1.13	-1.16
hsa-miR-338-5p	-1.32	**1.74**	-1.04	**2.40**
hsa-miR-342-3p	-1.37	-1.30	**-1.77**	-1.25
hsa-miR-409-5p	-1.28	1.08	1.18	**1.66**
hsa-miR-4267	-1.28	-1.04	**1.56**	1.06
hsa-miR-483-3p	-1.04	1.24	**1.71**	1.04
hsa-miR-513a-3p	**1.64**	1.06	1.24	-1.01
hsa-miR-520a-3p	**1.52**	-1.04	-1.04	-1.01
hsa-miR-548u	**1.95**	-1.34	-1.30	-1.24
hsa-miR-587	**1.53**	1.03	1.04	-1.14
hsa-miR-92a-2-star	**1.98**	-1.06	-1.06	-1.12

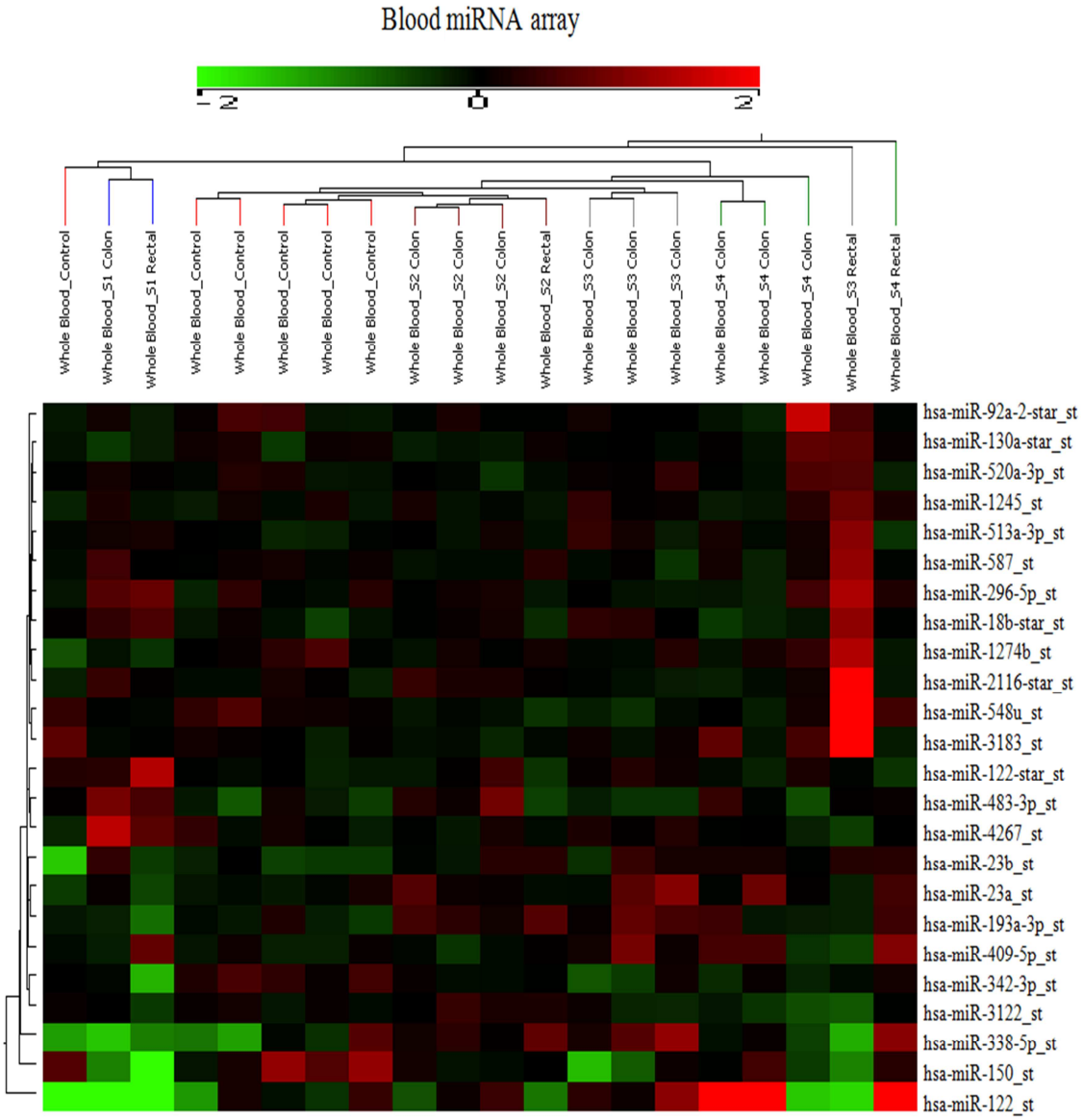

Figure 4.7: Heat map of blood miRNA array. The heat map shows the hierarchical clustering analysis of 24 miRNAs that were found to be differentially regulated between the cancer and the control groups.

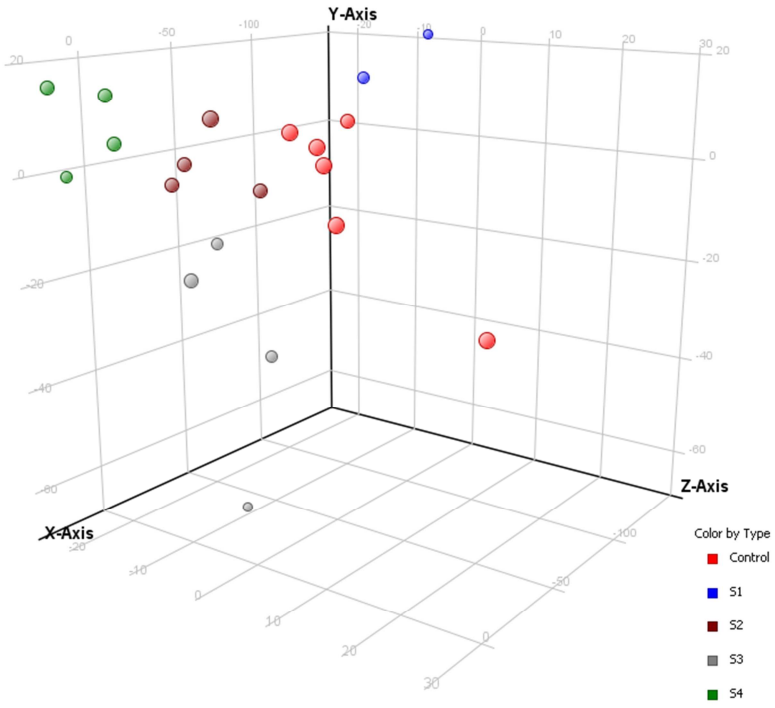

Figure 4.8: 3D PCA plot of blood miRNA array. Samples from the same stage were found to be clustered together. Colour by type, red: control; blue: stage I; brown: stage II; grey: stage III; green: stage IV.

4.4 Selection of miRNAs for validation study

The tissue miRNA array revealed a higher number of deregulated miRNAs and those that were concurrently expressed in the blood miRNA array were selected for further validation. The selected miRNAs consisted of five up-regulated (miR-193a-3p, miR-23a, miR-23b, miR-338-5p and miR-483-3p) and two down-regulated (miR-150 and miR-342-3p) miRNAs (Figure 4.9).

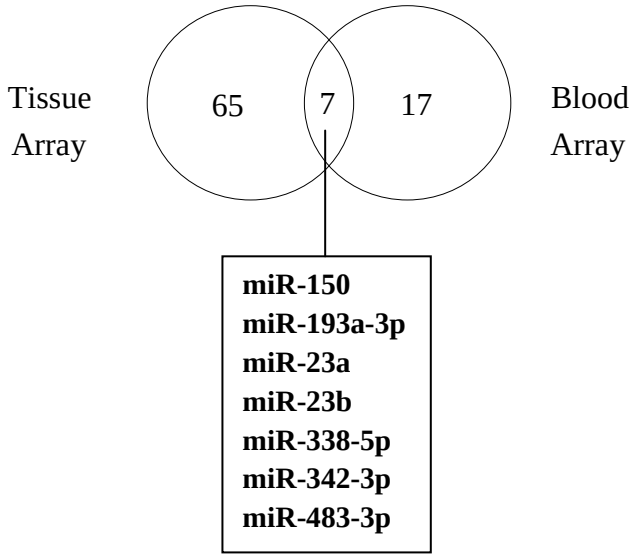

Figure 4.9: Venn diagram of differentially expressed miRNAs.

A two-step validation protocol involving the RT step using miRNA-specific primer and the qPCR technology using TaqMan probe was utilised. An independent set of 30 paired cancer tissues (stage II, n = 10; stage III, n = 10; stage IV, n = 10), 70 blood samples from CRC patients (stage I, n = 19; stage II, n = 20; stage III, n = 19; stage IV, n = 12) and 32 blood samples from healthy controls were used in the validation study (Appendix 6). The clinical samples were grouped into early-stage tumour (stage I-II) and advanced-stage tumour (stage III-IV) for statistical analysis.

RNU48 was chosen as the endogenous control for data normalisation. Its expression has been found to be reasonably stable and reproducible in CRC (K. H. Chang, Mestdagh, Vandesompele, Kerin, & Miller, 2010; Davoren, McNeill, Lowery, Kerin, & Miller, 2008). The tissue (p = 0.311) and blood (p = 0.524) levels of RNU48 between the cancer and normal/control samples were confirmed to be statistically insignificant.

4.4.1 Validation of the panel of seven miRNAs in tissue samples

The validation study was performed using 30 paired cancer tissues. The tissue RT-qPCR analysis indicated that the C_T values for the panel of seven miRNAs and endogenous control were within the detectable limit of less than 36 (Figure 4.10). Significant deregulations were noticed in the panel of seven miRNAs using paired *t*-test (p = 0.039 for miR-150, p = 0.037 for miR-193a-3p, p = 0.031 for miR-23a, p = 0.025 for miR-23b, p = 0.023 for miR-338-5p, p = 0.025 for miR-342-3p and p = 0.009 for miR-483-3p). The bar charts of paired tissue miR-150, miR-193a-3p, miR-23a, miR-23b, miR-338-5p, miR-342-3p and miR-483-3p expressions are illustrated in Figures 4.11 to 4.17. The basal fold change of the normal colonic mucosa was set at 1. Hence, a fold change above 1 in the cancer tissue was determined as up-regulation while a fold change below 1 was determined as down-regulation. The miRNAs expression levels of each sample are tabulated in Appendix 7.

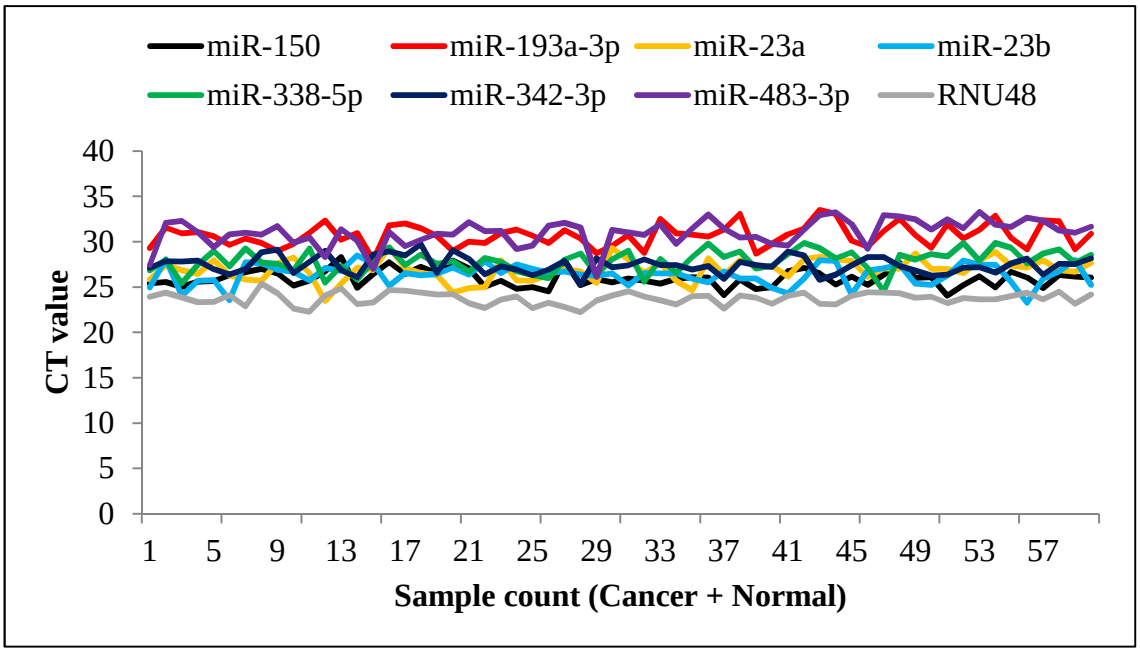

Figure 4.10: C_T values of miRNAs and endogenous control in tissue validation. Colour legend, black: miR-150; red: miR-193a-3p, orange: miR-23a; light blue: miR-23b, green: miR-338-5p; dark blue: miR-342-3p; purple: miR-483-3p; grey: RNU48.

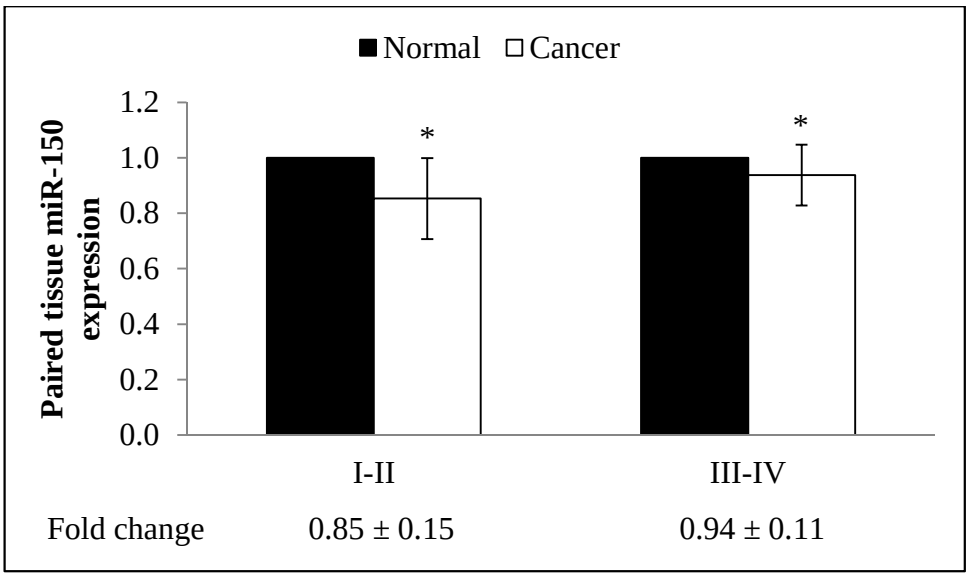

Figure 4.11: Paired tissue miR-150 expression. Relative expression is expressed as fold change of cancer tissue versus normal colonic mucosa. Fold change below 1 indicates down-regulation. Data are presented as mean ± SEM. * $p < 0.05$.

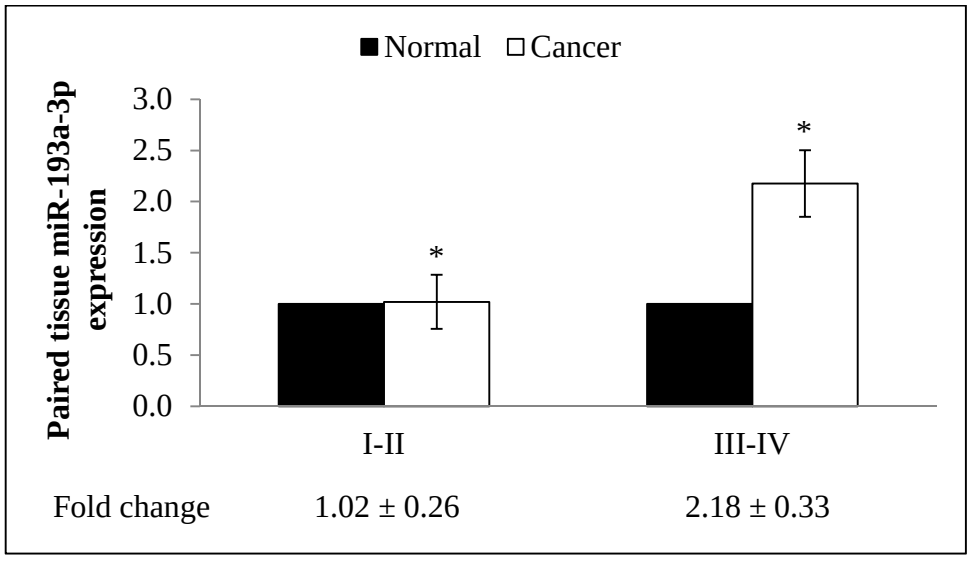

Figure 4.12: Paired tissue miR-193a-3p expression. Relative expression is expressed as fold change of cancer tissue versus normal colonic mucosa. Fold change above 1 indicates up-regulation. Data are presented as mean ± SEM. * $p < 0.05$.

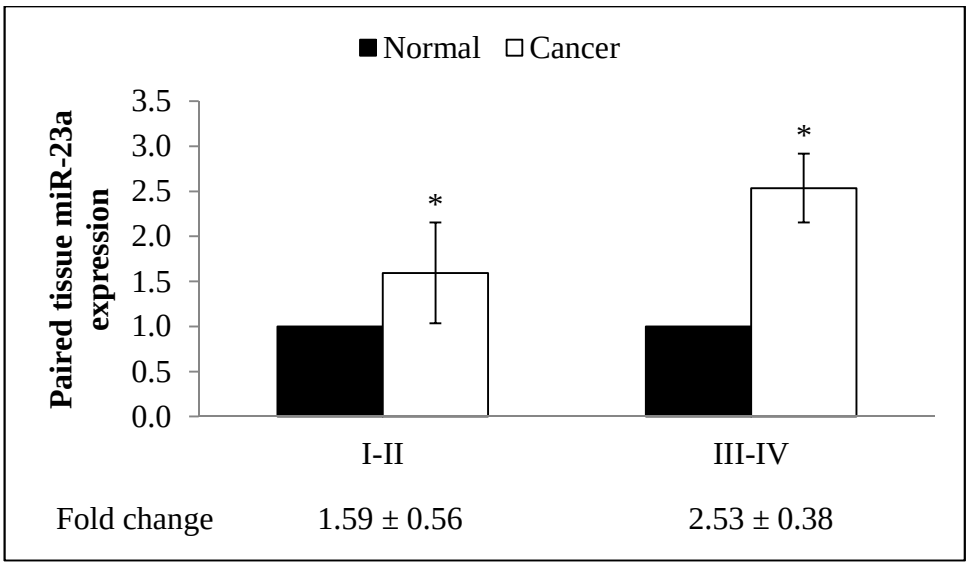

Figure 4.13: Paired tissue miR-23a expression. Relative expression is expressed as fold change of cancer tissue versus normal colonic mucosa. Fold change above 1 indicates up-regulation. Data are presented as mean ± SEM. * $p < 0.05$.

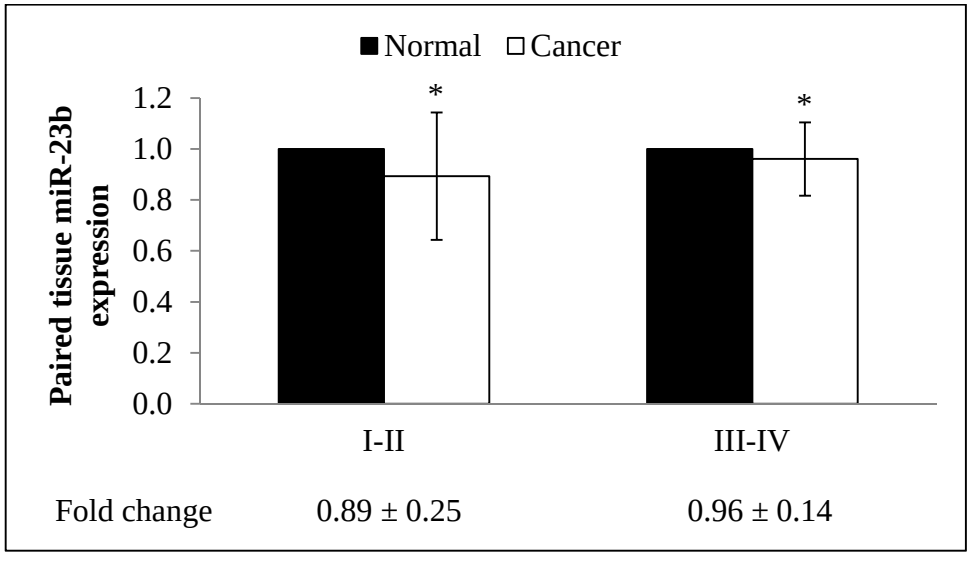

Figure 4.14: Paired tissue miR-23b expression. Relative expression is expressed as fold change of cancer tissue versus normal colonic mucosa. Fold change below 1 indicates down-regulation. Data are presented as mean ± SEM. * $p < 0.05$.

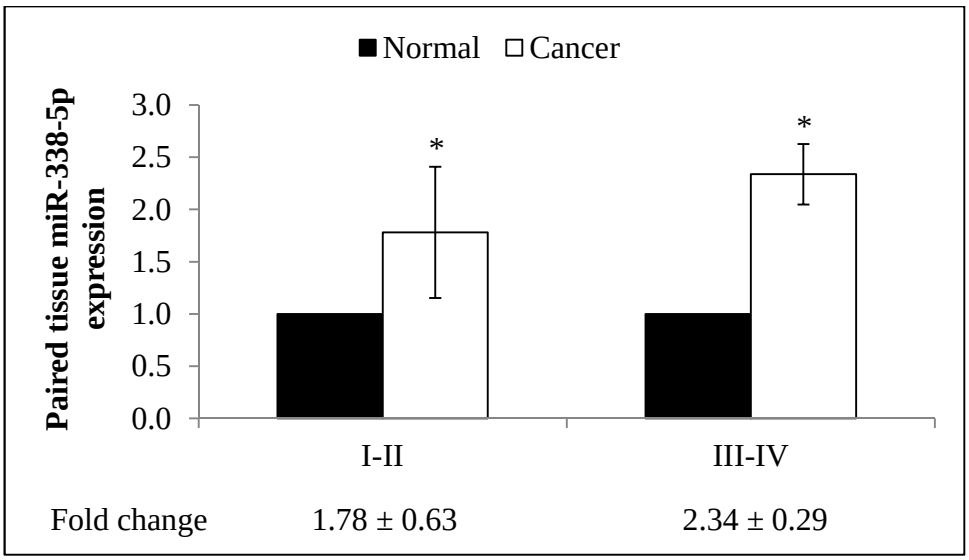

Figure 4.15: Paired tissue miR-338-5p expression. Relative expression is expressed as fold change of cancer tissue versus normal colonic mucosa. Fold change above 1 indicates up-regulation. Data are presented as mean ± SEM. * $p < 0.05$.

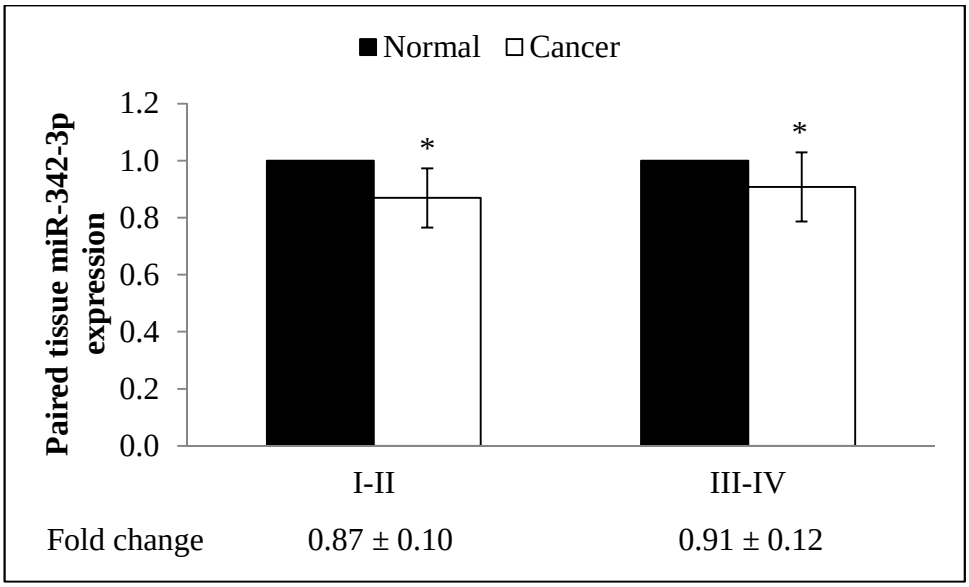

Figure 4.16: Paired tissue miR-342-3p expression. Relative expression is expressed as fold change of cancer tissue versus normal colonic mucosa. Fold change below 1 indicates down-regulation. Data are presented as mean ± SEM. * $p < 0.05$.

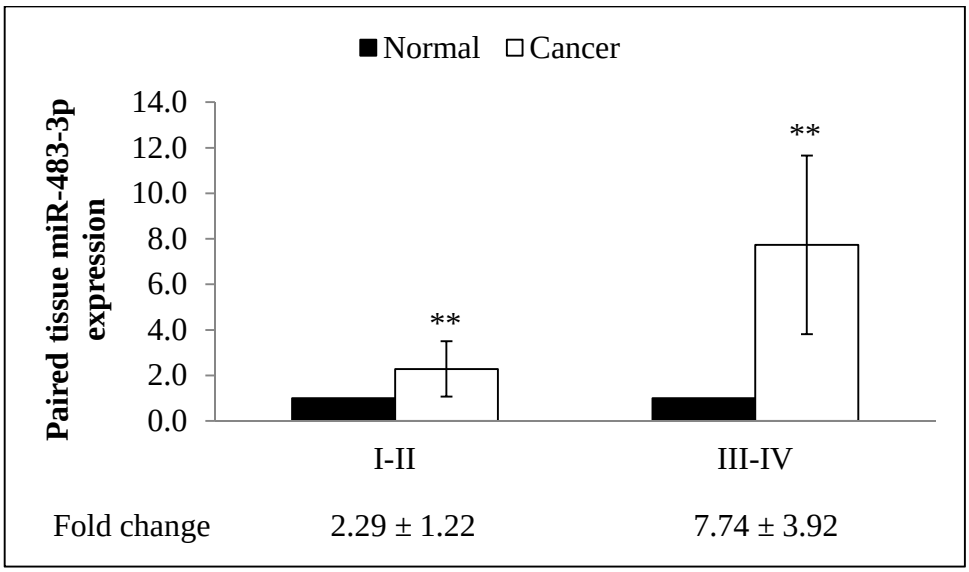

Figure 4.17: Paired tissue miR-483-3p expression. Relative expression is expressed as fold change of cancer tissue versus normal colonic mucosa. Fold change above 1 indicates up-regulation. Data are presented as mean ± SEM. ** $p < 0.01$.

4.4.2 Validation of the panel of seven miRNAs in blood samples

The validation study was conducted using 70 CRC and 32 healthy control samples. The blood RT-qPCR analysis revealed that the C_T values for the panel of seven miRNAs and endogenous control were within the detectable limit of less than 36 (Figure 4.18). Significant up-regulations were detected in the levels of miR-193a-3p ($p < 0.001$), miR-23a ($p = 0.043$), miR-23b ($p = 0.045$), miR-338-5p ($p < 0.001$) and miR-483-3p ($p = 0.010$) using unpaired *t*-test. However, no significant differences were observed in the levels of miR-150 ($p = 0.450$) and miR-342-3p ($p = 0.560$). The bar charts of blood miR-150, miR-193a-3p, miR-23a, miR-23b, miR-338-5p, miR-342-3p and miR-483-3p expressions are illustrated in Figures 4.19 to 4.25. The basal fold change of the control group was set at 1. Hence, a fold change above 1 in the CRC group was determined as up-regulation while a fold change below 1 was determined as down-regulation. The miRNAs expression levels of each sample are tabulated in Appendix 8.

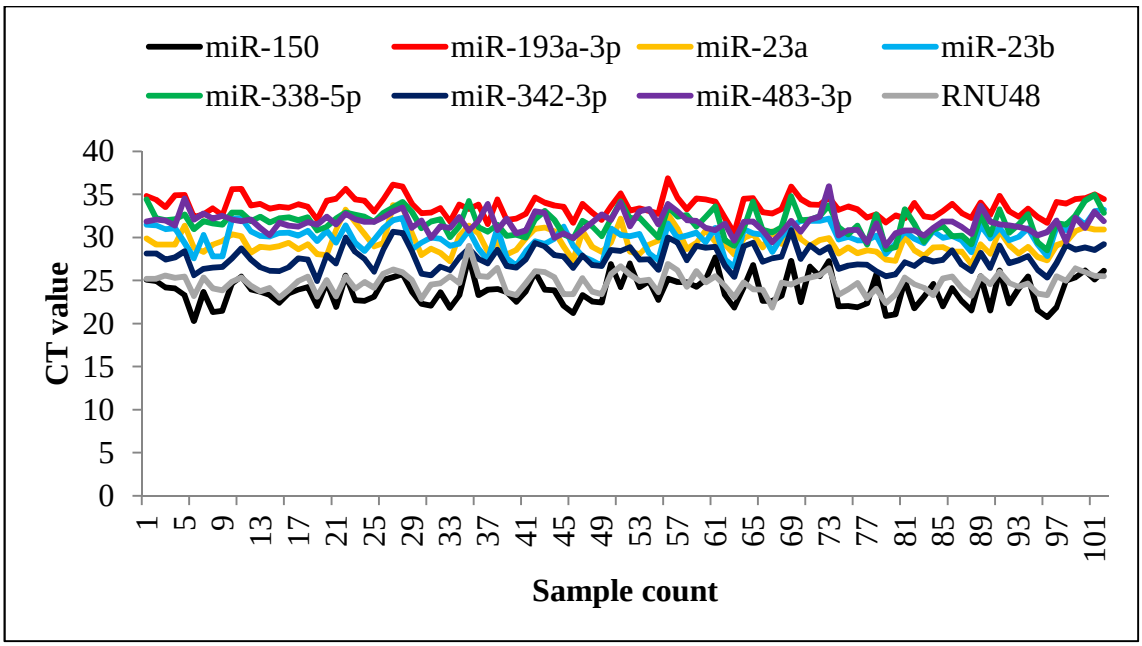

Figure 4.18: C_T values of miRNAs and endogenous control in blood validation. Colour legend, black: miR-150; red: miR-193a-3p, orange: miR-23a; light blue: miR-23b, green: miR-338-5p; dark blue: miR-342-3p; purple: miR-483-3p; grey: RNU48.

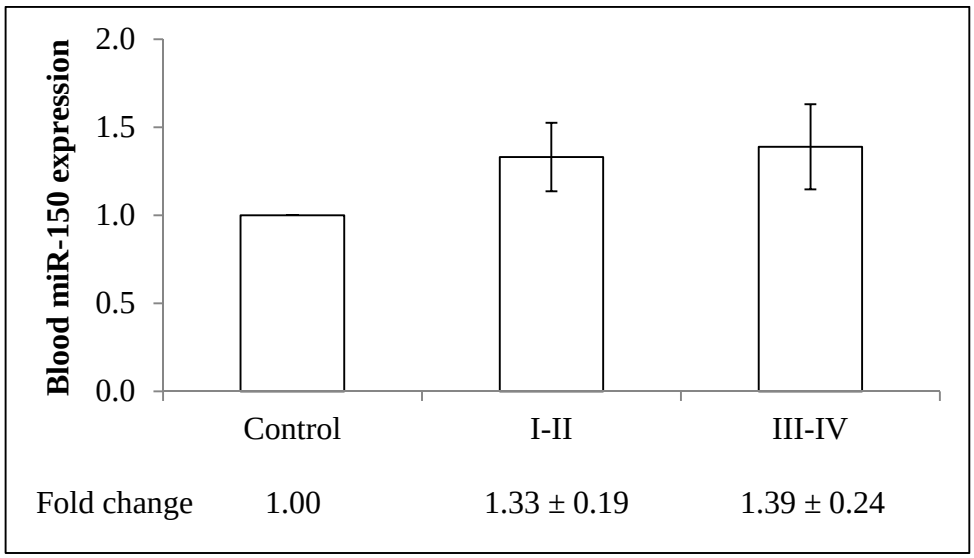

Figure 4.19: Blood miR-150 expression. Data are expressed as fold change of TNM stage versus control. The blood miR-150 expression was not statistically significant. Data are presented as mean ± SEM.

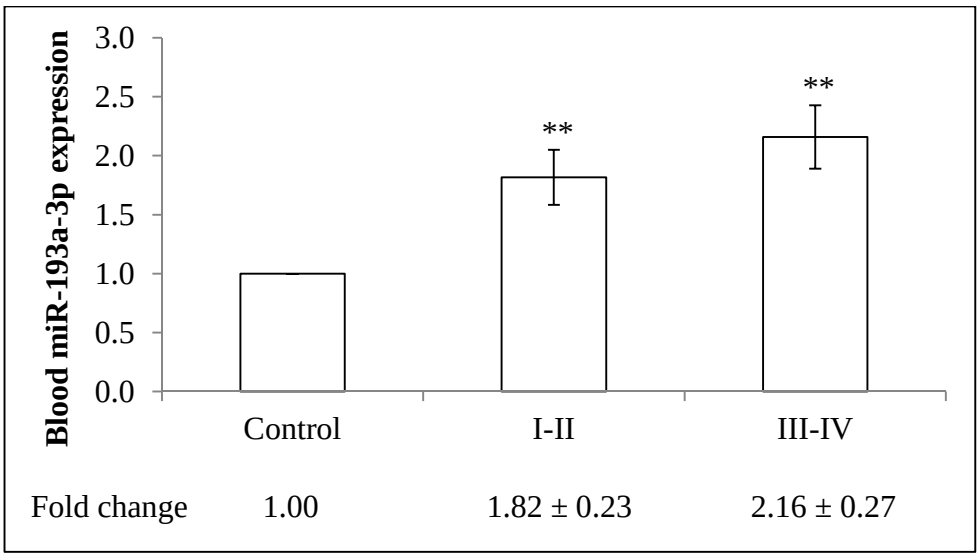

Figure 4.20: Blood miR-193a-3p expression. Data are expressed as fold change of TNM stage versus control. Fold change above 1 indicates up-regulation. Data are presented as mean ± SEM. ** $p < 0.01$.

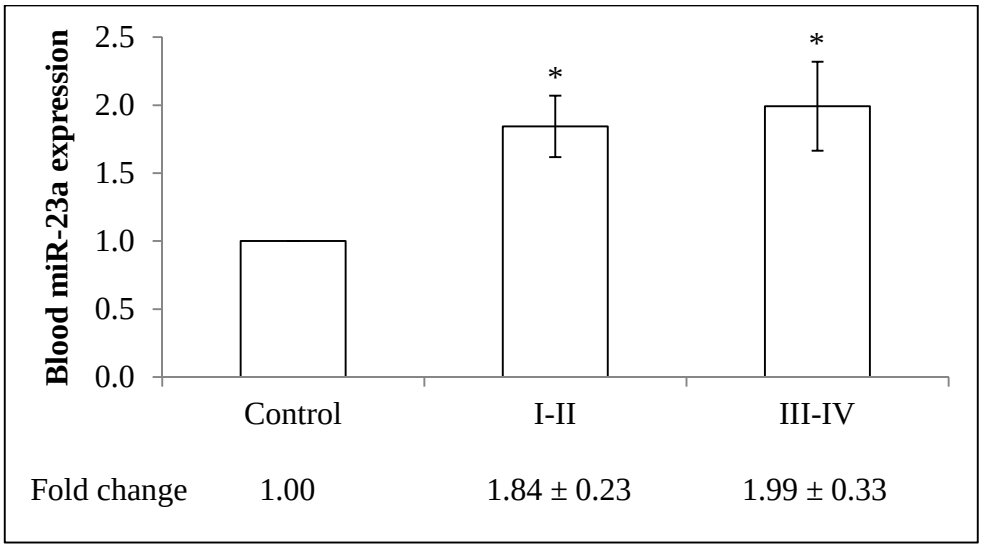

Figure 4.21: Blood miR-23a expression. Data are expressed as fold change of TNM stage versus control. Fold change above 1 indicates up-regulation. Data are presented as mean ± SEM. * $p < 0.05$.

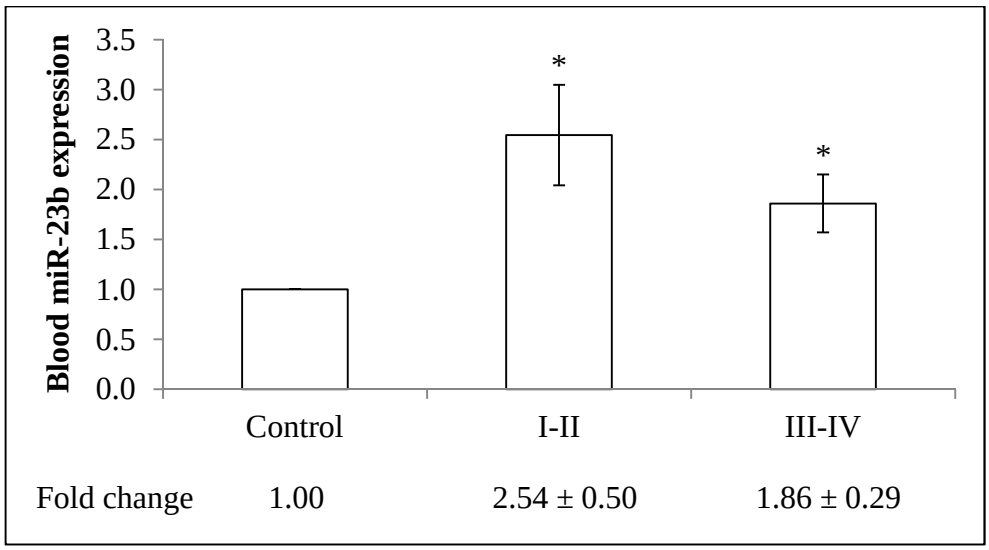

Figure 4.22: Blood miR-23b expression. Data are expressed as fold change of TNM stage versus control. Fold change above 1 indicates up-regulation. Data are presented as mean ± SEM. * $p < 0.05$.

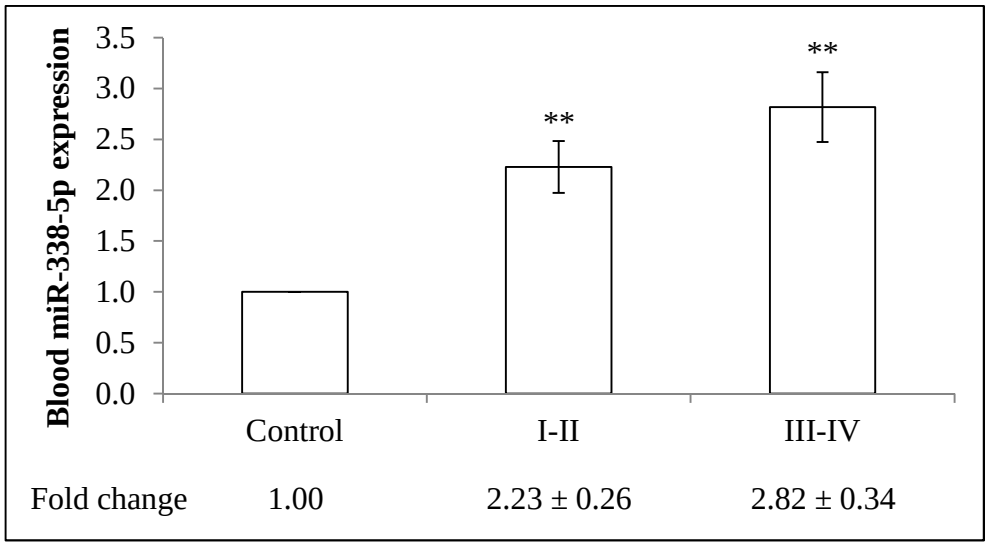

Figure 4.23: Blood miR-338-5p expression. Data are expressed as fold change of TNM stage versus control. Fold change above 1 indicates up-regulation. Data are presented as mean ± SEM. ** $p < 0.01$.

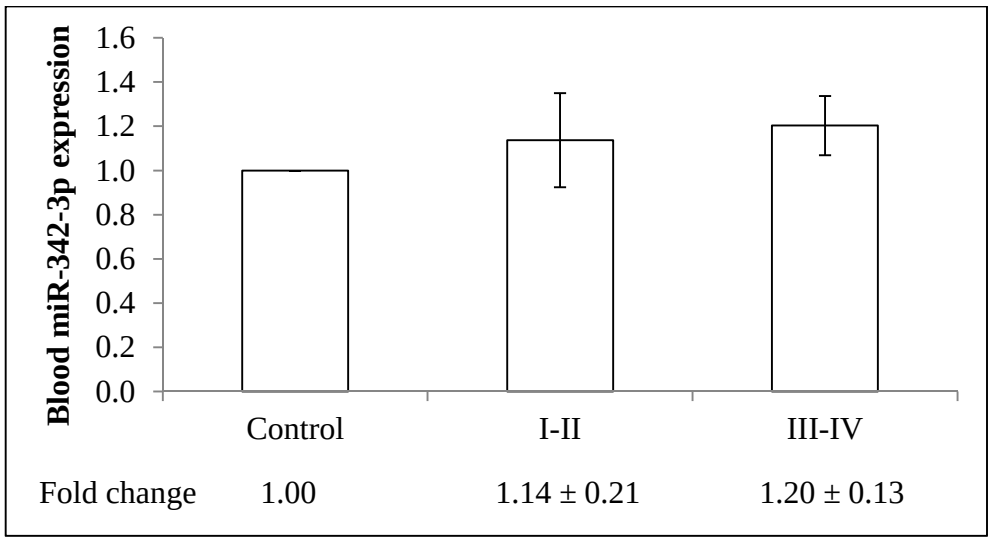

Figure 4.24: Blood miR-342-3p expression. Data are expressed as fold change of TNM stage versus control. The blood miR-342-3p expression was not statistically significant. Data are presented as mean ± SEM.

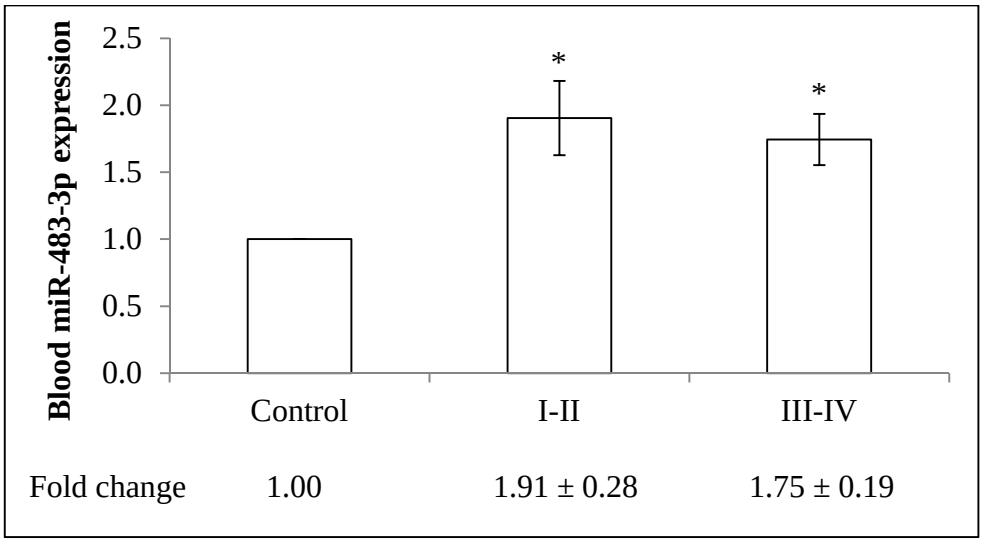

Figure 4.25: Blood miR-483-3p expression. Data are expressed as fold change of TNM stage versus control. Fold change above 1 indicates up-regulation. Data are presented as mean ± SEM. * $p < 0.05$.

4.5 Relationship between tissue and blood miRNAs

The miR-193a-3p, miR-23a, miR-23b, miR-338-5p and miR-483-3p expressions were found to be significantly deregulated in both tissue and blood validation studies. The correlation between the tissue and blood miRNAs was investigated. The purpose is to provide a stronger confirmation that the deregulated miRNAs in the systemic circulation may serve as potential indicators of what is happening at the tissue level. Controlling for age, gender, race and staging, correlation analyses between tissue and blood RT-qPCR data for miR-193a-3p ($r = 0.811$; $p < 0.001$), miR-23a ($r = 0.827$; $p < 0.001$), miR-23b ($r = 0.044$; $p = 0.819$), miR-338-5p ($r = 0.831$; $p < 0.001$) and miR-483-3p ($r = 0.373$; $p = 0.042$) were conducted. The results indicated significant positive correlations in the levels of miR-193a-3p, miR-23a and miR-338-5p between the tissue and blood samples. The miR-23b expression was not significantly correlated while the miR-483-3p expression revealed weak correlation. Thus, miR-193a-3p, miR-23a and miR-338-5p were selected as the triple miRNA classifier in this study. Moreover, an increasing trend of expression was observed in these circulating blood miRNAs as the tumour progressed from stage I-II to stage III-IV when compared with the control group (Figures 4.20, 4.21 and 4.23).

4.6 Diagnostic value of the triple miRNA classifier: miR-193a-3p, miR-23a and miR-338-5p in CRC

The predictive performance of the individual blood miRNA and the triple miRNA classifier for defining CRC were demonstrated by multivariate logistic regression analysis (Table 4.5). The triple miRNA classifier of miR-193a-3p, miR-23a and miR-338-5p gave the best performance and thus, suggested as a potential group of biomarkers in the detection of CRC. The optimal cut-off value for sensitivity and

specificity was determined based on the highest Youden's Index in ROC curve analysis (Obuchowski, 2005). The triple miRNA classifier has a stronger differentiation power than individual or double combination of miRNAs. The classifier has an increased area under the ROC curve (AUC) of 0.887 (95% confidence interval [CI]: 0.821 - 0.953) with 80.0% sensitivity, 84.4% specificity and 83.3% accuracy, illustrating an improved diagnostic value of these triple combination of miRNAs (Figure 4.26).

Table 4.5: Multivariate logistic regression analysis of individual blood miRNA and triple miRNA classifier of miR-193a-3p, miR-23a and miR-338-5p.

Statistical parameters	**miR-193a-3p**	**miR-23a**	**miR-338-5p**	**miR-193a-3p + miR-23a**	**miR-193a-3p + miR-338-5p**	**miR-23a + miR-338-5p**	**miR-193a-3p + miR-23a + miR-338-5p**
AUC	0.852	0.787	0.871	0.852	0.872	0.873	0.887
95% CI	0.768 - 0.935	0.685 - 0.889	0.800 - 0.942	0.770 - 0.935	0.798 - 0.946	0.803 - 0.942	0.821 - 0.953
Sensitivity (%)	100.0	94.3	81.4	74.3	94.3	81.4	80.0
Specificity (%)	56.2	53.1	75.0	81.2	65.6	75.0	84.4
Accuracy (%)	83.3	81.4	83.3	83.3	83.3	82.4	83.3
Youden's Index[a]	0.562	0.474	0.564	0.555	0.599	0.564	0.644
Cut-off value	0.346	0.502	0.640	0.745	0.474	0.636	0.728

[a]Youden's Index = sensitivity + specificity – 1

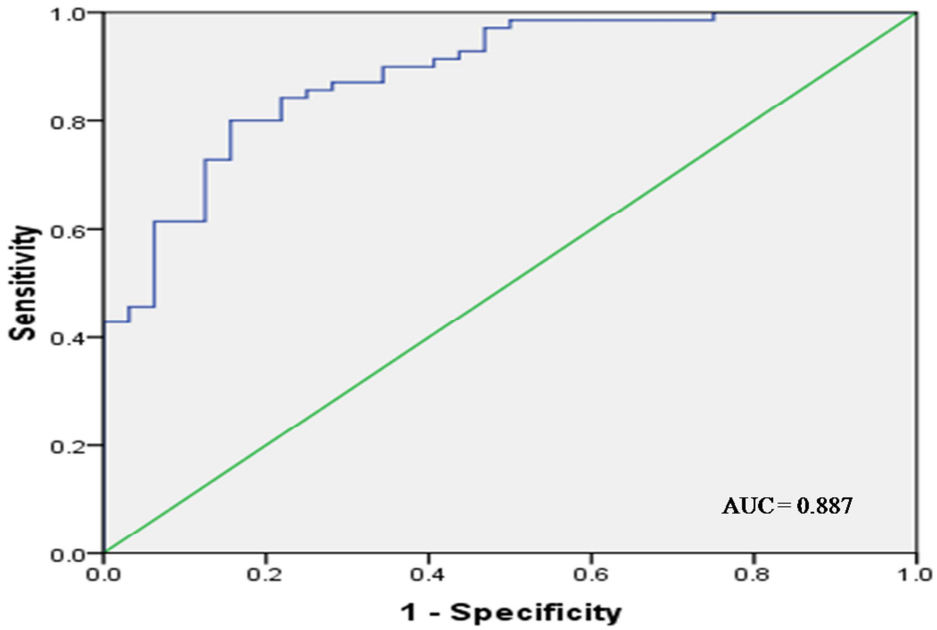

Figure 4.26: ROC curve analysis for the triple miRNA classifier of miR-193a-3p, miR-23a and miR-338-5p. The triple miRNA classifier yielded an AUC of 0.887 (95% CI: 0.821 - 0.953) with 80.0% sensitivity, 84.4% specificity and 83.3% accuracy.

4.7 Functional and miRNA:mRNA target validation studies

The subsequent phase of the research was the investigation on the roles and targets of miR-193a-3p, miR-23a and miR-338-5p. Two CRC cell lines (SW480 and SW620) with same genetic background but different metastatic potential were utilised. The presence of the three miRNAs in both cell lines was verified via RT-qPCR, with C_T values less than 36. The functional assays tested were cell viability, apoptosis, migration and invasion assays using miRNA mimics and inhibitors. Luciferase assays were performed for the validation of target mRNAs. The expression levels of target mRNAs and proteins in the CRC cell lines and clinical samples were assessed using RT-qPCR and Western blot.

4.7.1 miR-193a-3p transfection

4.7.1.1 Effect on cell viability rate following miR-193a-3p transfection

Cell viability studies of SW480 and SW620 cells post-transfections (24 h, 48 h and 72 h) were performed using MTT assay. The transfection of miR-193a-3p mimic or miR-193a-3p inhibitor in both cell lines did not significantly increase or decrease cell viability ($p > 0.05$) (Figure 4.27A, B). The cells were highly viable even after 72 h of transfection.

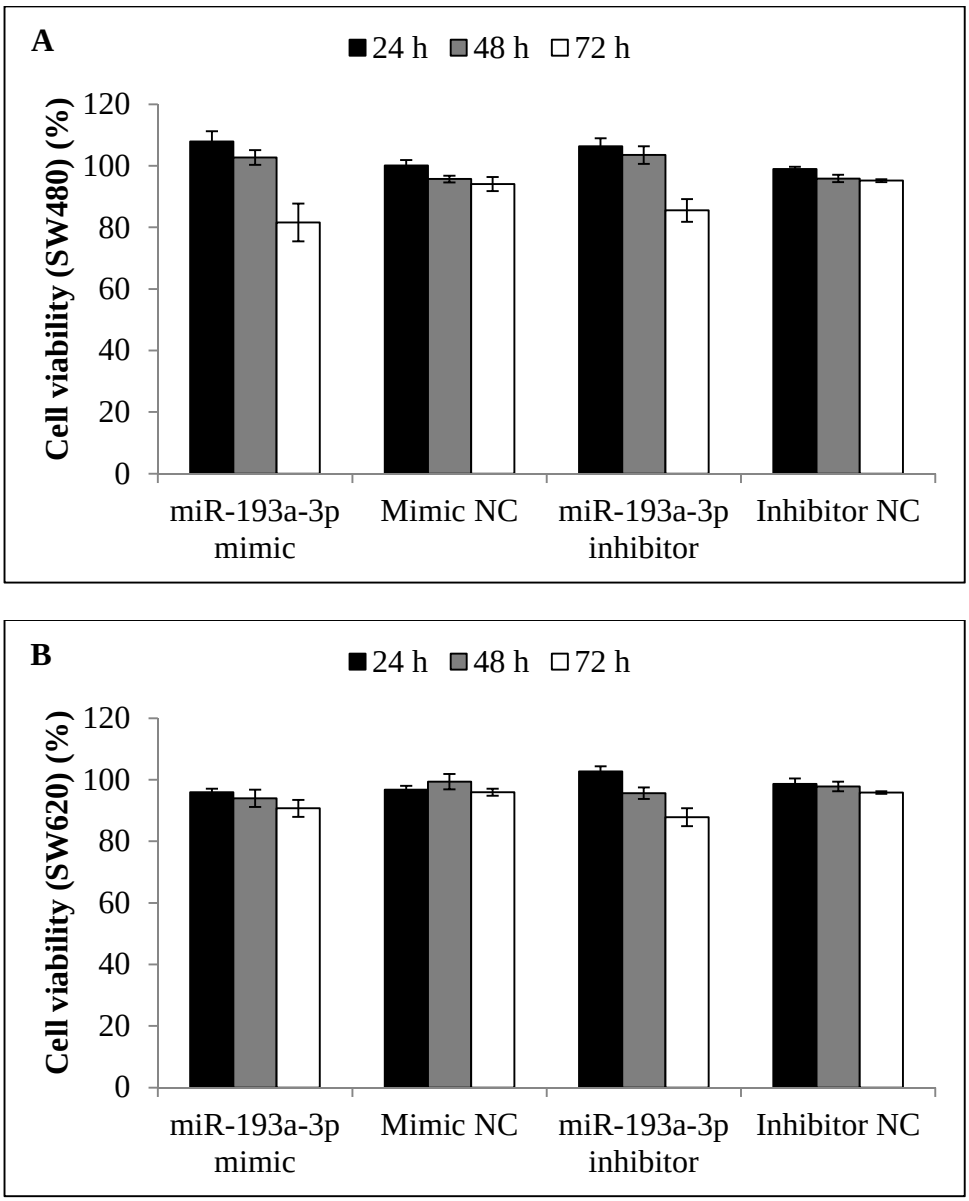

Figure 4.27: Cell viability of (A) SW480 and (B) SW620 cells following miR-193a-3p transfection. No statistical significance was observed ($p > 0.05$). Data are presented as mean ± SEM ($n = 3$).

4.7.1.2 Effect on apoptosis rate following miR-193a-3p transfection

Apoptosis assay was conducted using Annexin V and PI double staining procedure. Cell proportions in live, dead and apoptotic stages were quantitated using Invitrogen Tali image-based cytometer (Table 4.6). A sample of the cell analysis report is shown in Appendix 9. Doxorubicin, a well-known apoptosis-inducing agent, was used as the positive control. It is capable of inducing DNA damage by intercalating and cross-linking DNA double helix (Lüpertz et al., 2008). The miR-193a-3p mimic or miR-193a-3p inhibitor transfection did not produce any significant effect to the relative apoptosis rate of SW480 and SW620 cells ($p > 0.05$) (Figure 4.28).

Table 4.6: Quantification of live, dead and apoptotic cells in SW480 and SW620 cells using Invitrogen Tali image-based cytometer (miR-193a-3p transfection). Data are presented as mean ± SEM (*n* = 3).

Treatment	**SW480**			**SW620**		
	Live (%)	**Dead (%)**	**Apoptotic (%)**	**Live (%)**	**Dead (%)**	**Apoptotic (%)**
NTC	84.33 ± 0.33	10.33 ± 0.33	5.33 ± 0.33	84.00 ± 2.00	12.33 ± 1.76	3.67 ± 0.67
Mock	87.00 ± 1.53	11.00 ± 0.00	2.00 ± 1.53	81.67 ± 0.67	16.00 ± 0.58	2.00 ± 0.00
miR-193a-3p mimic	75.67 ± 0.33	22.00 ± 0.58	2.33 ± 0.88	79.67 ± 0.33	17.00 ± 2.00	3.33 ± 1.86
Mimic NC	83.67 ± 0.88	13.00 ± 0.58	2.67 ± 0.33	78.33 ± 0.88	14.00 ± 0.58	7.33 ± 0.88
miR-193a-3p inhibitor	84.67 ±1.33	14.00 ± 1.53	2.00 ± 0.58	77.33 ± 1.45	17.67 ± 0.33	5.00 ± 1.73
Inhibitor NC	85.00 ± 1.53	11.67 ± 0.67	3.67 ± 1.20	78.67 ± 1.20	15.00 ± 0.58	6.00 ± 1.15
Doxorubicin	54.33 ± 4.67	23.67 ± 0.88	22.33 ± 5.33	48.33 ± 4.84	27.00 ± 2.08	24.33 ± 2.91

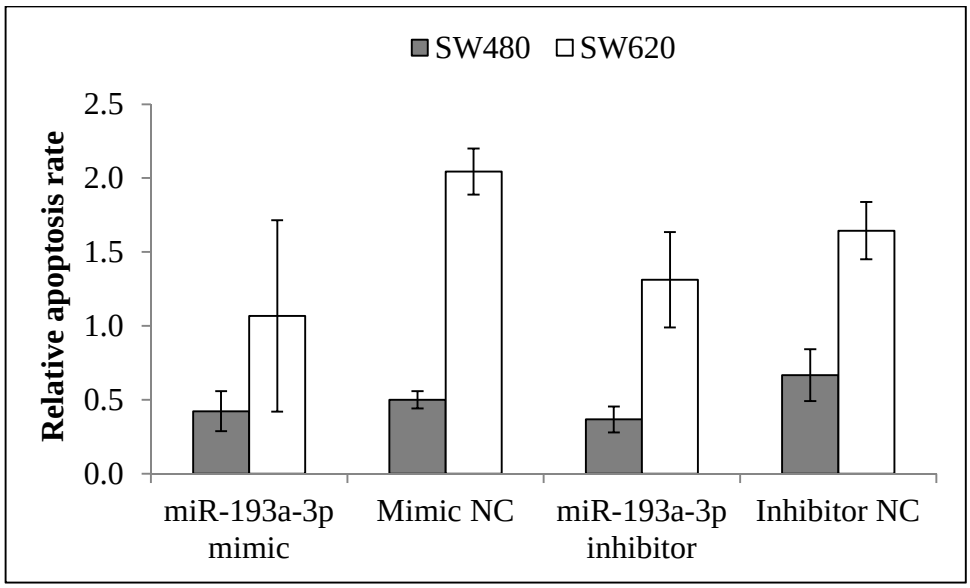

Figure 4.28: Relative apoptosis rate of SW480 and SW620 cells following miR-193a-3p transfection. No statistical significance was determined ($p > 0.05$). Data are presented as mean ± SEM ($n = 3$).

4.7.1.3 Effect on migration and invasion activity following miR-193a-3p transfection

The migration and invasion potential of SW480 and SW620 cells was evaluated. Significant results were obtained from miR-193a-3p mimic and miR-193a-3p inhibitor transfections ($p < 0.01$). The relative migration activity was increased by 1.62 ± 0.06-fold (SW480) and 1.78 ± 0.09-fold (SW620) in miR-193a-3p mimic-transfected cells and decreased by 0.52 ± 0.03-fold (SW480) and 0.45 ± 0.01-fold (SW620) in miR-193a-3p inhibitor-transfected cells. On the contrary, the relative invasion activity was increased by 1.39 ± 0.07-fold (SW480) and 1.83 ± 0.05-fold (SW620) in miR-193a-3p mimic-transfected cells and decreased by 0.58 ± 0.01-fold (SW480) and 0.63 ± 0.01-fold (SW620) in miR-193a-3p inhibitor-transfected cells. Normalised data are expressed

as relative value against the respective negative controls. Figure 4.29A-D shows the relative migration and invasion activity of SW480 and SW620 cells.

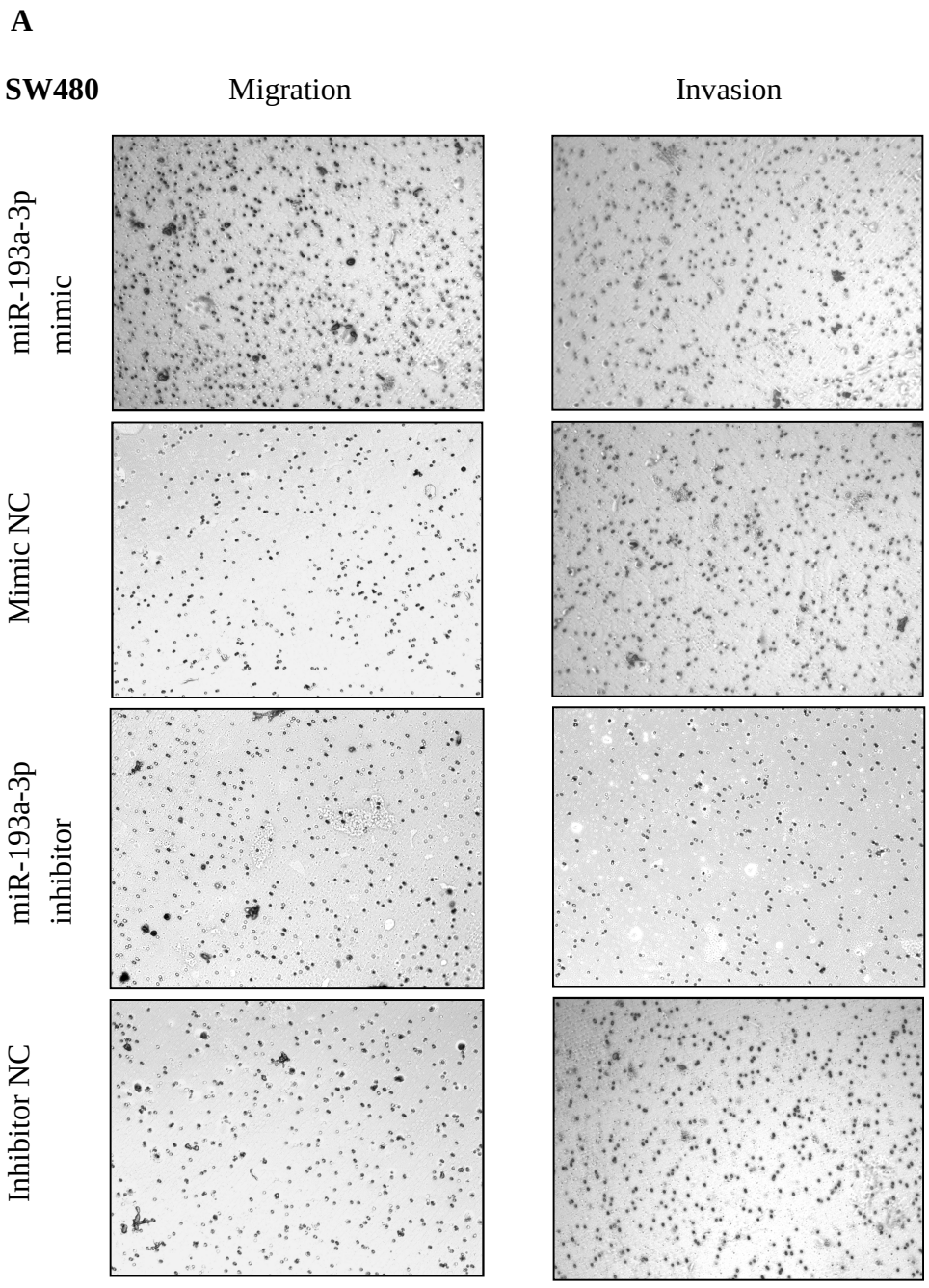

B

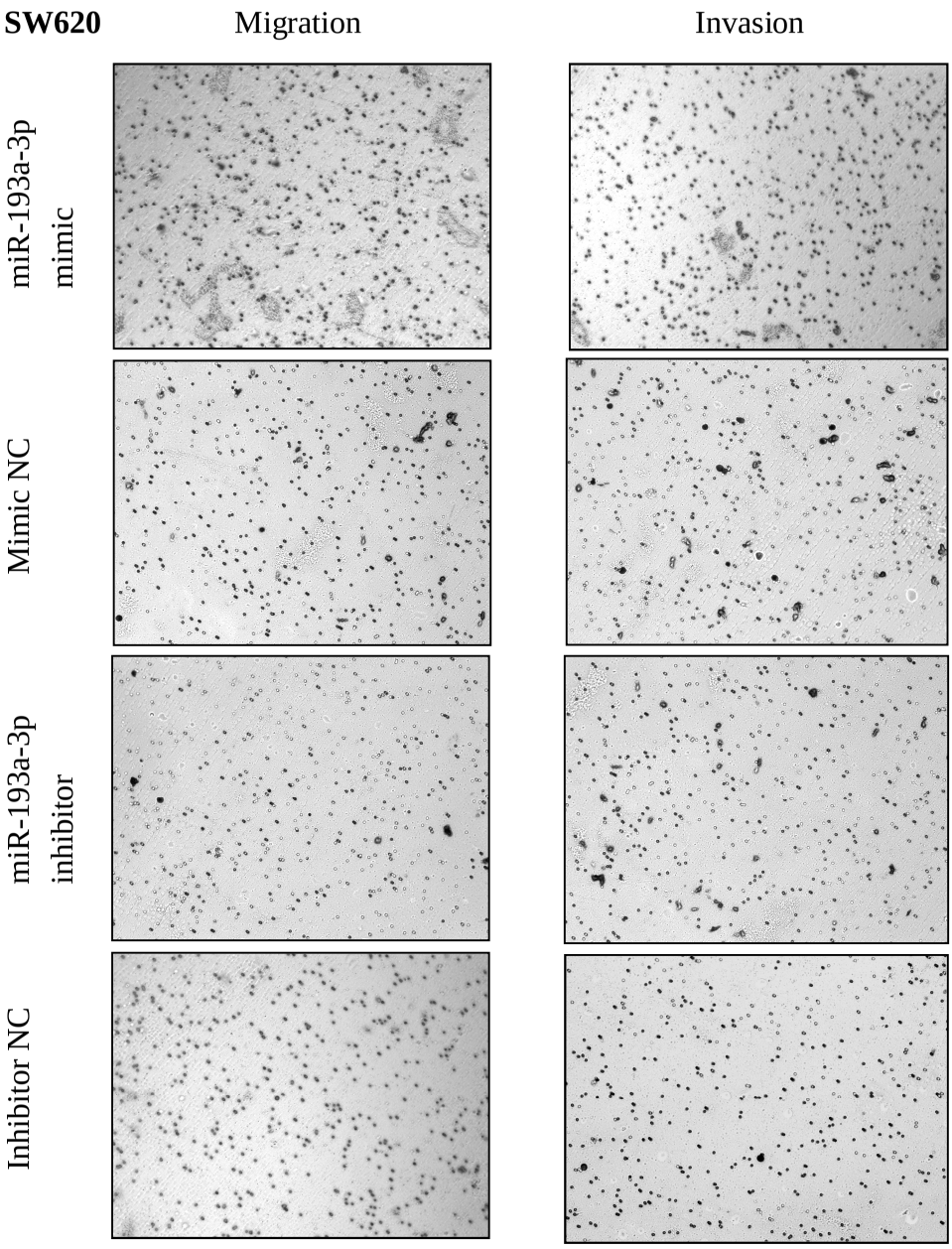
SW620
Migration
Invasion
miR-193a-3p mimic
Mimic NC
miR-193a-3p inhibitor
Inhibitor NC

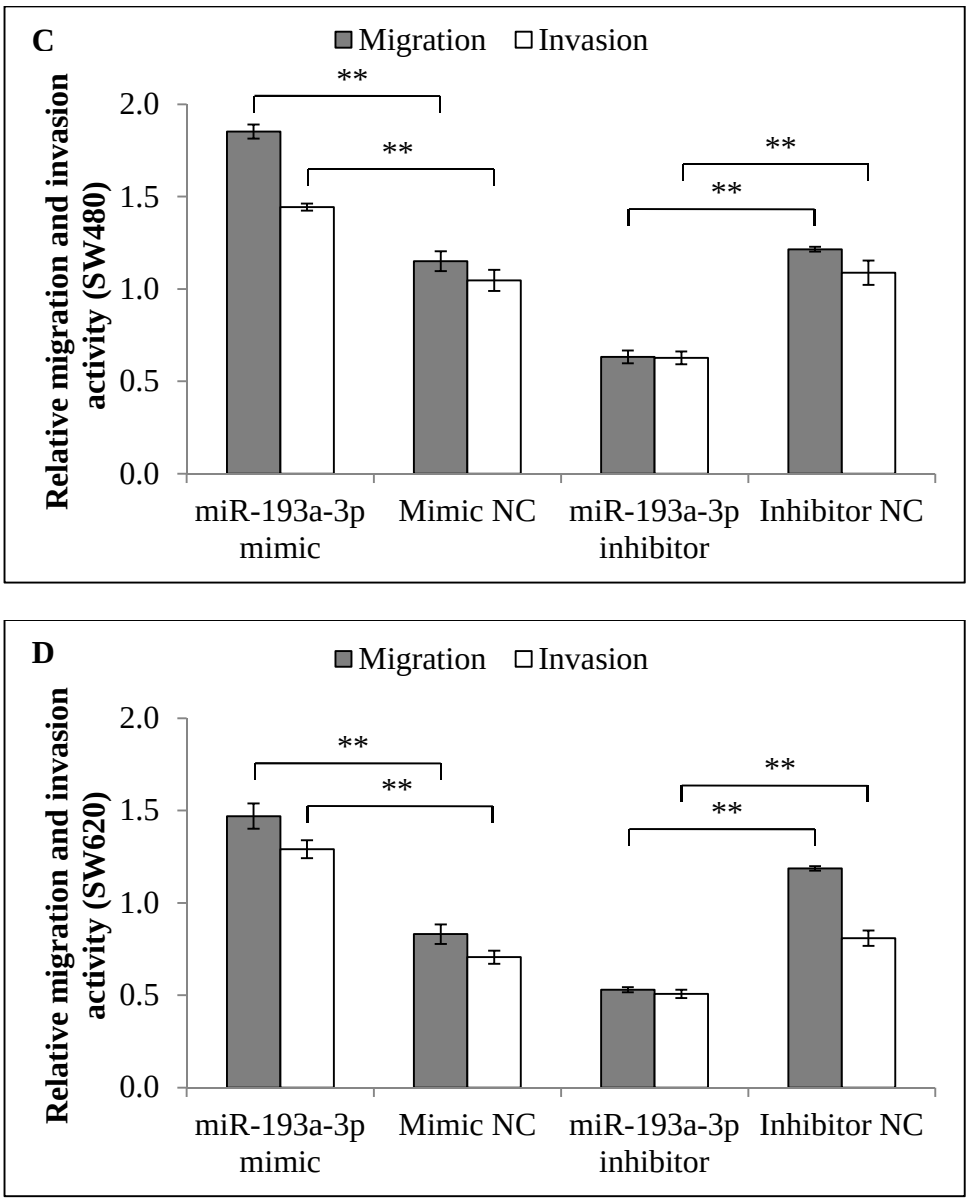

Figure 4.29: Relative migration and invasion activity of SW480 and SW620 cells following miR-193a-3p transfection. (A, B) Representative fields of migratory (left) and invasive (right) cells on plate insert. (C, D) Bar charts of relative migration and invasion activity. Data are presented as mean ± SEM (n = 3). ** $p < 0.01$.

4.7.1.4 Screening of miR-193a-3p targets

miRNA target prediction was computed using miRWalk database, whereby an informative prediction was assumed when a putative target was concordantly identified by five of the most common algorithms (DIANA-MicroT, miRanda, miRWalk, MirTarget2/miRDB, PicTar, RNA22, RNAhybrid and TargetScan Human). The preliminary screening process yielded a long list of mRNAs. Comprehensive literature search on CRC relevant genes was conducted. Five highly cited review papers were used as the basis of the search (Markowitz & Bertagnolli, 2009; Schetter, Okayama, & Harris, 2012; Slaby et al., 2009; Søreide et al., 2009; Vermaat et al., 2012). Several putative targets of miR-193a-3p that have been found to be associated with CRC were obtained, namely, *ACVR2B*, *AXIN2*, *CCND1*, *FAS*, *FOXO4*, *FZD4*, *FZD5*, *KRAS*, *MAPK1*, *PDGFRA*, *PTEN*, *SMAD4*, *SOS2* and *TGFBR1* (Appendix 10). Among these, forkhead box O4 (*FOXO4*) gene was selected for further investigation, with the consideration of its role as a tumour suppressor and possible implication in cell migration and invasion.

4.7.1.5 Construction of *FOXO4* luciferase reporters

The miRNA recognition site on the 3'-UTR of *FOXO4* mRNA was predicted using TargetScan Human 6.2. The recognition site that revealed the highly conserved seed match was used in the cloning assay.

FOXO4 (NM_005938.3) mRNA consists of 3365 bp. The length of the 3'-UTR is 1413 bp. A fragment of the *FOXO4* 3'-UTR containing the recognition site for miR-193a-3p at nucleotide position 2192-2491 was cloned via GeneArt gene synthesis service (Invitrogen, Carlsbad, CA, USA) (Appendix 11). The corresponding site-directed

mutant containing the mutated seed sequence (5'-GGCCAGU-3' to 5'-GCCGAUU-3') was also constructed (Appendix 12). Each customised fragment was inclusive of the HindIII and SpeI restriction sites (312 bp). The predicted pairing region between miR-193a-3p and *FOXO4* mRNA is presented in Table 4.7. Two luciferase reporter constructs containing the wild-type *FOXO4* 3'-UTR fragment (Luc-FOXO4-wt) and the mutated *FOXO4* 3'-UTR fragment (Luc-FOXO4-mt) were generated by sub-cloning the respective gene fragments from the GeneArt pMA-T vectors (Figure 4.30A, B) into the pMIR-REPORT firefly luciferase reporter vector (Figure 4.31) at the HindIII and SpeI sites. A luciferase vector without *FOXO4* 3'-UTR (Luc-FOXO4-ctl) was used as the experimental control. All constructs were verified by DNA sequencing.

Table 4.7: Conserved miR-193a-3p target site on human *FOXO4* 3'-UTR (NM_005938.3). *FOXO4* 3'-UTR length: 1413 bp. Seed match region at nucleotide position 444-450 is shown in bold italics. Mutations are marked with the symbol †.

FOXO4 3'-UTR	5'	...UGCAGUGGCCCCUUA***GGCCAGU***G...
		| | | | | | |
hsa-miR-193a-3p	3'	UGACCCUGAAACAU***CCGGUCA***A
Mutated *FOXO4* 3'-UTR	5'	...UGCAGUGGCCCCUUA***GCCGAUU***G ...
		| † | † | † |
hsa-miR-193a-3p	3'	UGACCCUGAAACAU***CCGGUCA***A

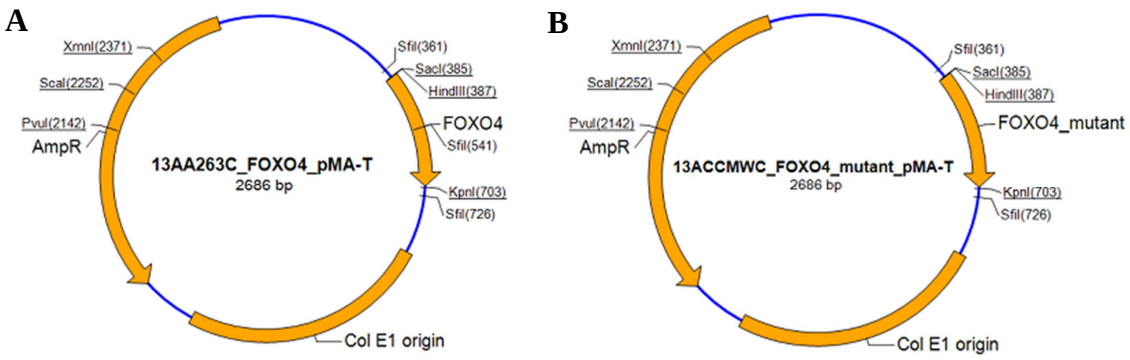

Figure 4.30: Images of customised GeneArt pMA-T vectors containing (A) *FOXO4* 3'-UTR fragment and (B) mutated *FOXO4* 3'-UTR fragment. The pMA-T vectors were sub-cloned into the pMIR-REPORT firefly luciferase reporter vector at the HindIII and SpeI sites to generate the Luc-FOXO4-wt and Luc-FOXO4-mt constructs.

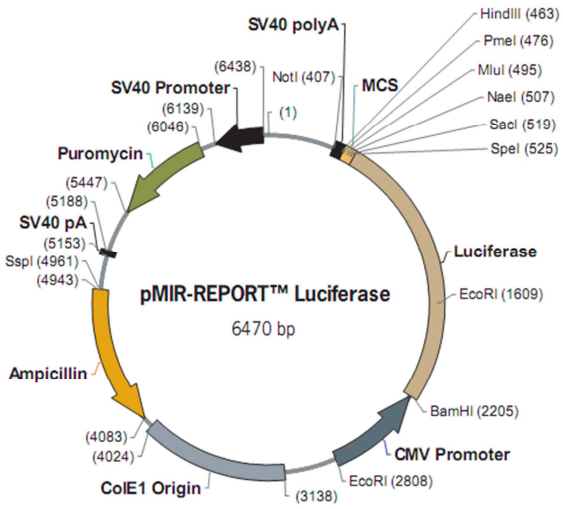

Figure 4.31: Image of pMIR-REPORT firefly luciferase reporter vector. Gene fragment from the GeneArt pMA-T vector was sub-cloned into the pMIR-REPORT firefly luciferase vector at the HindIII and SpeI sites.

(Image source: Invitrogen, Carlsbad, CA, USA)

4.7.1.6 miR-193a-3p:*FOXO4* target validation study

The functional interaction between miR-193a-3p and *FOXO4* 3'-UTR was investigated via luciferase assay. Co-transfection of SW480 cells with Luc-FOXO4-wt and miR-193a-3p mimic has resulted in a significant down-regulation of luciferase activity (0.77 ± 0.06-fold; $p = 0.005$) with respect to the Luc-FOXO4-ctl while co-transfection with Luc-FOXO4-mt and miR-193a-3p mimic has resulted in a significant up-regulation of luciferase activity (1.10 ± 0.04-fold; $p = 0.008$) when compared to the Luc-FOXO4-wt (Figure 4.32). No significant differences were observed following co-transfections of Luc-FOXO4-ctl, Luc-FOXO4-wt or Luc-FOXO4-mt with miR-193a-3p inhibitor ($p > 0.05$). Mutagenesis at the seed match region of *FOXO4* 3'-UTR has successfully attenuated the miR-193a-3p-induced decrease of luciferase activity. Therefore, miR-193a-3p could modulate the expression of *FOXO4* via the regulatory element exhibited in the 3'-UTR region.

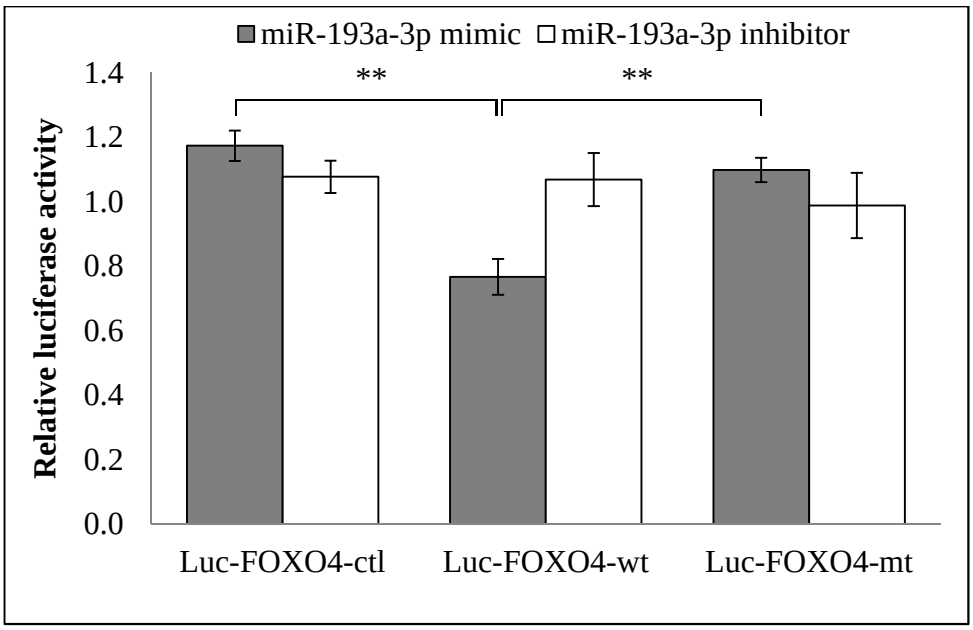

Figure 4.32: Relative luciferase activity following co-transfection of *FOXO4* luciferase reporters and miR-193a-3p into SW480 cells. Luminescence values obtained from the transfected cells were background-subtracted with the non-transfected cells. Firefly/*Renilla* luciferase activities were expressed as relative value against the respective negative controls. Functional interaction between Luc-FOXO4-wt and miR-193a-3p mimic was depicted via the down-regulation of luciferase activity with respect to Luc-FOXO4-ctl. Restoration of luciferase activity was observed in the co-transfection of Luc-FOXO4-mt and miR-193a-3p mimic with respect to Luc-FOXO4-wt. Fold change below 1 indicates down-regulation. Data are presented as mean ± SEM (n = 3). ** $p < 0.01$.

4.7.1.7 Modulation of *FOXO4* expression in SW480 and SW620 cell lines

The CRC cell lines studied were the non-metastatic SW480 and the metastatic SW620. In the RT-qPCR experiment for miRNA, RNU48 was used as the endogenous control. miRNA inhibitor positive control that targets the endogenous miR-16 was included. The transfection procedure was a success as the miR-16 level showed significant down-

regulation in both SW480 (0.06 ± 0.02-fold; $p = 0.012$) and SW620 (0.04 ± 0.01-fold; $p = 0.008$) cells. In the RT-qPCR experiment for mRNA, *β-actin* was used as the endogenous control. miRNA mimic positive control that targets the 3'-UTR of the housekeeping *GAPDH* gene was included. The *GAPDH* level revealed significant down-regulation in both SW480 (0.16 ± 0.01-fold; $p = 0.021$) and SW620 (0.18 ± 0.03-fold; $p = 0.013$) cells.

Following the transfection with miR-193a-3p mimic or inhibitor (Table 4.8), monitoring of *FOXO4* mRNA and FOXO4 protein expression levels was conducted via RT-qPCR and Western blot, respectively. As depicted in Figure 4.33, *FOXO4* mRNA expression was significantly down-regulated in SW480 (0.32 ± 0.07-fold; $p = 0.006$) and SW620 (0.49 ± 0.11-fold; $p = 0.016$) cells transfected with miR-193a-3p mimic and significantly up-regulated in SW480 (7.76 ± 1.26-fold; $p = 0.004$) and SW620 (3.63 ± 0.57-fold; $p < 0.001$) cells transfected with miR-193a-3p inhibitor. Alteration in the mRNA expression was reflected in the protein expression as well. The Western blot analysis showed that the level of FOXO4 protein was significantly decreased by 0.72 ± 0.07-fold; $p = 0.047$ (SW480) and 0.73 ± 0.07-fold; $p = 0.049$ (SW620) following miR-193a-3p mimic transfection and significantly increased by 1.77 ± 0.16-fold; $p = 0.048$ (SW480) and 1.45 ± 0.05-fold; $p = 0.042$ (SW620) following miR-193a-3p inhibitor transfection (Figure 4.34A, B). The transfection of miR-193a-3p inhibitor has resulted in a relatively higher induction of *FOXO4* mRNA and FOXO4 protein in the SW480 cells when compared to the SW620 cells.

Table 4.8: Relative miR-193a-3p expression in SW480 and SW620 cells following miR-193a-3p mimic or miR-193a-3p inhibitor transfection. Values are fold changes expressed as relative value against the respective negative controls. Fold change above 1 indicates up-regulation while fold change below 1 indicates down-regulation. Data are presented as mean ± SEM (n = 3).

Treatment	**Relative miR-193a-3p expression**	
	SW480	**SW620**
miR-193a-3p mimic	211.63 ± 41.79	177.53 ± 55.93
miR-193a-3p inhibitor	0.05 ± 0.01	0.18 ± 0.06

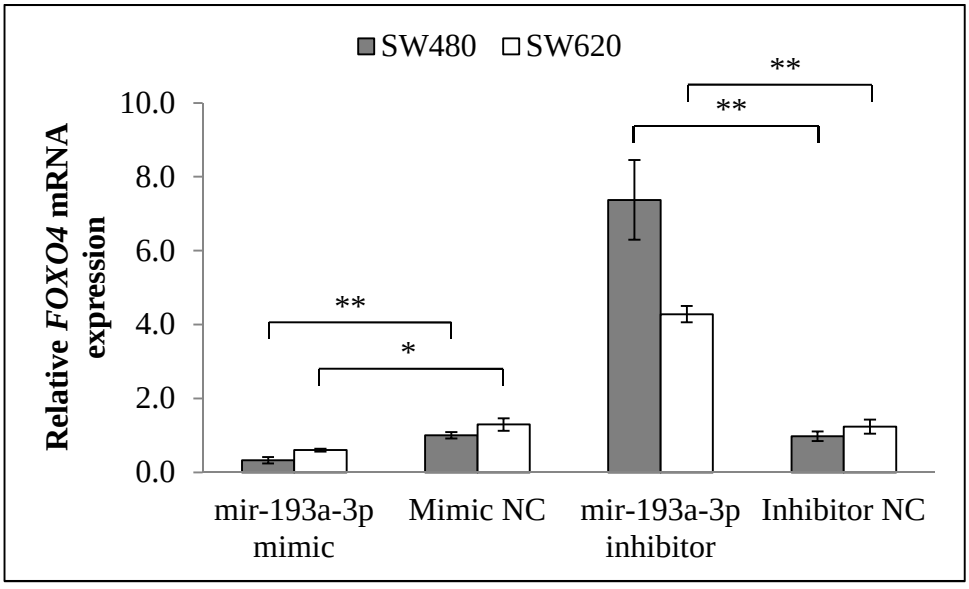

Figure 4.33: Relative *FOXO4* mRNA expression in SW480 and SW620 cells following miR-193a-3p transfection. *FOXO4* expression was down-regulated in miR-193a-3p mimic-transfected cells and up-regulated in miR-193a-3p inhibitor-transfected cells. Data are presented as mean ± SEM (n = 3). * $p < 0.05$; ** $p < 0.01$.

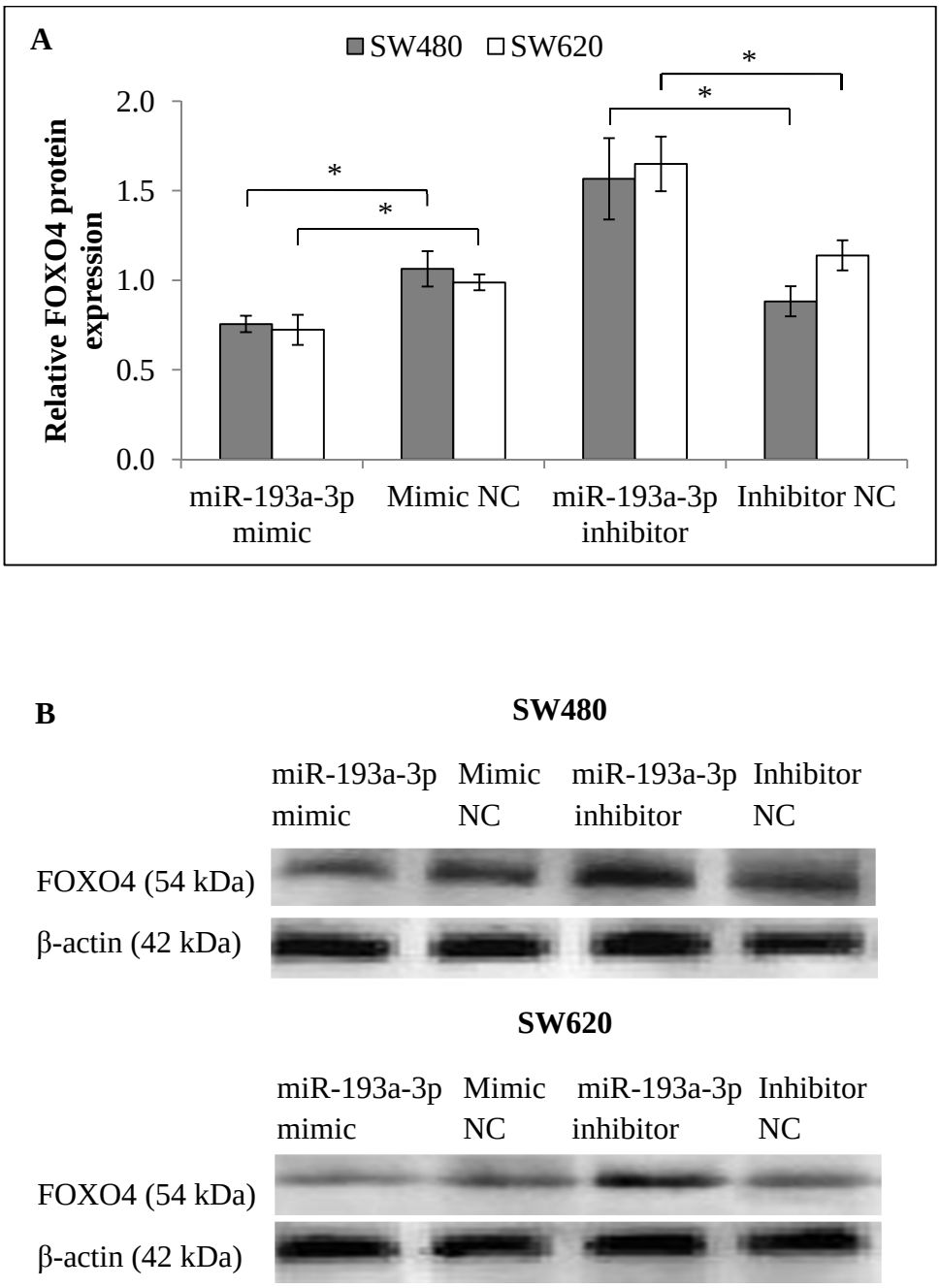

Figure 4.34: Relative FOXO4 protein expression in SW480 and SW620 cells following miR-193a-3p transfection. (A) FOXO4 expression was down-regulated in miR-193a-3p mimic-transfected cells and up-regulated in miR-193a-3p inhibitor-transfected cells. Data are presented as mean ± SEM (n = 3). * $p < 0.05$. (B) Representative blots of FOXO4 protein expression in SW480 and SW620 cells. β-actin was used as the loading control.

4.7.1.8 *FOXO4* expression in clinical CRC samples

The expression of *FOXO4* in CRC was evaluated using 102 whole blood samples (70 patients; 32 healthy controls) and 30 paired cancer tissues. *β-actin* was chosen as the endogenous control in RT-qPCR analysis. β-actin was also used as the loading control in Western blot analysis. The presence of *FOXO4* and *β-actin* mRNAs in the clinical samples was confirmed by RT-qPCR (Figure 4.35).

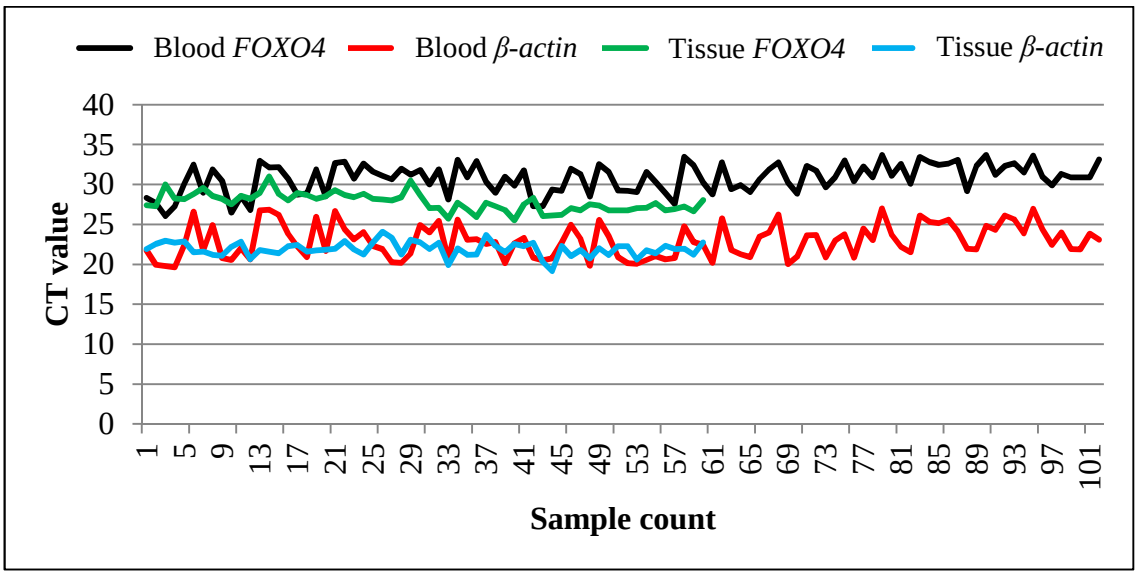

Figure 4.35: C_T values of blood and tissue *FOXO4* and *β-actin*. Colour legend, black: blood *FOXO4*; red: blood *β-actin*, green: tissue *FOXO4*; blue: tissue *β-actin*.

No significant differences were observed in the levels of *β-actin* mRNA (p = 0.992 in blood; p = 0.065 in tissue) and β-actin protein (p = 0.069 in tissue) between the cancer and normal/control samples. In contrast, *FOXO4* mRNA expression was found to be significantly down-regulated in the blood (p = 0.017) and tissue (p < 0.001) samples obtained from CRC patients. Pearson's correlation between the blood and tissue *FOXO4* levels was 0.549 (p = 0.002). A decreasing trend of expression was observed as the

tumour progressed from stage I-II to stage III-IV (Figures 4.36 and 4.37). The *FOXO4* mRNA expression of each sample is shown in Appendices 7 and 8. In addition, FOXO4 protein expression was determined to be lower in the cancer tissue when compared with the normal colonic mucosa ($p < 0.001$) (Figure 4.38A, B). The FOXO4 protein expression of each sample is shown in Appendix 13.

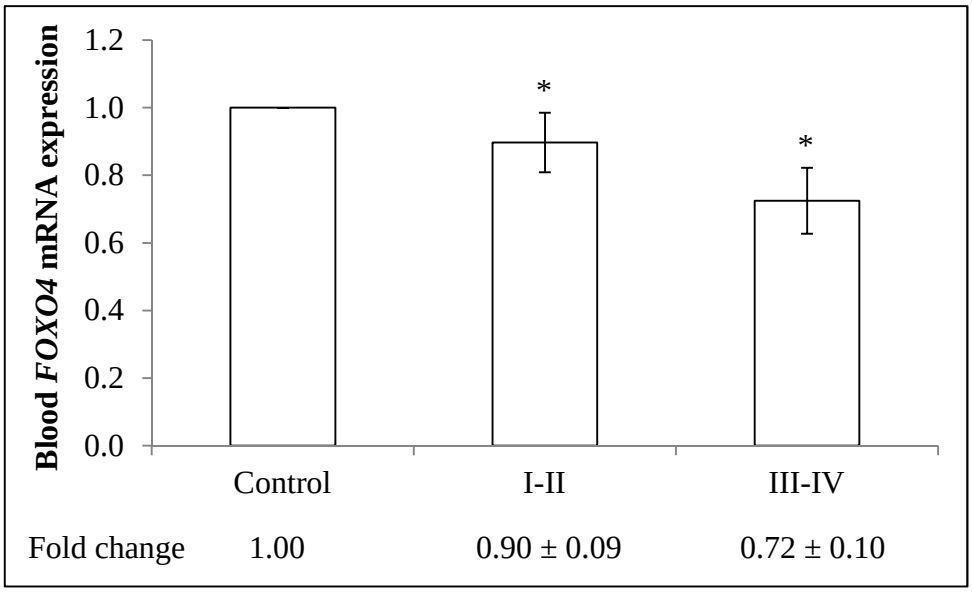

Figure 4.36: Blood *FOXO4* mRNA expression. The basal fold change of the control group was set at 1. Data are expressed as fold change of TNM stage versus control. Fold change below 1 indicates down-regulation. Data are presented as mean ± SEM. * $p < 0.05$.

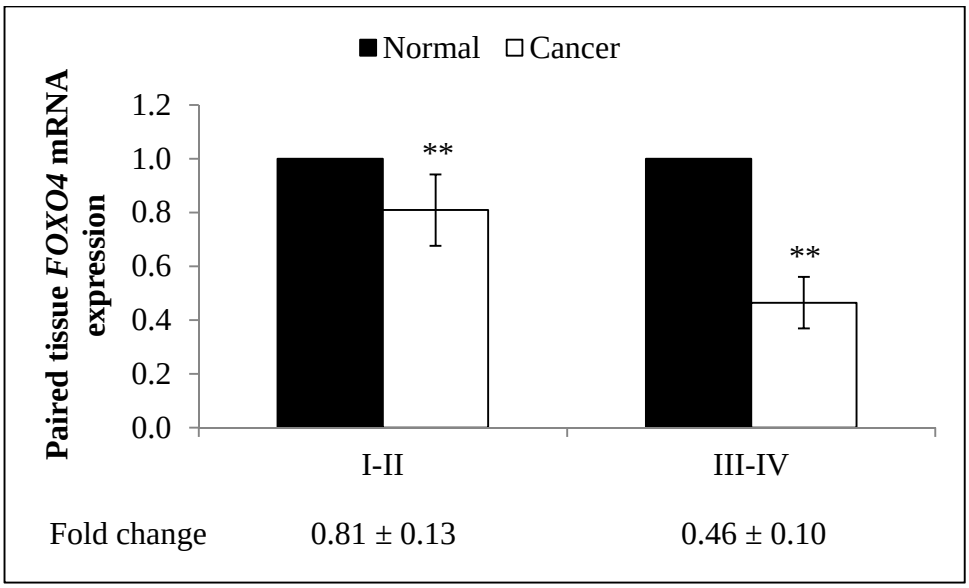

Figure 4.37: Paired tissue *FOXO4* mRNA expression. Relative expression is expressed as fold change of cancer tissue versus normal colonic mucosa. Fold change below 1 indicates down-regulation. Data are presented as mean ± SEM. ** $p < 0.01$.

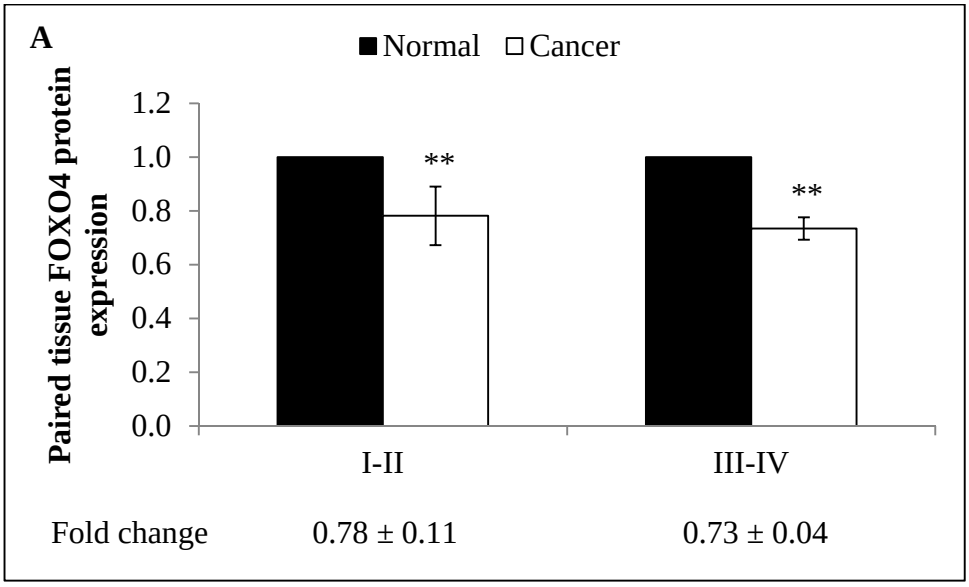

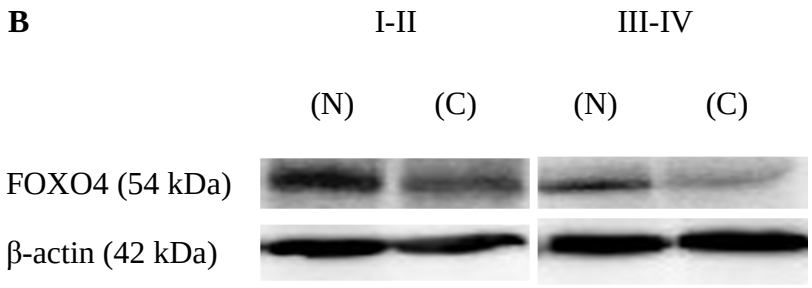

Figure 4.38: Paired tissue FOXO4 protein expression. (A) Relative expression is expressed as fold change of cancer tissue versus normal colonic mucosa. Fold change below 1 indicates down-regulation. Data are presented as mean ± SEM. $^{**}p < 0.01$. (B) Representative blots of FOXO4 protein expression in stage I-II and stage III-IV paired cancer tissues (N: normal colonic mucosa; C: cancer tissue). β-actin was used as the loading control.

Next, the relationship between miR-193a-3p and *FOXO4* mRNA or FOXO4 protein levels was analysed (Figure 4.39A-C). However, only tissue miR-193a-3p and tissue *FOXO4* mRNA showed significant negative correlation (r = -0.384; p = 0.036). No significant negative correlation was detected between blood miR-193a-3p and blood *FOXO4* mRNA (r = -0.138; p = 0.168) or between tissue miR-193a-3p and tissue FOXO4 protein (r = -0.094; p = 0.620). The expression between tissue *FOXO4* mRNA and FOXO4 protein was also found to be insignificantly correlated (r = 0.218; p = 0.248).

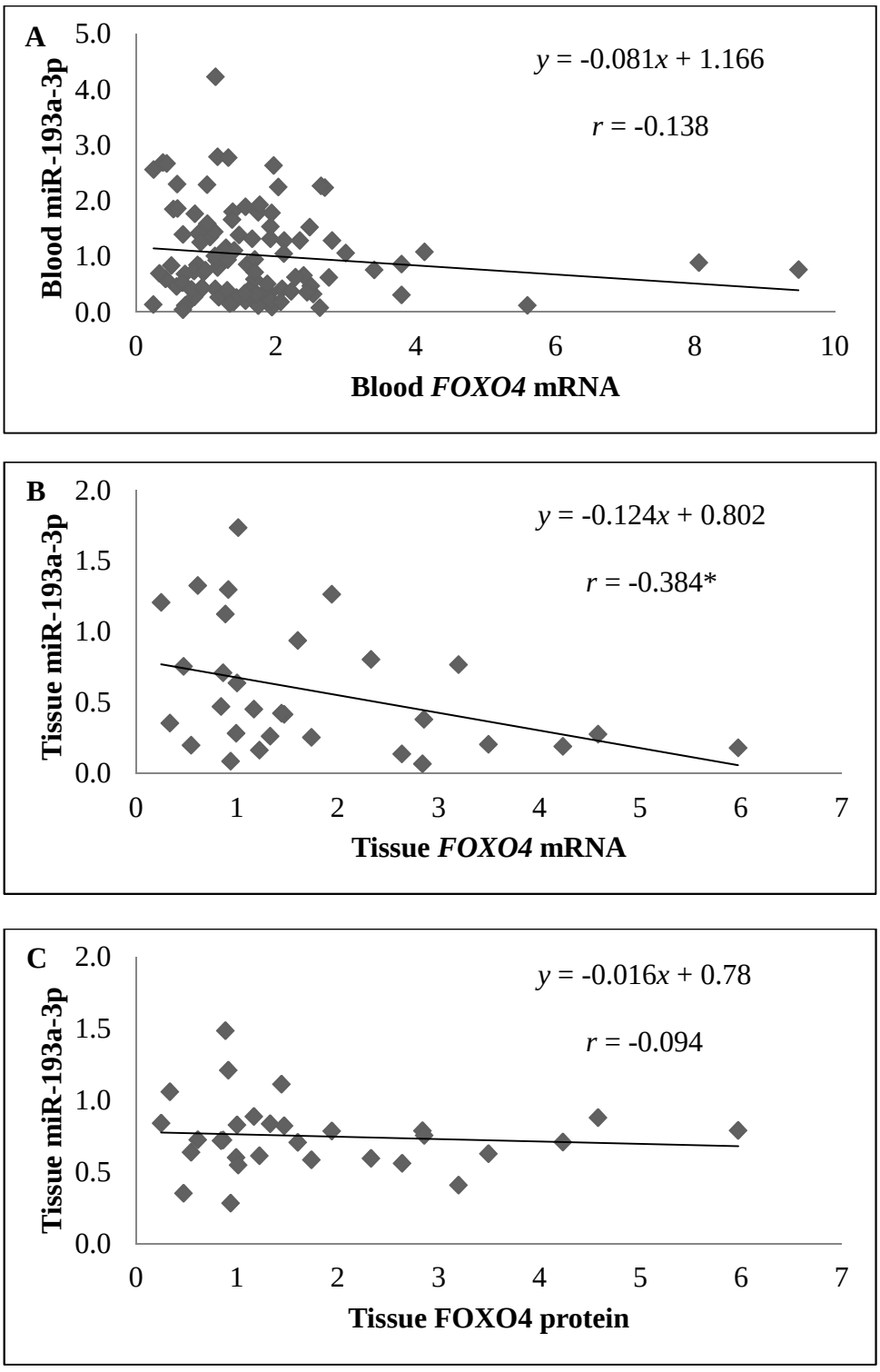

Figure 4.39: Correlation between miR-193a-3p and *FOXO4* mRNA or FOXO4 protein. (A) Blood miR-193a-3p and blood *FOXO4* mRNA. (B) Tissue miR-193a-3p and tissue *FOXO4* mRNA. (C) Tissue miR-193a-3p and tissue FOXO4 protein. * $p < 0.05$.

4.7.2 miR-23a transfection

4.7.2.1 Effect on cell viability rate following miR-23a transfection

Cell viability studies of SW480 and SW620 cells post-transfections (24 h, 48 h and 72 h) were conducted using MTT assay. No significant difference was observed at 24 h ($p > 0.05$). The cell viability of SW480 cells was significantly increased (118.08 ± 3.51%; $p = 0.003$) and decreased (67.94 ± 1.77%; $p < 0.001$) at 48 h following miR-23a mimic and miR-23a inhibitor transfections, respectively (Figure 4.40A). The cell viability of SW620 cells was also significantly increased (121.46 ± 2.70%; $p = 0.002$) and decreased (70.22 ± 2.56%; $p < 0.001$) at 48 h following miR-23a mimic and miR-23a inhibitor transfections, respectively (Figure 4.40B). At 72 h, only miR-23a inhibitor transfection revealed significant reduction of cell viability in both SW480 (67.85 ± 0.72%; $p < 0.001$) and SW620 (71.24 ± 4.26%; $p = 0.003$) cells. The miR-23a mimic transfection has no effect on cell viability after 72 h. The cells may have entered the stationary phase due to prolonged transfection, whereby cell proliferation is greatly reduced and further increase in cell viability is no longer possible (Davis, 2011). The optimal transfection period in the cell viability assay was 48 h.

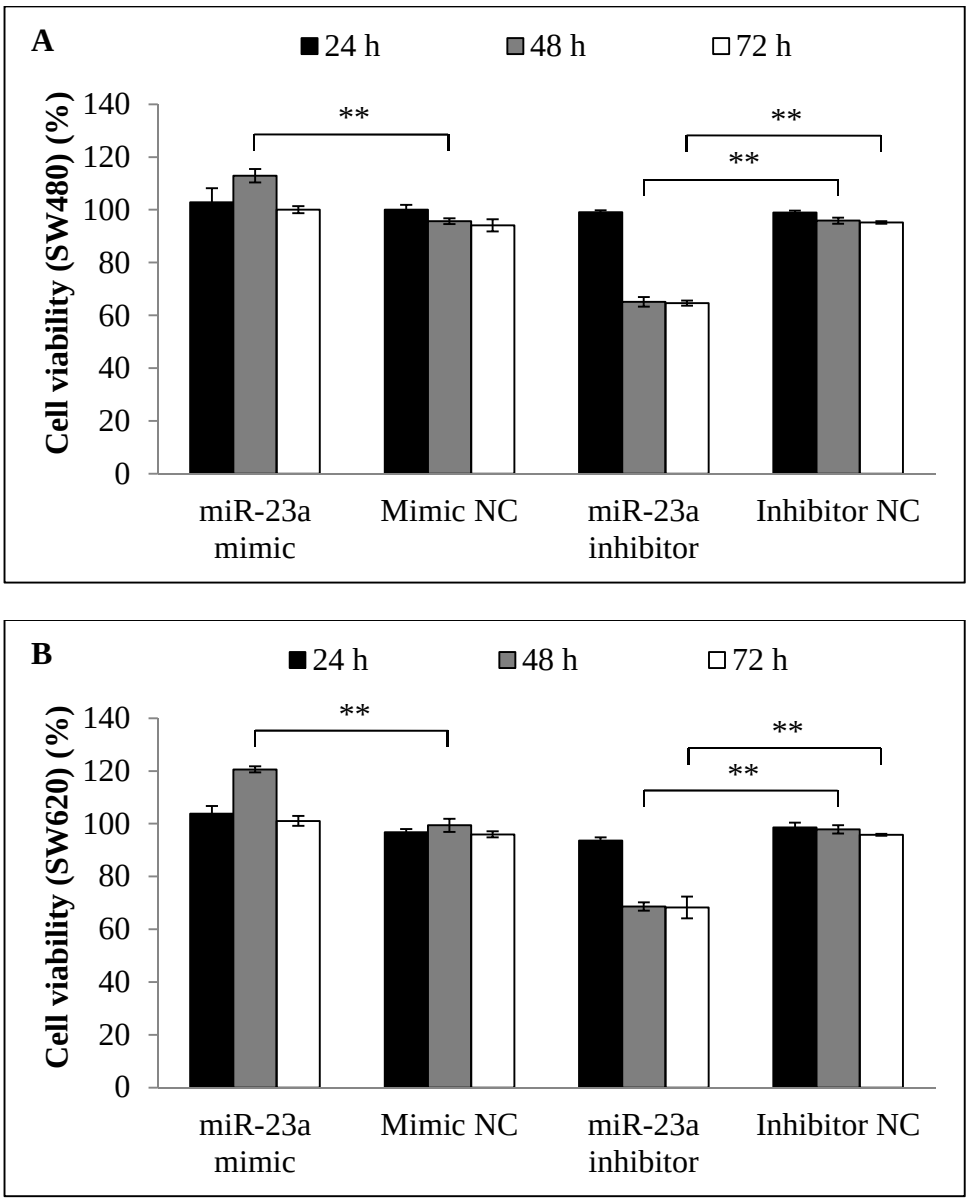

Figure 4.40: Cell viability of (A) SW480 and (B) SW620 cells following miR-23a transfection. The miR-23a inhibitor transfection has successfully reduced cell viability at 48 h and 72 h. Data are presented as mean ± SEM (n = 3). ** $p < 0.01$.

4.7.2.2 Effect on apoptosis rate following miR-23a transfection

Apoptosis assay was conducted using Annexin V and PI double staining procedure. Cell populations in live, dead and apoptotic stages were quantitated using Invitrogen Tali image-based cytometer (Table 4.9). The cytometric analysis demonstrated low percentages of apoptotic cells in the SW480 and SW620 cells following miR-23a mimic transfection and high percentages of apoptotic cells following miR-23a inhibitor transfection. Moreover, signs of apoptosis such as distorted cell morphology, membrane blebbling and cell lysis were noted under the microscope. The relative apoptosis rate was then calculated and the transfection of miR-23a inhibitor resulted in a significantly higher proportion of apoptotic cells in both SW480 (8.11 ± 1.93-fold; $p < 0.001$) and SW620 cells (3.24 ± 0.65-fold; $p = 0.002$) when compared to the miRNA inhibitor NC (Figure 4.41).

Table 4.9: Quantification of live, dead and apoptotic cells in SW480 and SW620 cells using Invitrogen Tali image-based cytometer (miR-23a transfection). Data are presented as mean ± SEM (*n* = 3).

Treatment	**SW480**			**SW620**		
	Live (%)	**Dead (%)**	**Apoptotic (%)**	**Live (%)**	**Dead (%)**	**Apoptotic (%)**
NTC	84.33 ± 0.33	10.33 ± 0.33	5.33 ± 0.33	84.00 ± 2.00	12.33 ± 1.76	3.67 ± 0.67
Mock	87.00 ± 1.53	11.00 ± 0.00	2.00 ± 1.53	81.67 ± 0.67	16.00 ± 0.58	2.00 ± 0.00
miR-23a mimic	85.33 ± 1.20	13.00 ± 1.00	1.33 ± 0.88	85.00 ± 1.15	10.00 ± 0.00	5.00 ± 1.15
Mimic NC	83.67 ± 0.88	13.00 ± 0.58	2.67 ± 0.33	78.33 ± 0.88	14.00 ± 0.58	7.33 ± 0.88
miR-23a inhibitor	65.67 ±1.45	9.00 ± 1.00	25.33 ± 1.86	68.00 ± 1.73	13.33 ± 0.67	18.33 ± 2.60
Inhibitor NC	85.00 ± 1.53	11.67 ± 0.67	3.67 ± 1.20	78.67 ± 1.20	15.00 ± 0.58	6.00 ± 1.15
Doxorubicin	54.33 ± 4.67	23.67 ± 0.88	22.33 ± 5.33	48.33 ± 4.84	27.00 ± 2.08	24.33 ± 2.91

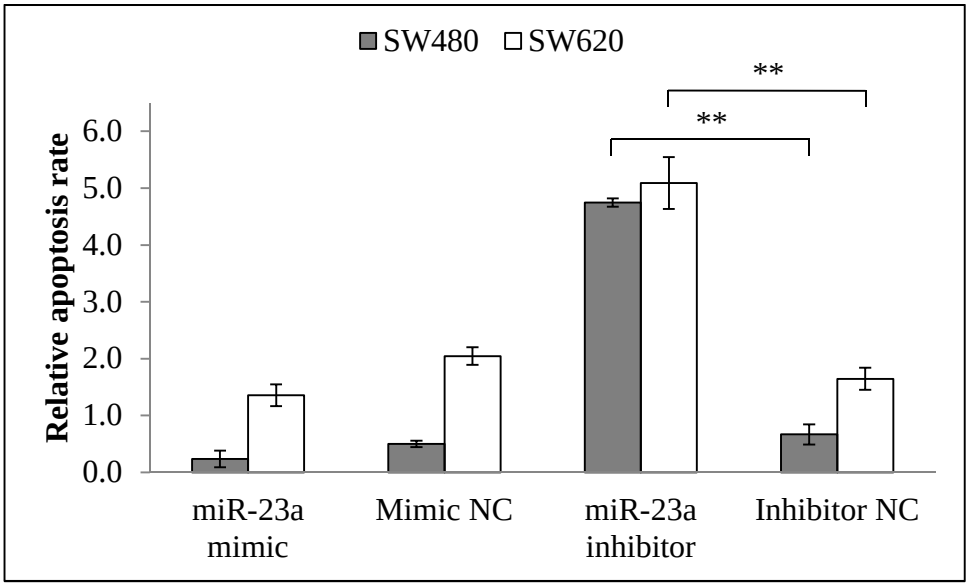

Figure 4.41: Relative apoptosis rate of SW480 and SW620 cells following miR-23a transfection. The miR-23a inhibitor transfection has successfully elevated cell apoptosis. Data are presented as mean ± SEM (n = 3). ** $p < 0.01$.

4.7.2.3 Effect on caspase 3/7 activity following miR-23a transfection

Caspase 3/7 activation analysis was performed to further elucidate the apoptotic role of miR-23a in CRC. The miR-23a inhibitor transfection induced significant activation of caspase 3/7 activity in both SW480 (198.42 ± 20.57%; p = 0.003) and SW620 (183.27 ± 7.60%; p = 0.004) cells (Figure 4.42). However, only SW480 cells showed significant reduction of caspase 3/7 activity (84.67 ± 4.12%; p = 0.048) following miR-23a mimic transfection.

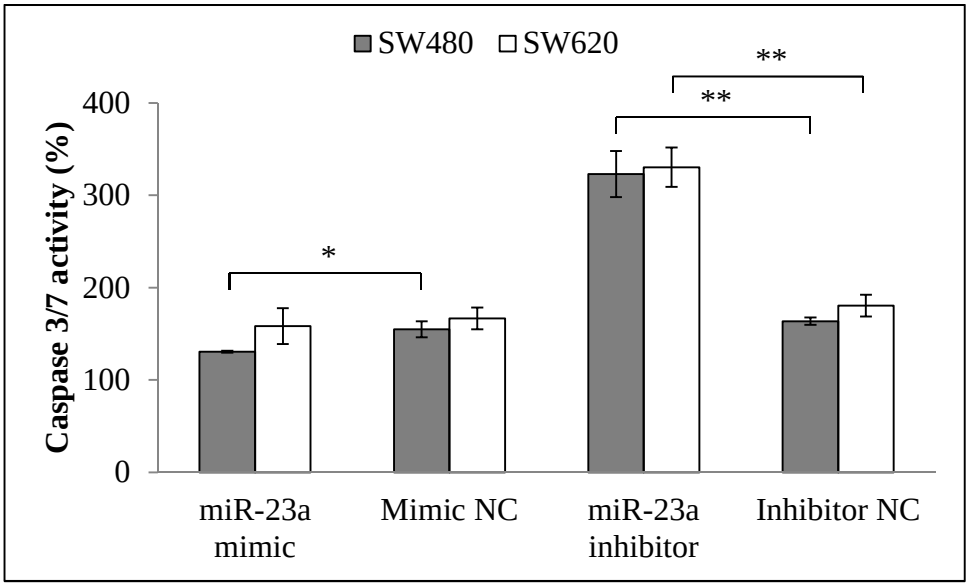

Figure 4.42: Caspase 3/7 activity of SW480 and SW620 cells following miR-23a transfection. The miR-23a inhibitor transfection has successfully increased caspase 3/7 activity. Data are presented as mean ± SEM (n = 3). * $p < 0.05$; ** $p < 0.01$.

4.7.2.4 Effect on migration and invasion activity following miR-23a transfection

The migratory and invasive ability of CRC cells was determined. However, no significant difference was observed in the relative migration and invasion activity of SW480 and SW620 cells following miR-23a transfection ($p > 0.05$) (Figure 4.43A-D).

A

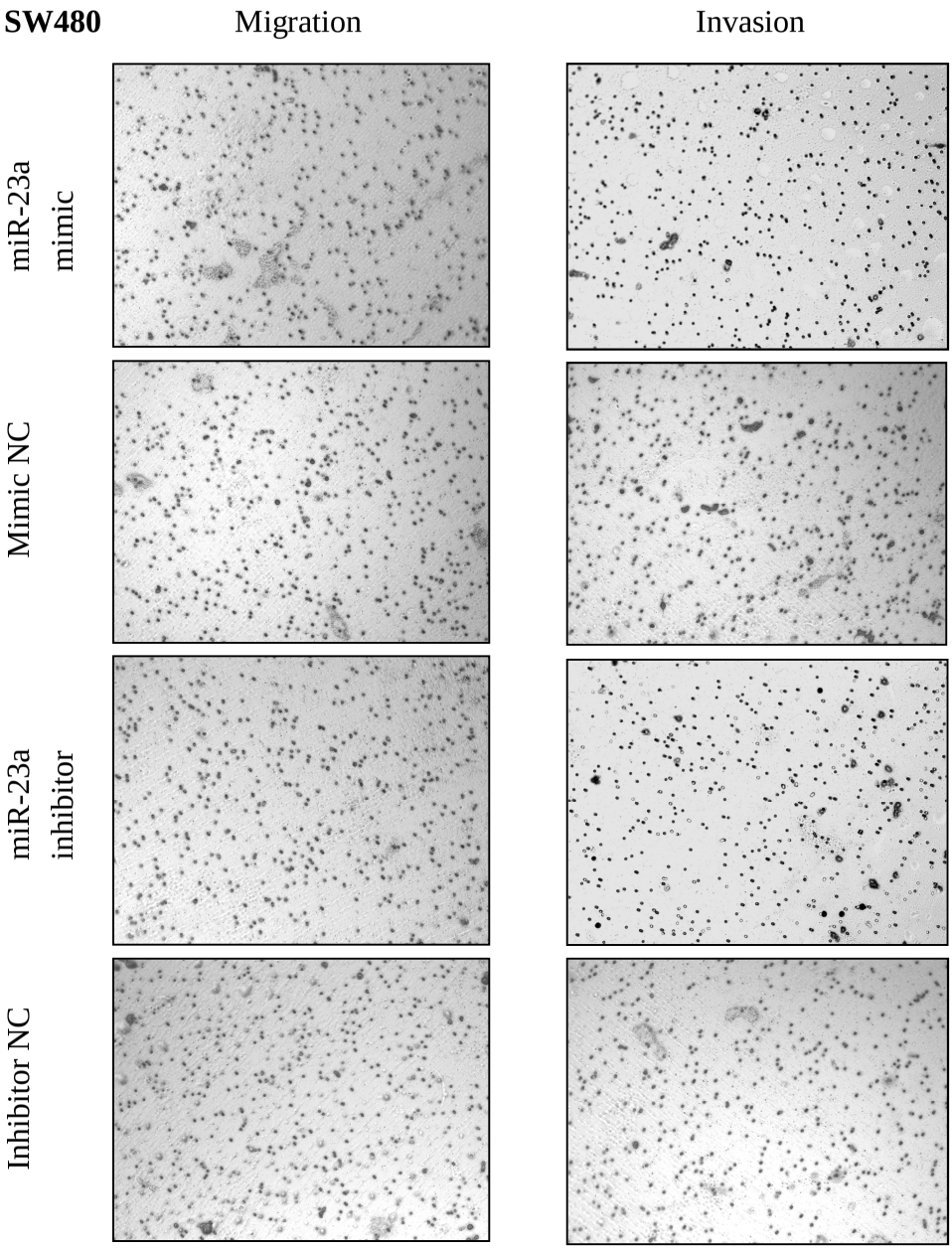
SW480
Migration
Invasion
miR-23a mimic
Mimic NC
miR-23a inhibitor
Inhibitor NC

B

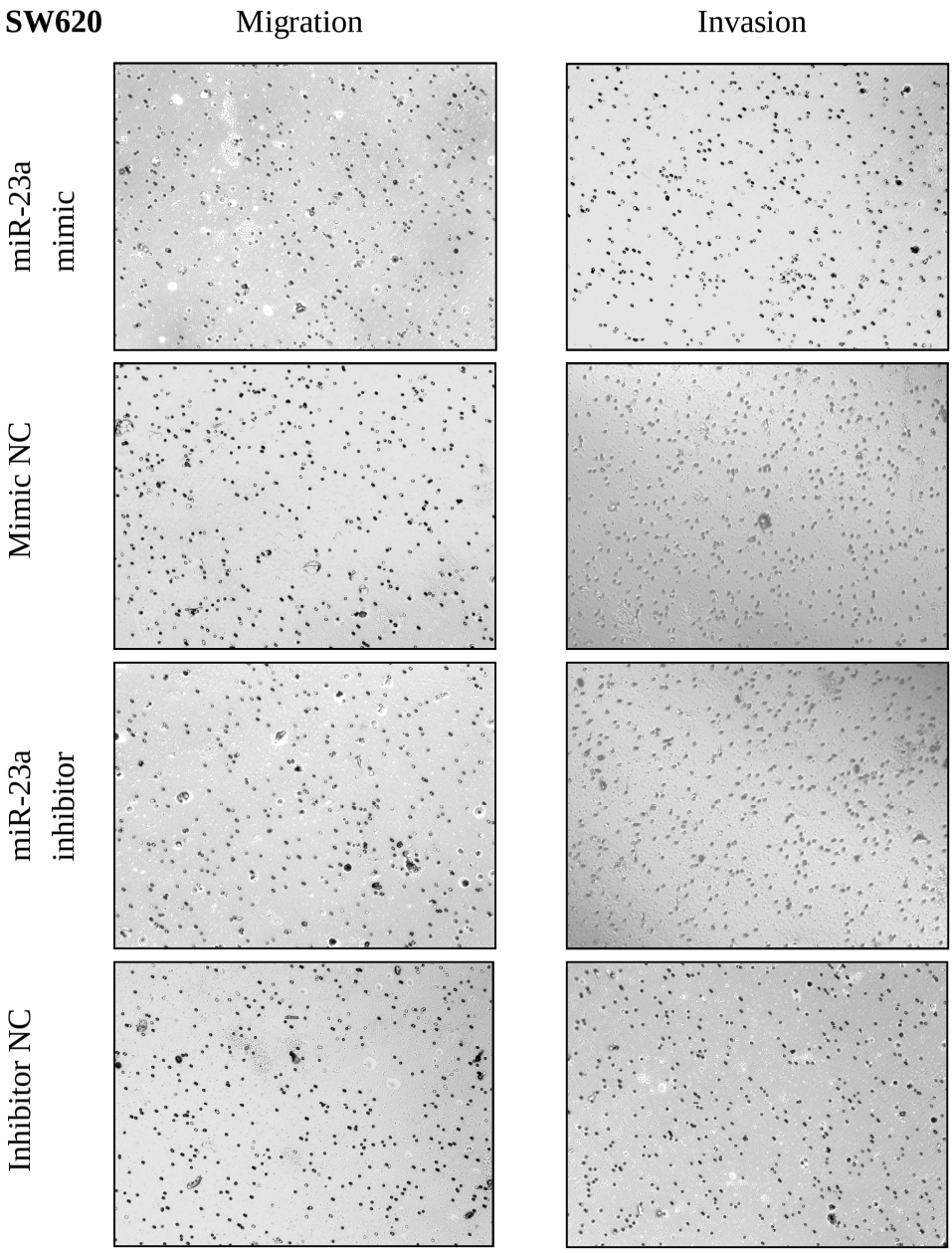
SW620
Migration
Invasion
miR-23a mimic
Mimic NC
miR-23a inhibitor
Inhibitor NC

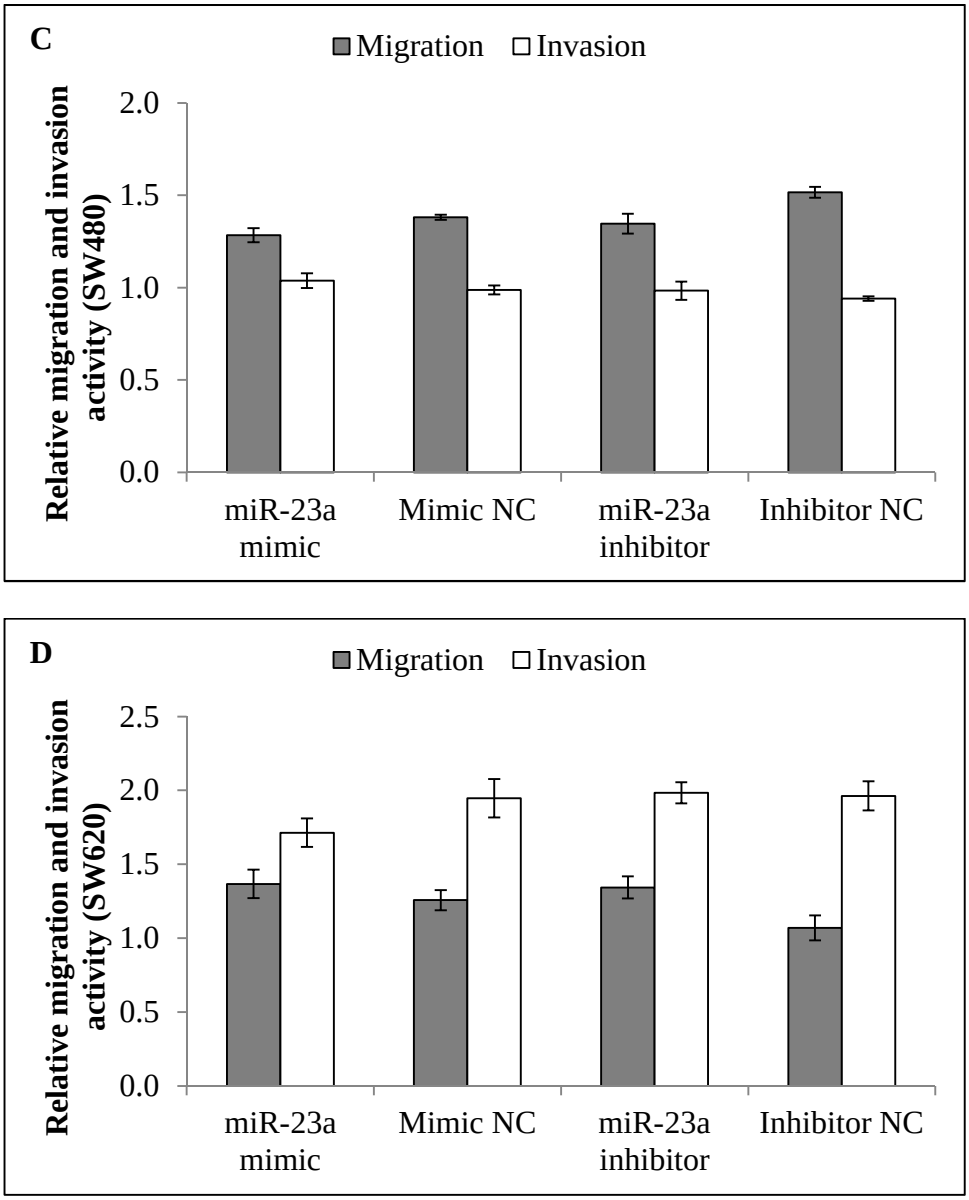

Figure 4.43: Relative migration and invasion activity of SW480 and SW620 cells following miR-23a transfection. (A, B) Representative fields of migratory (left) and invasive (right) cells on plate insert. (C, D) Bar charts of relative migration and invasion activity. No statistical significance was determined ($p > 0.05$). Data are presented as mean ± SEM ($n = 3$).

4.7.2.5 Screening of miR-23a targets

Similarly to section 4.7.1.4, miRNA target prediction for miR-23a was computed using miRWalk database. The initial screening process yielded a long list of mRNAs. Based on the comprehensive literature search on CRC relevant genes, several putative targets of miR-23a that have been found to be associated with CRC were determined, namely, *ACVR1C*, *ACVR2A*, *ACVR2B*, *APAF1*, *CASP7*, *CCND1*, *CREBBP*, *FAS*, *FZD4*, *FZD5*, *FZD7*, *ID4*, *PIK3R3*, *PTEN*, *RBL2*, *SMAD4*, *SOS1* and *TGFBR2* (Appendix 14). Among these, apoptotic peptidase activating factor 1 (*APAF1*) gene was selected for further investigation, with the consideration of its role in cell apoptosis.

4.7.2.6 Construction of *APAF1* luciferase reporters

Cloning of the *APAF1* 3'-UTR fragment was performed to verify a putative target site of miR-23a. The highly conserved site based on the TargetScan Human 6.2 prediction was chosen.

APAF1 (NM_013229.2) mRNA consists of 7171 bp. The length of the 3'-UTR is 2836 bp. A fragment of the *APAF1* 3'-UTR containing the recognition site for miR-23a at nucleotide position 5615-5914 was constructed via GeneArt gene synthesis service (Invitrogen, Carlsbad, CA, USA) (Appendix 15). The corresponding site-directed mutant containing the mutated seed sequence (5'-AAUGUGAA-3' to 5'-AUUCUGCA-3') was also generated (Appendix 16). Each customised fragment was inclusive of the HindIII and SpeI restriction sites (312 bp). The predicted pairing region between miR-23a and *APAF1* mRNA is presented in Table 4.10. The wild-type and mutated *APAF1* 3'-UTR fragments (Figure 4.44A, B) were cloned into the pMIR-REPORT firefly luciferase reporter vector (Figure 4.31) at the HindIII and SpeI sites and designated as

Luc-APAF1-wt and Luc-APAF1-mt, respectively. A luciferase vector without *APAF1* 3'-UTR (Luc-APAF1-ctl) was used as the experimental control. All constructs were verified by DNA sequencing.

Table 4.10: Conserved miR-23a target site on human *APAF1* 3'-UTR (NM_013229.2). *APAF1* 3'-UTR length: 2836 bp. Seed match region at nucleotide position 1474-1481 is shown in bold italics. Mutations are marked with the symbol †.

APAF1 3'-UTR	5'	...AAGAUUUUUCUAAGA***AAUGUGAA***...
		| | | | | | |
hsa-miR-23a	3'	CCUUUAGGGACCG***UUACACU***A
Mutated *APAF1* 3'-UTR	5'	...AAGAUUUUUCUAAGA***AUUCUGCA***...
		|†| †| | †
hsa-miR-23a	3'	CCUUUAGGGACCG***UUACACU***A

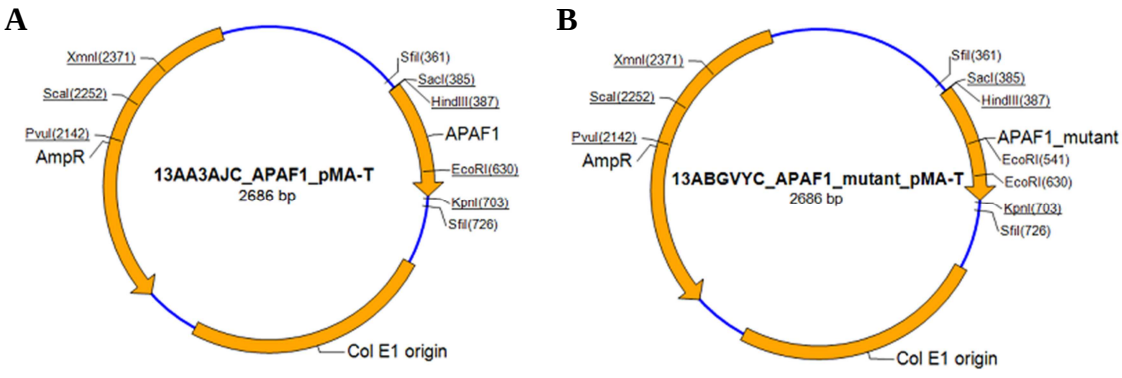

Figure 4.44: Images of customised GeneArt pMA-T vectors containing (A) *APAF1* 3'-UTR fragment and (B) mutated *APAF1* 3'-UTR fragment. The pMA-T vectors were sub-cloned into the pMIR-REPORT firefly luciferase reporter vector at the HindIII and SpeI sites to generate the Luc-APAF1-wt and Luc-APAF1-mt constructs.

4.7.2.7 miR-23a:*APAF1* target validation study

The functional interaction between miR-23a and *APAF1* 3'-UTR was determined using luciferase assay. Co-transfection of SW480 cells with Luc-APAF1-wt and miR-23a mimic has resulted in a significant down-regulation of luciferase activity (0.72 ± 0.05-fold; p = 0.001) with respect to the Luc-APAF1-ctl while co-transfection with Luc-APAF1-mt and miR-23a mimic has resulted in a significant up-regulation of luciferase activity (1.11 ± 0.04-fold; p = 0.003) when compared to the Luc-APAF1-wt (Figure 4.45). No significant differences were observed following co-transfections of Luc-APAF1-ctl, Luc-APAF1-wt or Luc-APAF1-mt with miR-23a inhibitor (p > 0.05). Mutation of the miR-23a target site in the *APAF1* 3'-UTR has successfully weakened the miR-23a-induced decrease of luciferase activity. Thus, miR-23a could influence the regulation of *APAF1* via the regulatory element present in the 3'-UTR region.

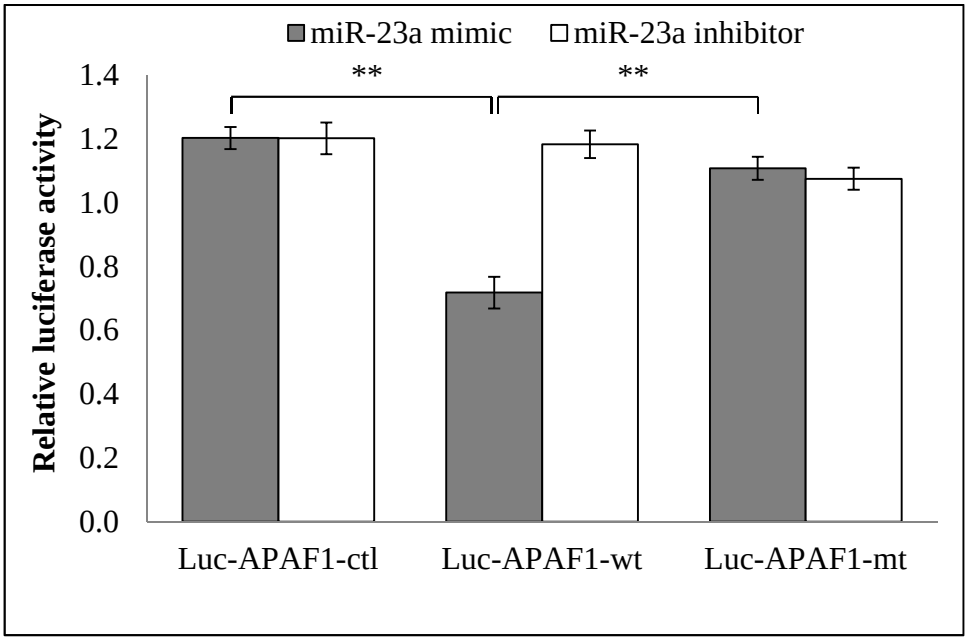

Figure 4.45: Relative luciferase activity following co-transfection of *APAF1* luciferase reporters and miR-23a into SW480 cells. Luminescence values obtained from the transfected cells were background-subtracted with the non-transfected cells. Firefly/*Renilla* luciferase activities were expressed as relative value against the respective negative controls. Functional interaction between Luc-APAF1-wt and miR-23a mimic was depicted via the down-regulation of luciferase activity with respect to Luc-APAF1-ctl. Restoration of luciferase activity was observed in the co-transfection of Luc-APAF1-mt and miR-23a mimic with respect to Luc-APAF1-wt. Fold change below 1 indicates down-regulation. Data are presented as mean ± SEM (n = 3). ** $p < 0.01$.

4.7.2.8 Modulation of *APAF1* expression in SW480 and SW620 cell lines

Following the transfection with miR-23a mimic or inhibitor (Table 4.11), monitoring of *APAF1* mRNA and APAF1 protein expression levels were conducted via RT-qPCR and Western blot, respectively. As depicted in Figure 4.46, *APAF1* mRNA expression was significantly down-regulated in SW480 (0.43 ± 0.11-fold; p = 0.015) and SW620 (0.62

± 0.11-fold; p = 0.048) cells transfected with miR-23a mimic and significantly up-regulated in SW480 (8.42 ± 1.99-fold; p = 0.041) and SW620 (3.24 ± 0.49-fold; p = 0.018) cells transfected with miR-23a inhibitor. Alteration in the mRNA expression was reflected in the protein expression as well. The Western blot analysis showed that the level of APAF1 protein was significantly decreased by 0.51 ± 0.08-fold; p = 0.006 (SW480) and 0.46 ± 0.17-fold; p = 0.033 (SW620) following miR-23a mimic transfection and significantly increased by 1.76 ± 0.28-fold; p = 0.043 (SW480) and 1.60 ± 0.22-fold; p = 0.049 (SW620) following miR-23a inhibitor transfection (Figure 4.47A, B). The transfection of miR-23a inhibitor has resulted in a relatively higher induction of *APAF1* mRNA and APAF1 protein in the non-metastatic SW480 cells when compared to the metastatic SW620 cells.

Table 4.11: Relative miR-23a expression in SW480 and SW620 cells following miR-23a mimic or miR-23a inhibitor transfection. Values are fold changes expressed as relative value against the respective negative controls. Fold change above 1 indicates up-regulation while fold change below 1 indicates down-regulation. Data are presented as mean ± SEM (n = 3).

Treatment	**Relative miR-23a expression**	
	SW480	**SW620**
miR-23a mimic	285.17 ± 50.11	234.59 ± 8.98
miR-23a inhibitor	0.03 ± 0.003	0.04 ± 0.005

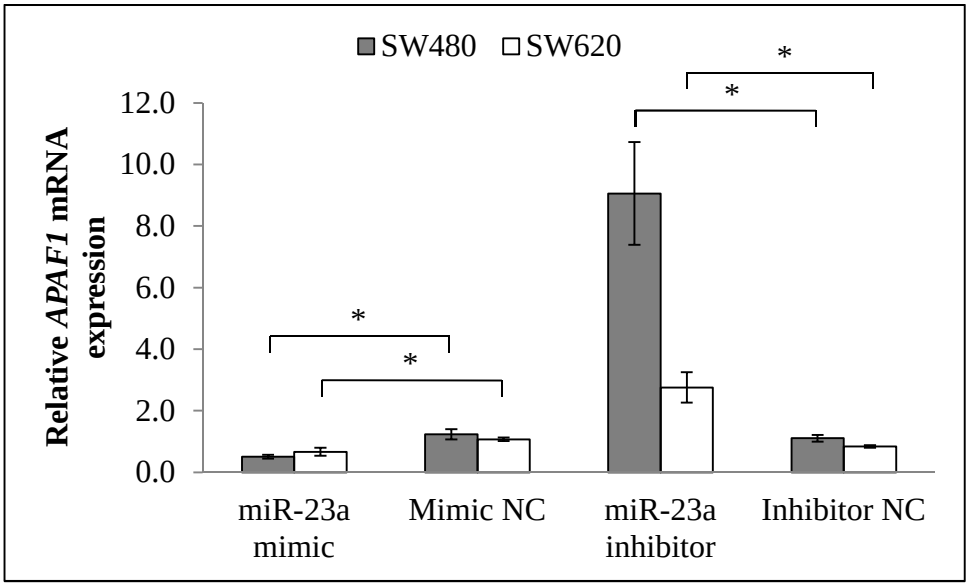

Figure 4.46: Relative *APAF1* mRNA expression in SW480 and SW620 cells following miR-23a transfection. *APAF1* expression was down-regulated in miR-23a mimic-transfected cells and up-regulated in miR-23a inhibitor-transfected cells. Data are presented as mean ± SEM (n = 3). * $p < 0.05$.

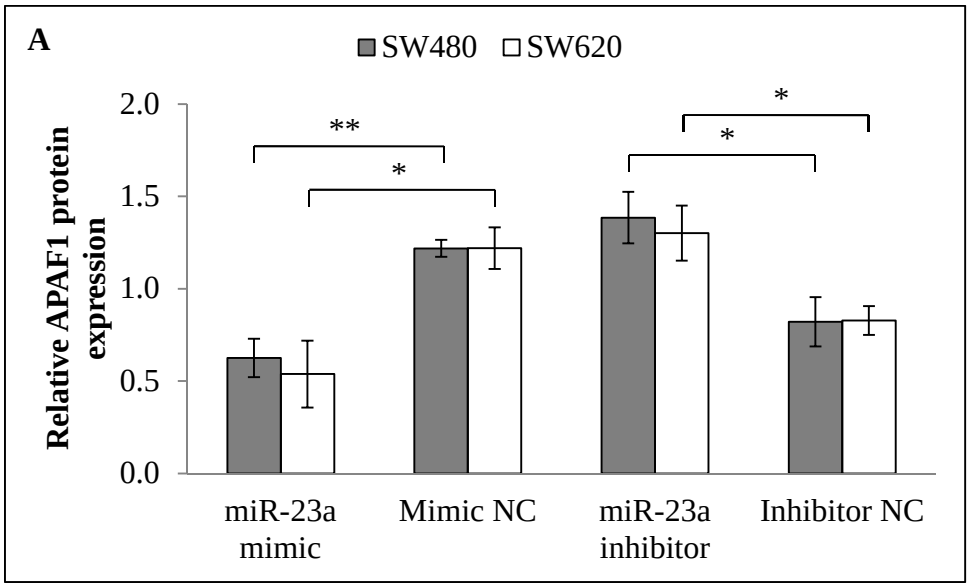

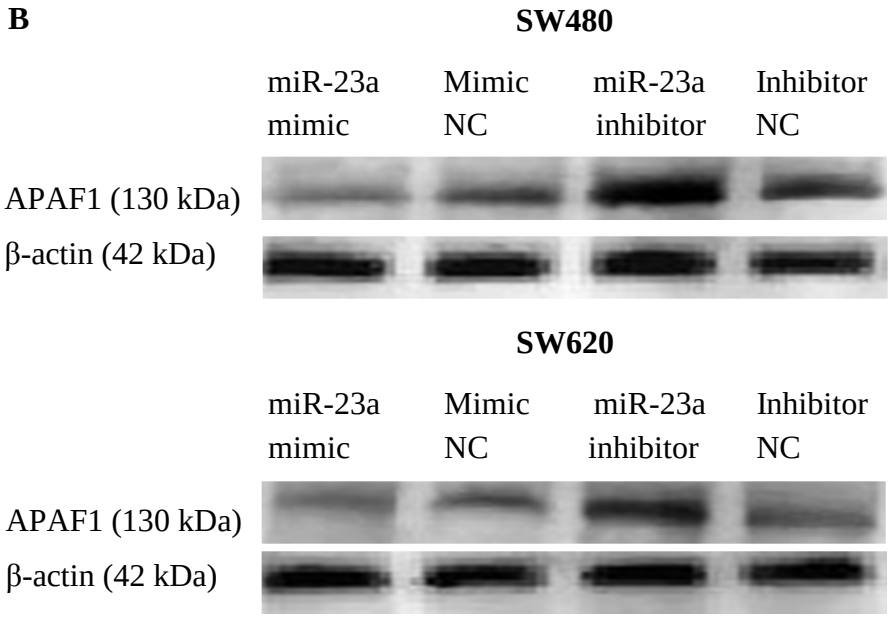

Figure 4.47: Relative APAF1 protein expression in SW480 and SW620 cells following miR-23a transfection. (A) APAF1 expression was down-regulated in miR-193a-3p mimic-transfected cells and up-regulated in miR-23a inhibitor-transfected cells. Data are presented as mean ± SEM (n = 3). * $p < 0.05$. (B) Representative blots of APAF1 protein expression in SW480 and SW620 cells. β-actin was used as the loading control.

4.7.2.9 *APAF1* expression in clinical CRC samples

Likewise in section 4.7.1.8, the expression of *APAF1* in CRC was evaluated using 102 whole blood samples (70 patients; 32 healthy controls) and 30 paired cancer tissues. The presence of *APAF1* and *β-actin* mRNAs in the clinical samples was confirmed by RT-qPCR (Figure 4.48).

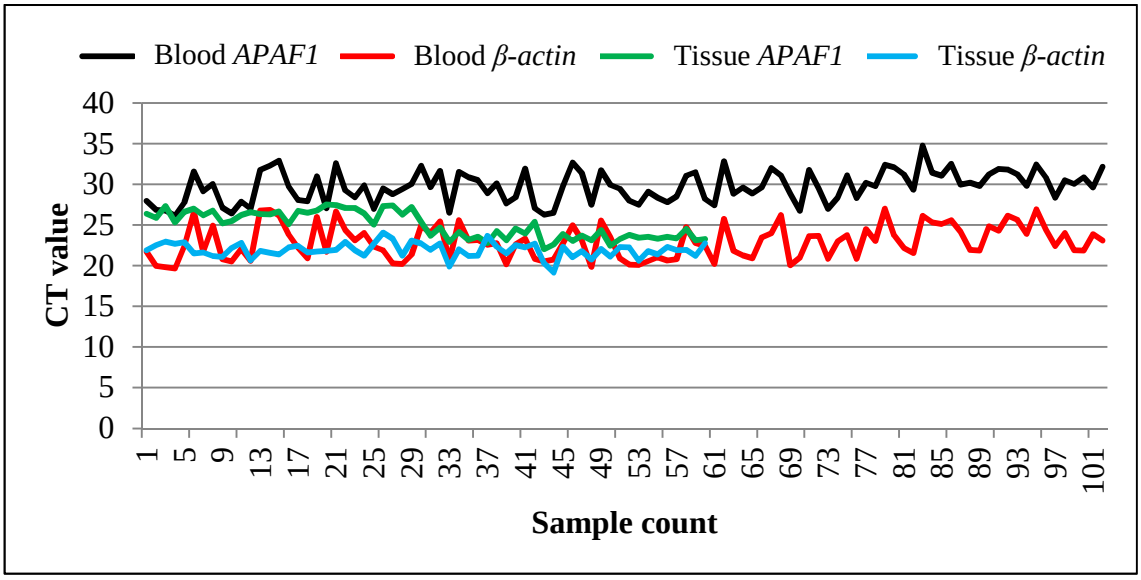

Figure 4.48: C_T values of blood and tissue *APAF1* and *β-actin*. Colour legend, black: blood *APAF1*; red: blood *β-actin*, green: tissue *APAF1*; blue: tissue *β-actin*.

No significant differences were observed in the levels of *β-actin* mRNA (p = 0.992 in blood; p = 0.065 in tissue) and β-actin protein (p = 0.069 in tissue) between the cancer and normal/control samples. In contrast, *APAF1* mRNA expression was determined to be significantly down-regulated in the blood (p = 0.002) and tissue (p < 0.001) samples obtained from CRC patients. Pearson's correlation between the blood and tissue *APAF1* levels was 0.378 (p = 0.039). A decreasing trend of expression was observed as the tumour progressed from stage I-II to stage III-IV (Figures 4.49 and 4.50). The *APAF1* mRNA expression of each sample is shown in Appendices 7 and 8. Besides that, APAF1 protein expression was determined to be lower in the cancer tissue when compared with the normal colonic mucosa (p < 0.001) (Figure 4.51A, B). The APAF1 protein expression of each sample is shown in Appendix 13.

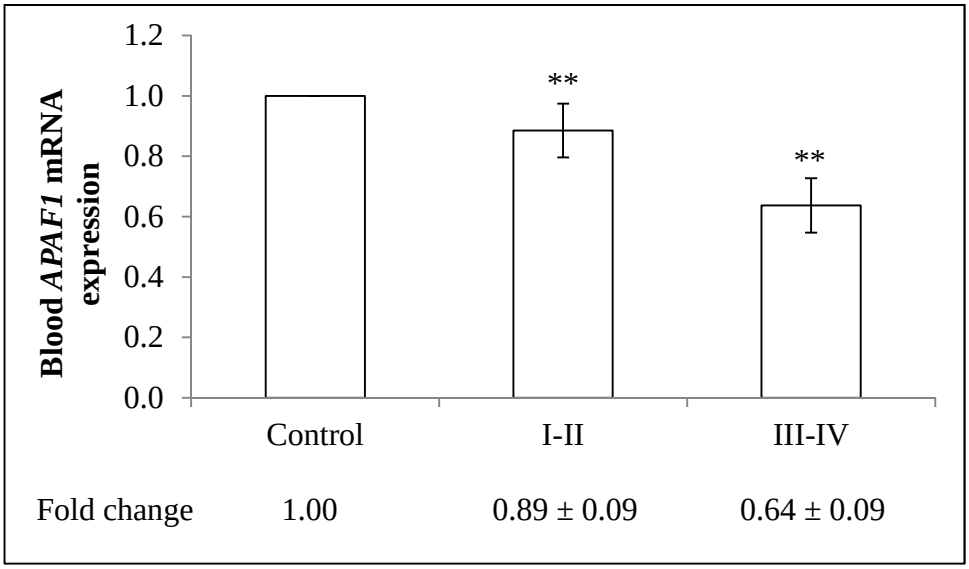

Figure 4.49: Blood *APAF1* mRNA expression. The basal fold change of the control group was set at 1. Data are expressed as fold change of TNM stage versus control. Fold change below 1 indicates down-regulation. Data are presented as mean ± SEM. ** $p < 0.01$.

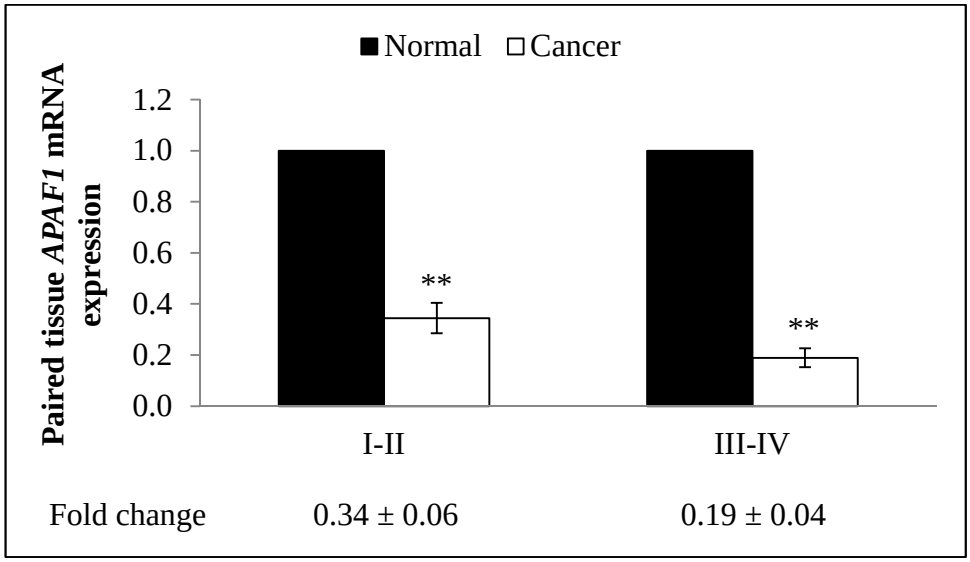

Figure 4.50: Paired tissue *APAF1* mRNA expression. Relative expression is expressed as fold change of cancer tissue versus normal colonic mucosa. Fold change below 1 indicates down-regulation. Data are presented as mean ± SEM. ** $p < 0.01$.

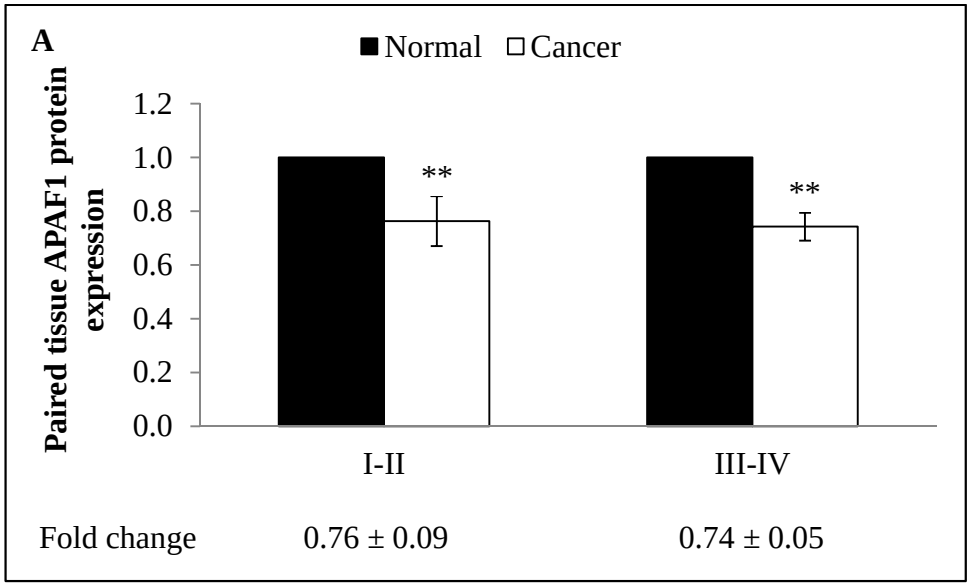

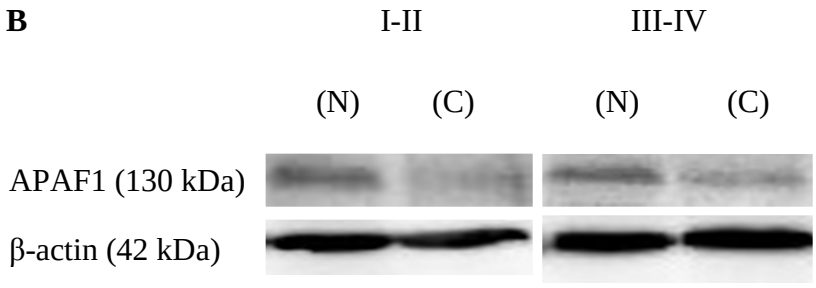

Figure 4.51: Paired tissue APAF1 protein expression. (A) Relative expression is expressed as fold change of cancer tissue versus normal colonic mucosa. Fold change below 1 indicates down-regulation. Data are presented as mean ± SEM. ** $p < 0.01$. (B) Representative blots of APAF1 protein expression in stage I-II and stage III-IV paired cancer tissues (N: normal colonic mucosa; C: cancer tissue). β-actin was used as the loading control.

Next, the relationship between miR-23a and *APAF1* mRNA or APAF1 protein levels was analysed (Figure 4.52A-C). Although significant negative correlation was not detected between miR-23a and *APAF1* mRNA (r = -0.135; p = 0.177) in the blood

samples, miR-23a was found to be inversely correlated with *APAF1* mRNA (r = -0.364; p = 0.048) and APAF1 protein (r = -0.443; p = 0.014) in the paired tissue samples. Moreover, the expression between tissue *APAF1* mRNA and APAF1 protein was also determined to be significantly correlated (r = 0.372; p = 0.043).

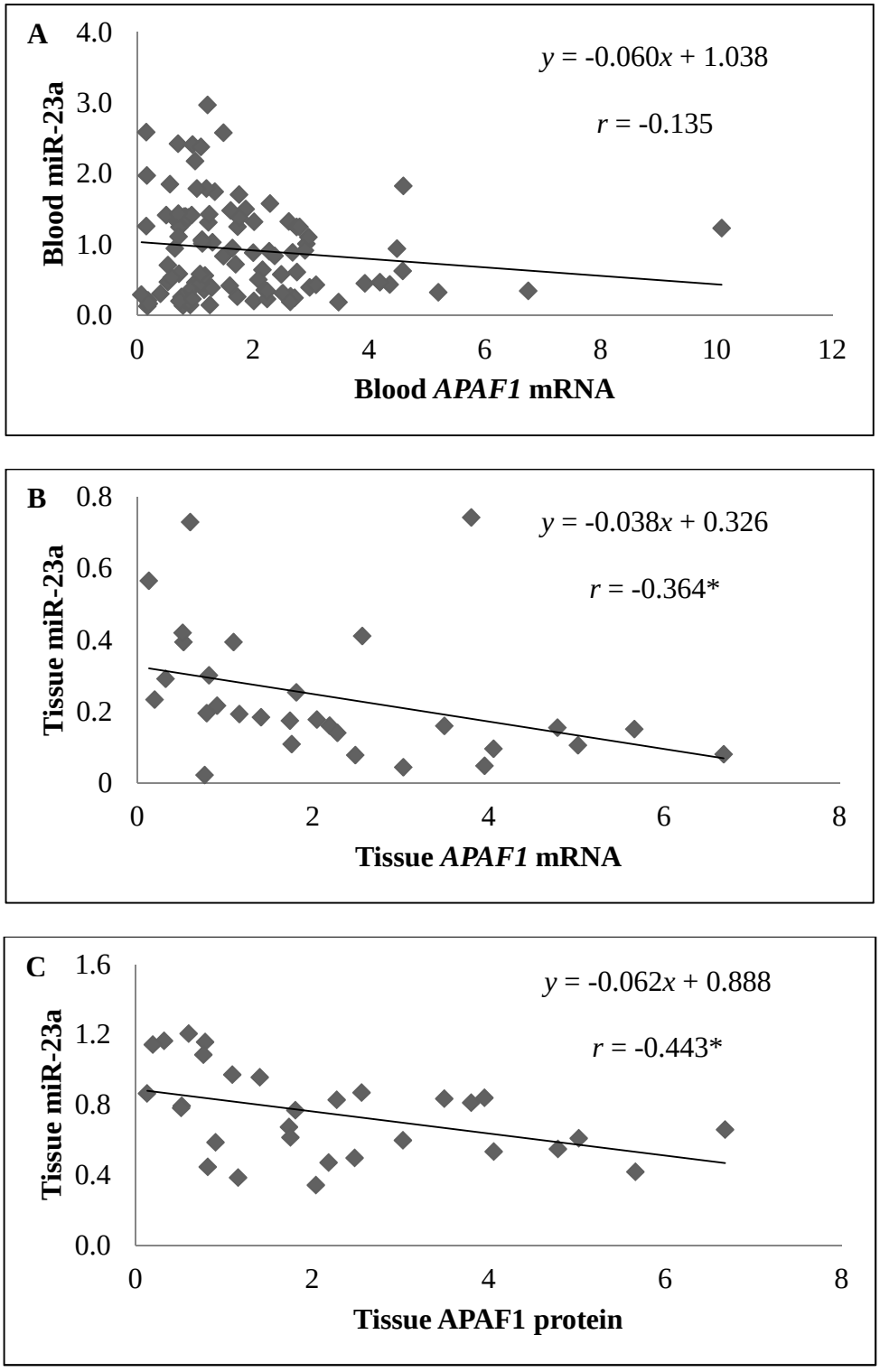

Figure 4.52: Correlation between miR-23a and *APAF1* mRNA or APAF1 protein. (A) Blood miR-23a and blood *APAF1* mRNA. (B) Tissue miR-23a and tissue *APAF1* mRNA. (C) Tissue miR-23a and tissue APAF1 protein. * $p < 0.05$.

4.7.3 miR-338-5p transfection

4.7.3.1 Effect on cell viability rate following miR-338-5p transfection

The transfection of miR-338-5p mimic or miR-338-5p inhibitor in SW480 and SW620 cells did not significantly increase or decrease cell viability ($p > 0.05$) (Figure 4.53).

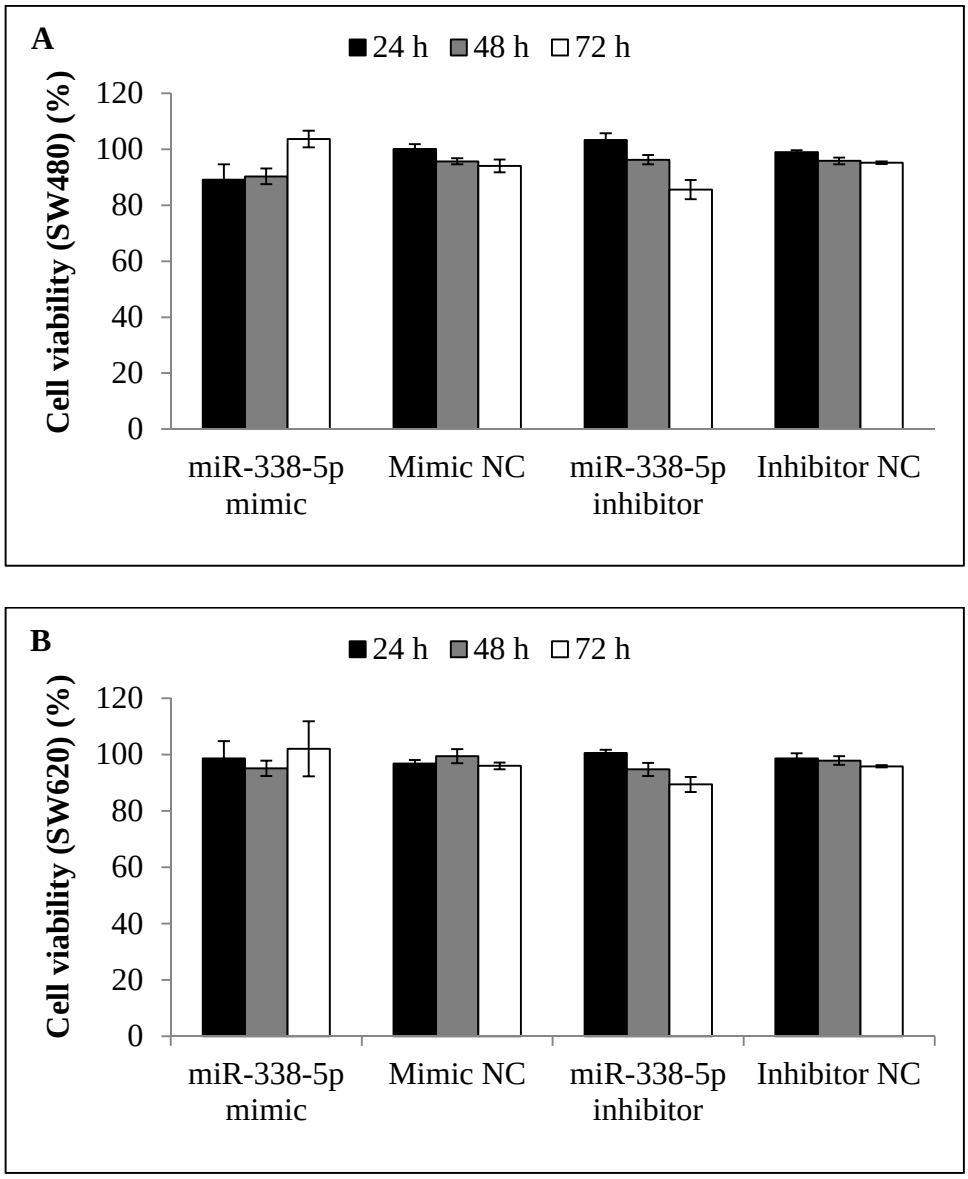

Figure 4.53: Cell viability of (A) SW480 and (B) SW620 cells following miR-338-5p transfection. No statistical significance was observed ($p > 0.05$). Data are presented as mean ± SEM ($n = 3$).

4.7.3.2 Effect on apoptosis rate following miR-338-5p transfection

Determination of cell apoptosis following miR-338-5p transfection was conducted. Cell populations in live, dead and apoptotic stages were quantitated using Invitrogen Tali image-based cytometer (Table 4.12). The relative apoptosis rate of SW480 and SW620 cells following miR-338-5p mimic or miR-338-5p inhibitor transfection was not statistically significant ($p > 0.05$) (Figure 4.54).

Table 4.12: Quantification of live, dead and apoptotic cells in SW480 and SW620 cells using Invitrogen Tali image-based cytometer (miR-338-5p transfection). Data are presented as mean ± SEM ($n = 3$).

Treatment	**SW480**			**SW620**		
	Live (%)	**Dead (%)**	**Apoptotic (%)**	**Live (%)**	**Dead (%)**	**Apoptotic (%)**
NTC	84.33 ± 0.33	10.33 ± 0.33	5.33 ± 0.33	84.00 ± 2.00	12.33 ± 1.76	3.67 ± 0.67
Mock	87.00 ± 1.53	11.00 ± 0.00	2.00 ± 1.53	81.67 ± 0.67	16.00 ± 0.58	2.00 ± 0.00
miR-338-5p mimic	85.00 ±0.58	13.00 ± 0.58	1.67 ± 0.67	71.00 ± 2.65	16.33 ± 2.40	12.33 ± 0.33
Mimic NC	83.67 ± 0.88	13.00 ± 0.58	2.67 ± 0.33	78.33 ± 0.88	14.00 ± 0.58	7.33 ± 0.88
miR-338-5p inhibitor	85.33 ±2.19	11.33 ± 1.45	3.33 ± 1.20	75.67 ± 0.67	18.00 ± 3.06	6.33 ± 2.67
Inhibitor NC	85.00 ± 1.53	11.67 ± 0.67	3.67 ± 1.20	78.67 ± 1.20	15.00 ± 0.58	6.00 ± 1.15
Doxorubicin	54.33 ± 4.67	23.67 ± 0.88	22.33 ± 5.33	48.33 ± 4.84	27.00 ± 2.08	24.33 ± 2.91

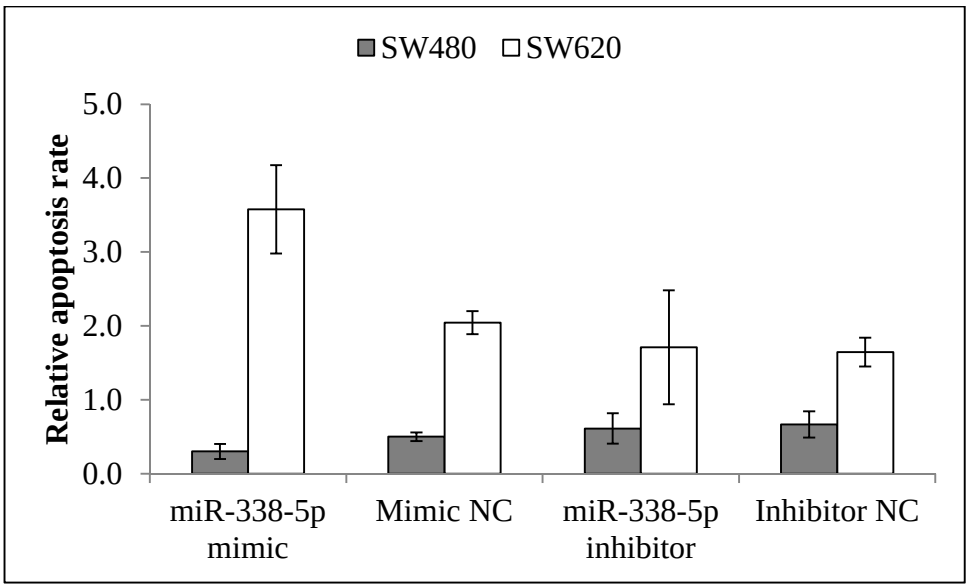

Figure 4.54: Relative apoptosis rate of SW480 and SW620 cells following miR-338-5p transfection. No statistical significance was determined ($p > 0.05$). Data are presented as mean ± SEM ($n = 3$).

4.7.3.3 Effect on migration and invasion activity following miR-338-5p transfection

The transfection of miR-338-5p mimic or miR-338-5p inhibitor in SW480 and SW620 cells did not significantly increase or decrease cell migration and invasion activity ($p > 0.05$) (Figure 4.55A-D).

A

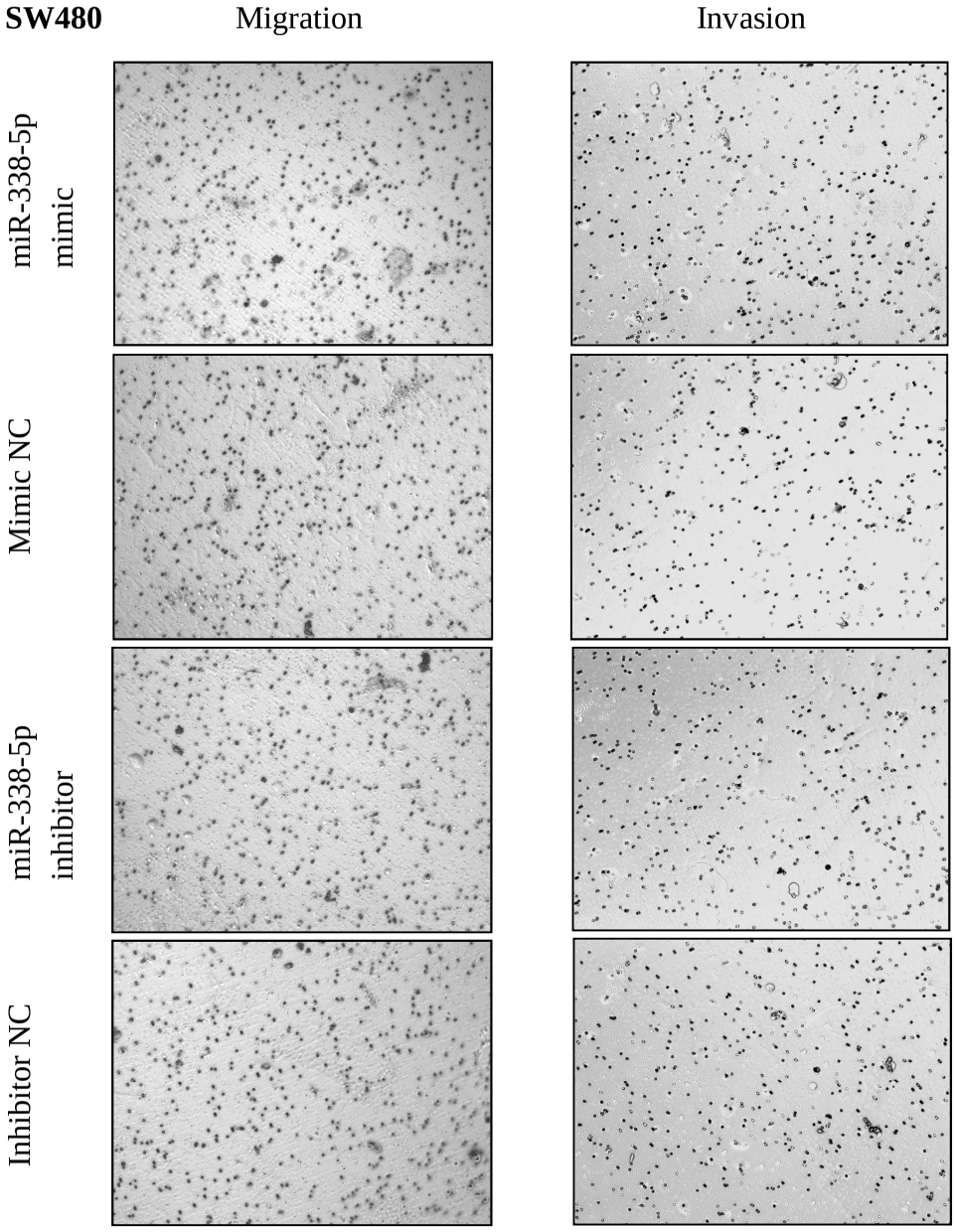
SW480
Migration
Invasion
miR-338-5p mimic
Mimic NC
miR-338-5p inhibitor
Inhibitor NC

B

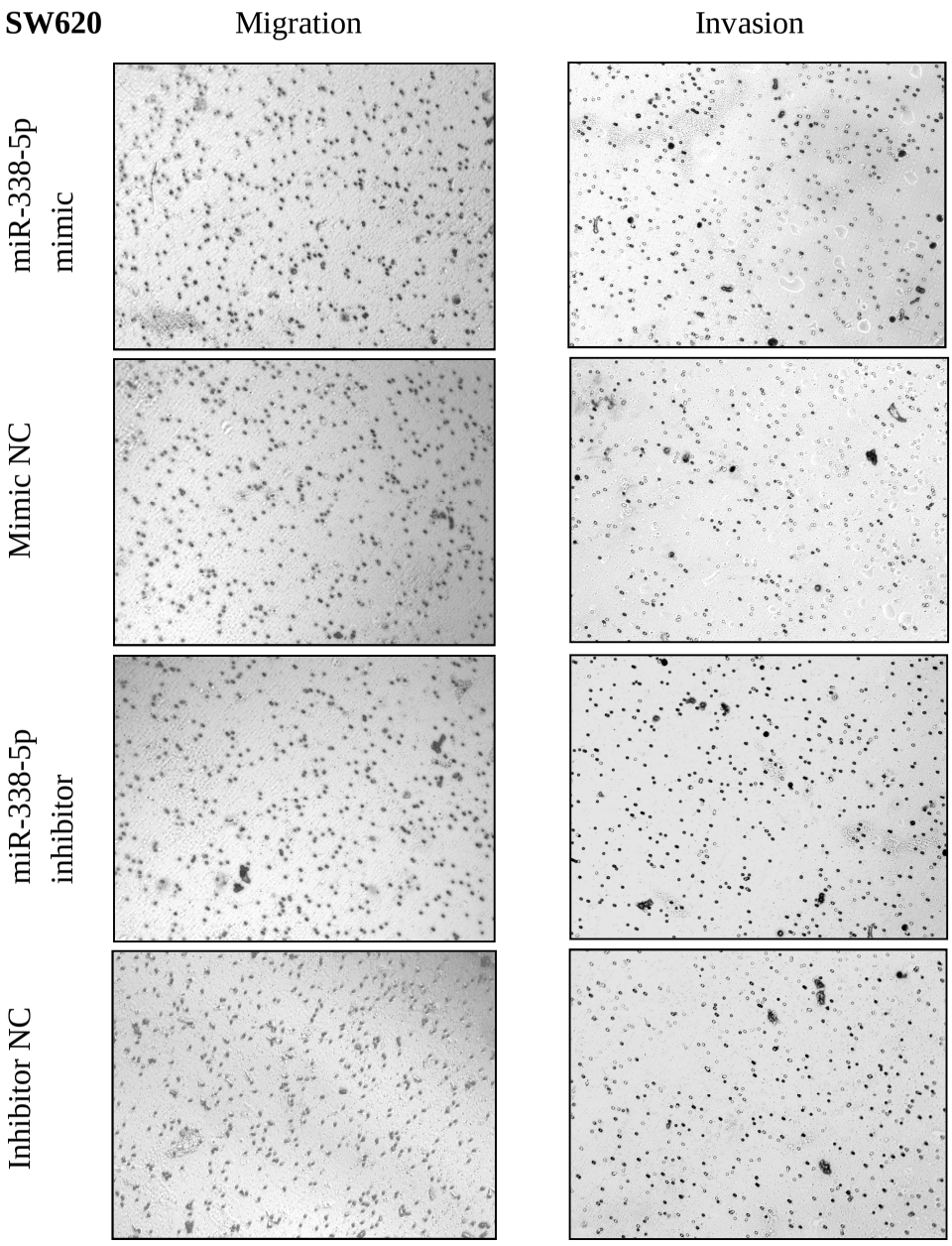
SW620
Migration
Invasion
miR-338-5p mimic
Mimic NC
miR-338-5p inhibitor
Inhibitor NC

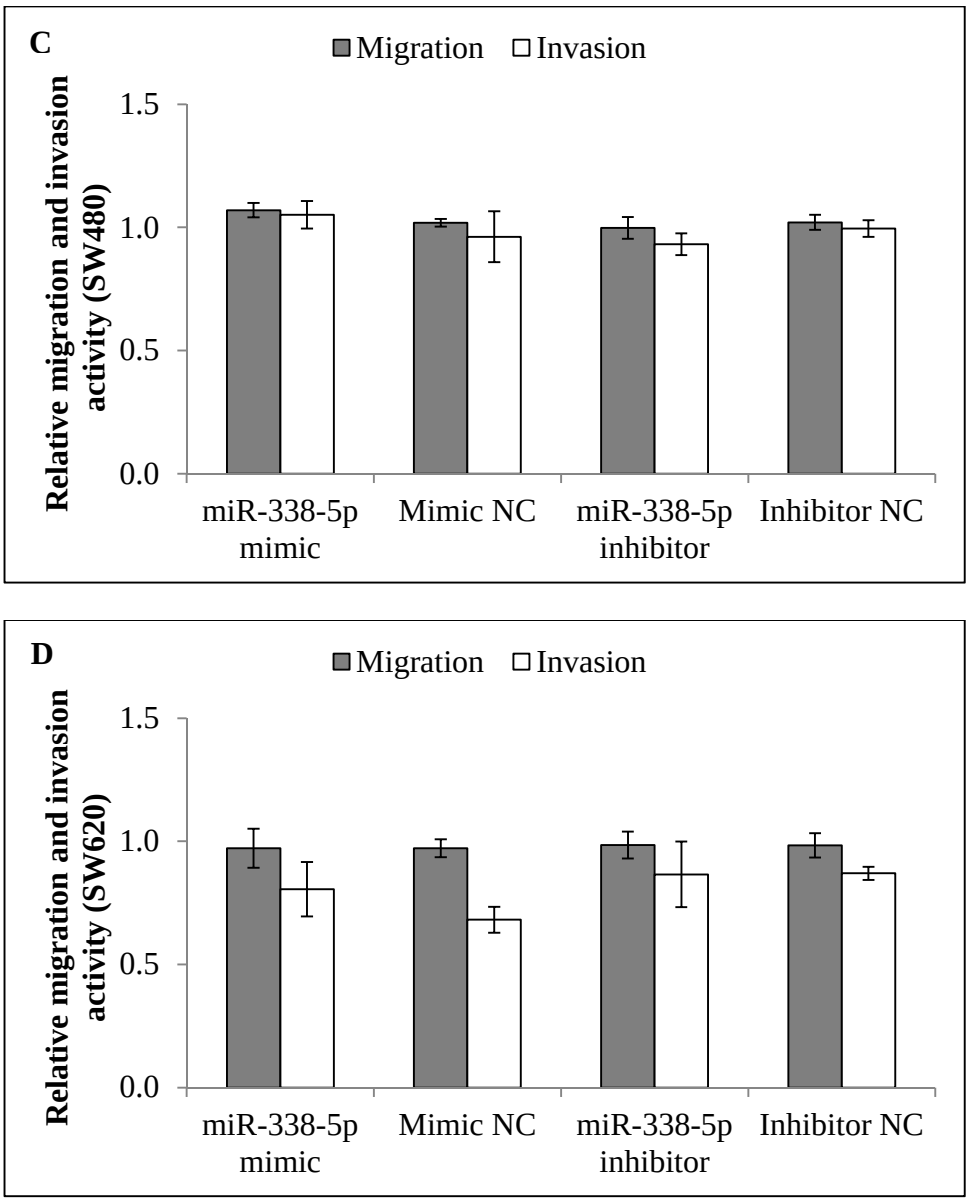

Figure 4.55: Relative migration and invasion activity of SW480 and SW620 cells following miR-338-5p transfection. (A, B) Representative fields of migratory (left) and invasive (right) cells on plate insert. (C, D) Bar charts of relative migration and invasion activity. No statistical significance was determined ($p > 0.05$). Data are presented as mean ± SEM ($n = 3$).

4.7.3.4 Screening of miR-338-5p targets

Despite the insignificant findings from the functional assays, *in silico* analysis was still being carried out to identify the possible targets of miR-338-5p. Several putative gene targets include *ACVR2A*, *APPL1*, *CCND1*, *CREBBP*, *EP300*, *FZD7*, *ID1*, *ID4*, *KRAS*, *MAPK1*, *MET*, *PDGFRA*, *PTEN*, *RBL2*, *RBX1*, *SMAD4*, *SMAD5*, *SOS1*, *SOS2* and *TGFBR1* (Appendix 17). Other functional experiments are required to further elucidate the role of miR-338-5p in CRC.

CHAPTER 5

DISCUSSION

5.1 Identification of differentially expressed miRNAs in CRC

5.1.1 Quality and integrity of extracted total RNA

The tissue and blood samples collected in this study were preserved in Ambion RNA*later* reagent. Samples stored in RNA*later* are protected from RNases and compatible with most RNA isolation procedures (Mutter et al., 2004). Samples preserved in this manner could be stored for extended periods at -80°C. As described in section 4.2, the extracted total RNA samples were deemed suitable for miRNA microarray and RT-qPCR assays. The samples were confirmed to be of high quality and integrity.

5.1.2 Marker discovery by miRNA microarray

The miRNA microarray is a high-throughput assay capable of screening the expression of thousands of miRNAs in a single experiment. The platform for Affymetrix GeneChip miRNA array used in this study is based on an enzymatic-labelling approach involving poly-adenosine tailling of the miRNA followed by ligation of a biotinylated signal molecule. The technology works on the basis of nucleic acid hybridisation between the target miRNAs and their corresponding complementary probes. The present study was designed to investigate the association between tissue and blood miRNA expression levels in CRC. Two independent miRNA profiling studies of tissue and blood samples were conducted. The tissue array revealed a panel of 72 differentially regulated

miRNAs (Table 4.3) while the blood array revealed a panel of 24 differentially regulated miRNAs (Table 4.4). The microarray data reported in this study are in accordance with the MIAME guidelines, which describe the minimum information for reporting microarray-based gene expression data (Brazma et al., 2001). The miRNAs that were concurrently expressed in the tissue and blood arrays were selected for further validation, i.e. miR-150, miR-193a-3p, miR-23a, miR-23b, miR-338-5p, miR-342-3p and miR-483-3p (Figure 4.9). This selection technique was proposed as a better method for marker validation, as compared to the classical procedure of selecting the highly expressed genes (Detours, Dumont, Bersini, & Maenhaut, 2003).

The Affymetrix GeneChip miRNA array platform has been employed by many research groups in the identification of miRNA biomarkers in cancer, in particularly CRC (Ahmed et al., 2012; Godfrey et al., 2013; Lajer et al., 2011; Piepoli et al., 2012). Although the differentially expressed miRNAs generated from multiple studies could be versatile, the presence of overlapping miRNAs has affirmed the reliability of the tissue and blood miRNA arrays data obtained in this study. Moreover, the reproducibility of certain miRNAs may provide valuable insights into their involvement in the carcinogenesis of CRC. For instance, a total of 17 miRNAs, namely, miR-10b, miR-1246, miR-138, miR-139-5p, miR-140-3p, miR-149, miR-182, miR-195, miR-21*, miR-224, miR-28-3p, miR-342-3p, miR-378, miR-422a, miR-429, miR-503 and miR-99a identified in the present tissue array, have been found to overlap with that of the tissue array performed by Piepoli et al. (2012). Moreover, the expression levels of miR-105, miR-1247, miR-139-5p, miR-195, miR-378, miR-378c, miR-383, miR-422a, miR-483-3p, miR-552 and miR-96 identified in the present tissue array, have been shown to be in agreement with those reported by Hamfjord et al. (2012). A recent miRNA profiling study by Perilli et al. (2014) has also revealed an overlap of miR-10b, miR-138, miR-150, miR-20a, miR-203, miR-21*, miR-215, miR-30a and miR-30a* in CRC

tissue. On the other hand, the first study that reported the applicability of the Affymetrix GeneChip miRNA array platform for blood-based miRNA profiling in CRC was conducted by Ahmed et al. (2012). miR-150, which was discovered to be down-regulated in the present blood array, was also found to be significantly down-regulated in their study.

Tissue-based miRNA profiling is known to provide a relatively sensitive and specific representation of miRNA deregulation in cancer (Callari et al., 2012; Piepoli et al., 2012). Although blood-based miRNA profiling is still far behind the advancement in tissue-based miRNA profiling, it offers the potential for early, non-invasive disease detection (Ahmed et al., 2012). Circulating miRNAs have recently emerged as candidate biomarkers for many diseases (Häusler et al., 2010; Z. Huang et al., 2010; Karolina et al., 2011; Schrauder et al., 2012; Sepramaniam et al., 2014). The circulating miRNAs are generally Ago-bound and protected from endogenous RNases, which enable them to serve as stable blood-based biomarkers (Kosaka, Iguchi, & Ochiya, 2010; Turchinovich, Weiz, Langheinz, & Burwinkel, 2011).

Tumour-derived miRNAs have been identified in plasma, serum and whole blood. The first discovery of tumour-derived miRNAs in plasma was done by Mitchell et al. (2008) when they identified that plasma miR-629* and miR-660 could be used to differentiate xenografted mice with prostate cancer from the controls. On the other hand, the first serum miRNA biomarker discovered was miR-21, when Lawrie and his colleagues indicated that elevated serum levels of miR-21 in patients with diffuse large B-cell lymphoma was associated with higher relapse-free survival (Lawrie et al., 2008). The first study on the use of whole blood as miRNA biomarker was reported by Heneghan et al. (2010). They have demonstrated that the up-regulation of miR-195 in the whole blood of breast cancer patients was reflective of that in the breast tumour tissues. Since the usage of plasma, serum and whole blood has been proven suitable for investigations

as blood-based biomarkers, whole blood was utilised in the present investigation. Whole blood includes all possible sources of circulating miRNAs from red blood cells, white blood cells and plasma (J. Wang, Zhang, Liu, & Sen, 2014). Previously, Heneghan et al. (2010) have reported a strong preference of using whole blood to plasma or serum for systemic miRNA detection and quantification. They have discovered a higher yield of miRNAs in the whole blood, as compared to plasma or serum. Moreover, the white cell counts, haemoglobin and haematocrit levels have been determined to be similar in the cancer and control samples, hence ruling out any potential bias attributed to cellular and protein components (Heneghan et al., 2010). In addition, the presence of cellular fraction in the whole blood has been suggested to ameliorate the miRNA profiles of cancer patients, as the immunosuppressive and pro-angiogenic signals sent out during tumour formation are commonly imprinted in the blood cells (Häusler et al., 2010). Thus, the detection of miRNA deregulation at early stages of tumour development is possible with the use of whole blood (J. Wang et al., 2014). Nevertheless, the actual mechanism on how tumour-derived miRNAs enter the blood circulation remains to be clarified. Chin and Slack (2008) have proposed two possibilities regarding this issue. First, tumour miRNAs may be present in the bloodstream due to tumour cell death and lyses. Second, tumour cells may secrete miRNAs into the tumour microenvironment and intravasate into the bloodstream via exosome transfer. It is clear that the present investigation was necessary to determine whether the differentially expressed miRNAs identified in the circulating blood of primary CRC patients would be reflective of those in the cancer tissue.

5.1.3 Marker validation by RT-qPCR

The RT-qPCR is an established technique for miRNA quantification. It is recognised as the gold standard for the validation of microarray data (Min & Yoon, 2010). The validation of differentially expressed miRNAs using an independent set of samples is necessary before drawing any conclusion from the microarray experiment. The samples in this study were grouped into early (stage I-II) and advanced (stage III-IV) CRC for statistical analysis. The rationality behind this conformed to one of the study objectives, i.e. to determine the feasibility of the miRNA biomarkers for discriminating early and advanced CRC. The cases were grouped on the basis of their similarities in clinical pathophysiology and tumour stromal microenvironmental elements (Compton et al., 2012). Stage I and II tumours are localised to the bowel and have not spread to lymph nodes or distant organs, hence the growth usually could be treated effectively with surgery alone without any adjuvant systemic therapy. However, for stage III and IV tumours, the growth has spread beyond the bowel, thus systemic treatment is needed to treat the residual cancer after surgery. The miRNAs that could discriminate between early and advanced CRC may serve as diagnostic and prognostic biomarkers for improving patient treatment protocols.

In the present study, the RT-qPCR validation procedure using miRNA-specific primer and TaqMan probe was performed in accordance with the Minimum Information for Publication of Quantitative Real-time PCR Experiments (MIQE) guidelines (Bustin et al., 2009). The TaqMan assay involves the utilisation of a fluorogenic-labelled probe that has a fluorescent reporter dye attached to its 5’ end and a quencher dye at its 3’ end (Heid, Stevens, Livak, & Williams, 1996). In the presence of the target sequence, the fluorogenic probe anneals downstream from one of the primer sites and is cleaved by the 5’ nuclease activity of the *Taq* DNA polymerase, resulting in fluorescence emission (Arya et al., 2005). In contrast, the fluorescence emission of the reporter dye is

quenched when the probe is in an intact form. The fluorescence intensity is directly proportional to the amount of product amplified in each PCR cycle (Overbergh et al., 2003). Post-PCR processing is not required. This assay is specific as proper hybridisation between the probe and target is needed to generate fluorescent signals (Ginzinger, 2002). Moreover, the probes can be labelled with distinct reporter dyes that allow the amplification and detection of two different sequences in one reaction (Overbergh et al., 2003). The primary disadvantage of the TaqMan chemistry is the requirement to synthesise multiple probes for different sequences, which increases assay setup and cost (Arya et al., 2005).

The validation analyses of the concurrently identified miRNAs (miR-150, miR-193a-3p, miR-23a, miR-23b, miR-338-5p, miR-342-3p and miR-483-3p) are discussed in the following sub-sections. These miRNAs are suggested to be biologically and clinically relevant to the carcinogenesis of CRC.

5.1.3.1 miR-150

In the present study, miR-150 expression was determined to be significantly down-regulated in the tissue and blood miRNA arrays. Even though significant down-regulation of miR-150 expression was not detected in the blood RT-qPCR analysis (Figure 4.19), the miR-150 expression was reported to be significantly down-regulated in the tissue RT-qPCR analysis (Figure 4.11). Furthermore, the down-regulation of miR-150 level in CRC has been reported by other research groups (C. Guo et al., 2008; Y. Ma et al., 2012; Q. Wang et al., 2012). Y. Ma et al. (2012) have indicated that the low expression levels of miR-150 in both colorectal adenoma and carcinoma tissues were associated with shorter survival and worse response to adjuvant chemotherapy. The miR-150 expression has been discovered to be significantly down-regulated in the

plasma CRC samples and several CRC cell lines, i.e. V9m, V855, V410 and V478 (C. Guo et al., 2008; Q. Wang et al., 2012). The miR-150 gene locus is located on chromosomal region 19q13.33 (Y. Ma et al., 2012). Based on the available literature, the validation of miR-150 target genes in CRC has not been confirmed. The lack of knowledge on the target genes has hindered the detailed understanding of miR-150 function in CRC. Nevertheless, the deregulation of miR-150 and its target genes has been detected in other gastrointestinal diseases. The miR-150 has been shown to be down-regulated in pancreatic cancer, and the restoration of the level has been found to suppress pancreatic cell growth, clonogenicity, migration and invasion by modulating the expression of mucin 4 (*MUC4*) gene (Srivastava et al., 2011). On the other hand, miR-150 has been reported to be up-regulated in irritable bowel syndrome (Fourie et al., 2014). It has been found to target the serine-threonine protein kinase *AKT2* gene, which is an important regulator in inflammatory pathways (Anderson & Wong, 2010; Fourie et al., 2014). Moreover, miR-150 has been determined to promote gastric cancer cell proliferation by negatively regulating the pro-apoptotic early growth response 2 (*EGR2*) gene (Q. Wu et al., 2010).

In this context, the variances in miR-150 expression indicate cell type-specific regulation of this miRNA. Thus, more studies are needed to identify the functions and targets of miR-150 in CRC.

5.1.3.2 miR-193a-3p

The information on the role of miR-193a-3p in colorectal carcinogenesis remains largely unknown. The miR-193a-3p is derived from the 3’ arm of miR-193a. The gene locus for miR-193a is found on chromosomal region 17q11.2 (Nakano, Yamada, Miyazawa, & Yoshida, 2013). The present study has been published as the first study on

the up-regulation of miR-193a-3p in CRC (Yong, Law, & Wang, 2013). This miRNA was found to be significantly up-regulated in the miRNA array and RT-qPCR validation studies (Figures 4.12 and 4.20). Moreover, the miR-193a-3p expression was ascertained to be positively correlated in the tissue and blood samples. This miRNA has been chosen for further functional studies and is reported in section 5.2.1.

Recently, Ragusa and his co-workers have demonstrated an up-regulation of miR-193a-3p expression in the cells and exosomes secreted by Caco2 and HCT116 CRC cells (Ragusa et al., 2014). The level of miR-193a-3p was successfully altered in Caco2 cells following Cetuximab treatment while no effect was observed in HCT116 cells, indicating the responsiveness of miR-193a-3p modulation in Caco2 cells. However, without specifying the arm origin, Iliopoulous and his colleagues have reported a down-regulation of miR-193a expression in colon-derived mice xenografts (Iliopoulos, Rotem, & Struhl, 2011). The contradicting results may be due to the specificity of the arm origin in cellular transformation and tumour growth, and the differences in genetically distinct CRC cells. Clearly, the role of miR-193a-3p in CRC has to be robustly investigated.

The miR-193a-3p level has been reported with varying conclusions in different cancers. The up-regulation of miR-193a-3p has been shown in pancreatic and bladder cancers while the down-regulation has been demonstrated in oral and ovarian cancers (Dyrskjøt et al., 2009; Kozaki, Imoto, Mogi, Omura, & Inazawa, 2008; Nakano et al., 2013; J. Yu, Li, Hong, Hruban, & Goggins, 2012). Moreover, miR-193a-3p has been reported to mediate the chemosensitivity of 5-FU and sorafenib drugs in hepatocellular carcinoma by targeting the serine/arginine-rich splicing factor 2 (*SRSF2*) and *uPA* genes, respectively (K. Ma et al., 2012; Salvi et al., 2013).

5.1.3.3 miR-23a

Based on the miRNA array and RT-qPCR analyses (Figures 4.13 and 4.21), the level of miR-23a was shown to be significantly elevated in CRC. Strong positive correlation was observed between the tissue and blood samples. In view of the present results, mounting evidence has suggested that miR-23a may serve as a promising biomarker in CRC. Ogata-Kawata et al. (2014) have found that miR-23a was over-expressed in the serum exosome of primary CRC patients and the level was remarkably reduced after tumour resection. X. Chen et al. (2008) have demonstrated a common up-regulation of blood miR-23a in CRC and lung cancer patients. Their study serves as a preliminary investigation that highlights the common physiological functions and relationship between CRC and lung cancer. The miR-23a level has also been detected to be higher in HCT116, HT29, RKO, SW48 and SW480 CRC cells when compared to normal colon-derived FHC cells (Ogata-Kawata et al., 2014). Furthermore, Jahid et al. (2012) have shown that miR-23a is involved in the promotion of CRC cell migration and invasion by down-regulating the metastasis suppressor 1 (*MTSS1*) gene. Apart from CRC, the up-regulation of miR-23a has been reported in other gastrointestinal cancers. Bao et al. (2014) have demonstrated that the increase of miR-23a expression in hepatocellular carcinoma was significantly associated with TNM stage and tumour size. The miR-23a has also been suggested to regulate the chemosensitivity of HepG2 hepatocellular carcinoma cells to etoposide drug (N. Wang et al., 2013). Furthermore, by using MGC803 gastric adenocarcinoma cell line, Zhu et al. (2010) have revealed a growth-promoting function of miR-23a via the regulation of interleukin 6 receptor (*IL6R*) gene. Subsequently, X. Liu et al. (2013) have shown that miR-23a can promote cellular proliferation and suppress paclitaxel-induced apoptosis in MGC803 cells by targeting the interferon regulatory factor 1 (*IRF1*) gene at the post-transcriptional level.

Besides the individualistic functions, miR-23a has also been shown to possess cooperative functions with miR-24 and miR-27a (Chhabra, Dubey, & Saini, 2010). The three miRNAs are derived from a single primary transcript, located on chromosomal locus 19p13.13 (Sikand, Slane, & Shukla, 2009). These miRNAs have been bioinformatically predicted to regulate the initiation of adenoma-carcinoma sequence in CRC via Wnt/β-catenin signalling pathway (Willert & Jones, 2006). In brief, miR-23a holds much potential as a biomarker in cancer. This miRNA has been selected for further functional studies and is reported in section 5.2.2.

5.1.3.4 miR-23b

In the present study, miR-23b level was found to be significantly up-regulated in the tissue and blood miRNA arrays. Although there was no elevation of miR-23b expression in the tissue RT-qPCR analysis (Figure 4.14), the miR-23b level was reported to be highly expressed in the blood samples of CRC patients (Figure 4.22). The miR-23b gene locus is found on chromosomal region 9q22.32 (Sikand et al., 2009). Prior to this study, H. Zhang et al. (2011) have introduced a self-assembled cell microarray that can be used to screen all potential miRNAs known to regulate metastasis-relevant cell behaviours. From their genome-wide screening, miR-23b has been identified as a miRNA with migratory function in CRC. It has been suggested to mediate tumour growth, invasion and angiogenesis by targeting a cohort of pro-metastatic genes (e.g. frizzled class receptor 7 [*FZD7*], mitogen-activated protein kinase kinase kinase 1 [*MAP3K1*], p21 protein [Cdc42/Rac]-activated kinase 2 [*PAK2*], *TGFBR2*, related RAS viral oncogene homologue 2 [*RRAS2*] and *uPA*) (H. Zhang et al., 2011). Recently, proline oxidase (*POX*), a p53-induced gene that is involved in the modulation of cell apoptosis and tumour growth in many gastrointestinal cancers, has

been identified as a direct target of miR-23b in renal cancer (W. Liu et al., 2010). Hence, miR-23b is predicted to be involved in the post-transcriptional regulation of *POX* gene in CRC as well (Y. Liu, Borchert, Surazynski, & Phang, 2008). In other instance, miR-23b, which is a paralog of miR-23a, has been demonstrated to possess an amplification effect with miR-23a in regulating the TGF-β signalling by targeting *SMAD* genes (Rogler et al., 2009). Moreover, both miR-23a and miR-23b have been reported to play certain roles in glutamine catabolism, cell cycle regulation and glucose metabolism via c-*MYC* regulation in CRC (Chhabra et al., 2010; Gao et al., 2009).

5.1.3.5 miR-338-5p

The miR-338-5p is derived from the 5' arm of miR-338. The gene encoding miR-338 is located in an intronic region within the apoptosis-associated tyrosine kinase (*AATK*) gene on chromosomal region 17q25.3 (Barik, 2008). In general, the over-expression of miR-338 has been observed in CRC, hepatocellular carcinoma and oral cancer (Budhu et al., 2008; T. S. Wong et al., 2008). Schetter et al. (2008) have found 37 miRNAs, including miR-338, to be differentially expressed in CRC tissues when compared with paired normal colonic tissues. The findings from the tissue and blood miRNA arrays in this work are in agreement with other reported studies, whereby mir-338-5p expression was shown to be up-regulated in the primary CRC patients. Furthermore, the RT-qPCR validation has revealed a significant positive correlation in the tissue and blood levels of miR-338-5p (Figures 4.15 and 4.23). The high level of expression was significantly associated with the advanced tumour (stage III-IV).

Recently, miR-338-5p has been discovered to be positively correlated with tumour metastasis in recurrent CRC (Ju et al., 2012). The study has been extended and Ju et al. (2013) have found that miR-338-5p can induce cell migration and suppress cell

autophagy by down-regulating the phosphatidylinositol 3-kinase, catalytic sub-unit type 3 (*PIK3C*3) and microtubule-associated protein 1A/1B-light chain 3 (*LC3*) genes. Moreover, miR-338-5p is predicted to suppress the carcinoma-related EF-hand (*CREF*) gene in many cancers, including CRC (Delgado, Brandao, Hamid, & Narayanan, 2013). The *CREF* encodes a calcium binding protein that can act as a tumour promoter or a tumour suppressor in different cell types (Salama, Malone, Mihaimeed, & Jones, 2008). In view of the clinical importance of miR-338-5p in CRC, patients who did not benefit from standard adjuvant chemotherapy have been determined to express higher expression levels of miR-338-5p as compared to those who benefited (Dou et al., 2013). Thus, miR-338-5p holds the potential as a predictive marker in monitoring patients' response to chemotherapy. This miRNA has been selected for further functional studies and is discussed in section 5.2.3.

5.1.3.6 miR-342-3p

The miR-342-3p is derived from the 3' arm of miR-342. The miR-342 gene locus is located between third and fourth exons of the Enah/Vasp-like (*EVL*) gene on chromosomal region 14q32.2 (Grady et al., 2008). This miRNA is known to be epigenetically silenced via CpG island methylation in CRC. Generally, methylation of the *EVL* gene could be found in approximately 86% and 67% of colorectal adenocarcinomas and adenomas, respectively (Grady et al., 2008). The miR-342-3p has been determined to play important roles in cell cycle control, proliferation, migration and angiogenesis (Ronchetti et al., 2008). It has been suggested to function as a tumour suppressor in CRC. Moreover, two independent miRNA profiling studies by Faltejskova et al. (2012) and Gaedcke et al. (2012) have demonstrated a significant down-regulation of miR-342-3p expression in CRC. The results obtained in the present

investigation are in agreement with the reported studies, whereby miR-342-3p was shown to be significantly down-regulated in both tissue and blood miRNA arrays. However, as shown in Figures 4.16 and 4.24, statistical significance was only achieved in the tissue RT-qPCR validation but not in the blood RT-qPCR validation. In line with this, Luo and his group have also obtained a similar discrepancy whereby their blood RT-qPCR validation analysis for miR-342-3p did not correlate significantly with the microarray data (Luo, Stock, Burwinkel, & Brenner, 2013). A validation study using a larger sample size is required to address the high variation of blood miR-342-3p expression.

On the contrary, the miR-342-3p expression has been shown to be up-regulated in patients with irritable bowel syndrome (Fourie et al., 2014). This miRNA may regulate inflammatory, pain signalling, smooth muscle contractility and gastrointestinal tract motility pathways (Fourie et al., 2014). The up-regulation of miR-342-3p expression has also been reported in patients with Hepatitis B virus (HBV) infection and HBV-positive hepatocellular carcinoma (L. M. Li et al., 2010). Furthermore, the miR-342-3p level has been shown to be affected by the treatment of cisplatin drug in KYSE410 oesophageal squamous cell carcinoma cell line (Hummel et al., 2011). On the basis of the evidence on miR-342-3p deregulation in the gastrointestinal system, the down-regulation of miR-342-3p expression appears to be specific for CRC. Further investigation may provide insight into the potential application of miR-342-3p as a biomarker in CRC.

5.1.3.7 miR-483-3p

The over-expression of miR-483-3p has been observed in many cancers such as Wilms' tumour, breast, colorectal, liver and pancreatic cancers (Hao, Zhang, Zhou, Hu, & Shao, 2011; N. Ma et al., 2012; Veronese et al., 2010). In this study, both of the miRNA array

and RT-qPCR validation analyses have revealed significant up-regulation of miR-483-3p expression levels in CRC tissue and blood samples (Figures 4.17 and 4.25). Although miR-483-3p was not chosen for further investigation due to the low correlation value between the tissue and blood RT-qPCR data, mounting evidence has suggested that this miRNA may act as an oncomiR in CRC (Oberg et al., 2011; Ragusa et al., 2012; Veronese, 2012).

The miR-483-3p is derived from the 3' arm of miR-483. The gene encoding miR-483 is located within intron two of the insulin-like growth factor 2 (*IGF2*) gene on chromosomal locus 11p15.5 (Veronese et al., 2010). A direct association between the over-expression of miR-483-3p and *IGF2* in CRC has been determined. Moreover, treatment with 5-FU chemotherapeutic drug has been found to result in the reduction of both miR-483-3p and *IGF2* levels in CRC (Veronese, 2012). Generally, the *IGF2* is epigenetically regulated and involved in cell growth and differentiation, mostly during foetal stage (Chao & D'Amore, 2008). The over-expression of *IGF2* in adult tissue may lead to tumour development. The loss of *IGF2* imprinting, commonly observed in 30% of CRC patients, is recognised as an early event in colorectal carcinogenesis (Cui et al., 2003). The miR-483-3p can function cooperatively with *IGF2* or independently as an autonomous oncogene by suppressing the level of pro-apoptotic BCL2-binding component 3 (*BBC3*) gene in CRC (Veronese et al., 2010). The encoded BBC3 protein is an essential mediator of p53-dependent and -independent apoptotic pathways that promotes apoptosis by inhibiting the anti-apoptotic factors BCL2 and BCLXL (Jeffers et al., 2003). In addition, the miR-483-3p can target the upstream stimulating factor 1 (*USF1*) gene via β-catenin induction (Veronese et al., 2011). The encoded USF1 protein is an evolutionarily conserved transcription factor that interacts at high affinity with E-box regulatory elements (Ratajewski, Walczak-Drzewiecka, Salkowska, & Dastych, 2012). The USF1 is a key regulator in stress and immune responses, cell cycle and

proliferation, and lipid and glucose metabolisms (Corre & Galibert, 2005). Since β-catenin is also a target of miR-483-3p, the negative regulatory loop that controls the miR-483-3p and β-catenin levels has to be tightly regulated to prevent aberrant cell proliferation (Veronese et al., 2011). On the other hand, the miR-483-3p has been validated to promote cellular proliferation by suppressing the expression levels of *SMAD4* in pancreatic cancer and suppressor of cytokine signalling 3 (*SOCS3*) in hepatocellular carcinoma (Hao et al., 2011; N. Ma et al., 2012).

5.2 Functional and target validation studies of miR-193a-3p, miR-23a and miR-338-5p

The present research aimed to identify the potential miRNA biomarkers for early detection of CRC. Through comprehensive miRNA microarray and RT-qPCR validation analyses, three miRNAs, namely, miR-193a-3p, miR-23a and miR-338-5p, were shown to be significantly up-regulated and highly correlated in the CRC tissue and blood samples. The triple miRNA classifier of miR-193a-3p, miR-23a and miR-338-5p was of high sensitivity (80.0%), specificity (84.4%) and accuracy (83.3%) in defining CRC (Table 4.5 and Figure 4.26).

In the subsequent study, a focused approach was adopted to examine the role of the individual miRNA in cell viablity, apoptosis, migration and invasion using SW480 and SW620 CRC cell lines. Functional and target validation experiments were performed to verify and establish the causal associations between the differentially expressed miRNAs and the predicted target genes. Generally, the common approach for miRNA:mRNA target validation is based on the combination of computational prediction and experimental validation. The binding of a mature miRNA to its target is largely dependent on the free energy of binding between the seed region of miRNA and

the 3'-UTR of mRNA (Doench & Sharp, 2004). A minute change in miRNA expression has been shown to have large-scale effects in fundamental cellular processes (Meltzer, 2005).

The SW480 cell line was derived from a primary Dukes' type B tumour obtained from the colon of a 50-year-old male Caucasian. The SW620 cell line was cultured a year later from a lymph node metastasis in the same patient diagnosed with metastatic Dukes' type C tumour (Leibovitz et al., 1976). The SW480 and SW620 cell lines have same genetic background but different metastatic potential (Hewitt et al., 2000). The two cell lines possess distinct appearances in culture (Leibovitz et al., 1976). Under light microscope, the SW480 cells are characterised by a spreading, epithelial-type morphology and form large, cohesive aggregates. On the contrary, the SW620 cells have a rounded, spindle-shaped, fibroblast-like morphology and form small, less cohesive aggregates. The SW480 and SW620 cell lines underlie the gene product modifications that have occurred as the cells acquire metastatic potential. The two cell lines serve as a useful model for studying the molecular events in CRC progression (Ghosh et al., 2011). In the current *in vitro* study, both cell lines were transiently transfected with synthetic miRNAs and/or plasmid DNAs through lipofection method by using Invitrogen Lipofectamine 2000 reagent. This method involves the injection of nucleic acids into the cells by means of cationic liposome formulations that can overcome the electrostatic repulsion of the cell membrane (Dalby et al., 2004). This method is well-known for its ease of use, limited toxicity and ability to transfect a wide range of cell types with relatively high efficiency (Ke et al., 2014; Salimzadeh, Jaberipour, Hosseini, & Ghaderi, 2013). Transiently transfected genetic materials are generally short-lived as the nucleic acids are not integrated into the genome and will be lost due to environmental factors and cell division (T. K. Kim & Eberwine, 2010). The peak transient expression is generally seen at 24 to 72 h following transfection (Dalby et

al., 2004). Thus, most analyses in this work were optimised to be carried out at 48 h post-transfection with the exception of cell viability assay, whereby the analysis was conducted at the periods of 24, 48 and 72 h post-transfections. A stable transfection method is not needed as the main purpose of the present transfection study was to demonstrate the interaction between a particular miRNA and its target gene with respect to its biological function.

5.2.1 Involvement of miR-193a-3p:*FOXO4* regulation axis in cell invasion and metastasis

Metastasis is a major cause of cancer-related death. It involves a series of interrelated events known as the invasion-metastasis cascade. Metastatic progression begins with (1) epithelial cells detachment from a well-confined primary tumour; (2) local invasion into the surrounding ECM and stromal cell layers; (3) transition of epithelial to mesenchymal phenotypes; (4) intravasation into blood or lymphatic vessels; (5) survival in the systemic circulation; (6) extravasation into the parenchyma of distant tissues; (7) micrometastasis formation and metastatic colonisation in the foreign microenvironments; and eventually (8) proliferation into clinically detectable metastatic growths (Liotta et al., 1991; Wan et al., 2013). A metastatic cancer is typically incurable due to its systemic dissemination and resistance to existing anti-cancer therapies (Valastyan & Weinberg, 2011). A huge repertoire of proteases, adhesion molecules, growth factors and transcription factors are involved in the regulation of cancer invasion and metastasis. Despite the substantial efforts in the search of suitable cancer biomarkers, a sensitive marker for the detection of early metastasis in CRC has not been discovered. A number of studies have indicated that miRNA regulation is important in the development and

progression of CRC. Several miRNAs with validated involvement in cell migration and invasion have been described in section 2.2.7.5.

The present investigation has shown that miR-193a-3p could act as a pro-metastasis miRNA in CRC via the promotion of cell migration and invasion. The miR-193a-3p expression was determined to be up-regulated in the clinical CRC tissue and blood samples. The effect of miR-193a-3p modulation in CRC cell progression was elucidated through the use of non-metastatic SW480 and metastatic SW620 cell lines. The findings from the functional studies revealed that the inhibition of miR-193a-3p in both cell lines has significantly impeded cell migration and invasion without the destruction of cellular viability (Figures 4.27 and 4.29). The over-expression of miR-193a-3p has no effect on cell viability as well, but it was sufficient to promote cell migration and invasion. Moreover, no significant finding was detected from the apoptosis assay (Figure 4.28). Hence, these results indicated that miR-193a-3p was necessary for the migration and invasion of CRC cells but not required for viability and apoptosis.

The use of Matrigel basement membrane matrix has facilitated the *in vitro* study of miR-193a-3p modulation on ECM-associated cancer cell growth (Price et al., 2012). As described previously by Cai, Mulatz, Ard, Nguyen, and Gee (2014), the capability of the SW620 cells to invade through the Matrigel-coated transwell inserts is greater than the SW480 cells. The migratory and invasive potential of the CRC cells is largely dependent on the cell capability for attachment (Hewitt et al., 2000). Thus, the higher capability of the SW620 cells for migration and invasion in this study was consistent with the more aggressive phenotype of the cells. Previous reports have demonstrated that the SW620 cells express a lower level of E-cadherin epithelial marker and a higher level of vimentin mesenchymal marker when compared to the SW480 cells (Katayama et al., 2006; Yehezkel, Cohen, Kliger, Manor, & Khalaila, 2012; Zirvi, Keogh, Slomiany, & Slomiany, 1991). The SW620 cells also display a greater metastatic ability

than the SW480 cells (Hewitt et al., 2000). Importantly, the SW620 cells secrete high levels of uPA and MMP proteinases that are needed for ECM breakdown (Takayama et al., 2006). Although the exact molecular mechanism on miR-193a-3p regulation in CRC metastasis is still ambiguous, the miR-193a-3p has been shown to affect *in vitro* cell migration and invasion and *in vivo* lung metastasis in non-small-cell lung cancer models by targeting the *ERBB4* and S6 kinase 2 (*S6K2*) genes (T. Yu et al., 2014). Moreover, the miR-193a-3p has been reported to be highly up-regulated in metastastic medullary thyroid carcinoma (Santarpia et al., 2013).

FOXO4 was identified as a target gene of miR-193a-3p in this study. This is the first study that reveals an interaction between miR-193a-3p and *FOXO4* in CRC via the luciferase assay (Figure 4.32). Mutagenesis at the seed match region of *FOXO4* 3'-UTR has confirmed the specificity of miR-193a-3p recognition. The over-expression of miR-193a-3p has caused a further decrease in the levels of *FOXO4* mRNA and FOXO4 protein while the forced inhibition of miR-193a-3p has resulted in the up-regulation of *FOXO4* mRNA and FOXO4 protein (Figures 4.33 and 4.34). The effects of these modulations were relatively stronger in the SW480 cells when compared to the SW620 cells. These findings have shown that miR-193a-3p could regulate CRC cell migration and invasion by targeting *FOXO4*. Based on the available literature, *FOXO4* has only been reported to be targeted by miR-214 in non-small-cell lung cancer, miR-223 in HBV-related hepatocellular carcinoma, miR-421 in nasopharyngeal carcinoma and miR-499-5p in CRC (L. Chen, Tang, Wang, Yan, & Xu, 2013; X. Liu et al., 2011; Salim et al., 2012; X. Xu et al., 2013). Such evidence implied that the study of miRNA-mediated control of *FOXO4* activity in cancer is still at its preliminary stage.

Generally, FOXO transcription factors belong to a large forkhead box (FOX) family of proteins (Katoh & Katoh, 2004). At least 19 sub-classes of FOX proteins have been determined, from A to S. The FOX domain is a conserved DNA binding domain

responsible for the recognition of protein-encoding genes and the recruitment of distinct factors needed for an activation or repression of gene transcription (Arden, 2006). The human FOXO family comprises of FOXO1 (also known as FKHR), FOXO3 (FKHRL1), FOXO4 (AFX) and FOXO6 (FOXO2) (Greer & Brunet, 2005). FOXO transcription factors are ubiquitously expressed in all mammalian tissues. Among these, *FOXO1*, *FOXO3* and *FOXO4* genes are commonly found at chromosomal translocations in human tumours, hence suggesting their involvement in carcinogenesis (Greer & Brunet, 2005). FOXO proteins regulate a series of target genes involved in cell growth, cell cycle arrest, DNA repair, stress, invasion and metastasis (X. Zhang, Tang, Hadden, & Rishi, 2011). FOXO proteins act as potent transcriptional activators when present in the nucleus. The transcriptional functions of FOXO proteins are often regulated by post-translational modifications, i.e. phosphorylation, ubiquitination and acetylation (Fu & Tindall, 2008). Firstly, FOXO phosphorylation is mainly regulated by the PI3K-AKT pathway in response to growth factor stimulation (Burgering & Kops, 2002). A variety of growth factors such as epidermal growth factors, insulin, insulin-like growth factors and erythropoietin can bind to the tyrosine kinase receptors and activate the serine/threonine kinases necessary for FOXO phosphorylation (Arden, 2006; Reagan-Shaw & Ahmad, 2007). Typically, the AKT serine/threonine kinases phosphorylate FOXO transcription factors at three regulatory sites conserved from *C. elegans* to mammals (threonine 28, serine 193, serine 258 in the FOXO4 sequence) and bind to 14-3-3 proteins, leading to the nuclear translocation of FOXO proteins into the cytoplasm and inhibition of FOXO-dependent transcription (Arden, 2006). Other serine/threonine kinases that have been shown to phosphorylate FOXO proteins include serum and glucocorticoid-inducible kinase (SGK), casein kinase 1 (CK1), dual-specificity tyrosine-phosphorylated and regulated kinase 1A (DYRK1A) and Ras-Ral pathway kinases (Greer & Brunet, 2005; Reagan-Shaw & Ahmad, 2007) (Figure 5.1). In contrast,

phosphorylation of FOXO proteins by JNK upon stress stimulation allows the nuclear import of FOXO proteins to restore the transcriptional regulatory potential (Kawamori et al., 2006). Several examples of stress stimuli are ultraviolet (UV) radiation, oxidative stress and heat shock. Secondly, the ubiquitination process via ubiquitin-proteasome pathway is involved in the degradation of FOXO proteins (Reagan-Shaw & Ahmad, 2007). The degradation of FOXO proteins often follows with cellular transformation in carcinogenesis (Greer & Brunet, 2005). FOXO ubiquitination is regulated by ubiquitin ligases and requires AKT phosphorylation as well. S-phase kinase-associated protein 2 (SKP2) and inhibitor kappa-B kinase β (IKKB) are the two common ubiquitin ligases that catalyse the degradation of FOXO1 and FOXO3, respectively (Hu et al., 2004; H. Huang et al., 2005). The impact of ubiquitination in the degradation of FOXO4 and FOXO6 remains to be clarified. The next mechanism involved in the modulation of FOXO-dependent transcription is the acetylation and deacetylation of FOXO proteins. The binding of FOXO proteins to the transcriptional co-activator and co-repressor complexes influences the FOXO acetylation levels (Reagan-Shaw & Ahmad, 2007). For instance, FOXO acetylation by the co-activators cAMP response element-binding protein (CREB)-binding protein (CREBBP) and p300/CBP-associated factor (PCAF) allows the activation of FOXO-mediated transcriptional activity (van der Heide & Smidt, 2005). On the other hand, FOXO deacetylation by the deacetylase SIRT1 in response to oxidative stress stimulates the activation of genes involved in stress and apoptosis resistance (van der Horst et al., 2004). In view of the critical roles of FOXO proteins in maintaining proper cell function and tumour suppression, the loss of FOXO4 activity could contribute to tumourigenesis (X. Q. Liu, Tang, Zhang, & Jin, 2011).

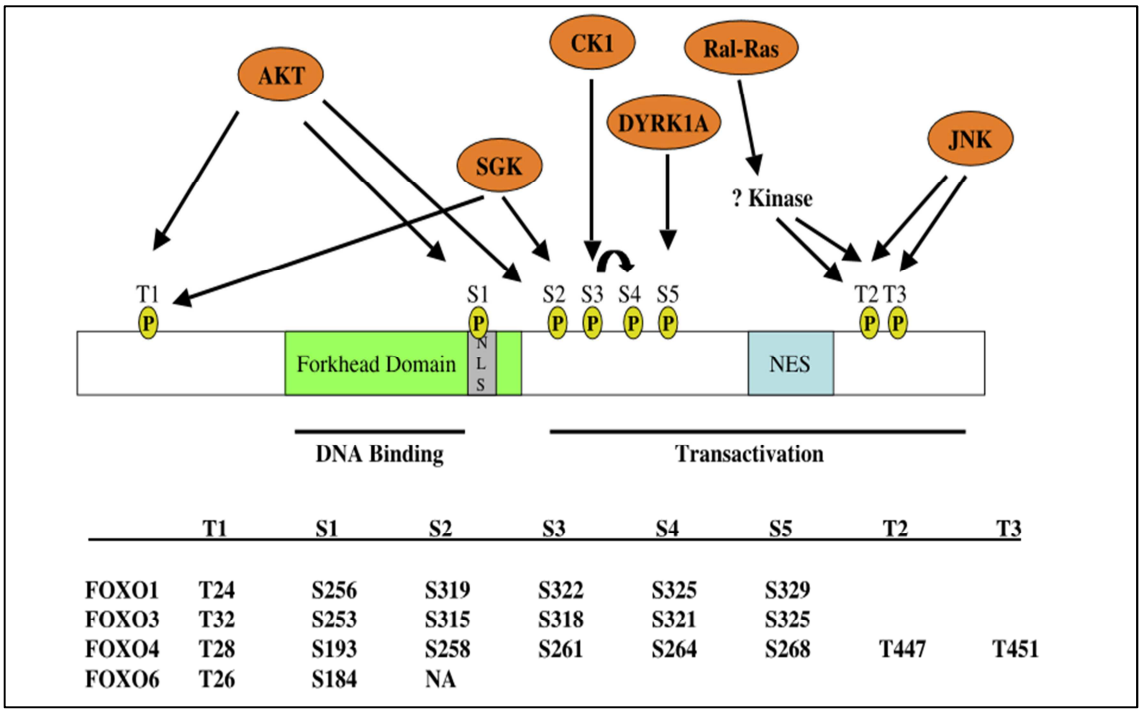

	T1	S1	S2	S3	S4	S5	T2	T3
FOXO1	T24	S256	S319	S322	S325	S329		
FOXO3	T32	S253	S315	S318	S321	S325		
FOXO4	T28	S193	S258	S261	S264	S268	T447	T451
FOXO6	T26	S184	NA					

Figure 5.1: Conformation and phosphorylation sites of FOXO transcription factors. The main components of FOXO are forkhead domain, nuclear localisation sequence (NLS) and nuclear export sequence (NES). FOXO-dependent transcription is mainly modulated by phosphorylation in response to growth factors and stress stimuli. The kinases involved are AKT, SGK, CK1, DYRK1A, Ral-Ras and JNK. The phosphorylation sites (T1, S1, S2, S3, S4, S5, T2, T3) with specific amino acid positions are shown.

(Source: Arden, 2006)

The gene that encodes FOXO4 is located on chromosomal locus Xq13.1 (Greer & Brunet, 2005). The down-regulation of FOXO4 transcription factor has been discovered in various types of epithelial cancer (Reagan-Shaw & Ahmad, 2007). An increase in HIF1 signalling due to low FOXO4 expression has been reported to be associated with tumour angiogenesis, invasion and metastasis (Dansen & Burgering, 2008). Yang, Zhao, Yang, and Lee (2005) have reported that FOXO4 positively regulates the cyclin-

dependent kinase inhibitor *p27KIP1* gene in cancers that over-express the *HER2* (also known as *ERBB2*) oncogene. HER2 over-expression has been detected in numerous cancers, including gastric and CRC (Blok, Kuppen, van Leeuwen, & Sier, 2013; Jørgensen & Hersom, 2012). The restoration of FOXO4 expression in nude mice transplanted with NIH3T3 fibroblast cells expressing the *FOXO4A3* gene has been shown to inhibit the HER2-activated cell growth and reduce tumour onset, size and progression (Yang et al., 2005). Annexin A8 (*ANXA8*) gene, which is associated with focal adhesion kinase expression and altered F-actin dynamics during EMT process, has been found to be transcriptionally down-regulated by epidermal growth factor-mediated FOXO4 phosphorylation (M. J. Lee et al., 2009). Furthermore, FOXO4-dependent transcription overlaps with the p53 pathway in the regulation of cell cycle control and tumour progression in CRC (Dansen & Burgering, 2008). FOXO4 has been shown to indirectly down-regulate the level of BCLXL via the induction of the BCL6 transcriptional repressor (Tang et al., 2002). This notion is further substantiated by the evidence that growth arrest and DNA damage-inducible protein 45 (*GADD45*), wild-type p53-induced phosphatase 1 (*WIP1*) and *SIRT1* genes are regulated by both FOXO4 and p53 pathways (Fiscella et al., 1997; Kastan et al., 1992; van der Horst et al., 2004). The transactivation activity of FOXO4 on *GADD45* has been determined to be suppresed by nicotinamide and enhanced by resveratrol through *SIRT1* interaction in HCT116 CRC cells (Y. Kobayashi et al., 2005). Besides that, FOXO4 can form a complex with β-catenin and sequester it from the TCF-dependent transcription to inhibit tumour progression in CRC (Kwon et al., 2010). The possible interaction between miR-193a-3p and FOXO4 in CRC progression is summarised in Figure 5.2.

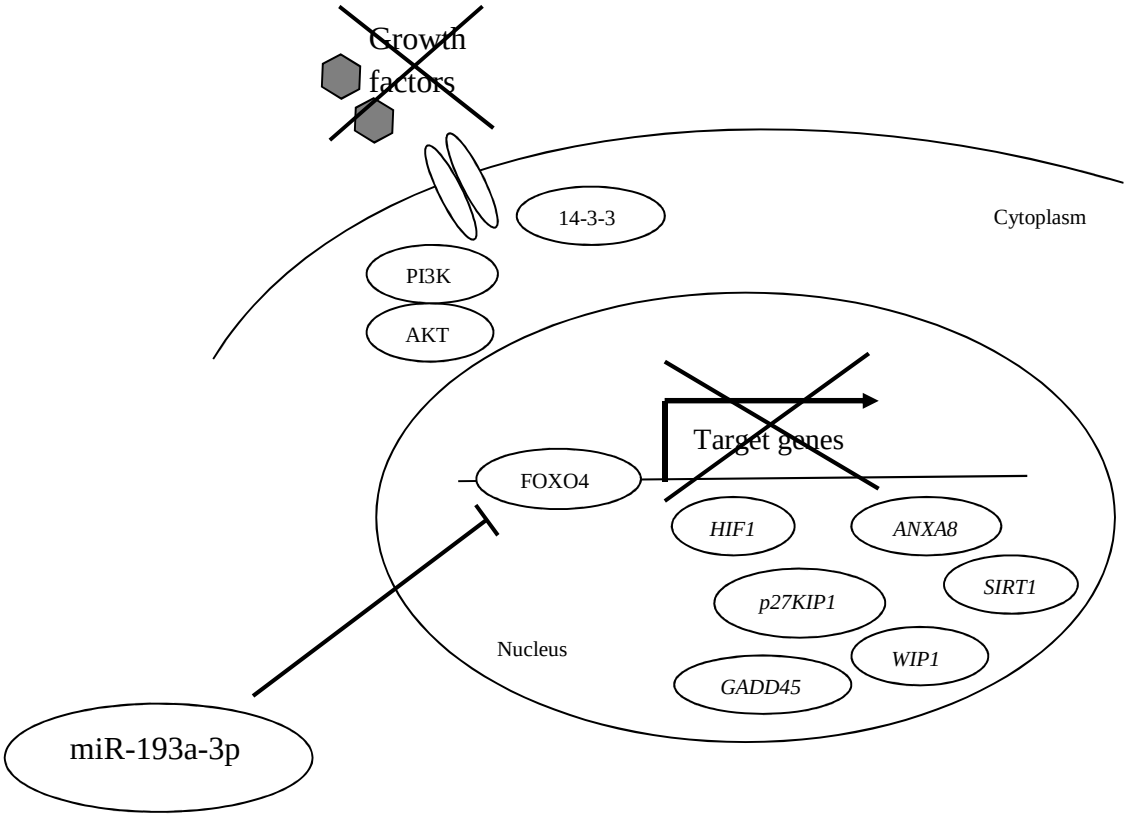

Figure 5.2: miR-193a-3p regulation on FOXO4 transcription factor in CRC progression. Generally, in the absence of growth factors, FOXO4 is localised in the nucleus and the FOXO4-dependent transcription is activated. miRNA regulation represents another level of modulation for FOXO4. In the present study, FOXO4 has been identified as a direct target of miR-193a-3p. This miRNA may suppress the expression of FOXO4 and lead to the repression of FOXO4-dependent transcription and promotion of cancer progression. *HIF1*, *p27KIP1*, *ANXA8*, *GADD45*, *WIP1* and *SIRT1* are examples of genes associated with tumour angiogenesis, invasion and metastasis.

The presence of negative correlation between miR-193a-3p and *FOXO4* mRNA or FOXO4 protein has been investigated. Significant inverse correlation between tissue miR-193a-3p and tissue *FOXO4* mRNA was detected (Figure 4.39B). Unfortunately, no statistical significance was determined in the negative correlation between blood miR-193a-3p and blood *FOXO4* mRNA (Figure 4.39A) or between tissue miR-193a-3p and tissue FOXO4 protein (Figure 4.39C). Despite the miRNA:mRNA target validation between miR-193a-3p and *FOXO4*, the exact correlation of tumour-derived miR-193a-3p and *FOXO4* expression levels in the clinical setting could not be elucidated in this study. However, individual deregulation of miR-193a-3p (r = 0.811) and *FOXO4* mRNA (r = 0.549) in the blood has been proven to be reflective of that in the CRC tissue. Pearson's correlation has been widely used as the statistical approach to determine the correlation between miRNAs and mRNAs in normally distributed data (Hauke & Kossowski, 2011; Roldo et al., 2006; F. Wang, Zheng, Guo, & Ding, 2010). As supported by Y. Li, Liang, Wong, Jin, and Zhang (2014), a larger number of samples may ameliorate the lack of negative correlations between certain miRNA:mRNA interactions in miRNA-based studies. Nevertheless, as the tumour progressed from the early-stage (I-II) to the advanced-stage (III-IV), an increasing trend of miR-193a-3p expression levels (Figures 4.12 and 4.20) and a decreasing trend of *FOXO4* mRNA and FOXO4 protein expression levels (Figures 4.36, 4.37 and 4.38) were observed in both tissue and blood samples. The results obtained are in agreement with the published report by X. Q. Liu et al. (2011), whereby FOXO4 expression was determined to be remarkably decreased and associated with tumour stage in CRC. The present work should therefore be seen as an exploratory study that highlights the role of miR-193a-3p as a pro-metastatic miRNA in CRC.

5.2.2 Involvement of miR-23a:*APAF1* regulation axis in apoptosis

Apoptosis is a coordinated, energy-dependent cell death process that involves the activation of a group of cysteine proteases known as caspases (Elmore, 2007). Apoptosis is viewed as an irreversible commitment to programmed cell death. Caspases are synthesised as inactive zymogens, which are activated by proteolytic cleavage at the aspartate cleavage sites in response to apoptotic stimuli (Degterev, Boyce, & Yuan, 2003). At least 14 different mammalian caspases have been discovered (Fan, Han, Cong, & Liang, 2005). A complex cascade of caspases activation is observed during apoptosis. Caspases are both the initiators and executioners in apoptotic cell death (Riedl & Shi, 2004; Shi, 2002). The two common pathways in apoptosis are extrinsic (death receptor) and intrinsic (mitochondrial) pathways (R. S. Y. Wong, 2011). Caspase-8 is the initiator caspase in the death receptor pathway that cleaves other effector caspases such as caspase-3 and -7 (Degterev et al., 2003). On the other hand, the mitochondrial pathway requires the generation of an apoptosome complex that recruits caspase-9 as the initiator caspase to activate downstream caspase-3 and -7 (Elmore, 2007). Caspase-3 and -7 are the main executioner caspases in apoptosis. Activated caspase-3 and -7 cleave distinct inhibitory sub-units of endonuclease family, cytoskeletal proteins, protein kinases and DNA repair proteins, leading to the formation of apoptotic bodies (Fan et al., 2005; R. S. Y. Wong, 2011). In the present study, caspase 3/7 activation assay was conducted to evaluate the execution event in the cultured cells following miR-23a transfection.

The morphological and biochemical hallmarks of apoptosis include cell shrinkage, chromatin condensation, nuclear fragmentation, DNA and protein breakdown, membrane blebbling and recognition by phagocytic cells (Hengartner, 2000). Apoptotic cell death occurs through both p53-dependent and -independent manners (Benchimol, 2001; Pan & Griep, 1995; Violette et al., 2002). Generally, apoptosis occurs during tissue development and aging as a homeostatic mechanism to maintain cell populations.

Apoptosis also occurs as a defence mechanism towards immune reactions and cell damages caused by diseases, radiation, drugs or chemicals. Therefore, resistance to apoptosis contributes to carcinogenesis and chemoradioresistance in cancer treatment. Mechanisms that lead to the evasion of apoptosis in cancer include impaired death receptor signalling, disrupted balance of BCL2 family of pro-apoptotic and anti-apoptotic proteins, defects or mutation in the *TP53* gene, reduced expression of caspases and increased expression of inhibitor of apoptosis proteins (R. S. Y. Wong, 2011). On top of that, miRNA deregulation also contributes to the aberration in apoptotic regulation. For instance, over-expression of miR-92a has been reported to cause uncontrollable cell proliferation in CRC via the down-regulation of pro-apoptotic molecule BCL2-interacting mediator of cell death (BIM) (Tsuchida et al., 2011). PDCD4, a tumour suppressor protein that is commonly down-regulated in CRC, has been determined to be associated with the up-regulation of miR-21 (Asangani et al., 2008; Yamamichi et al., 2009). Moreover, T. C. Chang et al. (2007) have shown the significance of miR-34a in the regulation of p53 network of cell cycle control and apoptosis in CRC. Based on a recent review by C. Li et al. (2012), numerous miRNAs have been reported to regulate the modulators of apoptosis (e.g. BCL2-antagonist/killer [BAK], BCL2-associated X protein [BAX], BBC3, BH3-interacting domain death antagonist [BID], Fas-associated death domain [FADD], caspase-3, -8 and -9).

The present investigation has demonstrated that miR-23a could harbour an apoptosis resistance function in CRC. The miR-23a expression was determined to be up-regulated in the clinical CRC tissue and blood samples. The elucidation of apoptosis function in the *in vitro* system via cell viability, apoptosis and caspase 3/7 activation analyses revealed significant reduction of cell viability and promotion of cell apoptosis following miR-23a inhibitor transfection (Figures 4.40, 4.41 and 4.42). No significant finding was observed in the migration and invasion assay (Figure 4.43). The results obtained have

indicated that miR-23a may exclusively regulate cell apoptosis in CRC. Currently, there is only a single study by Jahid et al. (2012) who have reported the involvement of miR-23a in CRC cell migration and invasion by targeting the *MTSS1* gene. The actual biological relevance of miR-23a in CRC metastasis remains to be clarified.

In the present study, *APAF1* has been determined to be directly targeted by miR-23a through the luciferase assay (Figure 4.45). Mutagenesis at the seed match region of *APAF1* 3'-UTR has affirmed the specificity of miR-23a recognition. These findings have clearly shown that miR-23a could regulate apoptosis by targeting *APAF1*. Previously, Huerta et al. (2007) have reported that the endogenous *APAF1* expression was significantly lower in the SW620 than the SW480 cells. The transfection of miR-23a inhibitor in the present investigation has revealed a relatively stronger induction of *APAF1* mRNA and APAF1 protein in the non-metastatic SW480 cells when compared to the metastatic SW620 cells. The SW620 cell line is believed to have lower susceptibility to gene modulation and apoptosis induction due to increased genetic mutations (Hewitt et al., 2000; Huerta et al., 2007).

Typically, APAF1, APAF2 and APAF3 are the three members of the APAF family (Cain, Bratton, & Cohen, 2002). APAF1 is the mammalian homologue of the *C. elegans* pro-apoptotic cell death 4 (CED-4) protein (Hickman & Helin, 2002). APAF2 is commonly identified as cytochrome c while APAF3 is also known as caspase-9 (P. Li et al., 1997; X. Liu, Kim, Yang, Jemmerson, & Wang, 1996). APAF1 has been suggested as a tumour suppressor in cancer (Lowe & Lin, 2000). It is one of the key regulators in the mitochondrial apoptotic pathway (Zlobec et al., 2007). The gene that encodes APAF1 is located on chromosomal locus 12q23 (Umetani et al., 2004). The protein molecular weight for APAF1 is 130 kDa (Cain et al., 2002). It is a cytosolic protein that consists of three domains, namely, N-terminal caspase recruitment domain (CARD), CED-4-like domain necessary for nucleotide binding and C-terminal domain containing

multiple repeats of tryptophan and aspartate residues (WD40 repeats) responsible for protein-protein interactions (Campioni et al., 2005; Corvaro & Cecconi, 2004) (Figure 5.3A). In the presence of an apoptotic stimulus, cytochrome c released from the mitochondrion binds to the WD40 repeats to reveal the nucleotide binding site for deoxyadenosine triphosphate (dATP) (Hickman & Helin, 2002). Following the attachment of dATP, APAF1 protein undergoes further conformational changes and unmasks the CARD domain, which allows the recruitment of procaspase-9 (Campioni et al., 2005). Subsequent oligomerisation of the APAF1 protein through its CED-4-like domain permits the formation of a large apoptosome complex (~700-1400 kDa) (Cain et al., 2002). The procaspase-9 is activated by autocatalytic cleavage to form active caspase-9 necessary for downstream caspases activation (Cecconi, Alvarez-Bolado, Meyer, Roth, & Gruss, 1998) (Figure 5.3B). Thus, the absence of APAF1 protein could prevent the activation of downstream effector caspases, leading to cellular resistance to apoptotic stimuli (Yoshida et al., 1998).

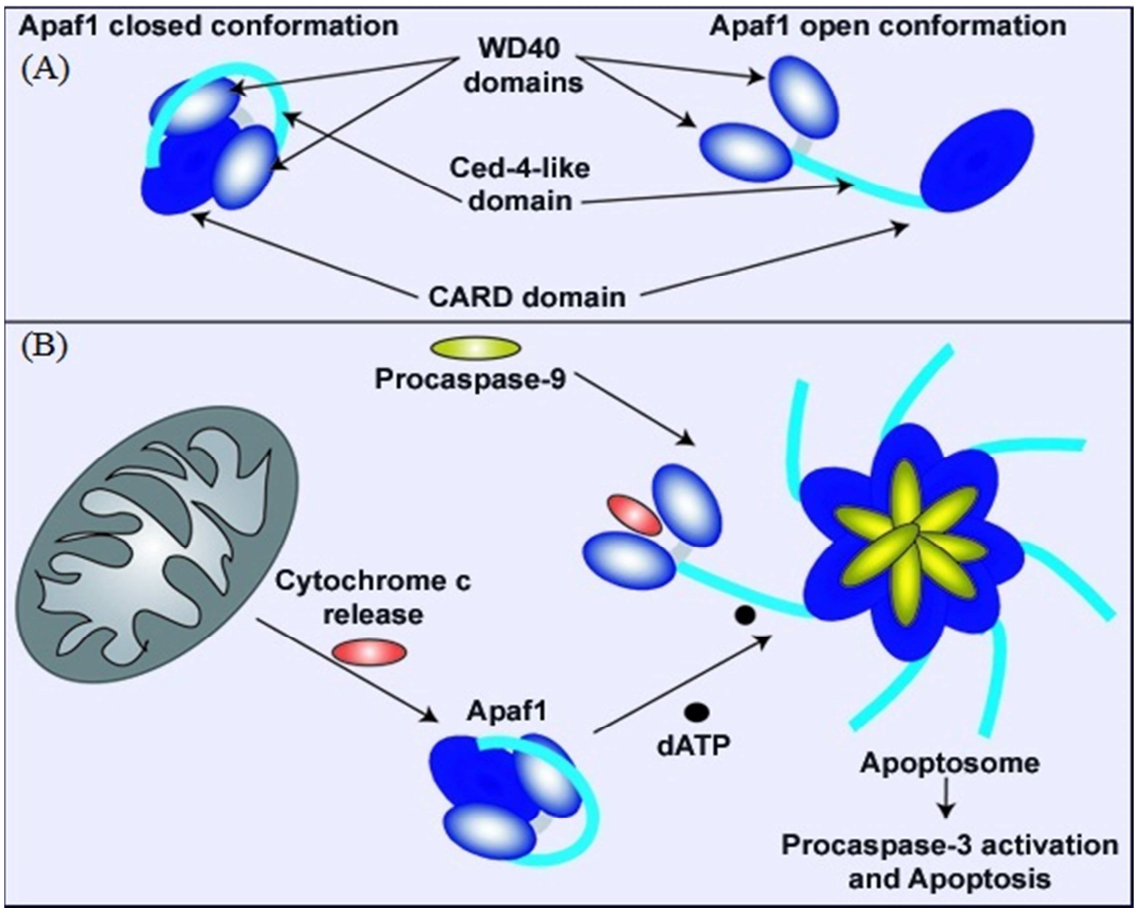

Figure 5.3: (A) Conformation of APAF1 protein. (B) Formation and regulation of apoptosome complex in apoptosis.

(Source: Corvaro & Cecconi, 2004)

Independently, studies on miR-23a up-regulation and *APAF1* down-regulation in relation to apoptosis have been reported. B. Li et al. (2013) have shown the involvement of miR-23a in the regulation of cell death in mice thymic lymphoma model by targeting the pro-apoptotic factor Fas. The up-regulation of miR-23a has also been reported to suppress the expression of UVB-induced topoisomerase 1, caspase-7 and serine/threonine kinase 4 (STK4) apoptotic factors in HaCaT keratinocyte cells (Z. Guo et al., 2013). On the other hand, APAF1 down-regulation has been linked to decreased apoptosis and correlated with an aggressive phenotype and adverse prognosis in CRC (Paik et al., 2007; Zlobec et al., 2007). The likelihood of colorectal tumours to undergo

apoptosis is lower in the advanced-stage cancer. The APAF1 expression may serve as a predictive marker for chemotherapy response and drug resistance in CRC. Hector et al. (2012) have reported that patients with higher expression levels of APAF1 protein showed better recurrence-free and overall survival following 5-FU-based adjuvant chemotherapy. Another study by Zlobec, Vuong, and Compton (2006) has indicated that the APAF1 expression is a substantial marker for monitoring tumour regression in rectal cancer patients who have received neoadjuvant radiotherapy. The *APAF1* mRNA has been found to be under epigenetic control, whereby allelic imbalance of the *APAF1* locus may contribute to the development and progression of CRC (Umetani et al., 2004). Apart from CRC, APAF1 has also been suggested as a marker of tumour progression in brain cancer, melanoma and gastric cancer (Johnson et al., 2007; Mustika, Budiyanto, Nishigori, Ichihashi, & Ueda, 2005; H. L. Wang, Bai, Li, Sun, & Wang, 2007). Mouhamad, Galluzzi, Zermati, Castedo, and Kroemer (2007) have demonstrated that APAF1 suppression in cancer can compromise the arrest of DNA synthesis in response to DNA damages by cisplastin, UVC radiation and gamma irradiation.

Prior to this work, three independent research groups have reported the association between miR-23a and *APAF1* in apoptosis. Q. Chen et al. (2014) have determined that miR-23a can alleviate hypoxia-induced neuronal apoptosis by suppressing the *APAF1* gene. Lian et al. (2013) have shown that the transfection of miR-23a inhibitor in glioma cell lines can restore the *APAF1* expression and promote cell apoptosis. Shang et al. (2014) have revealed that miR-23a inhibition can enhance 5-FU drug chemosensitivity through APAF1/caspase-9 apoptotic pathway in HCT116 and HT29 CRC cells. The results obtained in this study are comparable with the published reports. In clinical CRC tissue samples, the expression level of miR-23a was found to be inversely correlated with the expression levels of *APAF1* mRNA and APAF1 protein (Figure 4.52B, C). The miR-23a has been proven to bind to the 3'-UTR of *APAF1* and dramatically decreasing

the levels of *APAF1* mRNA and APAF1 protein. A limitation in the present study is the lack of a statistical power in the negative correlation between miR-23a and *APAF1* mRNA in the CRC blood samples (Figure 4.52A). Nonetheless, individual deregulation of miR-23a (r = 0.827) and *APAF1* mRNA (r = 0.378) in the blood has been proven to be reflective of that in the CRC tissue. In addition, as the tumour progressed from the early-stage (I-II) to the advanced-stage (III-IV), an increasing trend of miR-23a expression levels (Figures 4.13 and 4.21) and a decreasing trend of *APAF1* mRNA and APAF1 protein expression levels were noticed in both tissue and blood samples (Figures 4.49, 4.50 and 4.51). Blood circulation represents a complex environment in the human body (Luo, Burwinkel, Tao, & Brenner, 2011). The relatively small sample size in the present study may hinder the absolute confirmation of whether the deregulated miR-23a:*APAF1* expression in the systemic circulation was related to CRC alone or as a general mechanism in histological progression to cancer. This is the first report that accesses the clinical correlation between the expression of miR-23a and *APAF1* in the blood circulation of CRC patients. This study serves as a proof-of-concept example to highlight the physiological significance of miR-23a:*APAF1* regulation axis as a biomarker to monitor tumour progression in CRC. Since apoptosis is the primary cytotoxic mechanism of chemotherapeutic agents, grouping the patients into early and advanced CRC may provide a general overview of the miR-23a:*APAF1* regulation in the population that is most likely to be subjected for systemic chemotherapy.

Recently, N. Wang et al. (2013) have revealed that the expression of miR-23a is transcriptional activated by the *TP53* gene. Clinically, colorectal tumours tend to accumulate p53 mutations as they progress into late stages of carcinogenesis (Huerta et al., 2007). The SW480 and SW620 cell lines used in this study have been proven to express high levels of mutated p53 proteins (Rodrigues et al., 1990; Violette et al., 2002). Since p53 mutation is a common genetic abnormality in CRC, the regulation of

cell apoptosis via p53-dependent pathway is greatly disrupted (Lacopetta, 2003). *APAF1*, which was found to be down-regulated in the present study, is an essential downstream effector of p53-mediated apoptosis (Fortin et al., 2001; Robles, Bemmels, Foraker, & Harris, 2001). This defect could lead to decreased apoptosis and thus, may contribute to chemoradioresistance. Collectively, the reported findings correspond to this notion whereby the increase of *APAF1* mRNA and APAF1 protein following miR-23a inhibition has rescued the downstream caspase-3 and -7 activities, leading to promotion of cell apoptosis. The possible involvement of p53 and miR-23a in the regulation of *APAF1* is illustrated in Figure 5.4.

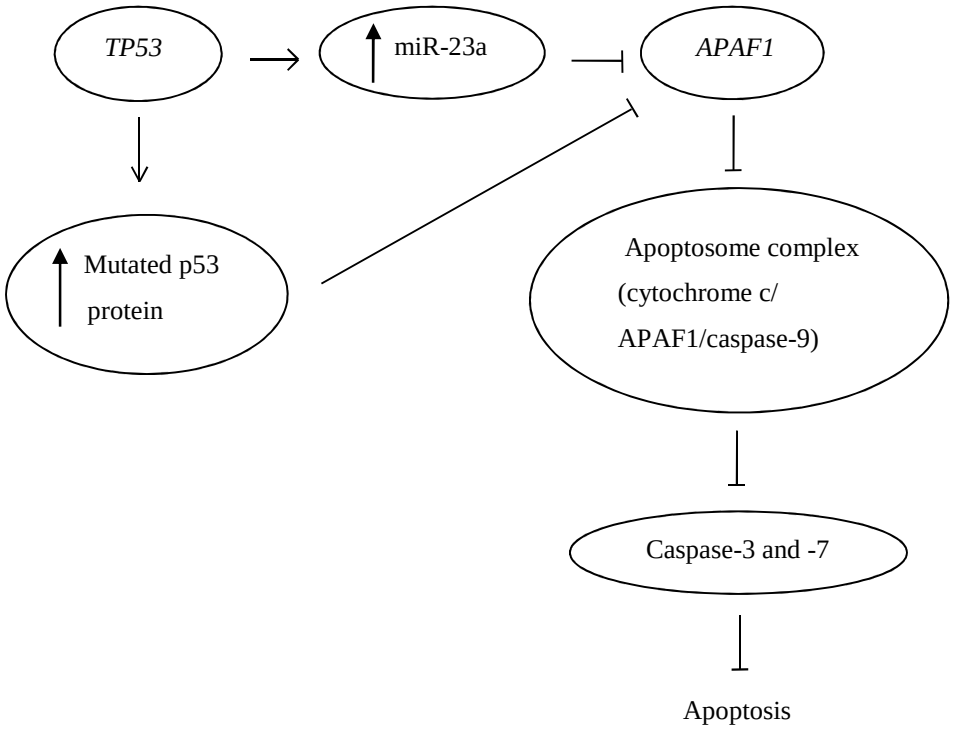

Figure 5.4: Involvement of p53 and miR-23a in the regulation of *APAF1* in CRC. The up-regulation of miR-23a and the increased synthesis of mutated p53 protein may lead to the down-regulation of *APAF1* that interrupts the normal regulation of cell apoptosis.

5.2.3 miR-338-5p transfection in CRC

miR-338-5p transfection was performed to study the effect of miR-338-5p modulation in CRC cells. However, the data from the MTT cell viability, Annexin V-FITC apoptosis and Matrigel migration and invasion analyses in both SW480 and SW620 cell lines did not reveal any statistical significance. Despite the up-regulation in the clinical samples (Figures 4.15 and 4.23), the biological relevance of miR-338-5p in CRC cell apoptosis, migration and invasion could not be elucidated in this study. Based on the available literature regarding the role of miR-338-5p in CRC (section 5.1.3.5), only Ju et al. (2013) have validated the involvement of miR-338-5p in CRC cell migration and autophagy. The transfection protocol and experimental assays used by Ju and his colleagues were different from the present work. Thus, these differences may account for the discrepancy between the two studies. The information on the role and regulation of miR-338-5p in CRC is limited. Other functional assays such as wound healing, cell cycle, oxidative stress and epigenetics assays could be performed in the future to further elucidate the function of miR-338-5p in CRC.

CHAPTER 6

CONCLUSION

6.1 Summary and significance of the study

The present study was carried out to determine the potential blood miRNA biomarkers for early detection of CRC. Seven miRNAs (miR-150, miR-193a-3p, miR-23a, miR-23b, miR-338-5p, miR-342-3p and miR-483-3p) have been found to be concurrently expressed in the tissue and blood miRNA arrays. Through comprehensive RT-qPCR validation and statistical analyses, miR-193a-3p, miR-23a and miR-338-5p have been demonstrated as a triple miRNA classifier for CRC detection, with an AUC of 0.887 (80.0% sensitivity, 84.4% specificity and 83.3% accuracy). These miRNAs have been determined to be significantly up-regulated and positively correlated in the tissue and blood samples obtained from primary CRC patients. The findings have collectively implicated that the deregulation of miR-193a-3p, miR-23a and miR-338-5p in the circulating blood is reflective of those in the CRC tissue.

The subsequent work involved the elucidation of miR-193a-3p, miR-23a and miR-338-5p functions in the carcinogenesis of CRC. Each of these miRNAs was studied separately using SW480 and SW620 CRC cell lines. These cell lines have been shown to be a useful *in vitro* model for the analysis of gene expression changes during CRC progression. The effects of the deregulated miRNAs in cell viability, apoptosis, migration and invasion assays have been examined. Firstly, miR-193a-3p has been identified to be involved in the promotion of CRC cell migration and invasion. *FOXO4* has been experimentally validated as a direct target of miR-193a-3p. Clinically, as the tumour progressed from the early- to advanced-stage, an increasing trend of miR-193a-

3p expression and a decreasing trend of *FOXO4* expression were observed. Significant inverse correlation was detected in the tissue levels of miR-193a-3p and *FOXO4* mRNA. Secondly, miR-23a has been shown to possess apoptosis resistance function in CRC. *APAF1* has been experimentally validated as a direct target of miR-23a. Clinically, as the tumour progressed from the early- to advanced-stage, an increasing trend of miR-23a expression and a decreasing trend of *APAF1* expression were determined. The miR-23a up-regulation was negatively correlated with *APAF1* mRNA and APAF1 protein down-regulation in CRC tissue samples. However, statistical significance was not detected in the correlation between miR-193a-3p and *FOXO4* mRNA or between miR-23a and *APAF1* mRNA in the blood samples. This is the first study that reports the clinical correlation between the expression levels of miR-193a-3p and *FOXO4* or miR-23a and *APAF1* in CRC though the expression levels in the blood were not statistically significant. Further studies are warranted to explore the existing potential of miR-193a-3p:*FOXO4* and miR-23a:*APAF1* regulation axes as biomarkers for miRNA-based therapy and prognostication. In this study, the modulation of miR-338-5p expression has been concluded with negative findings in the cell viability, apoptosis, migration and invasion analyses.

6.2 Limitations and future prospects of the study

In this research, there is a limitation in the tissue collection of stage I CRC samples. Surgically resected growths were usually small and thus the priority was given to the pathologists for histological analysis. The present work serves as an exploratory basis for further investigations in larger prospective and randomised clinical studies with higher number of samples from healthy controls and patients of advanced adenoma and various stages of CRC. A non-invasive miRNA screening assay using the triple miRNA

classifier of miR-193a-3p, miR-23a and miR-338-5p could then be developed to identify asymptomatic individuals with colorectal neoplasia prior to the invasive colonoscopy examination. The study may be extended to determine the feasibility of the three miRNAs as follow-up markers for the detection of CRC recurrence. Blood sample collection during surgical follow-up could be initiated to allow prospective evaluation of the changes in miRNA profiles. As technologies continue to advance, miRNA profiling will get even easier and cheaper. Moreover, the lack of negative correlations in the blood expression levels of miR-193a-3p:*FOXO4* and miR-23a:*APAF1* may also be addressed by a larger sample size.

The limitation in the present functional study is the inability to screen all the available functional assays in cancer due to cost and time constraints. Since miR-338-5p was not found to be associated with apoptosis, migration and invasion functions in this investigation, future work involving other functional assays such as wound healing, cell cycle, oxidative stress and epigenetics assays could be performed to investigate the role of miR-338-5p in CRC.

This research serves as a proof-of-concept example that highlights the potentiality of miR-193a-3p:*FOXO4* and miR-23a:*APAF1* regulation axes as therapeutic targets in CRC. The study may be extended into *in vivo* settings to generate more relevant data representing the living systems. Furthermore, it will be of interest to test the changes in the miRNA and mRNA levels following exposure to cytotoxic stimuli such as chemotherapeutic drugs and radiation in both *in vitro* and *in vivo* studies. Another future prospect of this study includes the effort to validate other gene targets of miR-193a-3p and miR-23a. *In silico* analysis has predicted the presence of thousands of miRNA:mRNA target pairs, of which only a small number have been experimentally validated.

All in all, the present research provides a promising rationale to explore and translate the findings into possible clinical applications in the diagnosis, prognosis and treatment of CRC.

REFERENCES

Ahlquist, D. A., Zou, H., Domanico, M., Mahoney, D. W., Yab, T. C., Taylor, W. R., . . . Lidgard, G. P. (2012). Next-generation stool DNA test accurately detects colorectal cancer and large adenomas. *Gastroenterology, 142*(2), 248-256.

Ahmed, F. E., Amed, N. C., Vos, P. W., Bonnerup, C., Atkins, J. N., Casey, M., . . . Allison, R. R. (2012). Diagnostic microRNA markers to screen for sporadic human colon cancer in blood. *Cancer Genomics and Proteomics, 9*(4), 179-192.

Akao, Y., Nakagawa, Y., & Naoe, T. (2006). let-7 microRNA functions as a potential growth suppressor in human colon cancer cells. *Biological and Pharmaceutical Bulletin, 29*(5), 903-906.

Allison, J. E., Tekawa, I. S., Ransom, L. J., & Adrain, A. L. (1996). A comparison of fecal occult-blood tests for colorectal-cancer screening. *The New England Journal of Medicine, 334*(3), 155-159.

Ambros, V., Bartel, B., Bartel, D. P., Burge, C. B., Carrington, J. C., Chen, X., . . . Tuschl, T. (2003). A uniform system for microRNA annotation. *RNA, 9*(3), 277-279.

American Cancer Society. (2011). Colorectal cancer facts & figures 2011-2013. Atlanta: American Cancer Society.

Anderson, E. C., & Wong, M. H. (2010). Caught in the Akt: regulation of Wnt signaling in the intestine. *Gastroenterology, 139*(3), 718-722.

André, T., Boni, C., Navarro, M., Tabernero, J., Hickish, T., Topham, C., . . . de Gramont, A. (2009). Improved overall survival with oxaliplatin, fluorouracil, and leucovorin as adjuvant treatment in stage II or III colon cancer in the MOSAIC trial. *Journal of Clinical Oncology, 27*(19), 3109-3116.

Arden, K. C. (2006). Multiple roles of FOXO transcription factors in mammalian cells point to multiple roles in cancer. *Experimental Gerontology, 41*(8), 709-717.

Arya, M., Shergill, I. S., Williamson, M., Gommersall, L., Arya, N., & Patel, H. R. (2005). Basic principles of real-time quantitative PCR. *Expert Review of Molecular Diagnostics, 5*(2), 209-219.

Asangani, I. A., Rasheed, S. A., Nikolova, D. A., Leupold, J. H., Colburn, N. H., Post, S., & Allgayer, H. (2008). MicroRNA-21 (miR-21) post-transcriptionally downregulates tumor suppressor Pdcd4 and stimulates invasion, intravasation and metastasis in colorectal cancer. *Oncogene, 27*(15), 2128-2136.

Austin, K. L., Power, E., Solarin, I., Atkin, W. S., Wardle, J., & Robb, K. A. (2009). Perceived barriers to flexible sigmoidoscopy screening for colorectal cancer among UK ethnic minority groups: a qualitative study. *Journal of Medical Screening, 16*(4), 174-179.

Babashah, S., & Soleimani, M. (2011). The oncogenic and tumour suppresive roles of microRNAs in cancer and apoptosis. *European Journal of Cancer, 47*(8), 1127-1137.

Bader, A. G. (2012). miR-34 - a microRNA replacement therapy is headed to the clinic. *Frontiers in Genetics, 3*, 120.

Bagga, S., Bracht, J., Hunter, S., Massirer, K., Holtz, J., Eachus, R., & Pasquinelli, A. E. (2005). Regulation by let-7 and lin-4 miRNAs results in target mRNA degradation. *Cell, 122*(4), 553-563.

Bandi, P., Cokkinides, V., Smith, R. A., & Jemal, A. (2012). Trends in colorectal cancer screening with home-based fecal occult blood tests in adults ages 50 to 64 years, 2000-2008. *Cancer, 118*(20), 5092-5099.

Bao, L., Zhao, J., Dai, X., Wang, Y., Ma, R., Su, Y., . . . Ren, X. (2014). Correlation between miR-23a and onset of hepatocellular carcinoma. *Clinics and Research in Hepatology and Gastroenterology, 38*(3), 318-330.

Barik, S. (2008). An intronic microRNA silences genes that are functionally antagonistic to its host gene. *Nucleic Acids Research, 36*(16), 5232-5241.

Bartel, D. P. (2004). MicroRNAs: genomics, biogenesis, mechanism, and function. *Cell, 116*(2), 281-297.

Bartel, D. P. (2009). MicroRNAs: target recognition and regulatory functions. *Cell, 136*(2), 215-233.

Benchimol, S. (2001). p53-dependent pathways of apoptosis. *Cell Death and Differentiation, 8*(11), 1049-1051.

Berezikov, E., Cuppen, E., & Plasterk, R. H. (2006). Approaches to microRNA discovery. *Nature Genetics, 38*, S2-S7.

Bhattacharyya, S. N., Habermacher, R., Martine, U., Closs, E. I., & Filipowicz, W. (2006). Relief of microRNA-mediated translational repression in human cells subjected to stress. *Cell, 125*(6), 1111-1124.

Biswas, S., Chytil, A., Washington, K., Romero-Gallo, J., Gorska, A. E., Wirth, P. S., . . . Grady, W. M. (2004). Transforming growth factor beta receptor type II inactivation promotes the establishment and progression of colon cancer. *Cancer Research, 64*(14), 4687-4692.

Blok, E. J., Kuppen, P. J. K., van Leeuwen, J. E. M., & Sier, C. F. M. (2013). Cytoplasmic overexpression of HER2: a key factor in colorectal cancer. *Clinical Medicine Insights: Oncology, 7*, 41-51.

Blosser, W., Vakana, E., Wyss, L. V., Swearingen, M. L., Stewart, J., Stancato, L., & Tate, C. M. (2014). A method to assess target gene involvement in angiogenesis in vitro and in vivo using lentiviral vectors expressing shRNA. *PLoS ONE, 9*(4), e96036.

Borel, F., van Logtenstein, R., Koornneef, A., Maczuga, P., Ritsema, T., Petry, H., . . . Konstantinova, P. (2011). In vivo knock-down of multidrug resistance transporters ABCC1 and ABCC2 by AAV-delivered shRNAs and by artificial miRNAs. *Journal of RNAi and Gene Silencing, 7*, 434-442.

Bouchie, A. (2013). First microRNA mimic enters clinic. *Nature Biotechnology, 31*(7), 577.

Boudreau, R. L., Martins, I., & Davidson, B. L. (2009). Artificial microRNAs as siRNA shuttles: improved safety as compared to shRNAs in vitro and in vivo. *Molecular Therapy, 17*(1), 169-175.

Bray, F., Jemal, A., Grey, N., Ferlay, J., & Forman, D. (2012). Global cancer transitions according to the Human Development Index (2008-2030): a population-based study. *The Lancet Oncology, 13*(8), 790-801.

Brazma, A., Hingamp, P., Quackenbush, J., Sherlock, G., Spellman, P., Stoeckert, C., . . . Vingron, M. (2001). Minimum information about a microarray experiment (MIAME)-toward standards for microarray data. *Nature Genetics, 29*(4), 365-371.

Bremnes, R. M., Dønnem, T., Al-Saad, S., Al-Shibli, K., Andersen, S., Sirera, R., . . . Busund, L. T. (2011). The role of tumor stroma in cancer progression and prognosis: emphasis on carcinoma-associated fibroblasts and non-small cell lung cancer. *Journal of Thoracic Oncology, 6*(1), 209-217.

Brenner, H., Chang-Claude, J., Jansen, L., Knebel, P., Stock, C., & Hoffmeister, M. (2013). Reduced risk of colorectal cancer up to 10 years after screening, surveillance, or diagnostic colonoscopy. *Gastroenterology, 146*(3), 709-717.

Broderick, J. A., & Zamore, P. D. (2011). MicroRNA therapeutics. *Gene Therapy, 18*, 1104-1110.

Bruce, W. R., Wolever, T. M., & Giacca, A. (2000). Mechanisms linking diet and colorectal cancer: the possible role of insulin resistance. *Nutrition and Cancer, 37*(1), 19-26.

Budhu, A., Jia, H. L., Forgues, M., Liu, C. G., Goldstein, D., Lam, A., . . . Wang, X. W. (2008). Identification of metastasis-related microRNAs in hepatocellular carcinoma. *Hepatology, 47*(3), 897-907.

Burgering, B. M., & Kops, G. J. (2002). Cell cycle and death control: long live Forkheads. *Trends in Biochemical Sciences, 27*(7), 352-360.

Burgos, K. L., Javaherian, A., Bomprezzi, R., Ghaffari, L., Rhodes, S., Courtright, A., . . . Van Keuren-Jensen, K. (2013). Identification of extracellular miRNA in human cerebrospinal fluid by next-generation sequencing. *RNA, 19*(5), 712-722.

Burk, U., Schubert, J., Wellner, U., Schmalhofer, O., Vincan, E., Spaderna, S., & Brabletz, T. (2008). A reciprocal repression between ZEB1 and members of the miR-200 family promotes EMT and invasion in cancer cells. *EMBO Reports, 9*(6), 582-589.

Bustin, S. A., Benes, V., Garson, J. A., Hellemans, J., Huggett, J., Kubista, M., . . . Wittwer, C. T. (2009). The MIQE guidelines: minimum information for publication of quantitative real-time PCR experiments. *Clinical Chemistry, 55*(4), 611-622.

Cai, K., Mulatz, K., Ard, R., Nguyen, T., & Gee, S. H. (2014). Increased diacylglycerol kinase ζ expression in human metastatic colon cancer cells augments Rho GTPase activity and contributes to enhanced invasion. *BMC Cancer, 14*, 208.

Cain, K., Bratton, S. B., & Cohen, G. M. (2002). The apaf-1 apoptosome: a large caspase-activating complex. *Biochimie, 84*(2-3), 203-214.

Calin, G. A., Dumitru, C. D., Shimizu, M., Bichi, R., Zupo, S., Noch, E., . . . Croce, C. M. (2002). Frequent deletions and down-regulation of micro-RNA genes miR15 and miR16 at 13q14 in chronic lymphocytic leukemia. *Proceedings of the National Academy of Sciences of the United States of America, 99*(24), 15524-15529.

Calin, G. A., Sevignani, C., Dumitru, C. D., Hyslop, T., Noch, E., Yendamuri, S., . . . Croce, C. M. (2004). Human microRNA genes are frequently located at fragile sites and genomic regions involved in cancers. *Proceedings of the National Academy of Sciences of the United States of America, 101*(9), 2999-3004.

Callari, M., Dugo, M., Musella, V., Marchesi, E., Chiorino, G., Grand, M. M., . . . De Cecco, L. (2012). Comparison of microarray platforms for measuring differential microRNA expression in paired normal/cancer colon tissues. *PLoS ONE, 7*(9), e45105.

Campioni, M., Santini, D., Tonini, G., Murace, R., Dragonetti, E., Spugnini, E. P., & Baldi, A. (2005). Role of Apaf-1, a key regulator of apoptosis, in melanoma progression and chemoresistance. *Experimental Dermatology, 14*(11), 811-818.

Caraguel, C. G. B., Stryhn, H., Gagné, N., Dohoo, I. R., & Hammell, K. L. (2011). Selection of a cutoff value for real-time polymerase chain reaction results to fit a diagnostic purpose: analytical and epidemiologic approaches. *Journal of Veterinary Diagnostic Investigation, 23*(1), 2-15.

Carrato, A. (2008). Adjuvant treatment of colorectal cancer. *Gastrointestinal Cancer Research, 2*(4), S42-S46.

Castanotto, D., Sakurai, K., Lingeman, R., Li, H., Shively, L., Aagaard, L., . . . Rossi, J. J. (2007). Combinatorial delivery of small interfering RNAs reduces RNAi efficacy by selective incorporation into RISC. *Nucleic Acids Research, 35*(15), 5154-5164.

Castro, G., Azrak, M. F., Seeff, L. C., & Royalty, J. (2013). Outpatient colonoscopy complications in the CDC's Colorectal Cancer Screening Demonstration Program: a prospective analysis. *Cancer, 119*(15), 2849-2854.

Cecconi, F., Alvarez-Bolado, G., Meyer, B. I., Roth, K. A., & Gruss, P. (1998). Apaf1 (CED-4 homolog) regulates programmed cell death in mammalian development. *Cell, 94*(6), 727-737.

Chan, S. P., & Slack, F. J. (2006). microRNA-mediated silencing inside P-bodies. *RNA Biology, 3*(3), 97-100.

Chang, K. H., Mestdagh, P., Vandesompele, J., Kerin, M. J., & Miller, N. (2010). MicroRNA expression profiling to identify and validate reference genes for relative quantification in colorectal cancer. *BMC Cancer, 10*, 173.

Chang, K. H., Miller, N., Kheirelseid, E. A., Ingoldsby, H., Hennessy, E., Curran, C. E., . . . Kerin, M. J. (2011). MicroRNA-21 and PDCD4 expression in colorectal cancer. *European Journal of Surgical Oncology, 37*(7), 597-603.

Chang, T. C., Wentzel, E. A., Kent, O. A., Ramachandran, K., Mullendore, M., Lee, K. H., . . . Mendell, J. T. (2007). Transactivation of miR-34a by p53 broadly influences gene expression and promotes apoptosis. *Molecular Cell, 26*(5), 745-752.

Chao, W., & D'Amore, P. A. (2008). IGF2: epigenetic regulation and role in development and disease. *Cytokine and Growth Factor Reviews, 19*(2), 111-120.

Chen, L., Tang, Y., Wang, J., Yan, Z., & Xu, R. (2013). miR-421 induces cell proliferation and apoptosis resistance in human nasopharyngeal carcinoma via downregulation of FOXO4. *Biochemical and Biophysical Research Communications, 435*(4), 745-750.

Chen, Q., Xu, J., Li, L., Li, H., Mao, S., Zhang, F., . . . Zhang, Q. (2014). MicroRNA-23a/b and microRNA-27a/b suppress Apaf-1 protein and alleviate hypoxia-induced neuronal apoptosis. *Cell Death and Disease, 5*, e1132.

Chen, X., Ba, Y., Ma, L., Cai, X., Yin, Y., Wang, K., . . . Zhang, C. Y. (2008). Characterization of microRNAs in serum: a novel class of biomarkers for diagnosis of cancer and other diseases. *Cell Research, 18*(10), 997-1006.

Chen, X., Guo, X., Zhang, H., Xiang, Y., Chen, J., Yin, Y., . . . Zhang, C. Y. (2009). Role of miR-143 targeting KRAS in colorectal tumorigenesis. *Oncogene, 28*(10), 1385-1392.

Chhabra, R., Dubey, R., & Saini, N. (2010). Cooperative and individualistic functions of the microRNAs in the miR-23a~27a~24-2 cluster and its implication in human diseases. *Molecular Cancer, 9*, 232.

Chin, L. J., & Slack, F. J. (2008). A truth serum for cancer-microRNAs have major potential as cancer biomarkers. *Cell Research, 18*(10), 983-984.

Choong, M. K., & Tsafnat, G. (2012). Genetic and epigenetic biomarkers of colorectal cancer. *Clinical Gastroenterology and Hepatology, 10*(1), 9-15.

Compton, C. C., Byrd, D. R., Garcia-Aguilar, J., Kurtzman, S. H., Olawaiye, A., & Washington, M. K. (Eds.). (2012). *AJCC Cancer Staging Atlas: a companion to the seventh editions of the AJCC Cancer Staging Manual and Handbook*. New York, NY: Springer.

Corney, D. C., Flesken-Nikitin, A., Godwin, A. K., Wang, W., & Nikitin, A. Y. (2007). MicroRNA-34b and MicroRNA-34c are targets of p53 and cooperate in control of cell proliferation and adhesion-independent growth. *Cancer Research, 67*(18), 8433-8438.

Corre, S., & Galibert, M. D. (2005). Upstream stimulating factors: highly versatile stress-responsive transcription factors. *Pigment Cell Research, 18*(5), 337-348.

Corvaro, M., & Cecconi, F. (2004). APAF1 (apoptotic protease activating factor 1). *Atlas of Genetics and Cytogenetics in Oncology and Haematology, 8*(4), 296-301.

Cotton, P. B., Durkalski, V. L., Pineau, B. C., Palesch, Y. Y., Mauldin, P. D., Hoffman, B., . . . Butler, H. (2004). Computed tomographic colonography (virtual colonoscopy): a multicenter comparison with standard colonoscopy for detection of colorectal neoplasia. *The Journal of the American Medical Association, 291*(14), 1713-1719.

Creeden, J., Junker, F., Vogel-Ziebolz, S., & Rex, D. (2011). Serum tests for colorectal cancer screening. *Molecular Diagnosis and Therapy, 15*(3), 129-141.

Cui, H., Cruz-Correa, M., Giardiello, F. M., Hutcheon, D. F., Kafonek, D. R., Brandenburg, S., . . . Feinberg, A. P. (2003). Loss of IGF2 imprinting: a potential marker of colorectal cancer risk. *Science, 299*(5613), 1753-1755.

Dalby, B., Cates, S., Harris, A., Ohki, E. C., Tilkins, M. L., Price, P. J., & Ciccarone, V. C. (2004). Advanced transfection with Lipofectamine 2000 reagent: primary neurons, siRNA, and high-throughput applications. *Methods, 33*(2), 95-103.

Dansen, T. B., & Burgering, B. M. (2008). Unravelling the tumor-suppressive functions of FOXO proteins. *Trends in Cell Biology, 18*(9), 421-429.

Davis, J. M. (Ed.). (2011). *Animal cell culture: essential methods*. New York, NY: John Wiley & Sons, Inc.

Davoren, P. A., McNeill, R. E., Lowery, A. J., Kerin, M. J., & Miller, N. (2008). Identification of suitable endogenous control genes for microRNA gene expression analysis in human breast cancer. *BMC Molecular Biology, 9*, 76.

Degterev, A., Boyce, M., & Yuan, J. (2003). A decade of caspases. *Oncogene, 22*(53), 8543-8567.

Delgado, A. P., Brandao, P., Hamid, S., & Narayanan, R. (2013). Mining the dark matter of the cancer proteome for novel biomarkers. *Current Cancer Therapy Reviews, 9*(4), 265-277.

Detours, V., Dumont, J. E., Bersini, H., & Maenhaut, C. (2003). Integration and cross-validation of high-throughput gene expression data: comparing heterogeneous data sets. *FEBS Letters, 546*(1), 98-102.

deVos, T., Tetzner, R., Model, F., Weiss, G., Schuster, M., Distler, J., . . . Lofton-Day, C. (2009). Circulating methylated SEPT9 DNA in plasma is a biomarker for colorectal cancer. *Clinical Chemistry, 55*(7), 1337-1346.

Dews, M., Homayouni, A., Yu, D., Murphy, D., Sevignani, C., Wentzel, E., . . . Thomas-Tikhonenko, A. (2006). Augmentation of tumor angiogenesis by a Myc-activated microRNA cluster. *Nature Genetics, 38*(9), 1060-1065.

Doench, J. G., & Sharp, P. A. (2004). Specificity of microRNA target selection in translational repression. *Genes and Development, 18*(5), 504-511.

Dou, R., Deng, Y., Huang, L., Fu, S., Tan, S., Wang, L., . . . Wang, J. (2013). Multi-microarray identifies lower AQP9 expression in adjuvant chemotherapy nonresponders with stage III colorectal cancer. *Cancer Letters, 336*(1), 106-113.

Dukes, C. E., & Bussey, H. J. R. (1958). The spread of rectal cancer and its effect on prognosis. *British Journal of Cancer, 12*(3), 309-320.

Dweep, H., Sticht, C., Pandey, P., & Gretz, N. (2011). miRWalk - database: prediction of possible miRNA binding sites by "walking" the genes of three genomes. *Journal of Biomedical Informatics, 44*(5), 839-847.

Dyrskjøt, L., Ostenfeld, M. S., Bramsen, J. B., Silahtaroglu, A. N., Lamy, P., Ramanathan, R., . . . Orntoft, T. F. (2009). Genomic profiling of microRNAs in bladder cancer: miR-129 is associated with poor outcome and promotes cell death in vitro. *Cancer Research, 69*(11), 4851-4860.

Earle, J. S. L., Luthra, R., Romans, A., Abraham, R., Ensor, J., Yao, H., & Hamilton, S. R. (2010). Association of microRNA expression with microsatellite instability status in colorectal adenocarcinoma. *The Journal of Molecular Diagnostics, 12*(4), 433-440.

Ebert, M. S., & Sharp, P. A. (2010). MicroRNA sponges: progress and possibilities. *RNA, 16*(11), 2043-2050.

Edge, S. B., & Compton, C. C. (2010). The American Joint Committee on Cancer: the 7th edition of the AJCC Cancer Staging Manual and the future of TNM. *Annals of Surgical Oncology, 17*(6), 1471-1474.

Eis, P. S., Tam, W., Sun, L., Chadburn, A., Li, Z., Gomez, M. F., . . . Dahlberg, J. E. (2005). Accumulation of miR-155 and BIC RNA in human B cell lymphomas. *Proceedings of the National Academy of Sciences of the United States of America, 102*(10), 3627-3632.

Elmore, S. (2007). Apoptosis: a review of programmed cell death. *Toxicologic Pathology, 35*(4), 495-516.

Enright, A. J., John, B., Gaul, U., Tuschl, T., Sander, C., & Marks, D. S. (2003). MicroRNA targets in Drosophila. *Genome Biology, 5*(1), R1.

Esau, C., Davis, S., Murray, S. F., Yu, X. X., Pandey, S. K., Pear, M., . . . Monia, B. P. (2006). miR-122 regulation of lipid metabolism revealed by in vivo antisense targeting. *Cell Metabolism, 3*(2), 87-98.

Esau, C. C., & Monia, B. P. (2007). Therapeutic potential for microRNAs. *Advanced Drug Delivery Reviews, 59*(2-3), 101-114.

Esquela-Kerscher, A., & Slack, F. J. (2006). Oncomirs - microRNAs with a role in cancer. *Nature Reviews Cancer, 6*(4), 259-269.

Faltejskova, P., Svoboda, M., Srutova, K., Mlcochova, J., Besse, A., Nekvindova, J., . . . Slaby, O. (2012). Identification and functional screening of microRNAs highly deregulated in colorectal cancer. *Journal of Cellular and Molecular Medicine, 16*(11), 2655-2666.

Fan, T. J., Han, L. H., Cong, R. S., & Liang, J. (2005). Caspase family proteases and apoptosis. *Acta Biochimica et Biophysica Sinica, 37*(11), 719-727.

Fang, J. Y., & Richardson, B. C. (2005). The MAPK signalling pathways and colorectal cancer. *The Lancet Oncology, 6*(5), 322-327.

Fearon, E. R., & Vogelstein, B. (1990). A genetic model for colorectal tumorigenesis. *Cell, 61*(5), 759-767.

Feng, B., Dong, T. T., Wang, L. L., Zhou, H. M., Zhao, H. C., Dong, F., & Zheng, M. H. (2012). Colorectal cancer migration and invasion initiated by microRNA-106a. *PLoS ONE, 7*(8), e43452.

Fenlon, H. M., Nunes, D. P., Schroy III, P. C., Barish, M. A., Clarke, P. D., & Ferrucci, J. T. (1999). A comparison of virtual and conventional colonoscopy for the detection of colorectal polyps. *The New England Journal of Medicine, 341*(20), 1496-1503.

Ferlay, J., Soerjomataram, I., Ervik, M., Dikshit, R., Eser, S., Mathers, C., . . . Bray, F. (2013). Cancer incidence and mortality worldwide: IARC CancerBase No. 11 Retrieved July 23, 2014, from http://globocan.iarc.fr

Filipowicz, W. (2005). RNAi: the nuts and bolts of the RISC machine. *Cell, 122*(1), 17-20.

Fiscella, M., Zhang, H., Fan, S., Sakaguchi, K., Shen, S., Mercer, W. E., . . . Appella, E. (1997). Wip1, a novel human protein phosphatase that is induced in response to ionizing radiation in a p53-dependent manner. *Proceedings of the National Academy of Sciences of the United States of America, 94*(12), 6048-6053.

Flitcroft, K. L., Irwig, L. M., Carter, S. M., Salkeld, G. P., & Gillespie, J. A. (2012). Colorectal cancer screening: why immunochemical fecal occult blood tests may be the best option. *BMC Gastroenterology, 12*, 183.

Fortin, A., Cregan, S. P., MacLaurin, J. G., Kushwaha, N., Hickman, E. S., Thompson, C. S., . . . Slack, R. S. (2001). APAF1 is a key transcriptional target for p53 in the regulation of neuronal cell death. *The Journal of Cell Biology, 155*(2), 207-216.

Fourie, N. H., Peace, R. M., Abey, S. K., Sherwin, L. B., Rahim-Williams, B., Smyser, P. A., . . . Henderson, W. A. (2014). Elevated circulating miR-150 and miR-342-3p in patients with irritable bowel syndrome. *Experimental and Molecular Pathology, 96*(3), 422-425.

Fu, Z., & Tindall, D. J. (2008). FOXOs, cancer and regulation of apoptosis. *Oncogene, 27*(16), 2312-2319.

Fujita, T., Yanagihara, K., Takeshita, F., Aoyagi, K., Nishimura, T., Takigahira, M., . . . Sasaki, H. (2013). Intraperitoneal delivery of a small interfering RNA targeting NEDD1 prolongs the survival of scirrhous gastric cancer model mice. *Cancer Science, 104*(2), 214-222.

Gaedcke, J., Grade, M., Camps, J., Søkilde, R., Kaczkowski, B., Schetter, A. J., . . . Litman, T. (2012). The rectal cancer microRNAome - microRNA expression in rectal cancer and matched normal mucosa. *Clinical Cancer Research, 18*(18), 4919-4930.

Gao, P., Tchernyshyov, I., Chang, T. C., Lee, Y. S., Kita, K., Ochi, T., . . . Dang, C. V. (2009). c-Myc suppression of miR-23 enhances mitochondrial glutaminase and glutamine metabolism. *Nature, 458*(7239), 762-765.

Garzon, R., Calin, G. A., & Croce, C. M. (2009). MicroRNAs in cancer. *Annual Review of Medicine, 60*, 167-179.

Geng, L., Sun, B., Gao, B., Wang, Z., Quan, C., Wei, F., & Fang, X. D. (2014). MicroRNA-103 promotes colorectal cancer by targeting tumor suppressor DICER and PTEN. *International Journal of Molecular Sciences, 15*(5), 8458-8472.

Ghosh, D., Yu, H., Tan, X. F., Lim, T. K., Zubaidah, R. M., Tan, H. T., . . . Lin, Q. (2011). Identification of key players for colorectal cancer metastasis by iTRAQ quantitative proteomics profiling of isogenic SW480 and SW620 cell lines. *Journal of Proteome Research, 10*(10), 4373-4387.

Gibbons, F. D., & Roth, F. P. (2002). Judging the quality of gene expression-based clustering methods using gene annotation. *Genome Research, 12*(10), 1574-1581.

Giles, R. H., van Es, J. H., & Clevers, H. (2003). Caught up in a Wnt storm: Wnt signaling in cancer. *Biochimica et Biophyisica Acta, 1653*(1), 1-24.

Ginzinger, D. G. (2002). Gene quantification using real-time quantitative PCR: an emerging technology hits the mainstream. *Experimental Hematology, 30*(6), 503-512.

Gluecker, T. M., Johnson, C. D., Harmsen, W. S., Offord, K. P., Harris, A. M., Wilson, L. A., & Ahlquist, D. A. (2003). Colorectal cancer screening with CT colonography, colonoscopy, and double-contrast barium enema examination: prospective assessment of patient perceptions and preferences. *Radiology, 227*(2), 378-384.

Godfrey, A. C., Xu, Z., Weinberg, C. R., Getts, R. C., Wade, P. A., Deroo, L. A., . . . Taylor, J. A. (2013). Serum microRNA expression as an early marker for breast cancer risk in prospectively collected samples from the Sister Study cohort. *Breast Cancer Research, 15*, R42.

Gold, P., & Freedman, S. O. (1965). Specific carcinoembryonic antigens of the human digestive system. *The Journal of Experimental Medicine, 122*(3), 467-481.

Grada, A., & Weinbrecht, K. (2013). Next-generation sequencing: methodology and application. *Journal of Investigative Dermatology, 133*(8), e11.

Grady, W. M., Myeroff, L. L., Swinler, S. E., Rajput, A., Thiagalingam, S., Lutterbaugh, J. D., . . . Markowitz, S. (1999). Mutational inactivation of transforming growth factor beta receptor type II in microsatellite stable colon cancers. *Cancer Research, 59*(2), 320-324.

Grady, W. M., Parkin, R. K., Mitchell, P. S., Lee, J. H., Kim, Y. H., Tsuchiya, K. D., . . . Tewari, M. (2008). Epigenetic silencing of the intronic microRNA hsa-miR-342 and its host gene EVL in colorectal cancer. *Oncogene, 27*(27), 3880-3888.

Gramantieri, L., Ferracin, M., Fornari, F., Veronese, A., Sabbioni, S., Liu, C. G., . . . Negrini, M. (2007). Cyclin G1 is a target of miR-122a, a microRNA frequently down-regulated in human hepatocellular carcinoma. *Cancer Research, 67*(13), 6092-6099.

Greer, E. L., & Brunet, A. (2005). FOXO transcription factors at the interface between longevity and tumor suppression. *Oncogene, 24*(50), 7410-7425.

Griffiths-Jones, S., Grocock, R. J., van Dongen, S., Bateman, A., & Enright, A. J. (2006). miRBase: microRNA sequences, targets and gene nomenclature. *Nucleic Acids Research, 34*, D140-D144.

Grimm, D., Streetz, K. L., Jopling, C. L., Storm, T. A., Pandey, K., Davis, C. R., . . . Kay, M. A. (2006). Fatality in mice due to oversaturation of cellular microRNA/short hairpin RNA pathways. *Nature, 441*(7092), 537-541.

Guo, C., Sah, J. F., Beard, L., Willson, J. K., Markowitz, S. D., & Guda, K. (2008). The noncoding RNA, miR-126, suppresses the growth of neoplastic cells by targeting phosphatidylinositol 3-kinase signaling and is frequently lost in colon cancers. *Genes, Chromosomes and Cancer, 47*(11), 939-946.

Guo, Z., Zhou, B., Liu, W., Xu, Y., Wu, D., Yin, Z., . . . Luo, D. (2013). MiR-23a regulates DNA damage repair and apoptosis in UVB-irradiated HaCaT cells. *Journal of Dermatological Science, 69*(1), 68-76.

Gupta, A., Swaminathan, G., Martin-Garcia, J., & Navas-Martin, S. (2012). MicroRNAs, hepatitis C virus, and HCV/HIV-1 co-infection: new insights in pathogenesis and therapy. *Viruses, 4*(11), 2485-2513.

Half, E., Bercovich, D., & Rozen, P. (2009). Familial adenomatous polyposis. *Orphanet Journal of Rare Diseases, 4*, 22.

Halligan, S., Wooldrage, K., Dadswell, E., Kralj-Hans, I., von Wagner, C., Edwards, R., . . . Atkin, W. (2013). Computed tomographic colonography versus barium enema for diagnosis of colorectal cancer or large polyps in symptomatic patients (SIGGAR): a multicentre randomised trial. *The Lancet, 381*(9873), 1185-1193.

Hamfjord, J., Stangeland, A. M., Hughes, T., Skrede, M. L., Tveit, K. M., Ikdahl, T., & Kure, E. H. (2012). Differential expression of miRNAs in colorectal cancer: comparison of paired tumor tissue and adjacent normal mucosa using high-throughput sequencing. *PLoS ONE, 7*(4), e34150.

Hamilton, S. R., & Aaltonen, L. A. (Eds.). (2000). *Pathology and genetics of tumours of the digestive system*. Lyon: IARC Press.

Hanahan, D., & Weinberg, R. A. (2011). Hallmarks of cancer: the next generation. *Cell, 144*(5), 646-674.

Hao, J., Zhang, S., Zhou, Y., Hu, X., & Shao, C. (2011). MicroRNA 483-3p suppresses the expression of DPC4/Smad4 in pancreatic cancer. *FEBS Letters, 585*(1), 207-213.

Hari, D. M., Leung, A. M., Lee, J. H., Sim, M. S., Vuong, B., Chiu, C. G., & Bilchik, A. J. (2013). AJCC Cancer Staging Manual 7th edition criteria for colon cancer: do the complex modifications improve prognostic assessment? *Journal of the American College of Surgeons, 217*(2), 181-190.

Harrison, S., & Benziger, H. (2011). The molecular biology of colorectal carcinoma and its implications: a review. *The Surgeon, 9*(4), 200-210.

Hauke, J., & Kossowski, T. (2011). Comparison of values of Pearson's and Spearman's correlation coefficients on the same sets of data. *Quaestiones Geographicae, 30*(2), 87-93.

Häusler, S. F., Keller, A., Chandran, P. A., Ziegler, K., Zipp, K., Heuer, S., . . . Wischhusen, J. (2010). Whole blood-derived miRNA profiles as potential new tools for ovarian cancer screening. *British Journal of Cancer, 103*(5), 693-700.

He, L., & Hannon, G. J. (2004). MicroRNAs: small RNAs with a big role in gene regulation. *Nature Reviews Genetics, 5*(7), 522-531.

Hector, S., Conlon, S., Schmid, J., Dicker, P., Cummins, R. J., Concannon, C. G., . . . Prehn, J. H. (2012). Apoptosome-dependent caspase activation proteins as prognostic markers in Stage II and III colorectal cancer. *British Journal of Cancer, 106*(9), 1499-1505.

Heichman, K. A. (2014). Blood-based testing for colorectal cancer screening. *Molecular Diagnosis and Therapy, 18*(2), 127-135.

Heid, C. A., Stevens, J., Livak, K. J., & Williams, P. M. (1996). Real time quantitative PCR. *Genome Research, 6*(10), 986-994.

Heneghan, H. M., Miller, N., Lowery, A. J., Sweeney, K. J., Newell, J., & Kerin, M. J. (2010). Circulating microRNAs as novel minimally invasive biomarkers for breast cancer. *Annals of Surgery, 251*(3), 499-505.

Hengartner, M. O. (2000). The biochemistry of apoptosis. *Nature, 407*(6805), 770-776.

Hewitt, R. E., McMarlin, A., Kleiner, D., Wersto, R., Martin, P., Tsokos, M., . . . Stetler-Stevenson, W. G. (2000). Validation of a model of colon cancer progression. *The Journal of Pathology, 192*(4), 446-454.

Hickman, E. S., & Helin, K. (2002). The regulation of APAF1 expression during development and tumourigenesis. *Apoptosis, 7*(2), 167-171.

Hong, X., Chen, G., Wang, M., Lou, C., Mao, Y., Li, Z., & Zhang, Y. (2012). STAT5a-targeting miRNA enhances chemosensitivity to cisplatin and 5-fluorouracil in human colorectal cancer cells. *Molecular Medicine Reports, 5*(5), 1215-1219.

Hu, M. C., Lee, D. F., Xia, W., Golfman, L. S., Ou-Yang, F., Yang, J. Y., . . . Hung, M. C. (2004). IkappaB kinase promotes tumorigenesis through inhibition of forkhead FOXO3a. *Cell, 117*(2), 225-237.

Huang, H., Regan, K. M., Wang, F., Wang, D., Smith, D. I., van Deursen, J. M., & Tindall, D. J. (2005). Skp2 inhibits FOXO1 in tumor suppression through ubiquitin-mediated degradation. *Proceedings of the National Academy of Sciences of the United States of America, 102*(5), 1649-1654.

Huang, Z., Huang, D., Ni, S., Peng, Z., Sheng, W., & Du, X. (2010). Plasma microRNAs are promising novel biomarkers for early detection of colorectal cancer. *International Journal of Cancer, 127*(1), 118-126.

Huerta, S., Heinzerling, J. H., Anguiano-Hernandez, Y. M., Huerta-Yepez, S., Lin, J., Chen, D., . . . Livingston, E. H. (2007). Modification of gene products involved in resistance to apoptosis in metastatic colon cancer cells: roles of Fas, Apaf-1, NFkappaB, IAPs, Smac/DIABLO, and AIF. *Journal of Surgical Research, 142*(1), 184-194.

Hummel, R., Wang, T., Watson, D. I., Michael, M. Z., Van der Hoek, M., Haier, J., & Hussey, D. J. (2011). Chemotherapy-induced modification of microRNA expression in esophageal cancer. *Oncology Reports, 26*(4), 1011-1017.

Idogawa, M., Sasaki, Y., Suzuki, H., Mita, H., Imai, K., Shinomura, Y., & Tokino, T. (2009). A single recombinant adenovirus expressing p53 and p21-targeting artificial microRNAs efficiently induces apoptosis in human cancer cells. *Clinical Cancer Research, 15*(11), 3725-3732.

Iliopoulos, D., Rotem, A., & Struhl, K. (2011). Inhibition of miR-193a expression by Max and RXRα activates K-Ras and PLAU to mediate distinct aspects of cellular transformation. *Cancer Research, 71*(15), 5144-5153.

Imperiale, T. F., Ransohoff, D. F., Itzkowitz, S. H., Turnbull, B. A., & Ross, M. E. (2004). Fecal DNA versus fecal occult blood for colorectal-cancer screening in an average risk population. *The New England Journal of Medicine, 351*(26), 2704-2714.

Irizarry, R. A., Hobbs, B., Collin, F., Beazer-Barclay, Y. D., Antonellis, K. J., Scherf, U., & Speed, T. P. (2003). Exploration, normalization, and summaries of high density oligonucleotide array probe level data. *Biostatistics, 4*(2), 249-264.

Jahid, S., Sun, J., Edwards, R. A., Dizon, D., Panarelli, N. C., Milsom, J. W., . . . Lipkin, S. M. (2012). miR-23a promotes the transition from indolent to invasive colorectal cancer. *Cancer Discovery, 2*(6), 540-553.

Jansen, A. P., Camalier, C. E., & Colburn, N. H. (2005). Epidermal expression of the translation inhibitor programmed cell death 4 suppresses tumourigenesis. *Cancer Research, 65*(14), 6034-6041.

Janssen, H. L., Reesink, H. W., Lawitz, E. J., Zeuzem, S., Rodriguez-Torres, M., Patel, K., . . . Hodges, M. R. (2013). Treatment of HCV infection by targeting microRNA. *The New England Journal of Medicine, 368*(18), 1685-1694.

Jeffers, J. R., Parganas, E., Lee, Y., Yang, C., Wang, J., Brennan, J., . . . Zambetti, G. P. (2003). Puma is an essential mediator of p53-dependent and -independent apoptotic pathways. *Cancer Cell, 4*(4), 321-328.

John, M., Constien, R., Akinc, A., Goldberg, M., Moon, Y. A., Spranger, M., . . . Bumcrot, D. (2007). Effective RNAi-mediated gene silencing without interruption of the endogenous microRNA pathway. *Nature, 449*(7163), 745-747.

Johnson, C. E., Huang, Y. Y., Parrish, A. B., Smith, M. I., Vaughn, A. E., Zhang, Q., . . . Deshmukh, M. (2007). Differential Apaf-1 levels allow cytochrome c to induce apoptosis in brain tumors but not in normal neural tissues. *Proceedings of the National Academy of Sciences of the United States of America, 104*(52), 20820-20825.

Jordan, J. A., & Durso, M. B. (2005). Real-time polymerase chain reaction for detecting bacterial DNA directly from blood of neonates being evaluated for sepsis. *The Journal of Molecular Diagnostics, 7*(5), 575-581.

Jørgensen, J. T., & Hersom, M. (2012). HER2 as a prognostic marker in gastric cancer - a systematic analysis of data from the literature. *Journal of Cancer, 3*, 137-144.

Josse, C., Bouznad, N., Geurts, P., Irrthum, A., Huynh-Thu, V. A., Servais, L., . . . Oury, C. (2014). Identification of a microRNA landscape targeting the PI3K/Akt signaling pathway in inflammation-induced colorectal carcinogenesis. *American Journal of Physiology - Gastrointestinal and Liver Physiology, 306*(3), G229-G243.

Ju, J. A., Huang, C. T., Lan, S. H., Wang, T. H., Lin, P. C., Lee, J. C., . . . Liu, H. S. (2013). Characterization of a colorectal cancer migration and autophagy-related microRNA miR-338-5p and its target gene PIK3C3. *Biomarkers and Genomic Medicine, 5*(3), 74-78.

Ju, J. A., Huang, Y. C., Lan, S. H., Wang, T. H., Lin, P. C., Lee, J. C., . . . Liu, H. S. (2012). Identification of colorectal cancer recurrence-related microRNAs. *Genomic Medicine, Biomarkers, and Health Sciences, 4*(1-2), 19-20.

Juven-Gershon, T., & Oren, M. (1999). Mdm2: the ups and downs. *Molecular Medicine, 5*(2), 71-83.

Kahi, C. J., Imperiale, T. F., Juliar, B. E., & Rex, D. K. (2009). Effect of screening colonoscopy on colorectal cancer incidence and mortality. *Clinical Gastroenterology and Hepatology, 7*(7), 770-775.

Karolina, D. S., Armugam, A., Tavintharan, S., Wong, M. T., Lim, S. C., Sum, C. F., & Jeyaseelan, K. (2011). MicroRNA 144 impairs insulin signaling by inhibiting the expression of insulin receptor substrate 1 in type 2 diabetes mellitus. *PLoS ONE, 6*(8), e22839.

Kastan, M. B., Zhan, Q., el-Deiry, W. S., Carrier, F., Jacks, T., Walsh, W. V., . . . Fornace Jr, A. J. (1992). A mammalian cell cycle checkpoint pathway utilizing p53 and GADD45 is defective in ataxia-telangiectasia. *Cell, 71*(4), 587-597.

Katayama, M., Nakano, H., Ishiuchi, A., Wu, W., Oshima, R., Sakurai, J., . . . Otsubo, T. (2006). Protein pattern difference in the colon cancer cell lines examined by two-dimensional differential in-gel electrophoresis and mass spectrometry. *Surgery Today, 36*(12), 1085-1093.

Katoh, M., & Katoh, M. (2004). Human FOX gene family (Review). *International Journal of Oncology, 25*(5), 1495-1500.

Kawamori, D., Kaneto, H., Nakatani, Y., Matsuoka, T. A., Matsuhisa, M., Hori, M., & Yamasaki, Y. (2006). The forkhead transcription factor Foxo1 bridges the JNK pathway and the transcription factor PDX-1 through its intracellular translocation. *The Journal of Biological Chemistry, 281*(2), 1091-1098.

Ke, T. W., Hsu, H. L., Wu, Y. H., Chen, W. T. L., Cheng, Y. W., & Cheng, C. W. (2014). MicroRNA-224 suppresses colorectal cancer cell migration by targeting Cdc42. *Disease Markers, 2014*, 617150.

Khvorova, A., Reynolds, A., & Jayasena, S. D. (2003). Functional siRNAs and miRNAs exhibit strand bias. *Cell, 115*(2), 209-216.

Kim, T. K., & Eberwine, J. H. (2010). Mammalian cell transfection: the present and the future. *Analytical and Bioanalytical Chemistry, 397*(8), 3173-3178.

Kim, V. N., Han, J., & Siomi, M. C. (2009). Biogenesis of small RNAs in animals. *Nature Reviews Molecular Cell Biology, 10*(2), 126-139.

Kluiver, J., Gibcus, J. H., Hettinga, C., Adema, A., Richter, M. K. S., Halsema, N., . . . van den Berg, A. (2012). Rapid generation of microRNA sponges for microRNA inhibition. *PLoS ONE, 7*(1), e29275.

Kobayashi, H., Mochizuki, H., Sugihara, K., Morita, T., Kotake, K., Teramoto, T., . . . Muto, T. (2007). Characteristics of recurrence and surveillance tools after curative resection for colorectal cancer: a multicenter study. *Surgery, 141*(1), 67-75.

Kobayashi, Y., Furukawa-Hibi, Y., Chen, C., Horio, Y., Isobe, K., Ikeda, K., & Motoyama, N. (2005). SIRT1 is critical regulator of FOXO-mediated transcription in response to oxidative stress. *International Journal of Molecular Medicine, 16*(2), 237-243.

Konishi, M., Kikuchi-Yanoshita, R., Tanaka, K., Muraoka, M., Onda, A., Okumura, Y., . . . Miyaki, M. (1996). Molecular nature of colon tumors in hereditary nonpolyposis colon cancer, familial polyposis, and sporadic colon cancer. *Gastroenterology, 111*(2), 307-317.

Kosaka, N., Iguchi, H., & Ochiya, T. (2010). Circulating microRNA in body fluid: a new potential biomarker for cancer diagnosis and prognosis. *Cancer Science, 101*(10), 2087-2092.

Koturbash, I., Zemp, F. J., Pogribny, I., & Kovalchuk, O. (2011). Small molecules with big effects: the role of the microRNAome in cancer and carcinogenesis. *Mutation Research/Genetic Toxicology and Environmental Mutagenesis, 722*(2), 94-105.

Kozaki, K., Imoto, I., Mogi, S., Omura, K., & Inazawa, J. (2008). Exploration of tumor-suppressive microRNAs silenced by DNA hypermethylation in oral cancer. *Cancer Research, 68*(7), 2094-2105.

Kozomara, A., & Griffiths-Jones, S. (2014). miRBase: annotating high confidence microRNAs using deep sequencing data. *Nucleic Acids Research, 42*, D68-D73.

Krasinskas, A. M. (2011). EGFR signaling in colorectal carcinoma. *Pathology Research International, 2011*, 932932.

Krek, A., Grün, D., Poy, M. N., Wolf, R., Rosenberg, L., Epstein, E. J., . . . Rajewsky, N. (2005). Combinatorial microRNA target predictions. *Nature Genetics, 37*(5), 495-500.

Krichevsky, A. M., & Gabriely, G. (2009). miR-21: a small multi-faceted RNA. *Journal of Cellular and Molecular Medicine, 13*(1), 39-53.

Krützfeldt, J., Rajewsky, N., Braich, R., Rajeev, K. G., Tuschl, T., Manoharan, M., & Stoffel, M. (2005). Silencing of microRNAs in vivo with 'antagomirs'. *Nature, 438*(7068), 685-689.

Kwon, I. K., Wang, R., Thangaraju, M., Shuang, H., Liu, K., Dashwood, R., . . . Browning, D. D. (2010). PKG inhibits TCF signaling in colon cancer cells by blocking beta-catenin expression and activating FOXO4. *Oncogene, 29*(23), 3423-3434.

Labianca, R., Nordlinger, B., Beretta, G. D., Brouquet, A., & Cervantes, A. (2010). Primary colon cancer: ESMO Clinical Practice Guidelines for diagnosis, adjuvant treatment and follow-up. *Annals of Oncology, 21*(5), v70-v77.

Lacopetta, B. (2003). TP53 mutation in colorectal cancer. *Human Mutation, 21*(3), 271-276.

Lagos-Quintana, M., Rauhut, R., Lendeckel, W., & Tuschl, T. (2001). Identification of novel genes coding for small expressed RNAs. *Science, 294*(5543), 853-858.

Lajer, C. B., Nielsen, F. C., Friis-Hansen, L., Norrild, B., Borup, R., Garnæs, E., . . . von Buchwald, C. (2011). Different miRNA signatures of oral and pharyngeal squamous cell carcinomas: a prospective translational study. *British Journal of Cancer, 104*(5), 830-840.

Lamouille, S., Subramanyam, D., Blelloch, R., & Derynck, R. (2013). Regulation of epithelial–mesenchymal and mesenchymal–epithelial transitions by microRNAs. *Current Opinion in Cell Biology, 25*(2), 200-207.

Lanza, G., Ferracin, M., Gafà, R., Veronese, A., Spizzo, R., Pichiorri, F., . . . Negrini, M. (2007). mRNA/microRNA gene expression profile in microsatellite unstable colorectal cancer. *Molecular Cancer, 6*, 54.

Lawrie, C. H., Gal, S., Dunlop, H. M., Pushkaran, B., Liggins, A. P., Pulford, K., . . . Harris, A. L. (2008). Detection of elevated levels of tumour-associated microRNAs in serum of patients with diffuse large B-cell lymphoma. *British Journal of Haematology, 141*(5), 672-675.

le Sage, C., Nagel, R., Egan, D. A., Schrier, M., Mesman, E., Mangiola, A., . . . Agami, R. (2007). Regulation of the p27(Kip1) tumor suppressor by miR-221 and miR-222 promotes cancer cell proliferation. *The EMBO Journal, 26*(15), 3699-3708.

Lee, M. J., Yu, G. R., Yoo, H. J., Kim, J. H., Yoon, B. I., Choi, Y. K., & Kim, D. G. (2009). ANXA8 down-regulation by EGF-FOXO4 signaling is involved in cell scattering and tumor metastasis of cholangiocarcinoma. *Gastroenterology, 137*(3), 1138-1150.

Lee, R. C., Feinbaum, R. L., & Ambros, V. (1993). The C. elegans heterochronic gene lin-4 encodes small RNAs with antisense complementarity to lin-14. *Cell, 75*(5), 843-854.

Lee, S., Cho, N. Y., Yoo, E. J., Kim, J. H., & Kang, G. H. (2008). CpG island methylator phenotype in colorectal cancers: comparison of the new and classic CpG island methylator phenotype marker panels. *Archives of Pathology and Laboratory Medicine, 132*(10), 1657-1665.

Leibovitz, A., Stinson, J. C., McCombs III, W. B., McCoy, C. E., Mazur, K. C., & Mabry, N. D. (1976). Classification of human colorectal adenocarcinoma cell lines. *Cancer Research, 36*(12), 4562-4569.

Lennox, K. A., & Behlke, M. A. (2010). A direct comparison of anti-microRNA oligonucleotide potency. *Pharmaceutical Research, 27*(9), 1788-1799.

Levin, B., Lieberman, D. A., McFarland, B., Smith, R. A., Brooks, D., Andrews, K. S., . . . Winawer, S. J. (2008). Screening and surveillance for the early detection of colorectal cancer and adenomatous polyps, 2008: a joint guideline from the American Cancer Society, the US Multi-Society Task Force on Colorectal Cancer, and the American College of Radiology. *CA: A Cancer Journal for Clinicians, 58*(3), 130-160.

Levine, A. J. (1997). p53, the cellular gatekeeper for growth and division. *Cell, 88*(3), 323-331.

Lewis, B. P., Burge, C. B., & Bartel, D. P. (2005). Conserved seed pairing, often flanked by adenosines, indicates that thousands of human genes are microRNA targets. *Cell, 120*(1), 15-20.

Lewis, B. P., Shih, I. H., Jones-Rhoades, M. W., Bartel, D. P., & Burge, C. B. (2003). Prediction of mammalian microRNA targets. *Cell, 115*(7), 787-798.

Li, B., Sun, M., Gao, F., Liu, W., Yang, Y., Liu, H., . . . Cai, J. (2013). Up-regulated expression of miR-23a/b targeted the pro-apoptotic Fas in radiation-induced thymic lymphoma. *Cellular Physiology and Biochemistry, 32*(6), 1729-1740.

Li, C., Hashimi, S. M., Good, D. A., Cao, S., Duan, W., Plummer, P. N., . . . Wei, M. Q. (2012). Apoptosis and microRNA aberrations in cancer. *Clinical and Experimental Pharmacology and Physiology, 39*(8), 739-746.

Li, L. C., Okino, S. T., Zhao, H., Pookot, D., Place, R. F., Urakami, S., . . . Dahiya, R. (2006). Small dsRNAs induce transcriptional activation in human cells. *Proceedings of the National Academy of Sciences of the United States of America, 103*(46), 17337-17342.

Li, L. M., Hu, Z. B., Zhou, Z. X., Chen, X., Liu, F. Y., Zhang, J. F., . . . Zen, K. (2010). Serum microRNA profiles serve as novel biomarkers for HBV infection and diagnosis of HBV-positive hepatocarcinoma. *Cancer Research, 70*(23), 9798-9807.

Li, P., Nijhawan, D., Budihardjo, I., Srinivasula, S. M., Ahmad, M., Alnemri, E. S., & Wang, X. (1997). Cytochrome c and dATP-dependent formation of Apaf-1/caspase-9 complex initiates an apoptotic protease cascade. *Cell, 91*(4), 479-489.

Li, S., Li, Y., Wen, Z., Kong, F., Guan, X., & Liu, W. (2014). microRNA-206 overexpression inhibits cellular proliferation and invasion of estrogen receptor α-positive ovarian cancer cells. *Molecular Medicine Reports, 9*(5), 1703-1708.

Li, Y., Liang, C., Wong, K. C., Jin, K., & Zhang, Z. (2014). Inferring probabilistic miRNA–mRNA interaction signatures in cancers: a role-switch approach. *Nucleic Acids Research, 42*(9), e76.

Lian, S., Shi, R., Bai, T., Liu, Y., Miao, W., Wang, H., . . . Fan, Y. (2013). Anti-miRNA-23a oligonucleotide suppresses glioma cells growth by targeting apoptotic protease activating factor-1. *Current Pharmaceutical Design, 19*(35), 6382-6389.

Lin, P. C., Lin, J. K., Lin, C. C., Wang, H. S., Yang, S. H., Jiang, J. K., . . . Chang, S. C. (2012). Carbohydrate antigen 19-9 is a valuable prognostic factor in colorectal cancer patients with normal levels of carcinoembryonic antigen and may help predict lung metastasis. *International Journal of Colorectal Disease, 27*(10), 1333-1338.

Lin, S. L., Chang, S. J., & Ying, S. Y. (2006). Transgene-like animal models using intronic microRNAs. *Methods in Molecular Biology, 342*, 321-334.

Link, A., Balaguer, F., Shen, Y., Nagasaka, T., Lozano, J. J., Boland, C. R., & Goel, A. (2010). Fecal microRNAs as novel biomarkers for colon cancer screening. *Cancer Epidemiology, Biomarkers and Prevention, 19*(7), 1766-1774.

Liotta, L. A., Steeg, P. S., & Stetler-Stevenson, W. G. (1991). Cancer metastasis and angiogenesis: an imbalance of positive and negative regulation. *Cell, 64*(2), 327-336.

Liu, C., Dong, B., Lu, A., Qu, L., Xing, X., Meng, L., . . . Shou, C. (2010). Synuclein gamma predicts poor clinical outcome in colon cancer with normal levels of carcinoembryonic antigen. *BMC Cancer, 10*, 359.

Liu, C., Kelnar, K., Liu, B., Chen, X., Calhoun-Davis, T., Li, H., . . . Tang, D. G. (2011). The microRNA miR-34a inhibits prostate cancer stem cells and metastasis by directly repressing CD44. *Nature Medicine, 17*(2), 211-215.

Liu, C., Li, Y., Semenov, M., Han, C., Baeg, G. H., Tan, Y., . . . He, X. (2002). Control of beta-catenin phosphorylation/degradation by a dual-kinase mechanism. *Cell, 108*(6), 837-847.

Liu, K., Zhao, H., Yao, H., Lei, S., Lei, Z., Li, T., & Qi, H. (2013). MicroRNA-124 regulates the proliferation of colorectal cancer cells by targeting iASPP. *Biomed Research International, 2013*, 867537.

Liu, L., Chen, L., Xu, Y., Li, R., & Du, X. (2010). microRNA-195 promotes apoptosis and suppresses tumorigenicity of human colorectal cancer cells. *Biochemical and Biophysical Research Communications, 400*(2), 236-240.

Liu, L., Nie, J., Chen, L., Dong, G., Du, X., Wu, X., . . . Han, W. (2013). The oncogenic role of microRNA-130a/301a/454 in human colorectal cancer via targeting Smad4 expression. *PLoS ONE, 8*(2), e55532.

Liu, W., Zabirnyk, O., Wang, H., Shiao, Y. H., Nickerson, M. L., Khalil, S., . . . Phang, J. M. (2010). miR-23b targets proline oxidase, a novel tumor suppressor protein in renal cancer. *Oncogene, 29*(35), 4914-4924.

Liu, X., Fortin, K., & Mourelatos, Z. (2008). MicroRNAs: biogenesis and molecular functions. *Brain Pathology, 18*(1), 113-121.

Liu, X., Kim, C. N., Yang, J., Jemmerson, R., & Wang, X. (1996). Induction of apoptotic program in cell-free extracts: requirement for dATP and cytochrome c. *Cell, 86*(1), 147-157.

Liu, X., Ru, J., Zhang, J., Zhu, L. H., Liu, M., Li, X., & Tang, H. (2013). miR-23a targets interferon regulatory factor 1 and modulates cellular proliferation and paclitaxel-induced apoptosis in gastric adenocarcinoma cells. *PLoS ONE, 8*(6), e64707.

Liu, X., Zhang, Z., Sun, L., Chai, N., Tang, S., Jin, J., . . . Fan, D. (2011). microRNA-499-5p promotes cellular invasion and tumor metastasis in colorectal cancer by targeting FOXO4 and PDCD4. *Carcinogenesis, 32*(12), 1798-1805.

Liu, X. Q., Tang, S. H., Zhang, Z. Y., & Jin, H. F. (2011). Expression and clinical significance of FOX04 in colorectal cancer. *Chinese Journal of Cellular and Molecular Immunology, 27*(9), 969-971.

Liu, Y., Borchert, G. L., Surazynski, A., & Phang, J. M. (2008). Proline oxidase, a p53-induced gene, targets COX-2/PGE2 signaling to induce apoptosis and inhibit tumor growth in colorectal cancers. *Oncogene, 27*(53), 6729-6737.

Liu, Z., Sall, A., & Yang, D. (2008). MicroRNA: an emerging therapeutic target and intervention tool. *International Journal of Molecular Sciences, 9*(6), 978-999.

Lofton-Day, C., Model, F., Devos, T., Tetzner, R., Distler, J., Schuster, M., . . . Sledziewski, A. (2008). DNA methylation biomarkers for blood-based colorectal cancer screening. *Clinical Chemistry, 54*(2), 414-423.

Lowe, S. W., & Lin, A. W. (2000). Apoptosis in cancer. *Carcinogenesis, 21*(3), 485-495.

Luo, X., Burwinkel, B., Tao, S., & Brenner, H. (2011). MicroRNA signatures: novel biomarker for colorectal cancer? *Cancer Epidemiology, Biomarkers and Prevention, 20*(7), 1272-1286.

Luo, X., Stock, C., Burwinkel, B., & Brenner, H. (2013). Identification and evaluation of plasma microRNAs for early detection of colorectal cancer. *PLoS ONE, 8*(5), e62880.

Lüpertz, R., Chovolou, Y., Unfried, K., Kampkötter, A., Wätjen, W., & Kahl, R. (2008). The forkhead transcription factor FOXO4 sensitizes cancer cells to doxorubicin-mediated cytotoxicity. *Carcinogenesis, 29*(11), 2045-2052.

Lynch, H. T., & Lynch, J. F. (2005). What the physician needs to know about Lynch syndrome: an update. *Oncology (Williston Park), 19*(4), 455-463.

Ma, K., He, Y., Zhang, H., Fei, Q., Niu, D., Wang, D., . . . Zhu, J. (2012). DNA methylation-regulated miR-193a-3p dictates resistance of hepatocellular carcinoma to 5-fluorouracil via repression of SRSF2 expression. *The Journal of Biological Chemistry, 287*(8), 5639-5649.

Ma, N., Li, F., Li, D., Hui, Y., Wang, X., Qiao, Y., . . . Gao, X. (2012). Igf2-derived intronic miR-483 promotes mouse hepatocellular carcinoma cell proliferation. *Molecular and Cellular Biochemistry, 361*(1-2), 337-343.

Ma, Q., Wang, X., Li, Z., Li, B., Ma, F., Peng, L., . . . Jiang, B. (2013). microRNA-16 represses colorectal cancer cell growth in vitro by regulating the p53/survivin signaling pathway. *Oncology Reports, 29*(4), 1652-1658.

Ma, Y., Zhang, P., Wang, F., Zhang, H., Yang, J., Peng, J., . . . Qin, H. (2012). miR-150 as a potential biomarker associated with prognosis and therapeutic outcome in colorectal cancer. *Gut, 61*(10), 1447-1453.

Maczuga, P., Koornneef, A., Borel, F., Petry, H., van Deventer, S., Ritsema, T., & Konstantinova, P. (2012). Optimization and comparison of knockdown efficacy between polymerase II expressed shRNA and artificial miRNA targeting luciferase and Apolipoprotein B100. *BMC Biotechnology, 12*, 42.

Maragkakis, M., Alexiou, P., Papadopoulos, G. L., Reczko, M., Dalamagas, T., Giannopoulos, G., . . . Hatzigeorgiou, A. G. (2009). Accurate microRNA target prediction correlates with protein repression levels. *BMC Bioinformatics, 10*, 295.

Markowitz, S. D., & Bertagnolli, M. M. (2009). Molecular basis of colorectal cancer. *The New England Journal of Medicine, 361*(25), 2449-2460.

Marshall, K. W., Mohr, S., Khettabi, F. E., Nossova, N., Chao, S., Bao, W., . . . Liew, C. C. (2010). A blood-based biomarker panel for stratifying current risk for colorectal cancer. *International Journal of Cancer, 126*(5), 1177-1186.

Massagué, J., Blain, S. W., & Lo, R. S. (2000). TGFbeta signaling in growth control, cancer, and heritable disorders. *Cell, 103*(2), 295-309.

McFarland, E. G., Levin, B., Lieberman, D. A., Pickhardt, P. J., Johnson, C. D., Glick, S. N., . . . Smith, R. A. (2008). Revised colorectal screening guidelines: joint effort of the American Cancer Society, U.S. Multisociety Task Force on Colorectal Cancer, and American College of Radiology. *Radiology, 248*(3), 717-720.

McKenna, E. S., & Roberts, C. W. M. (2009). Epigenetics and cancer without genomic instability. *Cell Cycle, 8*(1), 23-26.

McManus, M. T., Petersen, C. P., Haines, B. B., Chen, J., & Sharp, P. A. (2002). Gene silencing using micro-RNA designed hairpins. *RNA, 8*(6), 842-850.

Meltzer, P. S. (2005). Cancer genomics: small RNAs with big impacts. *Nature, 435*(7043), 745-746.

Min, H., & Yoon, S. (2010). Got target?: computational methods for microRNA target prediction and their extension. *Experimental and Molecular Medicine, 42*(4), 233-244.

Miranda, K. C., Huynh, T., Tay, Y., Ang, Y. S., Tam, W. L., Thomson, A. M., . . . Rigoutsos, I. (2006). A pattern-based method for the identification of microRNA binding sites and their corresponding heteroduplexes. *Cell, 126*(6), 1203-1217.

Mitchell, P. S., Parkin, R. K., Kroh, E. M., Fritz, B. R., Wyman, S. K., Pogosova-Agadjanyan, E. L., . . . Tewari, M. (2008). Circulating microRNAs as stable blood-based markers for cancer detection. *Proceedings of the National Academy of Sciences of the United States of America, 105*(30), 10513-10518.

Moawad, F. J., Maydonovitch, C. L., Cullen, P. A., Barlow, D. S., Jenson, D. W., & Cash, B. D. (2010). CT colonography may improve colorectal cancer screening compliance. *American Journal of Roentgenology, 195*(5), 1118-1123.

Monteleone, G., Pallone, F., & Stolfi, C. (2012). The dual role of inflammation in colon carcinogenesis. *International Journal of Molecular Sciences, 13*(9), 11071-11084.

Morimoto, L. M., Newcomb, P. A., Ulrich, C. M., Bostick, R. M., Lais, C. J., & Potter, J. D. (2002). Risk factors for hyperplastic and adenomatous polyps: evidence for malignant potential? *Cancer Epidemiology, Biomarkers and Prevention, 11*(10), 1012-1018.

Mouhamad, S., Galluzzi, L., Zermati, Y., Castedo, M., & Kroemer, G. (2007). Apaf-1 deficiency causes chromosomal instability. *Cell Cyle, 6*(24), 3103-3107.

Mustika, R., Budiyanto, A., Nishigori, C., Ichihashi, M., & Ueda, M. (2005). Decreased expression of Apaf-1 with progression of melanoma. *Pigment Cell Research, 18*(1), 59-62.

Mutter, G. L., Zahrieh, D., Liu, C., Neuberg, D., Finkelstein, D., Baker, H. E., & Warrington, J. A. (2004). Comparison of frozen and RNALater solid tissue storage methods for use in RNA expression microarrays. *BMC Genomics, 5*, 88.

Nagel, R., le Sage, C., Diosdado, B., van der Waal, M., Oude Vrielink, J. A. F., Bolijn, A., . . . Agami, R. (2008). Regulation of the adenomatous polyposis coli gene by the miR-135 family in colorectal cancer. *Cancer Research, 68*(14), 5795-5802.

Nakano, H., Yamada, Y., Miyazawa, T., & Yoshida, T. (2013). Gain-of-function microRNA screens identify miR-193a regulating proliferation and apoptosis in epithelial ovarian cancer cells. *International Journal of Oncology, 42*(6), 1875-1882.

Natalwala, A., Spychal, R., & Tselepis, C. (2008). Epithelial-mesenchymal transition mediated tumourigenesis in the gastrointestinal tract. *World Journal of Gastroenterology, 14*(24), 3792-3797.

Neri, E., Faggioni, L., Cerri, F., Turini, F., Angeli, S., Cini, L., . . . Bartolozzi, C. (2010). CT colonography versus double-contrast barium enema for screening of colorectal cancer: comparison of radiation burden. *Abdominal Imaging, 35*(5), 596-601.

Nicolas, F. E. (2011). Experimental validation of microRNA targets using a luciferase reporter system. *Methods in Molecular Biology, 732*, 139-152.

Nielsen, B. S. (2012). MicroRNA in situ hybridization. *Methods in Molecular Biology, 822*, 67-84.

Novak, D. J., Liew, G. J., & Liew, C. C. (2012). GeneNews Limited: bringing the blood transcriptome to personalized medicine. *Pharmacogenomics, 13*(4), 381-385.

Oberg, A. L., French, A. J., Sarver, A. L., Subramanian, S., Morlan, B. W., Riska, S. M., . . . Thibodeau, S. N. (2011). miRNA expression in colon polyps provides evidence for a multihit model of colon cancer. *PLoS ONE, 6*(6), e20465.

Obrocea, F. L., Sajin, M., Marinescu, E. C., & Stoica, D. (2011). Colorectal cancer and the 7th revision of the TNM staging system: review of changes and suggestions for uniform pathologic reporting. *Romanian Journal of Morphology and Embryology, 52*(2), 537-544.

Obuchowski, N. A. (2005). ROC analysis. *American Journal of Roentgenology, 184*(2), 364-372.

Ogata-Kawata, H., Izumiya, M., Kurioka, D., Honma, Y., Yamada, Y., Furuta, K., . . . Tsuchiya, N. (2014). Circulating exosomal microRNAs as biomarkers of colon cancer. *PLoS ONE, 9*(4), e92921.

Overbergh, L., Giulietti, A., Valckx, D., Decallonne, R., Bouillon, R., & Mathieu, C. (2003). The use of real-time reverse transcriptase PCR for the quantification of cytokine gene expression. *Journal of Biomolecular Techniques, 14*(1), 33-43.

Paik, S. S., Jang, K. S., Song, Y. S., Jang, S. H., Min, K. W., Han, H. X., . . . Jang, S. J. (2007). Reduced expression of Apaf-1 in colorectal adenocarcinoma correlates with tumor progression and aggressive phenotype. *Annals of Surgical Oncology, 14*(12), 3453-3459.

Pan, H., & Griep, A. E. (1995). Temporally distinct patterns of p53-dependent and p53-independent apoptosis during mouse lens development. *Genes and Development, 9*(17), 2157-2169.

Paterson, E. L., Kazenwadel, J., Bert, A. G., Khew-Goodall, Y., Ruszkiewicz, A., & Goodall, G. J. (2013). Down-regulation of the miRNA-200 family at the invasive front of colorectal cancers with degraded basement membrane indicates EMT is involved in cancer progression. *Neoplasia, 15*(2), 180-191.

Perilli, L., Pizzini, S., Bisognin, A., Mandruzzato, S., Biasiolo, M., Facciolli, A., . . . Zanovello, P. (2014). Human miRNome profiling in colorectal cancer and liver metastasis development. *Genomics Data, 2*, 184-188.

Piepoli, A., Tavano, F., Copetti, M., Mazza, T., Palumbo, O., Panza, A., . . . Andriulli, A. (2012). Mirna expression profiles identify drivers in colorectal and pancreatic cancers. *PLoS ONE, 7*(3), e33663.

Place, R. F., Li, L. C., Pookot, D., Noonan, E. J., & Dahiya, R. (2008). MicroRNA-373 induces expression of genes with complementary promoter sequences. *Proceedings of the National Academy of Sciences of the United States of America, 105*(5), 1608-1613.

Price, K. J., Tsykin, A., Giles, K. M., Sladic, R. T., Epis, M. R., Ganss, R., . . . Leedman, P. J. (2012). Matrigel basement membrane matrix influences expression of microRNAs in cancer cell lines. *Biochemical and Biophysical Research Communications, 427*(2), 343-348.

Quintero, E., Castells, A., Bujanda, L., Cubiella, J., Salas, D., Lanas, Á., . . . González-Navarro, A. (2012). Colonoscopy versus fecal immunochemical testing in colorectal-cancer screening. *The New England Journal of Medicine, 366*(8), 697-706.

Ragusa, M., Statello, L., Maugeri, M., Barbagallo, C., Passanis, R., Alhamdani, M. S., . . . Purrello, M. (2014). Highly skewed distribution of miRNAs and proteins between colorectal cancer cells and their exosomes following Cetuximab treatment: biomolecular, genetic and translational implications. *Oncoscience, 1*(2), 132-157.

Ragusa, M., Statello, L., Maugeri, M., Majorana, A., Barbagallo, D., Salito, L., . . . Purrello, M. (2012). Specific alterations of the microRNA transcriptome and global network structure in colorectal cancer after treatment with MAPK/ERK inhibitors. *Journal of Molecular Medicine, 90*(12), 1421-1438.

Ratajewski, M., Walczak-Drzewiecka, A., Salkowska, A., & Dastych, J. (2012). Upstream stimulating factors regulate the expression of RORγT in human lymphocytes. *The Journal of Immunology, 189*(6), 3034-3042.

Reagan-Shaw, S., & Ahmad, N. (2007). The role of Forkhead-box Class O (FoxO) transcription factors in cancer: a target for the management of cancer. *Toxicology and Applied Pharmacology, 224*(3), 360-368.

Redfern, A. D., Colley, S. M., Beveridge, D. J., Ikeda, N., Epis, M. R., Li, X., . . . Leedman, P. J. (2013). RNA-induced silencing complex (RISC) proteins PACT, TRBP, and Dicer are SRA binding nuclear receptor coregulators. *Proceedings of the National Academy of Sciences of the United States of America, 110*(16), 6536-6541.

Rehmsmeier, M., Steffen, P., Hochsmann, M., & Giegerich, R. (2004). Fast and effective prediction of microRNA/target duplexes. *RNA, 10*(10), 1507-1517.

Reid, J. F., Sokolova, V., Zoni, E., Lampis, A., Pizzamiglio, S., Bertan, C., . . . Pierotti, M. A. (2012). miRNA profiling in colorectal cancer highlights miR-1 involvement in MET-dependent proliferation. *Molecular Cancer Research, 10*(4), 504-515.

Reinhart, B. J., Slack, F. J., Basson, M., Pasquinelli, A. E., Bettinger, J. C., Rougvie, A. E., . . . Ruvkun, G. (2000). The 21-nucleotide let-7 RNA regulates developmental timing in *Caenorhabditis elegans*. *Nature, 403*(6772), 901-906.

Riedl, S. J., & Shi, Y. (2004). Molecular mechanisms of caspase regulation during apoptosis. *Nature Reviews Molecular Cell Biology, 5*(11), 897-907.

Robinson, K. L., Liu, T., Vandrovcova, J., Halvarsson, B., Clendenning, M., Frebourg, T., . . . Lindblom, A. (2007). Lynch syndrome (hereditary nonpolyposis colorectal cancer) diagnostics. *Journal of the National Cancer Institute, 99*(4), 291-299.

Robles, A. I., Bemmels, N. A., Foraker, A. B., & Harris, C. C. (2001). APAF-1 is a transcriptional target of p53 in DNA damage-induced apoptosis. *Cancer Research, 61*(18), 6660-6664.

Rodrigues, N. R., Rowan, A., Smith, M. E., Kerr, I. B., Bodmer, W. F., Gannon, J. V., & Lane, D. P. (1990). p53 mutations in colorectal cancer. *Proceedings of the National Academy of Sciences of the United States of America, 87*(19), 7555-7559.

Rogler, C. E., Levoci, L., Ader, T., Massimi, A., Tchaikovskaya, T., Norel, R., & Rogler, L. E. (2009). MicroRNA-23b cluster microRNAs regulate transforming growth factor-beta/bone morphogenetic protein signaling and liver stem cell differentiation by targeting Smads. *Hepatology, 50*(2), 575-584.

Roldo, C., Missiaglia, E., Hagan, J. P., Falconi, M., Capelli, P., Bersani, S., . . . Croce, C. M. (2006). MicroRNA expression abnormalities in pancreatic endocrine and acinar tumors are associated with distinctive pathologic features and clinical behavior. *Journal of Clinical Oncology, 24*(29), 4677-4684.

Ronchetti, D., Lionetti, M., Mosca, L., Agnelli, L., Andronache, A., Fabris, S., . . . Neri, A. (2008). An integrative genomic approach reveals coordinated expression of intronic miR-335, miR-342, and miR-561 with deregulated host genes in multiple myeloma. *BMC Medical Genomics, 1*, 37.

Rossi, S., Kopetz, S., Davuluri, R., Hamilton, S. R., & Calin, G. A. (2010). MicroRNAs, ultraconserved genes and colorectal cancers. *The International Journal of Biochemistry and Cell Biology, 42*(8), 1291-1297.

Sachdeva, M., & Mo, Y. Y. (2010). miR-145-mediated suppression of cell growth, invasion and metastasis. *American Journal of Translational Research, 2*(2), 170-180.

Salama, I., Malone, P. S., Mihaimeed, F., & Jones, J. L. (2008). A review of the S100 proteins in cancer. *European Journal of Surgical Oncology, 34*(4), 357-364.

Salim, H., Akbar, N. S., Zong, D., Vaculova, A. H., Lewensohn, R., Moshfegh, A., . . . Zhivotovsky, B. (2012). miRNA-214 modulates radiotherapy response of non-small cell lung cancer cells through regulation of p38MAPK, apoptosis and senescence. *British Journal of Cancer, 107*(8), 1361-1373.

Salimzadeh, L., Jaberipour, M., Hosseini, A., & Ghaderi, A. (2013). Non-viral transfection methods optimized for gene delivery to a lung cancer cell line. *Avicenna Journal of Medical Biotechnology, 5*(2), 68-77.

Salvi, A., Conde, I., Abeni, E., Arici, B., Grossi, I., Specchia, C., . . . De Petro, G. (2013). Effects of miR-193a and sorafenib on hepatocellular carcinoma cells. *Molecular Cancer, 12*, 162.

Santarpia, L., Calin, G. A., Adam, L., Ye, L., Fusco, A., Giunti, S., . . . Gagel, R. F. (2013). A miRNA signature associated with human metastatic medullary thyroid carcinoma. *Endocrine-Related Cancer, 20*(6), 809-823.

Schepeler, T., Reinert, J. T., Ostenfeld, M. S., Christensen, L. L., Silahtaroglu, A. N., Dyrskjøt, L., . . . Andersen, C. L. (2008). Diagnostic and prognostic microRNAs in stage II colon cancer. *Cancer Research, 68*(15), 6416-6424.

Schetter, A. J., Leung, S. Y., Sohn, J. J., Zanetti, K. A., Bowman, E. D., Yanaihara, N., . . . Harris, C. C. (2008). MicroRNA expression profiles associated with prognosis and therapeutic outcome in colon adenocarcinoma. *The Journal of the American Medical Association, 299*(4), 425-436.

Schetter, A. J., Okayama, H., & Harris, C. C. (2012). The role of microRNAs in colorectal cancer. *Cancer Journal, 18*(3), 244-252.

Schmittgen, T. D., & Livak, K. J. (2008). Analyzing real-time PCR data by the comparative C(T) method. *Nature Protocols, 3*(6), 1101-1108.

Schoen, R. E., Pinsky, P. F., Weissfeld, J. L., Yokochi, L. A., Church, T., Laiyemo, A. O., . . . Berg, C. D. (2012). Colorectal-cancer incidence and mortality with screening flexible sigmoidoscopy. *The New England Journal of Medicine, 366*(25), 2345-2357.

Schrauder, M. G., Strick, R., Schulz-Wendtland, R., Strissel, P. L., Kahmann, L., Loehberg, C. R., . . . Fasching, P. A. (2012). Circulating micro-RNAs as potential blood-based markers for early stage breast cancer detection. *PLoS ONE, 7*(1), e29770.

Schroeder, A., Mueller, O., Stocker, S., Salowsky, R., Leiber, M., Gassmann, M., . . . Ragg, T. (2006). The RIN: an RNA integrity number for assigning integrity values to RNA measurements. *BMC Molecular Biology, 7*, 3.

Sepramaniam, S., Tan, J. R., Tan, K. S., DeSilva, D. A., Tavintharan, S., Woon, F. P., . . . Jeyaseelan, K. (2014). Circulating microRNAs as biomarkers of acute stroke. *International Journal of Molecular Sciences, 15*(1), 1418-1432.

Seto, A. G. (2010). The road toward microRNA therapeutics. *The International Journal of Biochemistry and Cell Biology, 42*(8), 1298-1305.

Shang, J., Yang, F., Wang, Y., Wang, Y., Xue, G., Mei, Q., . . . Sun, S. (2014). MicroRNA-23a antisense enhances 5-fluorouracil chemosensitivity through APAF-1/caspase-9 apoptotic pathway in colorectal cancer cells. *Journal of Cellular Biochemistry, 115*(4), 772-784.

Shen, L., Toyota, M., Kondo, Y., Lin, E., Zhang, L., Guo, Y., . . . Issa, J. P. (2007). Integrated genetic and epigenetic analysis identifies three different subclasses of colon cancer. *Proceedings of the National Academy of Sciences of the United States of America, 104*(47), 18654-18659.

Shi, Y. (2002). Mechanisms of caspase activation and inhibition during apoptosis. *Molecular Cell, 9*(3), 459-470.

Sikand, K., Slane, S. D., & Shukla, G. C. (2009). Intrinsic expression of host genes and intronic miRNAs in prostate carcinoma cells. *Cancer Cell International, 9*, 21.

Simons, P. C., Van Steenbergen, L. N., De Witte, M. T., & Janssen-Heijnen, M. L. (2013). Miss rate of colorectal cancer at CT colonography in average-risk symptomatic patients. *European Radiology, 23*(4), 908-913.

Sisik, A., Kaya, M., Bas, G., Basak, F., & Alimoglu, O. (2013). CEA and CA 19-9 are still valuable markers for the prognosis of colorectal and gastric cancer patients. *Asian Pacific Journal of Cancer Prevention, 14*(7), 4289-4294.

Skrypina, N. A., Timofeeva, A. V., Khaspekov, G. L., Savochkina, L. P., & Beabealashvilli, R. S. (2003). Total RNA suitable for molecular biology analysis. *Journal of Biotechnology, 105*(1-2), 1-9.

Slaby, O., Svoboda, M., Michalek, J., & Vyzula, R. (2009). MicroRNAs in colorectal cancer: translation of molecular biology in clinical application. *Molecular Cancer, 8*, 102.

Song, M. S., & Rossi, J. J. (2014). The anti-miR21 antagomir, a therapeutic tool for colorectal cancer, has a potential synergistic effect by perturbing an angiogenesis-associated miR30. *Frontiers in Genetics, 4*, 301.

Søreide, K., Nedrebø, B. S., Knapp, J. C., Glomsaker, T. B., Søreide, J. A., & Kørner, H. (2009). Evolving molecular classification by genomic and proteomic biomarkers in colorectal cancer: potential implications for the surgical oncologist. *Surgical Oncology, 18*(1), 31-50.

Sotillo, E., & Thomas-Tikhonenko, A. (2011). Shielding the messenger (RNA): microRNA-based anti cancer therapies. *Pharmacology and Therapeutics, 131*(1), 18-32.

Srivastava, S. K., Bhardwaj, A., Singh, S., Arora, S., Wang, B., Grizzle, W. E., & Singh, A. P. (2011). MicroRNA-150 directly targets MUC4 and suppresses growth and malignant behavior of pancreatic cancer cells. *Carcinogenesis, 32*(12), 1832-1839.

Strillacci, A., Griffoni, C., Sansone, P., Paterini, P., Piazzi, G., Lazzarini, G., . . . Tomasi, V. (2009). MiR-101 downregulation is involved in cyclooxygenase-2 overexpression in human colon cancer cells. *Experimental Cell Research, 315*(8), 1439-1447.

Su, B. B., Shi, H., & Wan, J. (2012). Role of serum carcinoembryonic antigen in the detection of colorectal cancer before and after surgical resection. *World Journal of Gastroenterology, 18*(17), 2121-2126.

Suehiro, Y., Wong, C. W., Chirieac, L. R., Kondo, Y., Shen, L., Webb, C. R., . . . Hamilton, S. R. (2008). Epigenetic-genetic interactions in the APC/WNT, RAS/RAF, and P53 pathways in colorectal carcinoma. *Clinical Cancer Research, 14*(9), 2560-2569.

Sun, X., Dong, B., Yin, L., Zhang, R., Du, W., Liu, D., . . . Mao, L. (2013). PMTED: a plant microRNA target expression database. *BMC Bioinformatics, 14*, 174.

Sung, J. J. Y., Lau, J. Y. W., Goh, K. L., & Leung, W. K. (2005). Increasing incidence of colorectal cancer in Asia: implications for screening. *The Lancet Oncology, 6*(11), 871-876.

Tai, J., Wang, G., Liu, T., Wang, L., Lin, C., & Li, F. (2012). Effects of siRNA targeting c-Myc and VEGF on human colorectal cancer Volo cells. *Journal of Biochemical and Molecular Toxicology, 26*(12), 499-505.

Takane, K., Fujishima, K., Watanabe, Y., Sato, A., Saito, N., Tomita, M., & Kanai, A. (2010). Computational prediction and experimental validation of evolutionarily conserved microRNA target genes in bilaterian animals. *BMC Genomics, 11*, 101.

Takayama, T., Miyanishi, K., Hayashi, T., Sato, Y., & Niitsu, Y. (2006). Colorectal cancer: genetics of development and metastasis. *Journal of Gastroenterology, 41*(3), 185-192.

Tan, E., Gouvas, N., Nicholls, R. J., Ziprin, P., Xynos, E., & Tekkis, P. P. (2009). Diagnostic precision of carcinoembryonic antigen in the detection of recurrence of colorectal cancer. *Surgical Oncology, 18*(1), 15-24.

Tang, T. T., Dowbenko, D., Jackson, A., Toney, L., Lewin, D. A., Dent, A. L., & Lasky, L. A. (2002). The forkhead transcription factor AFX activates apoptosis by induction of the BCL-6 transcriptional repressor. *The Journal of Biological Chemistry, 277*(16), 14255-14265.

Tao, W., & Levine, A. J. (1999). P19(ARF) stabilizes p53 by blocking nucleo-cytoplasmic shuttling of Mdm2. *Proceedings of the National Academy of Sciences of the United States of America, 96*(12), 6937-6941.

Tejpar, S., & Van Cutsem, E. (2002). Molecular and genetic defects in colorectal tumorigenesis. *Best Practice and Research Clinical Gastroenterology, 16*(2), 171-185.

ten Dijke, P., & Hill, C. S. (2004). New insights into TGF-beta-Smad signalling. *Trends in Biochemical Sciences, 29*(5), 265-273.

Teodoridis, J. M., Hardie, C., & Brown, R. (2008). CpG island methylator phenotype (CIMP) in cancer: causes and implications. *Cancer Letters, 268*(2), 177-186.

Thorn, C. F., Marsh, S., Carrillo, M. W., McLeod, H. L., Klein, T. E., & Altman, R. B. (2011). PharmGKB summary: fluoropyrimidine pathways. *Pharmacogenetics and Genomics, 21*(4), 237-242.

Tortora, G. J., & Derrickson, B. H. (2007). *Principles of anatomy and physiology*. Hoboken, NJ: John Wiley & Sons, Inc.

Toyota, M., Ahuja, N., Ohe-Toyota, M., Herman, J. G., Baylin, S. B., & Issa, J. P. (1999). CpG island methylator phenotype in colorectal cancer. *Proceedings of the National Academy of Sciences of the United States of America, 96*(15), 8681-8686.

Tsai, W. C., Hsu, P. W., Lai, T. C., Chau, G. Y., Lin, C. W., Chen, C. M., . . . Tsou, A. P. (2009). MicroRNA-122, a tumor suppressor microRNA that regulates intrahepatic metastasis of hepatocellular carcinoma. *Hepatology, 49*(5), 1571-1582.

Tsang, W. P., & Kwok, T. T. (2009). The miR-18a* microRNA functions as a potential tumor suppressor by targeting on K-Ras. *Carcinogenesis, 30*(6), 953-959.

Tsuchida, A., Ohno, S., Wu, W., Borjigin, N., Fujita, K., Aoki, T., . . . Kuroda, M. (2011). miR-92 is a key oncogenic component of the miR-17-92 cluster in colon cancer. *Cancer Science, 102*(12), 2264-2271.

Turchinovich, A., Weiz, L., Langheinz, A., & Burwinkel, B. (2011). Characterization of extracellular circulating miRNA. *Nucleic Acids Research, 39*(16), 7223-7233.

U.S. Preventive Services Task Force. (2008). Screening for colorectal cancer: U.S. Preventive Services Task Force recommendation statement. *Annals of Internal Medicine, 149*(9), 627-637.

Umetani, N., Fujimoto, A., Takeuchi, H., Shinozaki, M., Bilchik, A. J., & Hoon, D. S. (2004). Allelic imbalance of APAF-1 locus at 12q23 is related to progression of colorectal carcinoma. *Oncogene, 23*(50), 8292-8300.

United Nations Population Division. (2013). World population prospects: the 2012 revision, highlights and advance tables. New York, NY: United Nations.

Valastyan, S., Reinhardt, F., Benaich, N., Calogrias, D., Szász, A. M., Wang, Z. C., . . . Weinberg, R. A. (2009). A pleiotropically acting microRNA, miR-31, inhibits breast cancer metastasis. *Cell, 137*(6), 1032-1046.

Valastyan, S., & Weinberg, R. A. (2011). Tumor metastasis: molecular insights and evolving paradigms. *Cell, 147*(2), 275-292.

van der Heide, L. P., & Smidt, M. P. (2005). Regulation of FoxO activity by CBP/p300-mediated acetylation. *Trends in Biochemical Sciences, 30*(2), 81-86.

van der Horst, A., Tertoolen, L. G., de Vries-Smits, L. M., Frye, R. A., Medema, R. H., & Burgering, B. M. (2004). FOXO4 is acetylated upon peroxide stress and deacetylated by the longevity protein hSir2(SIRT1). *The Journal of Biological Chemistry, 279*(28), 28873-28879.

van Zijl, F., Krupitza, G., & Mikulits, W. (2011). Initial steps of metastasis: cell invasion and endothelial transmigration. *Mutation Research, 728*(1-2), 23-34.

Vara, J. A. F., Casado, E., de Castro, J., Cejas, P., Belda-Iniesta, C., & González-Barón, M. (2004). PI3K/Akt signalling pathway and cancer. *Cancer Treatment Reviews, 30*(2), 193-204.

Vermaat, J. S., Nijman, I. J., Koudijs, M. J., Gerritse, F. L., Scherer, S. J., Mokry, M., . . . Voest, E. E. (2012). Primary colorectal cancers and their subsequent hepatic metastases are genetically different: implications for selection of patients for targeted treatment. *Clinical Cancer Research, 18*(3), 688-699.

Veronese, A. (2012). Regulation of miR-483 locus in hepatocarcinoma cancer cells. *Journal of Cancer Science and Therapy, 4*(10), 51.

Veronese, A., Lupini, L., Consiglio, J., Visone, R., Ferracin, M., Fornari, F., . . . Negrini, M. (2010). Oncogenic role of miR-483-3p at the IGF2/483 locus. *Cancer Research, 70*(8), 3140-3149.

Veronese, A., Visone, R., Consiglio, J., Acunzo, M., Lupini, L., Kim, T., . . . Croce, C. M. (2011). Mutated beta-catenin evades a microRNA-dependent regulatory loop. *Proceedings of the National Academy of Sciences of the United States of America, 108*(12), 4840-4845.

Violette, S., Poulain, L., Dussaulx, E., Pepin, D., Faussat, A. M., Chambaz, J., . . . Lesuffleur, T. (2002). Resistance of colon cancer cells to long-term 5-fluorouracil exposure is correlated to the relative level of bcl-2 and bcl-xl in addition to bax and p53 status. *International Journal of Cancer, 98*(4), 498-504.

Volinia, S., Calin, G. A., Liu, C. G., Ambs, S., Cimmino, A., Petrocca, F., . . . Croce, C. M. (2006). A microRNA expression signature of human solid tumors defines cancer gene targets. *Proceedings of the National Academy of Sciences of the United States of America, 103*(7), 2257-2261.

Wan, L., Pantel, K., & Kang, Y. (2013). Tumor metastasis: moving new biological insights into the clinic. *Nature Medicine, 19*(11), 1450-1464.

Wan Puteh, S. E., Saad, N. M., Aljunid, S. M., Abdul Manaf, M. R., Sulong, S., Sagap, I., . . . Muhammad Annuar, M. A. (2013). Quality of life in Malaysian colorectal cancer patients. *Asia-Pacific Psychiatry, 5*(1), 110-117.

Wang, F., Zheng, Z., Guo, J., & Ding, X. (2010). Correlation and quantitation of microRNA aberrant expression in tissues and sera from patients with breast tumor. *Gynecologic Oncology, 119*(3), 586-593.

Wang, H. L., Bai, H., Li, Y., Sun, J., & Wang, X. Q. (2007). Rationales for expression and altered expression of apoptotic protease activating factor-1 gene in gastric cancer. *World Journal of Gastroenterology, 13*(38), 5060-5064.

Wang, J., Zhang, K. Y., Liu, S. M., & Sen, S. (2014). Tumor-associated circulating microRNAs as biomarkers of cancer. *Molecules, 19*(2), 1912-1938.

Wang, N., Zhu, M., Tsao, S. W., Man, K., Zhang, Z., & Feng, Y. (2013). MiR-23a-mediated inhibition of topoisomerase 1 expression potentiates cell response to etoposide in human hepatocellular carcinoma. *Molecular Cancer, 12*, 119.

Wang, Q., Huang, Z., Ni, S., Xiao, X., Xu, Q., Wang, L., . . . Du, X. (2012). Plasma miR-601 and miR-760 are novel biomarkers for the early detection of colorectal cancer. *PLoS ONE, 7*(9), e44398.

Wang, X. (2008). miRDB: a microRNA target prediction and functional annotation database with a wiki interface. *RNA, 14*(6), 1012-1017.

Wang, X., Lam, E. K., Zhang, J., Jin, H., & Sung, J. J. (2009). MicroRNA-122a functions as a novel tumor suppressor downstream of adenomatous polyposis coli in gastrointestinal cancers. *Biochemical and Biophysical Research Communications, 387*(2), 376-380.

Wang, Y., Tang, Q., Li, M., Jiang, S., & Wang, X. (2014). MicroRNA-375 inhibits colorectal cancer growth by targeting PIK3CA. *Biochemical and Biophysical Research Communications, 444*(2), 199-204.

Warren, J. D., Xiong, W., Bunker, A. M., Vaughn, C. P., Furtado, L. V., Roberts, W. L., . . . Heichman, K. A. (2011). Septin 9 methylated DNA is a sensitive and specific blood test for colorectal cancer. *BMC Medicine, 9*, 133.

Weber, J. A., Baxter, D. H., Zhang, S., Huang, D. Y., Huang, K. H., Lee, M. J., . . . Wang, K. (2010). The microRNA spectrum in 12 body fluids. *Clinical Chemistry, 56*(11), 1733-1741.

Wei, X., Lv, T., Chen, D., & Guan, J. (2014). Lentiviral vector mediated delivery of RHBDD1 shRNA down regulated the proliferation of human glioblastoma cells. *Technology in Cancer Research and Treatment, 13*(1), 87-93.

Weimer, E. A. C. (2007). The role of microRNAs in cancer: no small matter. *European Journal of Cancer, 43*(10), 1529-1544.

Weisenberger, D. J., Siegmund, K. D., Campan, M., Young, J., Long, T. I., Faasse, M. A., . . . Laird, P. W. (2006). CpG island methylator phenotype underlies sporadic microsatellite instability and is tightly associated with BRAF mutation in colorectal cancer. *Nature Genetics, 38*(7), 787–793.

Willert, K., & Jones, K. A. (2006). Wnt signaling: is the party in the nucleus? *Genes and Development, 20*(11), 1394-1404.

Winter, J., Jung, S., Keller, S., Gregory, R. I., & Diederichs, S. (2009). Many roads to maturity: microRNA biogenesis pathways and their regulation. *Nature Cell Biology, 11*(3), 228-234.

Wolpin, B. M., Meyerhardt, J. A., Mamon, H. J., & Mayer, R. J. (2007). Adjuvant treatment of colorectal cancer. *CA: A Cancer Journal for Clinicians, 57*(3), 168-185.

Wong, R. S. Y. (2011). Apoptosis in cancer: from pathogenesis to treatment. *Journal of Experimental and Clinical Cancer Research, 30*, 87.

Wong, T. S., Liu, X. B., Wong, B. Y. H., Ng, R. W. M., Yuen, A. P. W., & Wei, W. I. (2008). Mature miR-184 as potential oncogenic microRNA of squamous cell carcinoma of tongue. *Clinical Cancer Research, 14*(9), 2588-2592.

Wu, L., Fan, J., & Belasco, J. G. (2006). MicroRNAs direct rapid deadenylation of mRNA. *Proceedings of the National Academy of Sciences of the United States of America, 103*(11), 4034-4039.

Wu, Q., Jin, H., Yang, Z., Luo, G., Lu, Y., Li, K., . . . Fan, D. (2010). MiR-150 promotes gastric cancer proliferation by negatively regulating the pro-apoptotic gene EGR2. *Biochemical and Biophysical Research Communications, 392*(3), 340-345.

Xu, H., He, J. H., Xiao, Z. D., Zhang, Q. Q., Chen, Y. Q., Zhou, H., & Qu, L. H. (2010). Liver-enriched transcription factors regulate microRNA-122 that targets CUTL1 during liver development. *Hepatology, 52*(4), 1431-1442.

Xu, X., Fan, Z., Kang, L., Han, J., Jiang, C., Zheng, X., . . . Ye, Q. (2013). Hepatitis B virus X protein represses miRNA-148a to enhance tumorigenesis. *The Journal of Clinical Investigation, 123*(2), 630-645.

Xu, Y., & Pasche, B. (2007). TGF-beta signaling alterations and susceptibility to colorectal cancer. *Human Molecular Genetics, 16*(R1), R14-R20.

Yamakuchi, M., Ferlito, M., & Lowenstein, C. J. (2008). miR-34a repression of SIRT1 regulates apoptosis. *Proceedings of the National Academy of Sciences of the United States of America, 105*(36), 13421-13426.

Yamakuchi, M., Lotterman, C. D., Bao, C., Hruban, R. H., Karim, B., Mendell, J. T., . . . Lowenstein, C. J. (2010). P53-induced microRNA-107 inhibits HIF-1 and tumor angiogenesis. *Proceedings of the National Academy of Sciences of the United States of America, 107*(14), 6334-6339.

Yamamichi, N., Shimomura, R., Inada, K., Sakurai, K., Haraguchi, T., Ozaki, Y., . . . Iba, H. (2009). Locked nucleic acid in situ hybridization analysis of miR-21 expression during colorectal cancer development. *Clinical Cancer Research, 15*(12), 4009-4016.

Yan, X., Liang, H., Deng, T., Zhu, K., Zhang, S., Wang, N., . . . Chen, X. (2013). The identification of novel targets of miR-16 and characterization of their biological functions in cancer cells. *Molecular Cancer, 12*, 92.

Yang, H., Zhao, R., Yang, H. Y., & Lee, M. H. (2005). Constitutively active FOXO4 inhibits Akt activity, regulates p27 Kip1 stability, and suppresses HER2-mediated tumorigenicity. *Oncogene, 24*(11), 1924-1935.

Yeh, L. C., & Lee, J. C. (1988). Probing the RNA structure within the yeast 5 S RNA.L1a protein complex by fluorescence and enzymatic digestion. *The Journal of Biological Chemistry, 263*(34), 18213-18219.

Yehezkel, G., Cohen, L., Kliger, A., Manor, E., & Khalaila, I. (2012). O-linked β-N-acetylglucosaminylation (O-GlcNAcylation) in primary and metastatic colorectal cancer clones and effect of N-acetyl-β-D-glucosaminidase silencing on cell phenotype and transcriptome. *The Journal of Biological Chemistry, 287*(34), 28755-28769.

Yip, K. T., Das, P. K., Suria, D., Lim, C. R., Ng, G. H., & Liew, C. C. (2010). A case-controlled validation study of a blood-based seven-gene biomarker panel for colorectal cancer in Malaysia. *Journal of Experimental and Clinical Cancer Research, 29*, 128.

Yong, F. L., Law, C. W., & Wang, C. W. (2013). Potentiality of a triple microRNA classifier: miR-193a-3p, miR-23a and miR-338-5p for early detection of colorectal cancer. *BMC Cancer, 13*, 280.

Yoshida, H., Kong, Y. Y., Yoshida, R., Elia, A. J., Hakem, A., Hakem, R., . . . Mak, T. W. (1998). Apaf1 is required for mitochondrial pathways of apoptosis and brain development. *Cell, 94*(6), 739-750.

Young, P. E., & Womeldorph, C. M. (2013). Colonoscopy for colorectal cancer screening. *Journal of Cancer, 4*(3), 217-226.

Yu, D. C., Li, Q. C., Ding, X. W., & Ding, Y. T. (2011). Circulating microRNAs: potential biomarkers for cancer. *International Journal of Molecular Sciences, 12*(3), 2055-2063.

Yu, J., Li, A., Hong, S. M., Hruban, R. H., & Goggins, M. (2012). MicroRNA alterations of pancreatic intraepithelial neoplasias. *Clinical Cancer Research, 18*(4), 981-992.

Yu, T., Li, J., Yan, M., Liu, L., Lin, H., Zhao, F., . . . Yao, M. (2014). MicroRNA-193a-3p and -5p suppress the metastasis of human non-small-cell lung cancer by downregulating the ERBB4/PIK3R3/mTOR/S6K2 signaling pathway. *Oncogene*. doi: 10.1038/onc.2013.574.

Yuan, J. S., Reed, A., Chen, F., & Stewart Jr, C. N. (2006). Statistical analysis of real-time PCR data. *BMC Bioinformatics, 7*, 85.

Zainal Ariffin, O., & Nor Saleha, I. T. (2011). National Cancer Registry Report 2007: Ministry of Health, Malaysia.

Zhang, G., Zhou, H., Xiao, H., Liu, Z., Tian, H., & Zhou, T. (2014). MicroRNA-92a functions as an oncogene in colorectal cancer by targeting PTEN. *Digestive Diseases and Sciences, 59*(1), 98-107.

Zhang, H., Hao, Y., Yang, J., Zhou, Y., Li, J., Yin, S., . . . Xi, J. J. (2011). Genome-wide functional screening of miR-23b as a pleiotropic modulator suppressing cancer metastasis. *Nature Communications, 2*, 554.

Zhang, J., Guo, H., Qian, G., Ge, S., Ji, H., Hu, X., & Chen, W. (2010). MiR-145, a new regulator of the DNA Fragmentation Factor-45 (DFF45)-mediated apoptotic network. *Molecular Cancer, 9*, 211.

Zhang, J., Lu, Y., Yue, X., Li, H., Luo, X., Wang, Y., . . . Wan, J. (2013). MiR-124 suppresses growth of human colorectal cancer by inhibiting STAT3. *PLoS ONE, 8*(8), e70300.

Zhang, J., & Ma, L. (2012). MicroRNA control of epithelial-mesenchymal transition and metastasis. *Cancer and Metastasis Reviews, 31*(3-4), 653-662.

Zhang, X., Tang, N., Hadden, T. J., & Rishi, A. K. (2011). Akt, FoxO and regulation of apoptosis. *Biochimica et Biophyisica Acta, 1813*(11), 1978-1986.

Zhu, L. H., Liu, T., Tang, H., Tian, R. Q., Su, C., Liu, M., & Li, X. (2010). MicroRNA-23a promotes the growth of gastric adenocarcinoma cell line MGC803 and downregulates interleukin-6 receptor. *FEBS Journal, 277*(18), 3726-3734.

Zirvi, K. A., Keogh, J. P., Slomiany, A., & Slomiany, B. L. (1991). Transglutaminase activity in human colorectal carcinomas of differing metastatic potential. *Cancer Letters, 60*(1), 85-92.

Zlobec, I., Minoo, P., Baker, K., Haegert, D., Khetani, K., Tornillo, L., . . . Lugli, A. (2007). Loss of APAF-1 expression is associated with tumour progression and adverse prognosis in colorectal cancer. *European Journal of Cancer, 43*(6), 1101-1107.

Zlobec, I., Vuong, T., & Compton, C. C. (2006). The predictive value of apoptosis protease-activating factor 1 in rectal tumors treated with preoperative, high-dose-rate brachytherapy. *Cancer, 106*(2), 284-286.

Zou, H., Taylor, W. R., Harrington, J. J., Hussain, F. T. N., Cao, X., Loprinzi, C. L., . . . Ahlquist, D. A. (2009). High detection rates of colorectal neoplasia by stool DNA testing with a novel digital melt curve assay. *Gastroenterology, 136*(2), 459-470.

APPENDICES

Appendix 1: Approval letter for ethical clearance (reference number: 805.9).

UNIVERSITY OF MALAYA
KUALA LUMPUR
UM MEDICAL CENTRE

MEDICAL ETHICS COMMITTEE
UNIVERSITY MALAYA MEDICAL CENTRE
ADDRESS: LEMBAH PANTAI, 59100 KUALA LUMPUR, MALAYSIA
TELEPHONE: 03-79493209 FAXIMILE: 03-79494638

NAME OF ETHICS COMMITTEE/IRB: Medical Ethics Committee, University Malaya Medical Centre ADDRESS: LEMBAH PANTAI 59100 KUALA LUMPUR	ETHICS COMMITTEE/IRB REFERENCE NUMBER: 805.9
PROTOCOL NO: TITLE: MicroRNAs (miRNAs) as biomarkers in the prognosis of colorectal cancer (CRC)	
PRINCIPAL INVESTIGATOR: Dr. Law Chee Wei TELEPHONE: KOMTEL:	SPONSOR: UM Research Grant & MAKNA

The following item [✓] have been received and reviewed in connection with the above study to be conducted by the above investigator.

[✓] Borang Permohonan Penyelidikan	Ver date: 08 Aug 10
[✓] Study Protocol	Ver date:
[ ] Investigator's Brochure	Ver date:
[✓] Patient Information Sheet	Ver date:
[✓] Consent Form	Ver date:
[ ] Questionnaire	Ver date:
[✓] Investigator(s) CV's (Dr. Law Chee Wei)	

and have been [✓]

[✓] Approved
[ ] Conditionally approved (identify item and specify modification below or in accompanying letter)
[ ] Rejected (identify item and specify reasons below or in accompanying letter)

Comments:

Investigator are required to:

1) *follow instructions, guidelines and requirements of the Medical Ethics Committee.*
2) *report any protocol deviations/violations to Medical Ethics Committee.*
3) *provide annual and closure report to the Medical Ethics Committee.*
4) *comply with International Conference on Harmonization – Guidelines for Good Clinical Practice (ICH-GCP) and Declaration of Helsinki.*
5) *note that Medical Ethics Committee may audit the approved study.*

Date of approval: 18th AUGUST 2010

c.c Head
Department of Surgery

Deputy Dean (Research)
Faculty of Medicine

Secretary
Medical Ethics Committee
University Malaya Medical Centre

PROF. LOOI LAI MENG
Chairman
Medical Ethics Committee

Appendix 2: Demographic data of 50 healthy controls (CTL) and 112 CRC patients (C).

No.	Sample	Age	Race	Gender	TNM	Location	Grading	Blood sample	Paired tissue sample
1	CTL_UA	70	Indian	Female				√	-
2	CTL_UD	65	Chinese	Female				√	-
3	CTL_UE	70	Chinese	Male				√	-
4	CTL_UF	75	Indian	Female				√	-
5	CTL_UH	71	Indian	Female				√	-
6	CTL_UI	68	Indian	Male				√	-
7	CTL_UJ	70	Chinese	Female				√	-
8	CTL_UM	65	Malay	Male				√	-
9	CTL_UP	70	Indian	Female				√	-
10	CTL_UW	66	Chinese	Female				√	-
11	CTL_VA	73	Chinese	Female				√	-
12	CTL_VD	62	Indian	Male				√	-
13	CTL_VH	63	Indian	Male				√	-
14	CTL_VN	66	Indian	Female				√	-
15	CTL_VO	60	Malay	Female				√	-
16	CTL_VV	73	Indian	Female				√	-
17	CTL_VZ	66	Malay	Female				√	-
18	CTL_WA	69	Malay	Female				√	-
19	CTL_WB	59	Indian	Female				√	-
20	CTL_WC	52	Indian	Female				√	-
21	CTL_WD	72	Indian	Female				√	-
22	CTL_WF	54	Indian	Female				√	-
23	CTL_XF	44	Malay	Male				√	-
24	CTL_XL	73	Malay	Male				√	-
25	CTL_XM	51	Indian	Female				√	-
26	CTL_XU	44	Malay	Male				√	-
27	CTL_XZ	52	Malay	Male				√	-
28	CTL_YA	44	Chinese	Male				√	-
29	CTL_YC	48	Chinese	Male				√	-
30	CTL_YD	47	Chinese	Male				√	-
31	CTL_YF	51	Chinese	Female				√	-
32	CTL_YH	40	Chinese	Female				√	-
33	CTL_YJ	72	Chinese	Female				√	-
34	CTL_YL	54	Chinese	Female				√	-
35	CTL_YN	73	Chinese	Female				√	-
36	CTL_YO	57	Chinese	Female				√	-
37	CTL_YQ	68	Chinese	Female				√	-
38	CTL_YW	60	Chinese	Female				√	-
39	CTL_ZB	68	Malay	Male				√	-
40	CTL_ZF	54	Malay	Male				√	-
41	CTL_ZJ	42	Malay	Male				√	-
42	CTL_ZM	80	Malay	Male				√	-

Appendix 2: continued.

No.	Sample	Age	Race	Gender	TNM	Location	Grading	Blood sample	Paired tissue sample
43	CTL_ZN	44	Chinese	Male				√	-
44	CTL_ZP	69	Chinese	Male				√	-
45	CTL_ZQ	56	Malay	Male				√	-
46	CTL_ZR	59	Malay	Male				√	-
47	CTL_ZT	69	Malay	Male				√	-
48	CTL_ZW	68	Chinese	Male				√	-
49	CTL_ZY	65	Chinese	Male				√	-
50	CTL_ZZ	66	Chinese	Male				√	-
51	C_AA	65	Chinese	Female	I	Colon	G2	√	-
52	C_AB	55	Indian	Female	I	Colon	G2	√	-
53	C_AC	64	Indian	Female	II	Colon	G2	√	√
54	C_AE	68	Indian	Female	I	Rectum	G2	√	-
55	C_AF	56	Chinese	Female	III	Colon	G2	√	√
56	C_AH	70	Indian	Male	III	Colon	G2	√	√
57	C_AI	72	Malay	Female	III	Colon	G2	√	√
58	C_AJ	63	Malay	Male	II	Colon	G2	√	√
59	C_AK	74	Indian	Male	II	Colon	G2	√	√
60	C_AN	70	Chinese	Male	II	Colon	G2	√	√
61	C_AP	55	Malay	Male	II	Colon	G2	√	√
62	C_AQ	65	Chinese	Male	II	Colon	G2	√	√
63	C_AR	61	Indian	Male	III	Colon	G2	√	√
64	C_AS	63	Indian	Female	IV	Colon	G2	√	√
65	C_AT	52	Malay	Female	IV	Colon	G2	√	√
66	C_AU	59	Indian	Male	IV	Colon	G2	√	√
67	C_AV	52	Indian	Female	II	Rectum	G2	√	-
68	C_AX	76	Chinese	Female	III	Rectum	G2	√	-
69	C_AZ	78	Indian	Female	IV	Rectum	G2	√	-
70	C_BA	71	Indian	Female	IV	Rectum	G2	√	-
71	C_BB	60	Malay	Male	IV	Colon	G2	√	√
72	C_BC	64	Indian	Female	II	Rectum	G2	√	-
73	C_BF	65	Malay	Male	II	Colon	G2	√	√
74	C_BH	80	Indian	Female	I	Rectum	G2	√	-
75	C_BI	50	Indian	Female	I	Colon	G2	√	-
76	C_BK	64	Malay	Female	II	Colon	G2	√	√
77	C_BM	66	Indian	Female	III	Colon	G2	√	√
78	C_BN	52	Indian	Female	II	Colon	G2	√	√
79	C_BO	68	Indian	Female	III	Colon	G2	√	√
80	C_BP	56	Malay	Male	III	Colon	G2	√	√
81	C_BQ	71	Indian	Female	III	Colon	G2	√	√
82	C_BS	61	Malay	Male	IV	Colon	G2	√	√
83	C_BU	76	Malay	Female	I	Rectum	G2	√	-
84	C_BV	63	Indian	Female	II	Rectum	G2	√	-

Appendix 2: continued.

No.	Sample	Age	Race	Gender	TNM	Location	Grading	Blood sample	Paired tissue sample
85	C_BW	73	Malay	Female	III	Rectum	G2	√	-
86	C_BX	66	Chinese	Female	IV	Rectum	G2	√	-
87	C_BZ	54	Chinese	Male	IV	Colon	G2	√	√
88	C_C	71	Chinese	Female	IV	Colon	G2	√	√
89	C_CB	46	Malay	Female	IV	Colon	G2	√	√
90	C_D	60	Chinese	Female	III	Colon	G2	√	√
91	C_E	63	Indian	Female	IV	Colon	G2	√	√
92	C_F	61	Malay	Male	I	Colon	G2	√	-
93	C_G	44	Chinese	Male	II	Rectum	G1	√	-
94	C_H	66	Chinese	Female	IV	Rectum	G2	√	-
95	C_I	60	Indian	Female	IV	Colon	G2	√	√
96	C_J	54	Indian	Female	III	Rectum	G2	√	-
97	C_KA	68	Chinese	Male	II	Rectum	G3	√	-
98	C_KB	76	Chinese	Male	II	Colon	G1	√	√
99	C_KD	68	Malay	Male	I	Colon	G2	√	-
100	C_KF	55	Chinese	Male	II	Colon	G2	√	√
101	C_KG	56	Chinese	Female	IV	Colon	G1	√	√
102	C_KH	58	Chinese	Male	II	Rectum	G1	√	-
103	C_KI	72	Chinese	Male	II	Colon	G1	√	√
104	C_KJ	46	Malay	Male	I	Colon	G1	√	-
105	C_KK	76	Chinese	Male	I	Colon	G1	√	-
106	C_KM	73	Chinese	Male	II	Colon	G2	√	√
107	C_KN	71	Chinese	Male	II	Colon	G2	√	√
108	C_KR	75	Malay	Male	I	Colon	G2	√	-
109	C_KS	58	Chinese	Female	IV	Colon	G2	√	√
110	C_KT	56	Malay	Male	I	Rectum	G3	√	-
111	C_KU	64	Chinese	Female	IV	Colon	G3	√	√
112	C_KX	60	Chinese	Male	III	Colon	G1	√	√
113	C_KY	66	Chinese	Male	II	Colon	G3	√	√
114	C_KZ	63	Malay	Male	I	Colon	G2	√	-
115	C_LA	63	Malay	Male	I	Rectum	G1	√	-
116	C_LC	55	Chinese	Male	II	Colon	G1	√	√
117	C_LD	52	Malay	Male	I	Rectum	G3	√	-
118	C_LE	61	Chinese	Male	II	Colon	G2	√	√
119	C_LF	43	Chinese	Male	III	Colon	G1	√	√
120	C_LG	56	Malay	Male	I	Colon	G2	√	-
121	C_LI	70	Malay	Male	I	Rectum	G2	√	-
122	C_LJ	52	Chinese	Female	IV	Colon	G1	√	√
123	C_LK	57	Chinese	Female	IV	Colon	G2	√	√
124	C_LM	74	Chinese	Female	IV	Colon	G2	√	√
125	C_LN	72	Malay	Male	I	Rectum	G2	√	-
126	C_LO	63	Chinese	Male	I	Rectum	G2	√	-

Appendix 2: continued.

No.	Sample	Age	Race	Gender	TNM	Location	Grading	Blood sample	Paired tissue sample
127	C_LP	69	Chinese	Male	II	Colon	G2	√	√
128	C_LQ	70	Malay	Male	I	Colon	G2	√	-
129	C_LR	82	Chinese	Male	III	Colon	G1	√	√
130	C_LS	59	Malay	Male	I	Rectum	G1	√	-
131	C_LU	81	Chinese	Male	II	Rectum	G1	√	-
132	C_LX	49	Chinese	Male	III	Colon	G3	√	√
133	C_LY	85	Chinese	Male	III	Colon	G2	√	√
134	C_LZ	54	Chinese	Male	I	Rectum	G2	√	-
135	C_MA	67	Chinese	Male	II	Rectum	G3	√	-
136	C_MB	69	Chinese	Male	II	Rectum	G1	√	-
137	C_MC	63	Chinese	Male	III	Rectum	G2	√	-
138	C_MD	65	Chinese	Male	III	Rectum	G1	√	-
139	C_MG	56	Chinese	Male	III	Rectum	G3	√	-
140	C_MI	58	Chinese	Male	III	Rectum	G3	√	-
141	C_MK	74	Chinese	Female	III	Rectum	G1	√	-
142	C_ML	70	Chinese	Female	IV	Colon	G2	√	√
143	C_MN	62	Chinese	Female	IV	Colon	G2	√	√
144	C_MO	57	Chinese	Female	III	Colon	G2	√	√
145	C_MP	61	Chinese	Male	I	Colon	G2	√	-
146	C_MS	64	Chinese	Male	II	Colon	G1	√	√
147	C_MV	75	Chinese	Female	IV	Colon	G1	√	√
148	C_MW	68	Chinese	Male	III	Rectum	G2	√	-
149	C_MX	69	Chinese	Male	III	Rectum	G2	√	-
150	C_MY	58	Chinese	Female	IV	Colon	G2	√	√
151	C_MZ	77	Chinese	Female	III	Rectum	G2	√	-
152	C_NA	70	Chinese	Male	III	Colon	G1	√	√
153	C_ND	89	Chinese	Male	II	Rectum	G1	√	-
154	C_NG	60	Malay	Male	I	Rectum	G1	√	-
155	C_NH	64	Chinese	Male	II	Colon	G1	√	√
156	C_NI	76	Chinese	Male	III	Colon	G1	√	√
157	C_NL	52	Chinese	Male	I	Rectum	G2	√	-
158	C_NN	78	Chinese	Male	II	Rectum	G2	√	-
159	C_NQ	69	Chinese	Male	III	Colon	G3	√	√
160	C_NR	70	Chinese	Female	III	Colon	G2	√	√
161	C_NS	71	Chinese	Male	II	Rectum	G3	√	-
162	C_NV	73	Chinese	Male	III	Colon	G2	√	√

Appendix 3: Agarose gel electrophoresis images of extracted total RNA.

Images of 162 blood samples

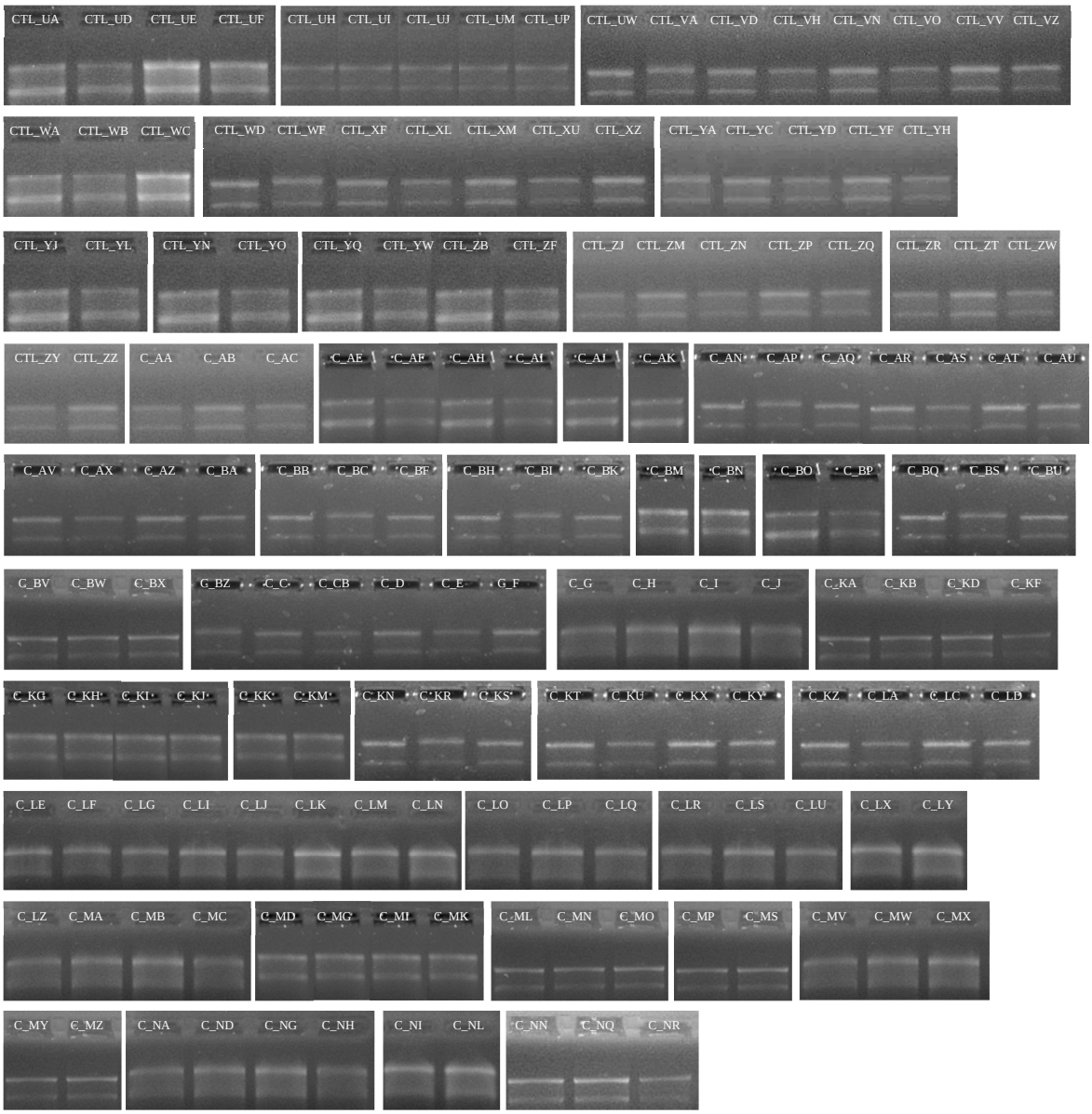

Appendix 3: continued.

Images of 60 paired tissue samples (cancer tissue)

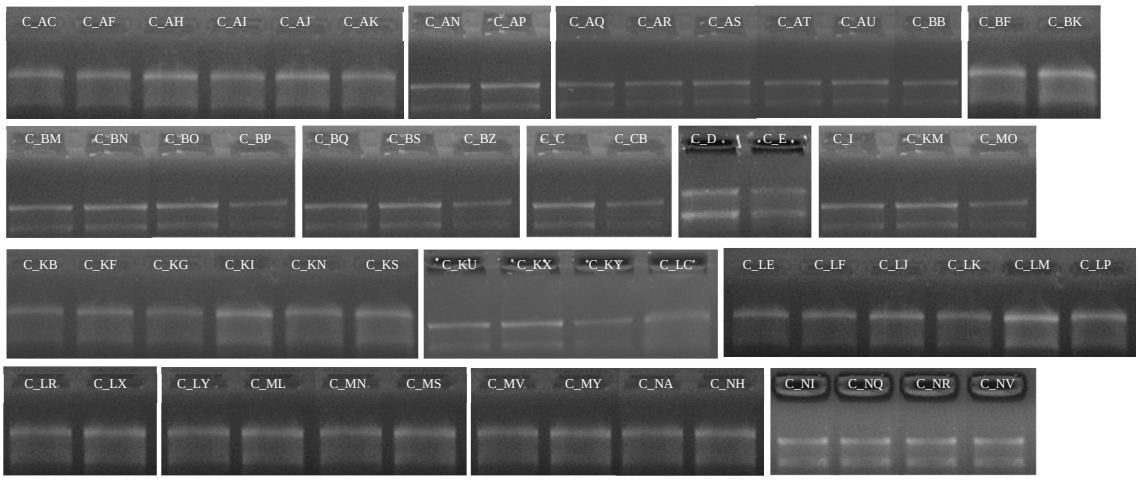

Images of 60 paired tissue samples (normal colonic tissue)

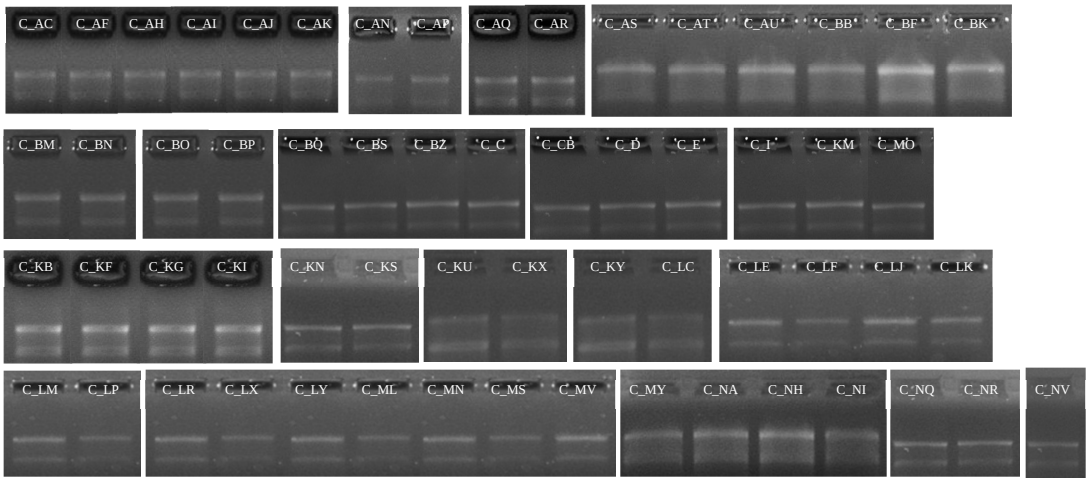

Appendix 4: Polyacrylamide gel electrophoresis images of extracted total RNA.

Images of 162 blood samples

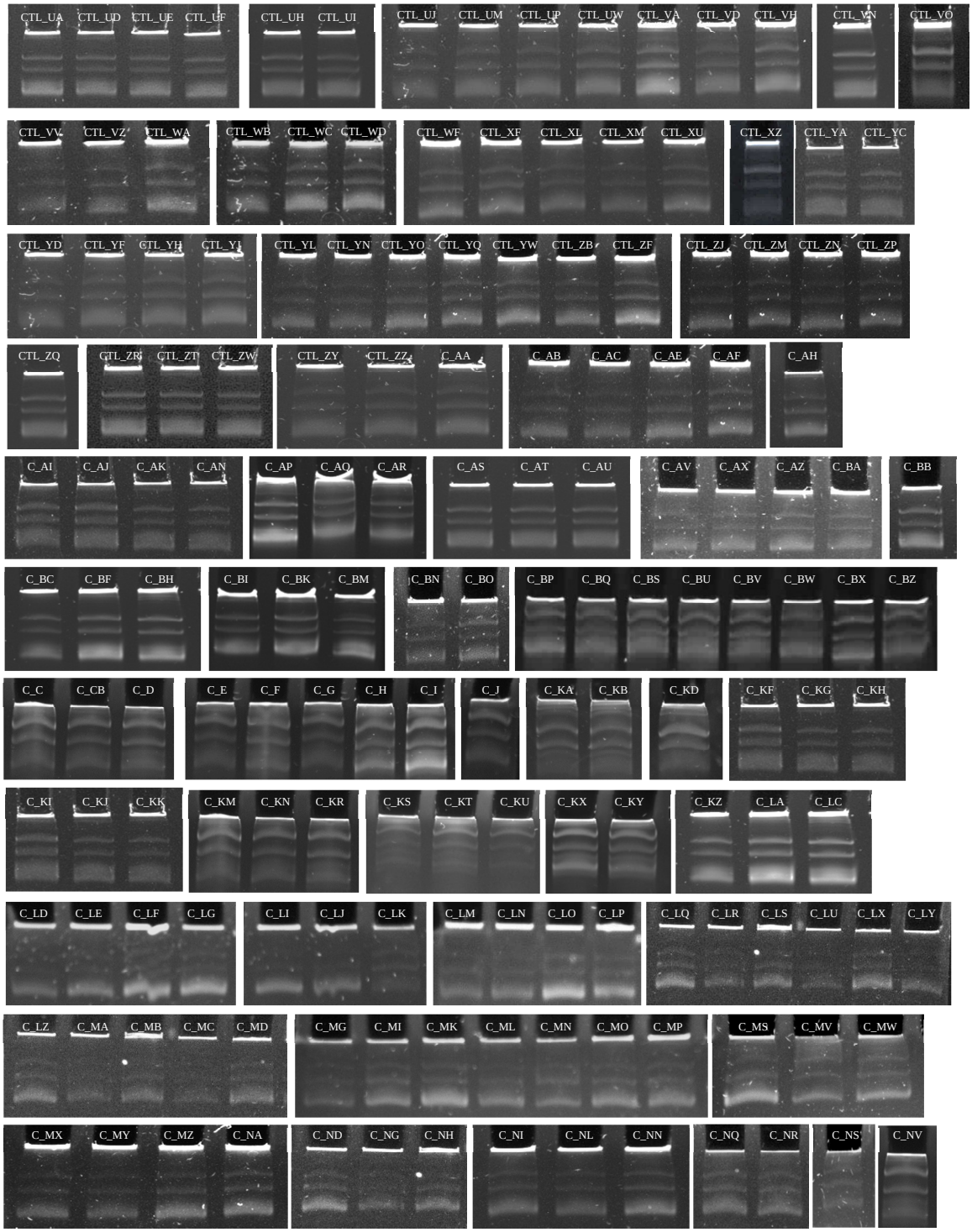

Appendix 4: continued.

Images of 60 paired tissue samples (cancer tissue)

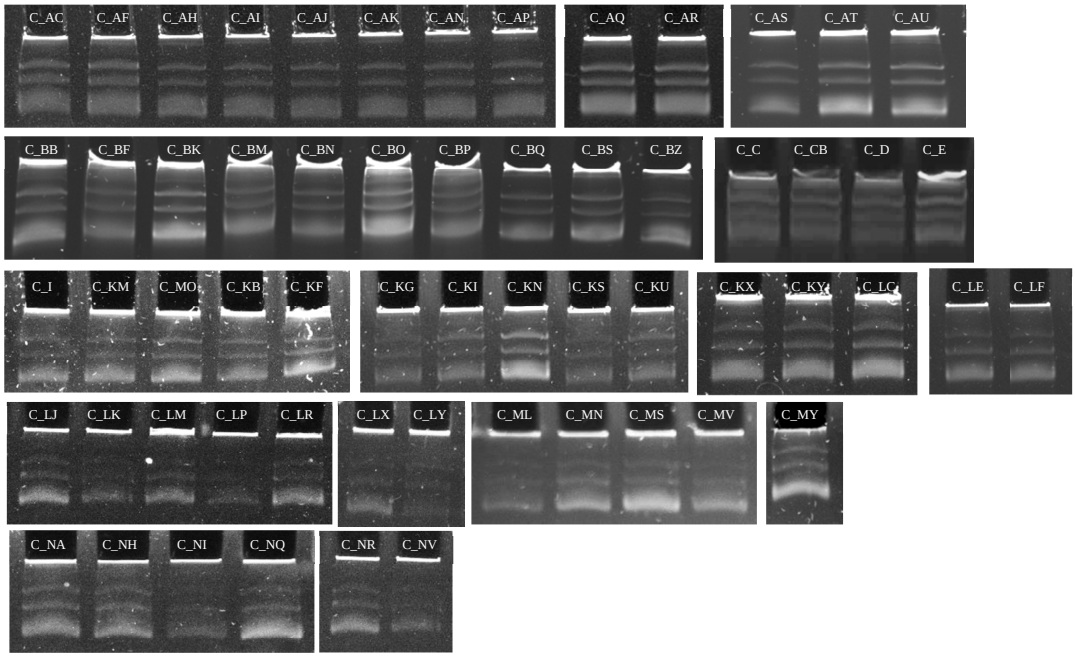

Images of 60 paired tissue samples (normal colonic tissue)

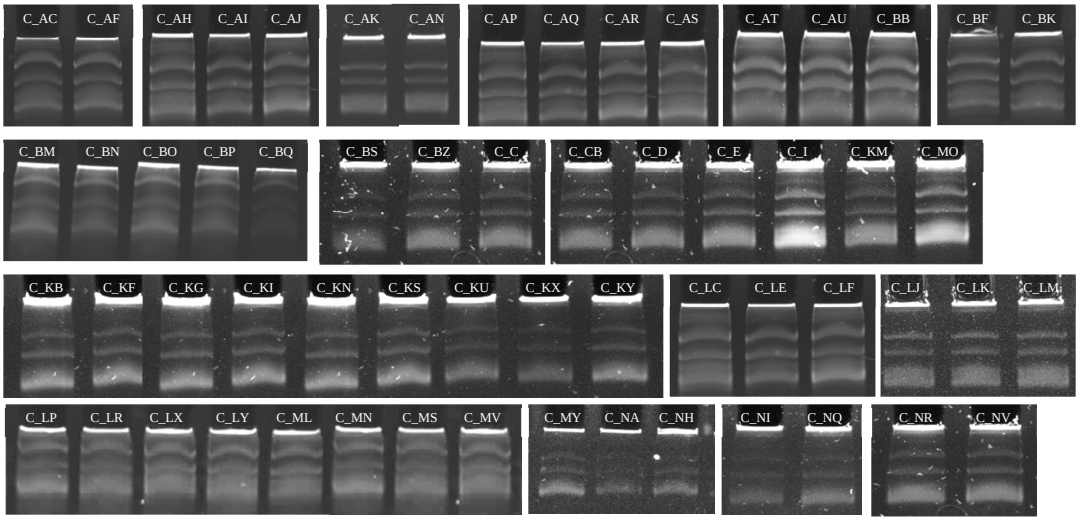

Appendix 5: RIN of total RNA samples used in miRNA microarray.

Blood array	RIN	Blood array	RIN
CTL_UA	7.0	C_BF	7.3
CTL_UD	8.5	C_BH	7.0
CTL_UE	7.5	C_BI	7.0
CTL_UF	8.4	C_BK	8.3
CTL_UH	8.8	C_BM	8.3
CTL_UI	9.5	C_BN	7.8
CTL_UJ	8.1	C_BO	7.8
CTL_UM	8.2	C_BP	7.2
CTL_UP	7.8	C_BQ	7.3
CTL_UW	8.6	C_BS	7.8
CTL_VA	7.1	C_BU	7.7
CTL_VD	7.7	C_BV	8.3
CTL_VH	8.1	C_BW	7.6
CTL_VN	8.3	C_BX	7.1
CTL_VO	8.2	C_BZ	7.0
CTL_VV	8.0	C_CB	7.1
CTL_VZ	7.9	C_D	7.1
CTL_WA	7.5	C_E	7.2
C_AA	8.5	C_I	7.1
C_AB	7.2	C_J	7.1
C_AC	9.2		
C_AE	7.3		
C_AF	8.2		
C_AH	8.5		
C_AI	8.5		
C_AJ	8.3		
C_AK	8.5		
C_AN	7.3		
C_AP	9.1		
C_AQ	9.0		
C_AR	9.8		
C_AS	8.2		
C_AT	8.4		
C_AU	9.0		
C_AV	9.5		
C_AX	8.8		
C_AZ	8.5		
C_BA	8.1		
C_BB	7.3		
C_BC	7.5		

Tissue array (Cancer)	RIN	Tissue array (Normal)	RIN
C_AC	7.1	C_AC	9.8
C_AF	7.4	C_AF	9.5
C_AH	7.0	C_AH	9.3
C_AI	9.2	C_AI	8.8
C_AJ	8.1	C_AJ	9.8
C_AK	7.6	C_AK	9.4
C_AN	9.1	C_AN	9.0
C_AP	7.3	C_AP	8.6
C_AQ	7.6	C_AQ	10.0
C_AR	8.1	C_AR	8.3
C_AS	7.2	C_AS	9.4
C_AT	7.2	C_AT	8.4
C_AU	9.2	C_AU	8.5
C_BB	7.6	C_BB	9.4
C_BF	8.0	C_BF	8.6
C_BK	7.3	C_BK	8.8
C_BM	7.4	C_BM	9.8
C_BN	8.5	C_BN	9.0
C_BO	7.7	C_BO	8.2
C_BP	7.2	C_BP	7.9
C_BQ	7.6	C_BQ	8.7
C_BS	7.7	C_BS	9.7
C_BZ	7.6	C_BZ	8.4
C_C	9.1	C_C	10.0
C_CB	8.6	C_CB	8.2
C_D	9.6	C_D	8.1
C_E	9.6	C_E	8.4
C_I	9.5	C_I	9.1
C_KM	8.9	C_KM	8.5
C_MO	9.4	C_MO	7.2

Appendix 6: Samples used in miRNA microarray, RT-qPCR and Western blot.

Blood microarray		Tissue microarray	Blood RT-qPCR			Tissue RT-qPCR & Western blot
CTL_UA	C_BC	C_AC	CTL_WB	C_KF	C_MG	C_KB
CTL_UD	C_BF	C_AF	CTL_WC	C_KG	C_MI	C_KF
CTL_UE	C_BH	C_AH	CTL_WD	C_KH	C_MK	C_KG
CTL_UF	C_BI	C_AI	CTL_WF	C_KI	C_ML	C_KI
CTL_UH	C_BK	C_AJ	CTL_XF	C_KJ	C_MN	C_KN
CTL_UI	C_BM	C_AK	CTL_XL	C_KK	C_MO	C_KS
CTL_UJ	C_BN	C_AN	CTL_XM	C_KM	C_MP	C_KU
CTL_UM	C_BO	C_AP	CTL_XU	C_KN	C_MS	C_KX
CTL_UP	C_BP	C_AQ	CTL_XZ	C_KR	C_MV	C_KY
CTL_UW	C_BQ	C_AR	CTL_YA	C_KS	C_MW	C_LC
CTL_VA	C_BS	C_AS	CTL_YC	C_KT	C_MX	C_LE
CTL_VD	C_BU	C_AT	CTL_YD	C_KU	C_MY	C_LF
CTL_VH	C_BV	C_AU	CTL_YF	C_KX	C_MZ	C_LJ
CTL_VN	C_BW	C_BB	CTL_YH	C_KY	C_NA	C_LK
CTL_VO	C_BX	C_BF	CTL_YJ	C_KZ	C_ND	C_LM
CTL_VV	C_BZ	C_BK	CTL_YL	C_LA	C_NG	C_LP
CTL_VZ	C_CB	C_BM	CTL_YN	C_LC	C_NH	C_LR
CTL_WA	C_D	C_BN	CTL_YO	C_LD	C_NI	C_LX
C_AA	C_E	C_BO	CTL_YQ	C_LE	C_NL	C_LY
C_AB	C_I	C_BP	CTL_YW	C_LF	C_NN	C_ML
C_AC	C_J	C_BQ	CTL_ZB	C_LG	C_NQ	C_MN
C_AE		C_BS	CTL_ZF	C_LI	C_NR	C_MS
C_AF		C_BZ	CTL_ZJ	C_LJ	C_NS	C_MV
C_AH		C_C	CTL_ZM	C_LK	C_NV	C_MY
C_AI		C_CB	CTL_ZN	C_LM		C_NA
C_AJ		C_D	CTL_ZP	C_LN		C_NH
C_AK		C_E	CTL_ZQ	C_LO		C_NI
C_AN		C_I	CTL_ZR	C_LP		C_NQ
C_AP		C_KM	CTL_ZT	C_LQ		C_NR
C_AQ		C_MO	CTL_ZW	C_LR		C_NV
C_AR			CTL_ZY	C_LS		
C_AS			CTL_ZZ	C_LU		
C_AT			C_C	C_LX		
C_AU			C_F	C_LY		
C_AV			C_G	C_LZ		
C_AX			C_H	C_MA		
C_AZ			C_KA	C_MB		
C_BA			C_KB	C_MC		
C_BB			C_KD	C_MD		

Appendix 7: Fold change ($2^{-\Delta\Delta CT}$) of miRNAs and mRNAs in paired tissue samples. Values are expressed as fold change of cancer tissue versus normal colonic mucosa.

Sample	miR-150	miR-193a-3p	miR-23a	miR-23b	miR-338-5p	miR-342-3p	miR-483-3p	*FOXO4*	*APAF1*
C_KB	0.9330	3.1977	5.6637	1.4008	5.6663	0.7894	12.9880	0.7674	0.1506
C_KF	1.5611	0.4717	0.5263	0.2091	0.6041	1.6245	0.3773	0.7553	0.3939
C_KG	1.6043	1.4425	1.0981	1.1764	4.1615	0.9462	0.4616	0.4247	0.3946
C_KI	1.4866	0.8849	0.6040	2.1829	0.5628	0.8564	0.4127	1.1259	0.7304
C_KN	0.8706	0.9152	0.3240	0.4397	0.7581	0.6416	2.9063	1.2983	0.2913
C_KS	0.8706	1.2221	1.7579	2.5377	2.6954	1.9928	2.1554	0.1634	0.1089
C_KU	0.2102	2.8400	0.7696	0.7019	0.5128	0.5716	1.7106	0.0661	0.0221
C_KX	1.1070	4.2319	6.6793	0.7623	3.2817	1.1790	0.3108	0.1907	0.0800
C_KY	0.4196	0.9931	2.0456	0.3283	0.7577	0.4292	0.4341	0.2827	0.1775
C_LC	0.6186	0.5450	0.5172	0.3608	0.7733	1.1005	0.9558	0.1978	0.4202
C_LE	0.6035	0.8632	0.8183	0.3724	0.3807	0.6356	0.6474	0.7101	0.3013
C_LF	1.0169	1.3300	5.0208	0.4662	4.3215	0.5482	1.6594	0.2626	0.1050
C_LJ	0.9330	2.8564	2.2800	0.6622	3.6548	1.5553	4.1400	0.3818	0.1404
C_LK	1.3214	5.9716	2.5638	0.9330	3.5777	1.2655	2.5640	0.1787	0.4111
C_LM	0.4866	0.9385	2.4835	0.1078	2.3345	0.2568	42.0531	0.0852	0.0774
C_LP	0.2087	0.2480	0.1329	2.2383	0.2660	0.7708	0.3521	1.2079	0.5655
C_LR	1.0833	0.3339	0.7905	1.6425	0.1319	1.0029	1.7147	0.3537	0.1955
C_LX	1.4105	2.3295	1.7387	2.0910	2.4196	0.2029	5.5233	0.8050	0.1741
C_LY	0.8972	1.1683	4.7860	0.4710	1.7289	1.5246	3.9408	0.4525	0.1548
C_ML	0.3324	0.8417	3.9549	0.3500	1.0937	0.1727	1.7789	0.4722	0.0482
C_MN	0.1232	2.6371	3.0303	1.1693	3.8745	0.2975	1.4810	0.1369	0.0437
C_MS	0.5398	1.4681	3.4987	1.0718	4.3790	0.8039	1.5105	0.4158	0.1597
C_MV	1.3439	1.6046	1.1640	0.9089	1.4105	0.9085	1.9583	0.9373	0.1930
C_MY	1.3680	3.4960	4.0591	1.1510	3.8906	0.9861	4.1386	0.2048	0.0959
C_NA	1.2858	1.0129	3.8037	0.3746	2.3329	0.9593	2.2978	1.7366	0.7431
C_NH	1.2887	0.6120	1.8119	0.3254	3.6569	1.0402	2.2873	1.3262	0.2538
C_NI	0.0656	1.9421	2.1900	0.4585	1.8374	0.1901	0.9519	1.2643	0.1603
C_NQ	0.4520	4.5815	1.4088	1.5053	1.4086	1.0057	2.6685	0.2753	0.1835
C_NR	1.5210	1.7395	0.9086	1.5207	0.9500	0.7970	71.8009	0.2529	0.2163
C_NV	1.3125	1.0008	0.1988	0.2225	1.1235	1.7980	1.4591	0.6384	0.2330

Appendix 8: Fold change ($2^{-\Delta\Delta CT}$) of miRNAs and mRNAs in blood samples.

Sample	miR-150	miR-193a-3p	miR-23a	miR-23b	miR-338-5p	miR-342-3p	miR-483-3p	*FOXO4*	*APAF1*
CTL_WB	0.5148	0.8405	1.2980	0.6112	0.3373	0.8825	1.5790	1.7702	1.0336
CTL_WC	0.5817	1.1649	2.1623	0.6657	1.5622	0.8902	1.3521	0.8046	0.6431
CTL_WD	1.2450	2.6990	2.7579	1.1662	2.3416	1.8772	1.8677	2.2420	0.6115
CTL_WF	1.1337	0.8774	2.3725	0.9019	1.8282	1.3293	2.3996	0.8526	0.8409
CTL_XF	2.1334	0.9135	0.5650	3.1998	1.3470	0.8839	0.2895	0.8215	1.8544
CTL_XL	3.6659	1.1660	0.7041	2.3277	0.9236	1.2778	0.3358	2.7917	2.4242
CTL_XM	1.5501	4.1288	4.3584	1.6065	2.1822	3.4802	0.9341	1.0873	0.4337
CTL_XU	3.2698	1.0555	0.9979	3.6872	1.0614	1.2799	0.5817	1.3496	2.1795
CTL_XZ	2.4999	1.5668	0.6516	3.2005	1.0125	1.0634	0.3910	0.2093	0.9474
CTL_YA	0.5526	0.3855	0.7401	0.3057	0.7618	1.0487	1.0735	2.6870	1.3008
CTL_YC	0.4539	0.5346	1.2297	0.4075	1.0818	0.6573	1.7144	1.8532	1.3128
CTL_YD	0.6237	1.0159	2.2761	0.5946	1.0839	0.8078	0.7617	2.2916	0.9059
CTL_YF	0.5010	0.5892	0.9529	0.5600	0.4915	0.9909	0.9792	2.3046	2.4128
CTL_YH	0.8645	1.1384	1.3371	0.7708	1.0238	1.7244	2.2704	4.2278	1.7461
CTL_YJ	0.7193	0.4389	0.5298	0.2604	0.3323	0.7966	0.3786	2.6727	0.7091
CTL_YL	0.6510	0.8958	0.7726	0.4833	0.5866	1.0976	0.8882	1.4124	1.2841
CTL_YN	0.9755	1.3833	2.6184	1.2451	1.4967	1.1041	2.0150	1.8092	1.3244
CTL_YO	1.1061	2.3960	2.4846	1.2096	1.6672	1.7438	1.9359	0.6643	0.5803
CTL_YQ	1.0175	1.3190	1.0988	0.5537	0.9596	1.9464	0.4866	2.7797	2.3799
CTL_YW	0.6041	1.1211	4.5931	0.9252	2.7004	0.9341	0.9658	1.4456	1.8306
CTL_ZB	1.1121	0.2509	0.1561	0.6379	0.3744	0.4826	0.4829	2.5639	1.2619
CTL_ZF	0.4490	0.5782	0.1544	0.7890	1.1750	0.3006	1.0352	0.4648	2.5886
CTL_ZJ	1.2093	0.5034	0.1636	1.2261	0.5196	0.3529	0.5959	0.8421	1.9763
CTL_ZM	2.2140	0.9388	0.6988	3.9502	1.0326	1.0526	1.2552	0.4372	1.3223
CTL_ZN	0.9913	1.4371	1.2166	1.0281	0.9876	1.8820	0.7924	0.2647	2.9708
CTL_ZP	0.8162	1.6426	2.9786	1.2679	1.5254	0.9926	1.7386	0.2875	0.3963
CTL_ZQ	0.8734	0.7022	0.1874	0.9001	1.3496	0.3207	1.4757	0.1264	0.2099
CTL_ZR	0.5436	0.6704	0.1758	0.6061	0.6922	0.2863	0.8422	0.0480	0.1302
CTL_ZT	1.2146	1.3944	0.7534	4.0720	0.8188	0.6795	2.4069	0.1819	0.1883
CTL_ZW	0.7103	0.6693	1.0035	0.5220	0.6836	0.9098	0.2929	1.4002	0.4654
CTL_ZY	2.6039	1.9677	1.8724	1.0777	1.2389	3.2129	3.6145	2.6344	1.5038
CTL_ZZ	0.9834	1.5665	2.9238	1.3432	1.1642	1.7831	1.6147	1.8936	1.0102
C_C	6.1957	8.0533	10.0868	4.1363	8.5458	4.2075	3.2142	0.8942	1.2307
C_F	1.2623	1.1553	0.7284	1.9839	2.0375	0.8600	0.7706	0.9369	1.2467
C_G	1.1652	3.4098	6.7512	14.1024	5.4913	8.6981	47.4744	0.7600	0.3446
C_H	2.2220	2.0682	1.0948	5.3096	3.9285	1.7042	1.8537	0.1873	0.4548
C_KA	1.3482	9.4800	4.4825	12.9335	5.2958	2.3098	0.4445	0.7692	0.9426
C_KB	2.6303	2.6458	4.1912	2.0557	6.1297	1.5744	7.4862	2.2707	0.4696
C_KD	0.4732	1.9417	1.5969	3.0299	2.1196	0.8059	0.4164	0.0931	0.4207
C_KF	0.8161	1.4012	0.8814	4.3600	1.5421	0.7355	1.0815	1.1098	1.3852
C_KG	0.9221	2.5001	0.8886	3.6747	5.0824	0.9959	2.2457	0.4768	0.1956
C_KH	0.5224	1.7693	1.1223	4.3351	3.0903	0.6985	1.2593	1.9302	1.0171
C_KI	1.9967	2.4842	0.9392	5.1282	1.4827	0.8835	1.3726	1.5313	1.4141

Appendix 8: continued.

Sample	miR-150	miR-193a-3p	miR-23a	miR-23b	miR-338-5p	miR-342-3p	miR-483-3p	*FOXO4*	*APAF1*
C_KJ	1.3969	2.0896	0.8325	2.2056	2.0191	1.1642	6.6554	0.4237	1.3964
C_KK	1.2236	0.5911	0.7216	0.2142	1.6724	0.3320	1.1983	1.8621	0.5864
C_KM	2.1609	2.1187	2.2030	0.9751	2.2104	0.8245	1.7451	1.2920	0.3590
C_KN	1.9242	1.6957	0.7668	8.5535	1.9958	1.1220	3.4084	0.5975	0.2584
C_KR	1.0673	1.1345	0.9345	3.9710	1.0465	0.8153	0.6064	0.4202	0.3744
C_KS	0.9361	1.6618	1.1212	4.8922	1.8881	0.7089	0.2589	1.3225	1.0523
C_KT	0.2138	2.7609	2.6839	1.2310	2.3303	0.9883	2.0306	0.6278	0.8877
C_KU	2.5974	1.8750	0.7299	3.9708	1.0789	2.0061	0.9572	0.5110	0.2022
C_KX	0.1924	3.7991	5.1983	2.2036	2.1320	0.7380	3.2047	0.3132	0.3260
C_KY	0.7850	1.9039	3.9284	1.0965	1.2124	1.2085	0.5733	0.3334	0.4523
C_KZ	0.5381	2.6302	2.0115	5.6923	3.1027	1.3089	0.5427	0.0815	0.2042
C_LA	0.8820	1.1830	0.5299	3.6419	2.4120	1.1074	0.6602	0.2725	0.4724
C_LC	1.5643	0.6633	0.5935	1.8223	2.0416	0.8038	1.2392	0.5318	0.5320
C_LD	1.2314	1.9230	1.1560	3.5250	2.6334	0.7254	1.3683	1.5404	0.3610
C_LE	0.3423	1.3028	1.6411	0.8008	0.6248	0.8117	0.7635	0.3958	0.9520
C_LF	1.7145	1.9319	3.4732	2.2078	5.6306	0.8907	2.7973	0.2153	0.1846
C_LG	0.3828	0.8291	0.5006	1.9386	1.0354	0.4224	1.9659	0.7420	1.4162
C_LI	0.1037	1.6444	2.0944	1.0006	0.7318	0.6357	3.8561	0.4361	0.5052
C_LJ	1.0162	2.8037	1.1709	5.8482	5.1034	1.3237	1.0713	1.2894	0.5610
C_LK	1.0872	3.7983	1.0853	4.2428	3.1842	1.3124	1.6477	0.8659	0.5820
C_LM	0.7041	0.7932	0.9533	0.6663	2.7062	0.3707	1.2053	0.4106	0.2313
C_LN	0.0681	0.4226	0.3992	0.5340	0.1712	0.1592	0.6758	0.5987	0.3053
C_LO	1.1973	1.2854	1.1179	0.5806	1.6306	0.7322	1.3394	1.1604	1.0678
C_LP	0.2761	0.3324	0.0724	0.5357	0.4649	0.1281	0.8252	0.7001	0.2916
C_LQ	1.3791	1.7469	1.4897	1.2030	2.3133	0.8366	2.8221	1.7984	2.5796
C_LR	0.0709	0.2465	0.2032	0.4398	0.1617	0.0856	0.9231	0.1414	0.1669
C_LS	2.8222	0.9667	1.2425	0.4128	1.6150	1.2229	3.1891	0.7192	1.4301
C_LU	0.1975	1.8704	2.6450	0.5019	1.9034	0.5108	1.4818	0.3997	0.2668
C_LX	0.5310	2.2824	2.0178	0.6205	1.7151	1.1088	1.4419	0.6308	1.3228
C_LY	0.2733	2.2180	2.9558	0.8798	1.2404	1.2216	0.2170	0.3772	1.1050
C_LZ	1.2033	0.6999	1.1938	0.5594	0.8463	0.8373	1.3482	0.6872	1.7919
C_MA	1.8514	0.8333	1.1491	0.7097	2.3880	1.0158	1.3618	0.2753	0.4676
C_MB	3.4144	1.7721	3.0863	1.5642	1.9739	1.5294	2.1790	0.2186	0.4327
C_MC	0.7324	0.9900	0.7103	0.4622	2.6603	0.4593	1.7256	0.7576	1.4348
C_MD	0.1538	1.6968	1.6959	0.6730	0.5103	1.6735	0.8164	0.7178	0.7204
C_MG	1.3463	1.0218	1.0279	0.9226	2.6900	0.7923	1.5782	1.5938	1.7903
C_MI	2.4059	1.1287	2.2409	0.8018	4.4161	1.3331	1.1588	1.0142	0.2308
C_MK	0.5930	5.6016	1.2518	1.1687	0.8202	1.9697	3.5767	0.1255	0.1457
C_ML	3.3106	0.9478	2.2431	1.2569	1.5769	1.5782	2.1274	0.4392	0.3427
C_MN	0.9949	2.1148	2.6407	1.3643	5.0855	0.6562	2.4035	1.0570	0.1910
C_MO	0.1971	1.3115	0.7173	0.2794	1.0175	0.4550	0.7152	0.9434	1.1146
C_MP	4.6035	3.0007	2.7526	1.8680	3.0106	1.5459	1.6451	1.0648	1.2497

Appendix 8: continued.

Sample	miR-150	miR-193a-3p	miR-23a	miR-23b	miR-338-5p	miR-342-3p	miR-483-3p	*FOXO4*	*APAF1*
C_MS	1.2156	1.9210	4.5832	1.8383	7.7985	0.8246	1.9035	1.3226	0.6276
C_MV	1.3526	1.5578	1.7642	1.0404	2.8597	1.0225	1.1294	0.3422	1.3794
C_MW	1.5588	1.2663	2.7149	1.4555	3.1267	0.9351	1.0908	1.1201	0.2476
C_MX	0.4776	1.7500	2.5130	0.8247	1.4438	1.0288	0.5397	0.1181	0.3123
C_MY	3.9467	2.4471	2.8983	1.2061	3.7175	1.8329	1.0299	0.3613	0.9169
C_MZ	0.4295	1.4753	1.2831	1.3779	1.3128	0.8209	3.4935	1.3870	0.3894
C_NA	2.4652	2.0341	1.6145	1.5831	3.5107	1.3855	1.5111	2.2486	1.4826
C_ND	0.5432	2.3441	2.2929	0.8716	1.3154	0.7943	1.2782	1.2915	1.5791
C_NG	0.2707	1.5906	1.7315	0.5646	0.7369	0.7476	1.9909	0.8602	1.2542
C_NH	1.8380	1.3730	1.7607	0.9137	3.1890	1.0121	1.4383	1.6639	1.7045
C_NI	2.8513	1.9393	2.0009	2.0573	5.3820	1.6473	0.9948	1.7863	0.8834
C_NL	5.8654	1.6979	2.8009	0.9065	2.7741	2.3815	1.8223	0.9492	1.2504
C_NN	0.4769	1.3208	1.4899	0.8099	2.2057	0.3765	6.7729	1.0578	0.8348
C_NQ	1.0347	2.5326	1.7284	0.7883	2.9380	1.5470	2.7320	0.3269	0.2657
C_NR	0.4221	1.7184	0.9127	1.0829	0.6367	0.9493	4.5663	0.3220	0.1450
C_NS	0.6419	0.9239	0.8104	0.2674	0.2941	0.8520	0.8940	1.2568	1.3975
C_NV	0.3099	1.3403	0.7897	0.2285	1.2302	0.5262	1.8883	0.1588	0.1392

Appendix 9: Sample of Invitrogen Tali image-based cytometry cell analysis report.

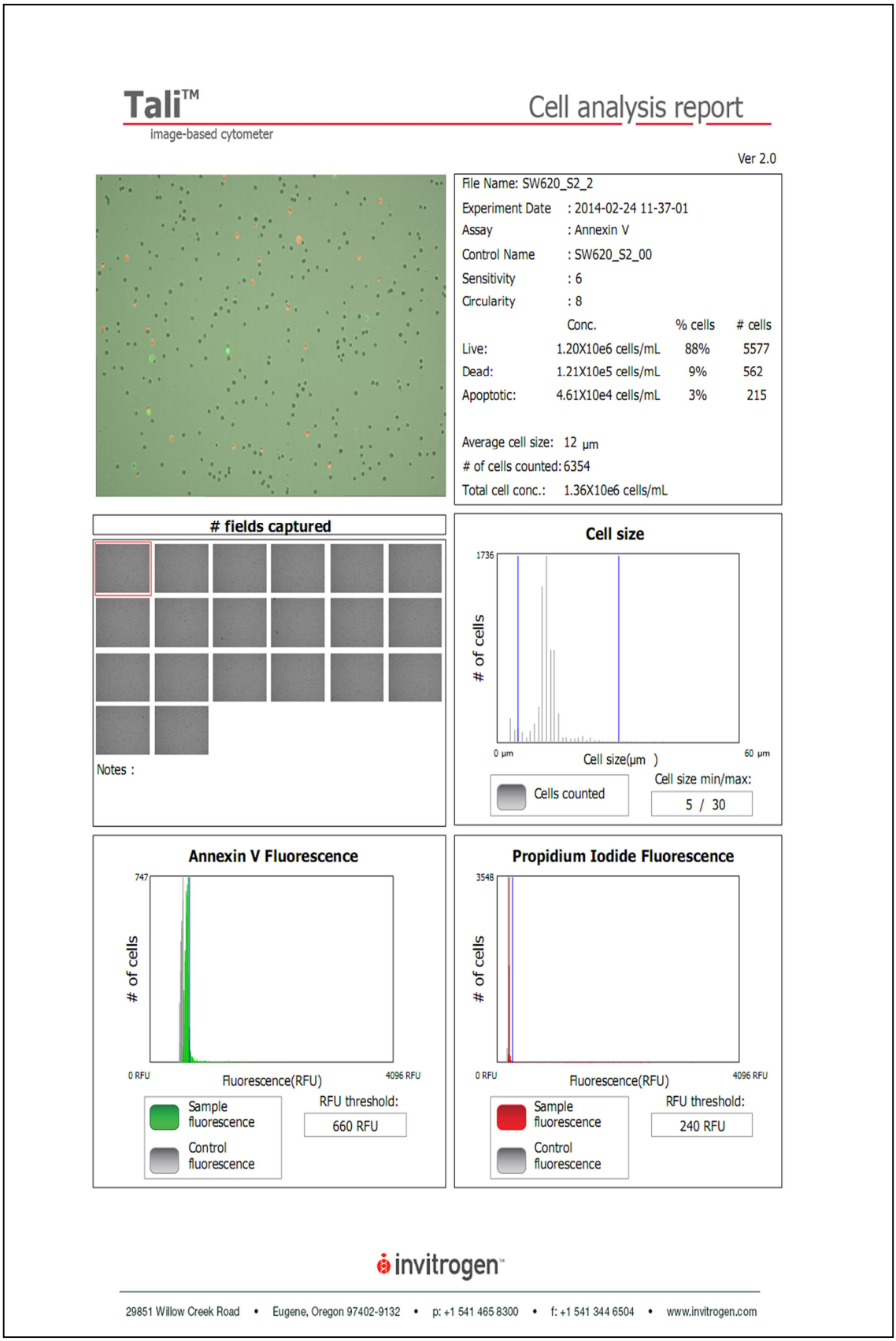

Appendix 10: Putative gene targets of miR-193a-3p.

Putative gene (*Homo sapiens*)	**Full name**	**NCBI reference sequence**	**Description (Source: NCBI database [http://www.ncbi.nlm.nih.gov/]; UniProt database [http://www.uniprot.org/])**
ACVR2B	Activin A receptor, type 2B	NM_001106.3	ACVR2B is an activin type 2 receptor that binds activins (dimeric growth and differentiation factors) and forms a stable complex with the activin type 1 receptor in TGF-β signalling.
AXIN2	Axin 2	NM_004655.3	Axin 2 is involved in the regulation of β-catenin stability in the Wnt/β-catenin pathway. Mutations in this gene have been linked to CRC with defective mismatch repair.
CCND1	Cyclin D1	NM_053056.2	Cyclin D1 is involved in the regulation of cell cycle, in particularly G1/S transition. It is a regulator of cyclin-dependent kinases 4 and 6. Mutations and over-expression of this gene are common in cancer.
FAS	Fas cell surface death receptor	NM_000043.4	Fas receptor is a member of the tumour necrosis factor receptor superfamily that contains a death domain. Fas receptor is involved in the regulation of programmed cell death via extrinsic apoptosis pathway. Mutations in this gene have been implicated in the pathogenesis of cancer and diseases of the immune system.

Appendix 10: continued.

Putative gene (*Homo sapiens*)	**Full name**	**NCBI reference sequence**	**Description (Source: NCBI database [http://www.ncbi.nlm.nih.gov/]; UniProt database [http://www.uniprot.org/])**
FOXO4	Forkhead box O4	NM_005938.3	FOXO4 is a transcription factor that belongs to a large FOX family of proteins. FOXO4 is involved in the regulation of cell growth, cell cycle arrest, DNA repair, stress, invasion and metastasis. FOXO4 has been identified as a tumour suppressor in cancer.
FZD4	Frizzled class receptor 4	NM_012193.3	FZD4 belongs to a family of G protein-coupled transmembrane proteins that serve as receptors in the Wnt/β-catenin pathway. It acts as a positive regulator in the Wnt/β-catenin signalling.
FZD5	Frizzled class receptor 5	NM_003468.3	FZD5 belongs to a family of G protein-coupled transmembrane proteins that serve as receptors in the Wnt/β-catenin pathway. It acts as a positive regulator in the Wnt/β-catenin signalling.
KRAS	Kirsten rat sarcoma viral oncogene homologue	NM_033360.3	*KRAS* is an oncogene. It encodes a protein that is a member of the small GTPase superfamily. Mutations in this gene have been implicated in various malignancies, including CRC.

Appendix 10: continued.

Putative gene (*Homo sapiens*)	**Full name**	**NCBI reference sequence**	**Description (Source: NCBI database [http://www.ncbi.nlm.nih.gov/]; UniProt database [http://www.uniprot.org/])**
MAPK1	Mitogen-activated protein kinase 1	NM_002745.4	MAPK1 is involved in the regulation of cell proliferation, differentiation and transcriptional activation/repression via EGFR pathway.
PDGFRA	Platelet-derived growth factor receptor, alpha polypeptide	NM_006206.4	PDGFRA is a cell surface tyrosine kinase receptor that binds platelet-derived growth factors, which are mitogens for cells of mesenchymal origin. PDGFRA is involved in the regulation of organ development, wound healing and tumour progression. Mutations in this gene have been associated with numerous cancers.
PTEN	Phosphatase and tensin homologue	NM_000314.4	*PTEN* is a tumour suppressor gene. It is involved in the regulation of PI3K-AKT pathway. Mutations in this gene are common in cancer.
SMAD4	SMAD family member 4	NM_005359.5	SMAD4 is a member of the SMAD family of signal transduction proteins. SMAD proteins are phosphorylated and activated by transmembrane serine-threonine receptor kinases in response to TGF-β signalling. *SMAD4* is a tumour suppressor gene. Mutations in this gene have been implicated in hereditary haemorrhagic telangiectasia syndrome, juvenile polyposis syndrome, pancreatic cancer and CRC.

Appendix 10: continued.

Putative gene (*Homo sapiens*)	**Full name**	**NCBI reference sequence**	**Description (Source: NCBI database [http://www.ncbi.nlm.nih.gov/]; UniProt database [http://www.uniprot.org/])**
SOS2	Son of sevenless homologue 2	NM_006939.2	*SOS2* encodes a protein that is a guanine nucleotide exchange factor that binds guanine nucleotides and prepares the GTP binding site for Ras proteins binding in the EGFR pathway. SOS2-dependent signalling is predominantly short-term, as compared to SOS1. Mutations in this gene have been associated with chronic myeloid leukaemia.
TGFBR1	Transforming growth factor beta receptor I	NM_004612.2	Upon binding to TGF-β ligand, TGFBR1 forms a heterodimeric complex with TGFBR2 and transmits the TGF-β signal from the cell surface to the cytoplasm. Mutations in this gene are common in the malignant transformation of CRC.

Appendix 11: *FOXO4* 3'-UTR fragment (NM_005938.3) containing the seed sequence. The customised fragment was inclusive of the HindIII and SpeI restriction sites (312 bp).

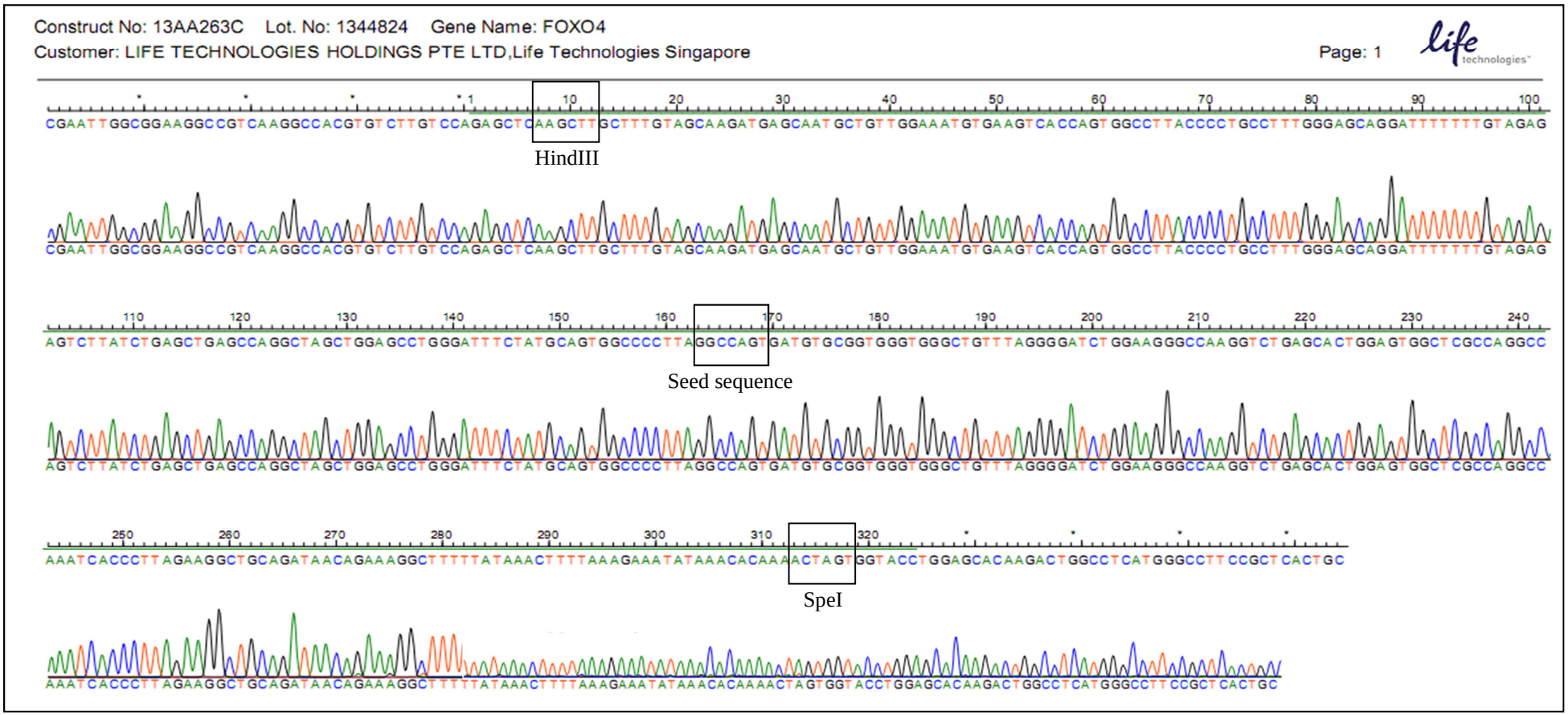

Appendix 12: *FOXO4* 3'-UTR fragment (NM_005938.3) containing the mutated seed sequence. The customised fragment was inclusive of the HindIII and SpeI restriction sites (312 bp).

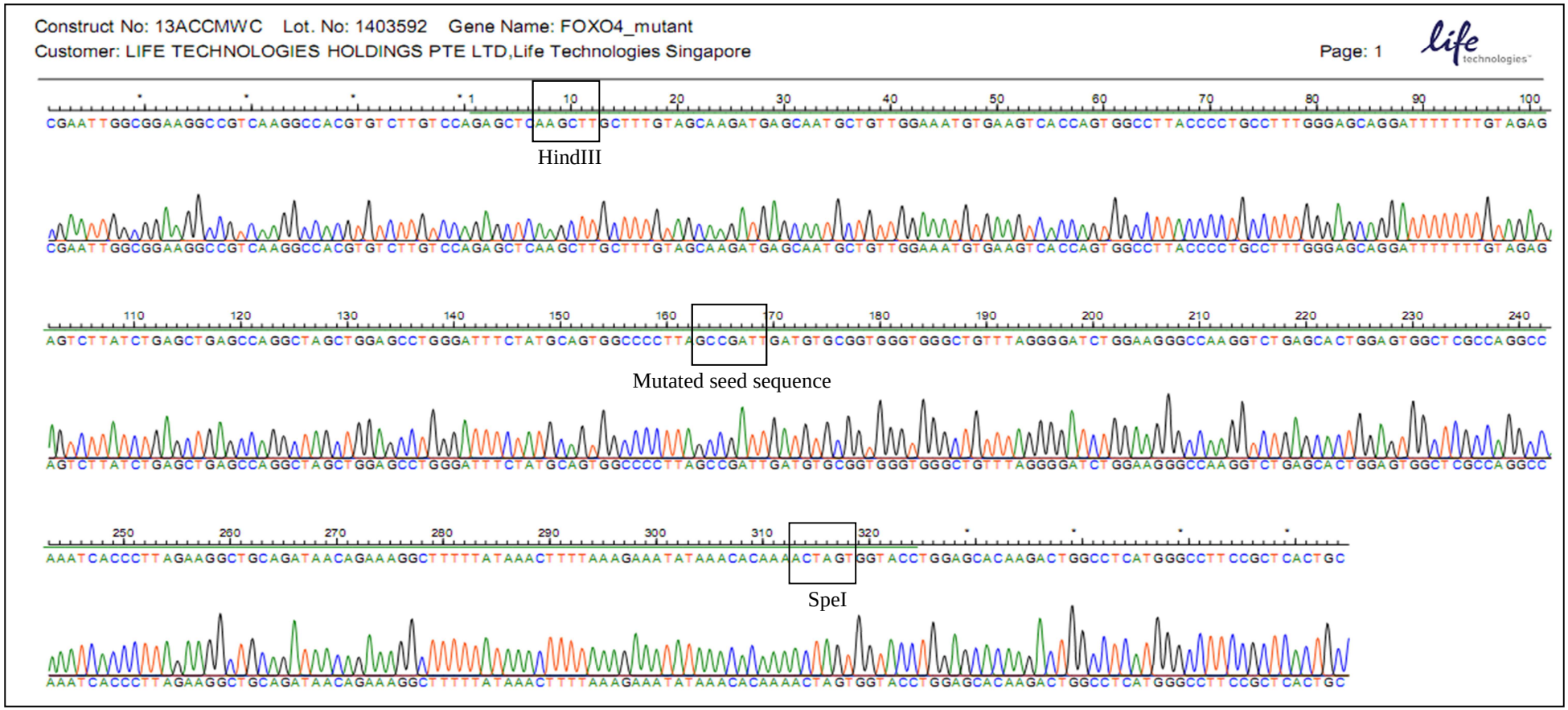

Appendix 13: Western blot images and fold change values of FOXO4 and APAF1 in paired tissue samples. β-actin was used as the loading control. N: normal colonic tissue; C: cancer tissue.

Sample	β-actin		FOXO4 protein			APAF1 protein		
	N	C	N	C	Fold change	N	C	Fold change
C_KB	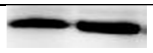		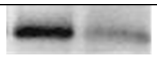		0.4103			0.4178
C_KF					0.3521			0.7943
C_KG					1.1133			0.9720
C_KI					1.4866			1.2070
C_KN					1.2110			1.1646
C_KS					0.6143			0.6136
C_KU					0.7889			1.0867
C_KX					0.7102			0.6592
C_KY					0.6020			0.3421
C_LC					0.6390			0.7827
C_LE					0.7234			0.4469
C_LF					0.8378			0.6098
C_LJ					0.7568			0.8293
C_LK					0.7909			0.8709
C_LM					0.2831			0.4970
C_LP					0.8408			0.8649
C_LR					1.0606			1.1586
C_LX					0.5964			0.6734
C_LY					0.8887			0.5479
C_ML					0.7191			0.8409
C_MN					0.5618			0.5981
C_MS					0.8240			0.8361
C_MV					0.7074			0.3855
C_MY					0.6290			0.5341
C_NA					0.5493			0.8116
C_NH					0.7260			0.7696
C_NI					0.7866			0.4717
C_NQ					0.8798			0.9567
C_NR					0.5865			0.5861
C_NV					0.8287			1.1435

Appendix 14: Putative gene targets of miR-23a.

Putative gene (*Homo sapiens*)	**Full name**	**NCBI reference sequence**	**Description (Source: NCBI database [http://www.ncbi.nlm.nih.gov/]; UniProt database [http://www.uniprot.org/])**
ACVR1C	Activin A receptor, type 1C	NM_145259.2	ACVR1C is an activin type 1 receptor that binds activins (dimeric growth and differentiation factors) and forms a stable complex with the activin type 2 receptor in TGF-β signalling.
ACVR2A	Activin A receptor, type 2A	NM_001278579.1	ACVR2A is an activin type 2 receptor that binds activins (dimeric growth and differentiation factors) and forms a stable complex with the activin type 1 receptor in TGF-β signalling.
ACVR2B	Activin A receptor, type 2B	NM_001106.3	ACVR2B is an activin type 2 receptor that binds activins (dimeric growth and differentiation factors) and forms a stable complex with the activin type 1 receptor in TGF-β signalling.
APAF1	Apoptotic peptidase activating factor 1	NM_013229.2	APAF1 is a cytoplasmic protein that is involved in the regulation of cell apoptosis via intrinsic apoptosis pathway.
CASP7	Caspase-7, apoptosis-related cysteine peptidase	NM_001227.4	Caspase-7 is a cysteine aspartic acid protease that plays a central role in the execution phase of cell apoptosis.

Appendix 14: continued.

Putative gene (*Homo sapiens*)	**Full name**	**NCBI reference sequence**	**Description (Source: NCBI database [http://www.ncbi.nlm.nih.gov/]; UniProt database [http://www.uniprot.org/])**
CCND1	Cyclin D1	NM_053056.2	Cyclin D1 is involved in the regulation of cell cycle, in particularly G1/S transition. It is a regulator of cyclin-dependent kinases 4 and 6. Mutations and over-expression of this gene are common in cancer.
CREBBP	cAMP response element-binding (CREB)-binding protein	NM_004380.2	CREBBP is ubiquitously expressed and is associated with transcriptional co-activation of a variety of transcription factors. It is involved in embryonic development, growth control and cellular homeostasis.
FAS	Fas cell surface death receptor	NM_000043.4	Fas receptor is a member of the tumour necrosis factor receptor superfamily that contains a death domain. Fas receptor is involved in the regulation of programmed cell death via extrinsic apoptosis pathway. Mutations in this gene have been implicated in the pathogenesis of cancer and diseases of the immune system.
FZD4	Frizzled class receptor 4	NM_012193.3	FZD4 belongs to a family of G protein-coupled transmembrane proteins that serve as receptors in the Wnt/β-catenin pathway. It acts as a positive regulator in the Wnt/β-catenin signalling.

Appendix 14: continued.

Putative gene (*Homo sapiens*)	**Full name**	**NCBI reference sequence**	**Description (Source: NCBI database [http://www.ncbi.nlm.nih.gov/]; UniProt database [http://www.uniprot.org/])**
FZD5	Frizzled class receptor 5	NM_003468.3	FZD5 belongs to a family of G protein-coupled transmembrane proteins that serve as receptors in the Wnt/β-catenin pathway. It acts as a positive regulator in the Wnt/β-catenin signalling.
FZD7	Frizzled class receptor 7	NM_003507.1	FZD7 belongs to a family of G protein-coupled transmembrane proteins that serve as receptors in the Wnt/β-catenin pathway. FZD7 may down-regulate APC function and enhance β-catenin-mediated signals in cancer.
ID4	Inhibitor of DNA binding 4, dominant negative helix-loop-helix protein	NM_001546.3	ID4 is a basic helix-loop-helix transcription factor. ID4 can act as a tumour suppressor though it lacks the DNA binding activity. The activity of ID4 depends on its protein binding partner.
PIK3R3	Phosphoinositide-3-kinase, regulatory sub-unit 3 (gamma)	NM_003629.3	PIK3R3 is a lipid kinase that binds to activated protein-tyrosine kinases through its SH2 domain and regulates the downstream signalling acitivties. It is involved in the regulation of cell proliferation, survival, degranulation, vesicular trafficking and migration.

Appendix 14: continued.

Putative gene (*Homo sapiens*)	**Full name**	**NCBI reference sequence**	**Description (Source: NCBI database [http://www.ncbi.nlm.nih.gov/]; UniProt database [http://www.uniprot.org/])**
PTEN	Phosphatase and tensin homologue	NM_000314.4	*PTEN* is a tumour suppressor gene. It is involved in the regulation of PI3K-AKT pathway. Mutations in this gene are common in cancer.
RBL2	Retinoblastoma-like 2	NM_005611.3	RBL2 is a key regulator in cell division. It is involved in heterochromatin formation by maintaining the overall chromatin structure. It is a potent inhibitor of E2F-mediated transactivation and may act as a tumour suppressor protein.
SMAD4	SMAD family member 4	NM_005359.5	SMAD4 is a member of the SMAD family of signal transduction proteins. SMAD proteins are phosphorylated and activated by transmembrane serine-threonine receptor kinases in response to TGF-β signalling. *SMAD4* is a tumour suppressor gene. Mutations in this gene have been implicated in hereditary haemorrhagic telangiectasia syndrome, juvenile polyposis syndrome, pancreatic cancer and CRC.
SOS1	Son of sevenless homologue 1	NM_005633.3	*SOS1* encodes a protein that is a guanine nucleotide exchange factor that binds guanine nucleotides and prepares the GTP binding site for Ras proteins binding in the EGFR pathway. Over-expression of SOS1 has been linked to the development of various solid tumours.

Appendix 14: continued.

Putative gene (*Homo sapiens*)	**Full name**	**NCBI reference sequence**	**Description (Source: NCBI database [http://www.ncbi.nlm.nih.gov/]; UniProt database [http://www.uniprot.org/])**
TGFBR2	Transforming growth factor beta receptor II	NM_001024847.2	Upon binding to TGF-β ligand, TGFBR2 forms a heterodimeric complex with TGFBR1 and transmits the TGF-β signal from the cell surface to the cytoplasm. Mutations in this gene are common in the malignant transformation of CRC.

Appendix 15: *APAF1* 3'-UTR fragment (NM_013229.2) containing the seed sequence. The customised fragment was inclusive of the HindIII and SpeI restriction sites (312 bp).

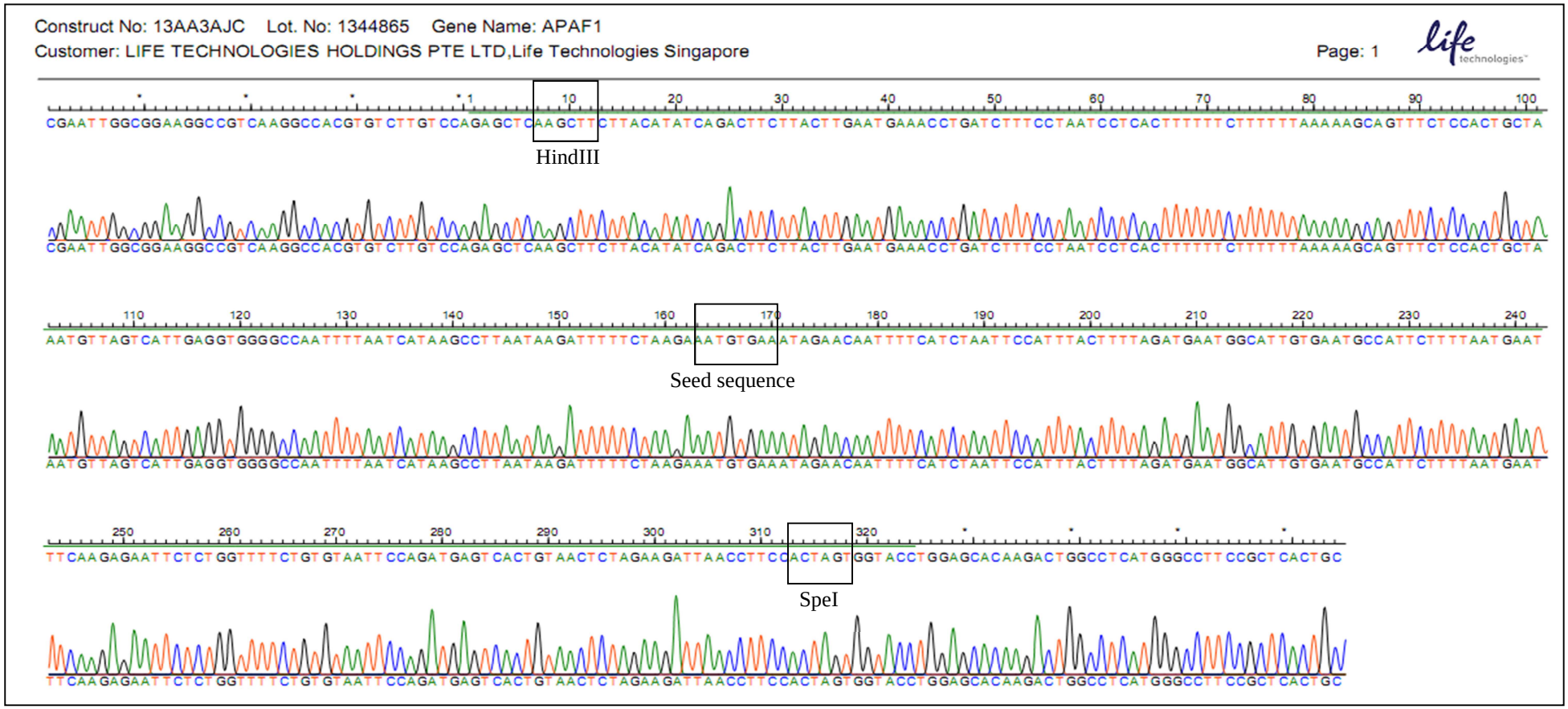

Appendix 16: *APAF1* 3'-UTR fragment (NM_013229.2) containing the mutated seed sequence. The customised fragment was inclusive of the HindIII and SpeI restriction sites (312 bp).

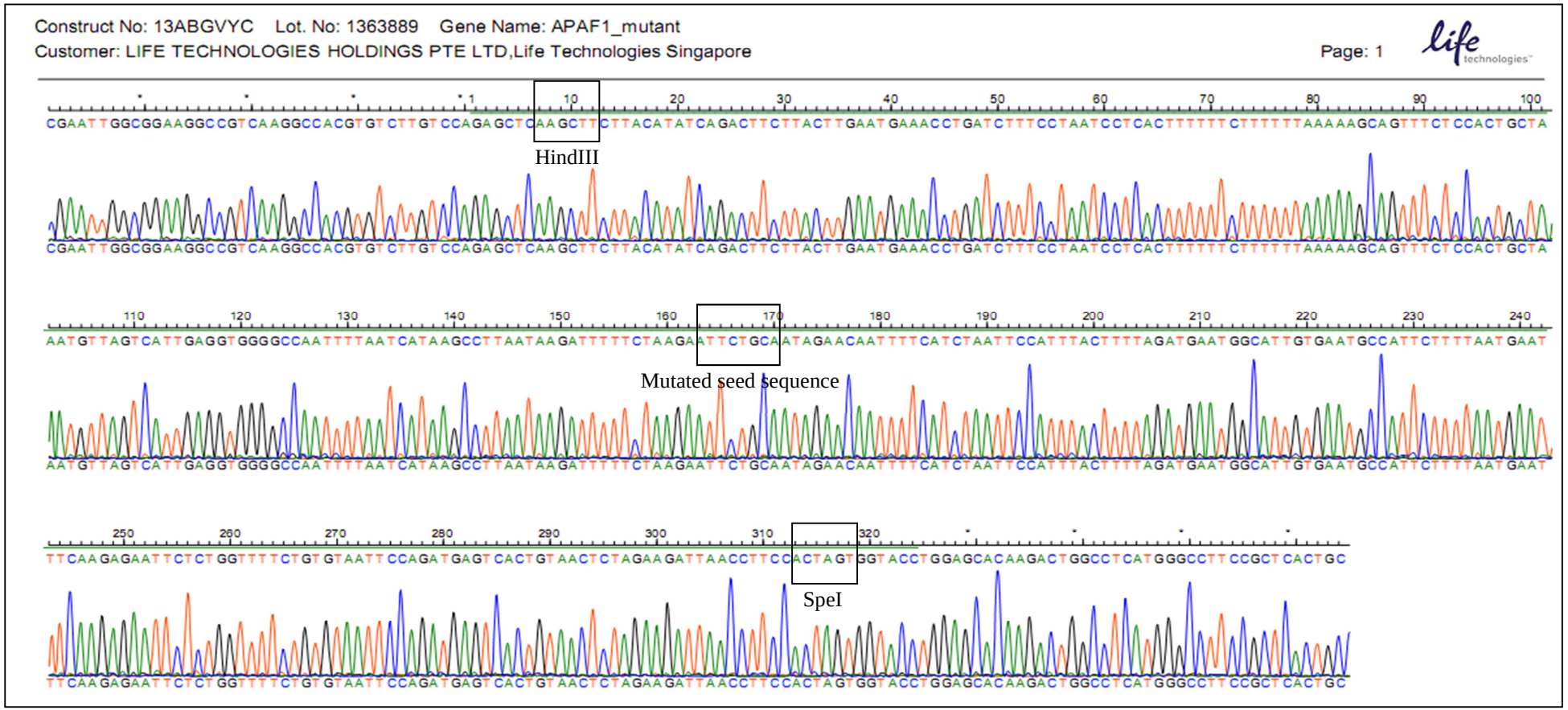

Appendix 17: Putative gene targets of miR-338-5p.

Putative gene (*Homo sapiens*)	**Full name**	**NCBI reference sequence**	**Description (Source: NCBI database [http://www.ncbi.nlm.nih.gov/]; UniProt database [http://www.uniprot.org/])**
ACVR2A	Activin A receptor, type 2A	NM_001278579.1	ACVR2A is an activin type 2 receptor that binds activins (dimeric growth and differentiation factors) and forms a stable complex with the activin type 1 receptor in TGF-β signalling.
APPL1	Adaptor protein, phosphotyrosine interaction, PH domain and leucine zipper containing 1	NM_012096.2	APPL1 is involved in the regulation of cell proliferation, adiponectin signalling and insulin signalling.
CCND1	Cyclin D1	NM_053056.2	Cyclin D1 is involved in the regulation of cell cycle, in particularly G1/S transition. It is a regulator of cyclin-dependent kinases 4 and 6. Mutations and over-expression of this gene are common in cancer.

Appendix 17: continued.

Putative gene (*Homo sapiens*)	**Full name**	**NCBI reference sequence**	**Description (Source: NCBI database [http://www.ncbi.nlm.nih.gov/]; UniProt database [http://www.uniprot.org/])**
CREBBP	cAMP response element-binding (CREB)-binding protein	NM_004380.2	CREBBP is ubiquitously expressed and is associated with transcriptional co-activation of a variety of transcription factors. It is involved in embryonic development, growth control and cellular homeostasis.
EP300	E1A binding protein p300	NM_001429.3	*EP300* encodes the adenovirus E1A-associated cellular p300 transcriptional co-activator protein. EP300 functions as histone acetyltransferase that regulates cellular transcription via chromatin remodelling. It is involved in the regulation of cell proliferation and differentiation. Mutations in this gene have been detected in epithelial cancer.
FZD7	Frizzled class receptor 7	NM_003507.1	FZD7 belongs to a family of G protein-coupled transmembrane proteins that serve as receptors in the Wnt/β-catenin pathway. FZD7 may down-regulate APC function and enhance β-catenin-mediated signals in cancer.

Appendix 17: continued.

Putative gene (*Homo sapiens*)	**Full name**	**NCBI reference sequence**	**Description (Source: NCBI database [http://www.ncbi.nlm.nih.gov/]; UniProt database [http://www.uniprot.org/])**
ID1	Inhibitor of DNA binding 1, dominant negative helix-loop-helix protein	NM_002165.3	ID1 is a basic helix-loop-helix transcription factor that lacks the DNA binding activity. It is involved in the regulation of cell growth, senescence, and differentiation.
ID4	Inhibitor of DNA binding 4, dominant negative helix-loop-helix protein	NM_001546.3	ID4 is a basic helix-loop-helix transcription factor. ID4 can act as a tumour suppressor though it lacks the DNA binding activity. The activity of ID4 depends on its protein binding partner.
KRAS	Kirsten rat sarcoma viral oncogene homologue	NM_033360.3	*KRAS* is an oncogene. It encodes a protein that is a member of the small GTPase superfamily. Mutations in this gene have been implicated in various malignancies, including CRC.

Appendix 17: continued.

Putative gene (*Homo sapiens*)	**Full name**	**NCBI reference sequence**	**Description (Source: NCBI database [http://www.ncbi.nlm.nih.gov/]; UniProt database [http://www.uniprot.org/])**
MAPK1	Mitogen-activated protein kinase 1	NM_002745.4	MAPK1 is involved in the regulation of cell proliferation, differentiation and transcriptional activation/repression via EGFR pathway.
MET	MET proto-oncogene, receptor tyrosine kinase	NM_001127500.1	The proto-oncogene MET product is the hepatocyte growth factor receptor with tyrosine kinase activity. Mutations in this gene generally lead to carcinogenesis.
PDGFRA	Platelet-derived growth factor receptor, alpha polypeptide	NM_006206.4	PDGFRA is a cell surface tyrosine kinase receptor that binds platelet-derived growth factors, which are mitogens for cells of mesenchymal origin. PDGFRA is involved in the regulation of organ development, wound healing and tumour progression. Mutations in this gene have been associated with numerous cancers.
PTEN	Phosphatase and tensin homologue	NM_000314.4	*PTEN* is a tumour suppressor gene. It is involved in the regulation of PI3K-AKT pathway. Mutations in this gene are common in cancer.
RBL2	Retinoblastoma-like 2	NM_005611.3	RBL2 is a key regulator in cell division. It is involved in heterochromatin formation by maintaining the overall chromatin structure. It is a potent inhibitor of E2F-mediated transactivation and may act as a tumour suppressor protein.

Appendix 17: continued.

Putative gene (*Homo sapiens*)	**Full name**	**NCBI reference sequence**	**Description (Source: NCBI database [http://www.ncbi.nlm.nih.gov/]; UniProt database [http://www.uniprot.org/])**
RBX1	Ring-box 1, E3 ubiquitin protein ligase	NM_014248.3	RBX1 is involved in ubiquitination during cell cycle progression.
SMAD4	SMAD family member 4	NM_005359.5	SMAD4 is a member of the SMAD family of signal transduction proteins. SMAD proteins are phosphorylated and activated by transmembrane serine-threonine receptor kinases in response to TGF-β signalling. *SMAD4* is a tumour suppressor gene. Mutations in this gene have been implicated in hereditary haemorrhagic telangiectasia syndrome, juvenile polyposis syndrome, pancreatic cancer and CRC.
SMAD5	SMAD family member 5	NM_005903.6	SMAD5 is a member of the SMAD family of signal transduction proteins. SMAD proteins are phosphorylated and activated by transmembrane serine-threonine receptor kinases in response to TGF-β signalling. Mutations in this gene have been detected in cancer.

Appendix 17: continued.

Putative gene (*Homo sapiens*)	**Full name**	**NCBI reference sequence**	**Description (Source: NCBI database [http://www.ncbi.nlm.nih.gov/]; UniProt database [http://www.uniprot.org/])**
SOS1	Son of sevenless homologue 1	NM_005633.3	*SOS1* encodes a protein that is a guanine nucleotide exchange factor that binds guanine nucleotides and prepares the GTP binding site for Ras proteins binding in the EGFR pathway. Over-expression of SOS1 has been linked to the development of various solid tumours.
SOS2	Son of sevenless homologue 2	NM_006939.2	*SOS2* encodes a protein that is a guanine nucleotide exchange factor that binds guanine nucleotides and prepares the GTP binding site for Ras proteins binding in the EGFR pathway. SOS2-dependent signalling is predominantly short-term, as compared to SOS1. Mutations in this gene have been associated with chronic myeloid leukaemia.
TGFBR1	Transforming growth factor beta receptor I	NM_004612.2	Upon binding to TGF-β ligand, TGFBR1 forms a heterodimeric complex with TGFBR2 and transmits the TGF-β signal from the cell surface to the cytoplasm. Mutations in this gene are common in the malignant transformation of CRC.

Appendix 18: List of publications and papers presented.

Research article

BMC Cancer (2013) - Impact factor: 3.32

Yong *et al. BMC Cancer* 2013, **13**:280
http://www.biomedcentral.com/1471-2407/13/280

BMC Cancer

RESEARCH ARTICLE **Open Access**

Potentiality of a triple microRNA classifier: miR-193a-3p, miR-23a and miR-338-5p for early detection of colorectal cancer

Fung Lin Yong[1*], Chee Wei Law[1] and Chee Woon Wang[2]

Abstract

Background: MicroRNAs (miRNAs) are short, non-coding RNA molecules that act as regulators of gene expression. Circulating blood miRNAs offer great potential as cancer biomarkers. The objective of this study was to correlate the differential expression of miRNAs in tissue and blood in the identification of biomarkers for early detection of colorectal cancer (CRC).

Methods: The study was divided into two phases: (I) Marker discovery by miRNA microarray using paired cancer tissues (n = 30) and blood samples (CRC, n = 42; control, n = 18). (II) Marker validation by stem-loop reverse transcription real time PCR using an independent set of paired cancer tissues (n = 30) and blood samples (CRC, n = 70; control, n = 32). Correlation analysis was determined by Pearson's test. Logistic regression and receiver operating characteristics curve analyses were applied to obtain diagnostic utility of the miRNAs.

Results: Seven miRNAs (miR-150, miR-193a-3p, miR-23a, miR-23b, miR-338-5p, miR-342-3p and miR-483-3p) have been found to be differentially expressed in both tissue and blood samples. Significant positive correlations were observed in the tissue and blood levels of miR-193a-3p, miR-23a and miR-338-5p. Moreover, increased expressions of these miRNAs were detected in the more advanced stages. MiR-193a-3p, miR-23a and miR-338-5p were demonstrated as a classifier for CRC detection, yielding a receiver operating characteristic curve area of 0.887 (80.0% sensitivity, 84.4% specificity and 83.3% accuracy).

Conclusion: Dysregulations in circulating blood miRNAs are reflective of those in colorectal tissues. The triple miRNA classifier of miR-193a-3p, miR-23a and miR-338-5p appears to be a potential blood biomarker for early detection of CRC.

Keywords: Colorectal cancer, MicroRNA, MiR-193a-3p, MiR-23a, MiR-338-5p

Background

Colorectal cancer (CRC) is the third most common cancer worldwide, with an estimation of 1.2 million new cases per year and more than 600,000 deaths [1-3]. The risk of CRC increases with age, whereby most cases are diagnosed in individuals aged 50 and above [4]. Incidence rate of CRC has been increasing in Asian countries. In Malaysia, it ranks the second after lung cancer and breast cancer in men and women, respectively [5]. The 5-year survival rate exceeds 90% when CRC is detected at an early, localized stage [6]. However, most cases are diagnosed at late stages due to inconvenient settings of current CRC screening tests and low population compliance. Colonoscopy has significant contribution in the detection of neoplastic lesions, but the requirements of bowel preparation, sedation and invasive nature have hindered its widespread application as a screening tool [7]. Other structural tests such as computed tomographic colonography and double contrast barium enema are limited by the concern of radiation exposure and cost [8]. Fecal-based analyses such as occult blood, immunochemical and stool DNA tests are common noninvasive

* Correspondence: flyong88@yahoo.com
[1]Department of Surgery, Faculty of Medicine, University of Malaya, 50603 Kuala Lumpur, Malaysia
Full list of author information is available at the end of the article

Appendix 18: continued.

Research article

International Journal of Molecular Sciences (2014) - Impact factor: 2.34

Int. J. Mol. Sci. **2014**, *15*, 11713-11729; doi:10.3390/ijms150711713

OPEN ACCESS
International Journal of
Molecular Sciences
ISSN 1422-0067
www.mdpi.com/journal/ijms

Article

The Involvement of miR-23a/*APAF1* Regulation Axis in Colorectal Cancer

Fung Lin Yong [1,*], Chee Woon Wang [2], April Camilla Roslani [1] and Chee Wei Law [1]

[1] Department of Surgery, Faculty of Medicine, University of Malaya, Kuala Lumpur 50603, Malaysia; E-Mails: aprilroslani@um.edu.my (A.C.R.); drcwlaw@gmail.com (C.W.L.)
[2] Department of Biochemistry, Faculty of Medicine, MAHSA University, Kuala Lumpur 59100, Malaysia; E-Mail: wang.chee@mahsa.edu.my

* Author to whom correspondence should be addressed; E-Mail: flyong88@yahoo.com; Tel.: +60-165-950-178; Fax: +60-379-586-360.

Received: 13 May 2014; in revised form: 2 June 2014 / Accepted: 4 June 2014 / Published: 2 July 2014

Abstract: Recent advances in microRNAome have made microRNAs (miRNAs) a compelling novel class of biomarker in cancer biology. In the present study, the role of miR-23a in the carcinogenesis of colorectal cancer (CRC) was investigated. Cell viability, apoptosis, and caspase 3/7 activation analyses were conducted to determine the potentiality of apoptosis resistance function of miR-23a in CRC. Luciferase assay was performed to verify a putative target site of miR-23a in the 3'-UTR of apoptosis protease activating factor 1 (*APAF1*) mRNA. The expression levels of miR-23a and *APAF1* in CRC cell lines (SW480 and SW620) and clinical samples were assessed using reverse transcription-quantitative real-time PCR (RT-qPCR) and Western blot. We found that the inhibition of miR-23a in SW480 and SW620 cell lines resulted in significant reduction of cell viability and promotion of cell apoptosis. Moreover, miR-23a up-regulation was coupled with *APAF1* down-regulation in CRC tissue samples. Taken together, miR-23a was identified to regulate apoptosis in CRC. Our study highlights the potential application of miR-23a/*APAF1* regulation axis in miRNA-based therapy and prognostication.

Keywords: miR-23a; APAF1; colorectal cancer; apoptosis; SW480; SW620

Appendix 18: continued.

Oral presentation; 6th Postgraduate Forum on Health Systems and Policies (2012)

BMC Public Health (2012) - Impact factor: 2.32

Yong *et al. BMC Public Health* 2012, **12**(Suppl 2):A22
http://www.biomedcentral.com/1471-2458/12/S2/A22

BMC Public Health

MEETING ABSTRACT Open Access

Role of microRNAs in the pathophysiology of sporadic colorectal cancer

Fung Lin Yong[1*], Chee Wei Law[1], Chee Woon Wang[2]

From 6th Postgraduate Forum on Health Systems and Policies
Melaka, Malaysia. 21-22 May 2012

Background
Colorectal cancer (CRC) is one of the leading causes of cancer-related mortality worldwide. Majority of the cases (~92%) are sporadic (nonhereditary), while the hereditary types constitute a lower percentage. The pathogenesis of sporadic CRC is heterogeneous and multi-factorial. In addition to environmental exposure, diet and lifestyle; accumulation of random somatic mutations also significantly affects the transcription of the genome and contributes to the carcinogenesis process. In recent years, microRNAs (miRNAs) have evolved as a unique class of endogenous regulators that offer great potential in the elucidation of cancer pathophysiology. The primary aim is to study the role of miRNAs as early biomarkers in sporadic CRC aetiology and pathogenesis.

Materials and methods
Matched-pairs of 30 cancerous and non-cancerous tissues, 47 blood samples from sporadic CRC patients and 30 blood samples from healthy controls have been collected from the University of Malaya Medical Centre. Total RNA was extracted and profiled using Affymetrix GeneChip miRNA 2.0 microarray chips. The microarray results and predicted targets have also been analyzed using miRNA bioinformatic softwares.

Results
A panel of significantly dysregulated miRNAs were identified ($p < 0.05$), namely miR-106a, -20a, -21, -223, -24 and -424. Based on TargetScan software, these miRNAs were found to participate in the regulation of keysignaling pathways in the adenoma-carcinoma sequences in CRC. Several predicted target genes involved were *APC*, *KRAS*, *PI3K*, *SMAD* and *MMPs*. These genes have been described to play crucial roles in inflammation, cell proliferation, apoptosis, angiogenesis, extracellular matrix remodelling and epithelial-mesenchymal transition.

Conclusions
miRNAs are informative in shedding light on the molecular mechanisms underlying the pathogenesis of sporadic CRC and circulating blood miRNAs are reflective of those in tissues. Further studies into the blood miRNA profiles would elucidate their potential roles as novel noninvasive biomarkers in CRC.

Author details
[1]Department of Surgery, Faculty of Medicine, University of Malaya, 50603 Kuala Lumpur, Malaysia. [2]Department of Biochemistry, Faculty of Medicine, MAHSA University College, 59100 Kuala Lumpur, Malaysia.

Published: 27 November 2012

doi:10.1186/1471-2458-12-S2-A22
Cite this article as: Yong *et al.*: Role of microRNAs in the pathophysiology of sporadic colorectal cancer. *BMC Public Health* 2012 12(Suppl 2):A22.

[1]Department of Surgery, Faculty of Medicine, University of Malaya, 50603 Kuala Lumpur, Malaysia
Full list of author information is available at the end of the article

Appendix 18: continued.

Oral presentation; 2nd International Conference on Bioinformatics and Biomedical Science (2013)

International Journal of Bioscience, Biochemistry and Bioinformatics (2013) - Non-ISI

International Journal of Bioscience, Biochemistry and Bioinformatics, Vol. 3, No. 5, September 2013

MicroRNAs that Potentially Regulate SOS1 Expression in Colon Cancer

Fung Lin Yong, Chee Wei Law, and Chee Woon Wang

***Abstract*—Colon cancer is one of the leading causes of cancer-associated morbidity and mortality worldwide. The development of colon cancer is closely related to epidermal growth factor receptor (EGFR) pathway. Son of Sevenless Homolog 1 (SOS1) gene is a key component in the EGFR pathway that has been reported to be overexpressed in cancer. The aim of the study was to investigate the microRNAs that potentially regulate SOS1 expression in colon cancer patients. A total of 60 cancerous and adjacent non-cancerous tissues were collected. Western blot, microRNA microarray and quantitative real-time PCR analyses were carried out. Significant overexpression of SOS1 and downregulation of miR-195 were determined ($p < 0.05$). The findings suggested a potential regulation of SOS1 expression by miR-195.**

***Index Terms*—Colon cancer, microRNA, SOS1, TNM.**

I. Introduction

Colon cancer is one of the leading causes of cancer-associated morbidity and mortality worldwide. A population-based study by Bray *et al.* [1] revealed an estimation of 1.2 million new cases per year and more than 600,000 deaths, primarily through liver metastasis. The pathogenesis of colon cancer is heterogeneous, multi-factorial and may take several decades. Several risk factors that might contribute to colon carcinogenesis include environmental exposure to carcinogens, diet, lifestyle and inflammation [2]. Colon cancer could develop sporadically through randomly acquired somatic mutations (92%) or as part of hereditary cancer syndromes such as Familial Adenomatous Polyposis (FAP) (<1%) and Hereditary NonPolyposis Colorectal Cancer (HNPCC) (8%) [3]-[6].

Son of Sevenless Homolog 1 (SOS1) is a gene of 8331 base pairs which is mapped to chromosome 2p21 (RefSeq Accession Number: NM_005633.3). SOS1 encodes a protein that is a guanine nucleotide exchange factor (GEF) that binds guanine nucleotides and prepares the GTP binding site for Ras proteins binding in the epidermal growth factor receptor (EGFR) pathway [7]. EGFR signaling is a common pathway that contributes to the progression of colon cancer [8]. SOS1 also possesses an opposite role in Ras proteins inactivation by facilitating the exchange of GTP for GDP [7]. Generally, a stimulation in the EGFR pathway would initiate the activation of adaptor proteins such as SH-2 containing protein (SHC) and growth-factor-receptor bound protein 2 (GRB2) that recruit SOS1 protein to the cell membrane [9]. The association with SOS1 will activate KRAS and further activate both RAF kinases and PI3Ks of the MAPK and PI3K/AKT pathways, respectively [9]. Gain-of-function mutations and/or overexpression of SOS1 gene has been found to be associated with Noonan syndrome type 4 [10] and gingival fibromatosis type 1 [11]. Although a DNA sequencing study by Swanson *et al.* [12] did not conclude SOS1 as a significant human oncogene, the overexpression of SOS1 is implicated in the pathobiology of various solid tumors. For instance, a study by Chen *et al.* [13] revealed the function of SOS1 in mediating Ras-induced Rac activation and metastatic colonization with the association with adaptor proteins EPS8 and ABI1. The silencing of any factor in the SOS1/EPS8/ABI1 tri-complex was reported to inhibit ovarian cancer cell migration and metastatic progression [13]. Timofeeva *et al.* [14] supported the role of SOS1 in cancer promotion and progression through a study in prostate cancer. Their group has successfully blocked prostate cancer cell migration and invasion through siRNA silencing of SOS1 [14].

MicroRNAs (miRNAs) are short (19-22 nucleotides), non-coding RNA molecules that act as regulators of gene expression [15]. MiRNAs are evolutionary conserved across species and play important roles in cancer pathophysiology such as cell proliferation, differentiation, apoptosis and metastasis [16]-[18]. MiRNAs can confer both oncogenic and tumor suppressive roles, depending upon their downstream targets [19]. Recently, miRNA-based study has become an important area in cancer research. In this study, differential expressions of miRNAs that correlate to the increased expression of SOS1 in colon cancer patients were evaluated.

II. Methods

A. Sample Collection

A total of 60 cancerous and adjacent non-cancerous tissues were collected from patients having surgical resection for primary colon cancer at the University of Malaya Medical Centre (UMMC), Malaysia between January 2011 and June 2012. The histology was confirmed by pathological analysis and staged according to the tumor-node-metastasis (TNM) staging system of the International Union against Cancer. The recruited patients were of sporadic cases and without

Manuscript received January 7, 2013; revised March 15, 2013. This work was supported in part by the University of Malaya (Malaysia) Research Grant (RG313-11HTM) and University of Malaya (Malaysia) Postgraduate Research Grant (PV020-2011A).

Fung Lin Yong and Chee Wei Law are with Department of Surgery, Faculty of Medicine, University of Malaya, 50603 Kuala Lumpur, Malaysia (e-mail: flyong88@yahoo.com, drcwlaw@gmail.com).

Chee Woon Wang is with Department of Biochemistry, Faculty of Medicine, MAHSA University College, 59100 Kuala Lumpur, Malaysia (e-mail: wang.chee@mahsa.edu.my).

DOI: 10.7763/IJBBB.2013.V3.248

Appendix 18: continued.

Poster presentation; Coloproctology Conference (2013)

UNIVERSITY OF MALAYA
KUALA LUMPUR
UM MEDICAL CENTRE

MAHSA UNIVERSITY COLLEGE

BLOOD MICRORNAS THAT POTENTIALLY REGULATE DELETED IN COLON CANCER (DCC) GENE AND DIFFERENTIATION-RELATED GENE 1 (DRG1) IN METASTATIC COLORECTAL CANCER

Fung Lin Yong[1], Chee Woon Wang[2], Chee Wei Law[1]

[1] Department of Surgery, Faculty of Medicine, University of Malaya, Kuala Lumpur, Malaysia
[2] Department of Biochemistry, Faculty of Medicine, MAHSA University College, Kuala Lumpur, Malaysia

INTRODUCTION

Colorectal cancer (CRC) metastasis occurs in diverse organs, most commonly in liver. *Deleted in colon cancer (DCC)* gene and *Differentiation-related gene 1 (DRG1)* are metastasis suppressor genes that play important roles in cancer metastasis[1]. In recent years, microRNAs (miRNAs) have been shown to hold much potential as novel non-invasive biomarkers for cancer diagnosis, prognosis and therapeutic approaches[2]. The first miRNA-based therapeutic that enters into human clinical trials is an inhibitor of miR-122 (Miravirsen, a β-D-oxy-LNA-modified phosphorothioate anti-sense oligonucleotide; Santaris Pharma A/S), and it is currently in phase 2a for the treatment of Hepatitis C[3].

OBJECTIVE

The objective of this study was to investigate the blood miRNA profile in metastatic CRC patients.

METHODS

Blood samples were collected from primary CRC patients from University of Malaya Medical Centre (UMMC). Total RNA (+miRNA) was extracted. MiRNA microarray was performed using pooled samples from healthy controls (n = 18) and CRC patients at stage II (n = 12), stage III (n = 12) and metastatic stage IV (n = 12). *In silico* miRNA target prediction was conducted using Targetscan software.

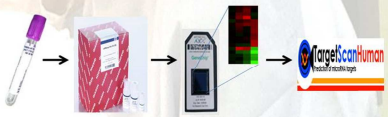

RESULTS

DCC and *DRG1* expressions have been shown to be down-regulated in metastatic CRC[1,4-5] (Table 1). Based on our *in silico* analysis, we have identified three miRNAs (miR-4267, miR-616* and miR-96) that could target *DCC* and one miRNA (miR-624*) that could target *DRG1* from the blood miRNA profile. These four miRNAs were found to be highly up-regulated in metastatic stage IV cases when compared to controls and could be used as targets for miRNA inhibition (Figure 1 and Table 2).

DCC	*DRG1*
• Metastasis suppressor gene • Down-regulated expression in metastatic CRC	
• DCC protein is a cell surface receptor • Involved in diverse cellular functions (e.g. axon guidance, induction of apoptosome) • Regulation of cell-cell and/or cell-extracellular matrix interactions	• DRG1 protein is an intracellular signaling molecule • Involved in several cancer-associated pathways: p53, PI3K/PTEN, PKC • Regulation of angiogenesis

Table 1. Roles of *DCC* and *DRG1* in CRC.

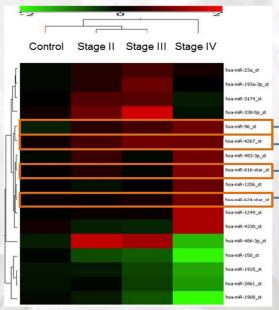

Figure 1. Blood miRNA profile of CRC patients. A total of 17 miRNAs were found to be differentially regulated. Fold change ≥ 1.5 (p < 0.05). Green: down-regulation; Red: up-regulation.

(A) *DCC*		Fold change of miRNA up-regulation	
		Stage IV vs. control	Mets vs. non-mets
Position 4071-4077 of DCC 3'UTR hsa-miR-96	5'…UAUCUAAAUACCUGU–UGCCAAAA… 3' UCGUUUUUACACGAUCACGGUUU	1.95	1.58
Position 4589-4595 of DCC 3'UTR hsa-miR-4267	5'…A–AGGGAGAUCUGGUUGGG… 3' UCUCCCUUGAGGGCACUUU	1.84	1.05#
Position 4968-4974 of DCC 3'UTR hsa-miR-616*	5'…GGUAUUUUGAGCCUACAAAAAG… 3' ACUCAAAACCCUUCAGUGACUU	1.87	1.69

(B) *DRG1*		Fold change of miRNA up-regulation	
		Stage IV vs. control	Mets vs. non-mets
Position 741-748 of DRG1 3'UTR hsa-miR-624*	5'…AUCAUGGUUUUUGAAGGCUUUA… 3' UAGUACCAGUACCUUGUGUUCA	1.88	1.75

Table 2. Predicted pairing region for (A) *DCC* and (B) *DRG1* at 3' untranslated region (3' UTR) with respective miRNAs using Targetscan software. The binding sites were highlighted in red. Fold changes of miRNAs up-regulations (metastatic stage IV vs. control; metastatic stage IV vs. non-metastatic stage II and III) were shown. #no significant difference.

CONCLUSION

These findings suggest the potentiality of blood miR-4267, miR-616*, miR-624* and miR-96 as prospective physiological regulators of cell invasion and metastasis. Further investigation via miRNA modulation would enhance our understanding of CRC metastasis and provide patient-specific insights to clinical prognostication and therapeutic strategies.

REFERENCES

1. Cook LM *et al.* (2011) *Semin Cancer Biol* 21(2): 113-122.
2. Seto AG (2010) *Int J Biochem Cell Biol* 42(8): 1298-1305.
3. Reesink HW *et al.* (2012) *J Hepatol* 56: pS1-S614. Suppl 2, A58.
4. Aschele C *et al.* (2004) *J Clin Oncol* 22(18): 3758-3765.
5. Shah MA *et al.* (2005) *Clin Cancer Res* 11(9): 3296-3302.

ACKNOWLEGDEMENTS

The study was funded by University of Malaya research grants (RG313-11HTM and PV020-2011A). The authors would like to thank the UMMC colorectal surgical team for blood samples collection.